MODELING HEAT TRANSFER IN BUTTER PRODUCTS

A thesis presented in partial fulfilment of
the requirements for the degree of

Doctor of Philosophy (PhD)

in

Bioprocess Engineering

Institute of Technology and Engineering
Massey University
Palmerston North, New Zealand

AMSHA NAHID
2007

ABSTRACT

Butter keeping quality and pallet physical stability during transport and storage are dependent on the temperature distribution through the product. Understanding these temperature changes are of vital importance for the dairy industry with regard to butter manufacture, storage and shipping.

Three dimensional mathematical models of heat transfer were developed to predict thawing and freezing in butter products. These models require accurate thermophysical data as an input. Specific heat capacity and enthalpy of butter with different composition was measured using Differential Scanning Calorimetry. The specific heat capacity of butter differs for cooling and heating operations due to significant supercooling and delayed crystallization of the fat fraction of butter at temperatures well below the equilibrium phase change temperature during cooling. This reduces the heat capacity for cooling relative to that for heating.

Thawing of individual blocks of butter was accurately predicted by the conduction only model (no mass transfer limitations) with equilibrium thermal properties giving accurate predictions when the butter was completely frozen before thawing. For partially frozen butter the conduction model with the measured temperature dependent specific heat capacity data for unfrozen butter including melting of some of the fat fraction gave accurate predictions.

For freezing it was observed that water in the butter supercools many degrees below its initial freezing point before freezing due to its water in oil structure. Experiments suggested that during freezing release of latent heat observed as a temperature rebound is controlled as much by the rate of crystallisation of water in each of the water droplets as by the rate of heat transfer. A conduction only model including water crystallization kinetics based on the Avrami Model predicted freezing in butter successfully. Simple models with equilibrium thermal properties and nucleation only kinetics (based on homogenous nucleation theory) or the sensible heat only model (no release of latent heat) gave poor predictions.

The models for individual blocks were extended to predict heat transfer in butter pallets. A butter pallet contains product, packaging material and the air entrapped between the packaging and butter cartons. Measurements were made for freezing and thawing of full and half pallets at a commercial storage facility and in the University laboratory. Thawing and freezing in wrapped tightly stacked

pallets was predicted accurately by the conduction only model with effective thermal properties (incorporating butter, packaging and air) estimated by the parallel model.

For unwrapped tightly stacked or loosely stacked pallets there is potential for air flow between the adjacent cartons of butter. An alternative approach was developed which consisted of modeling the pallet on block by block basis using effective heat transfer coefficients for each surface. Different heat transfer coefficients were used on different faces of the blocks depending on the location of the block in the pallet. This approach gave good predictions for both unwrapped tightly stacked and loosely stacked pallets using the estimated effective heat transfer coefficients from the measured data. Further experimental and/or modelling work is required in order to develop guidelines for estimating effective heat transfer coefficient values for internal block face for industrial scenarios.

ACKNOWLEDGEMENTS

It has been said by a wise person, "Preserve your knowledge by writing it". This PhD thesis consists of knowledge I gained during the last several years of my study at Massey University. Gaining this knowledge and its preservation would have not been possible without the help (and patience) of a number of people. I would like to thank to these people for a huge variety of reasons.

Firstly I like to thank my supervisors Associate Prof. **John Bronlund**, Professor **Don Cleland** (Massey University) and **Bruce Philpott** (Fonterra Co-operative Group Limited) for their continuous support, guidance and constructive criticism while supervising this work. I could not have imagined having a better supervising team for my PhD.

My special thanks to Dr. **Ashraf Choudhary** (Member of New Zealand Parliament) for helping me to come and study in Massey University and advising me to pursue Doctoral research.

I am grateful to The **New Zealand Foundation for Research, Science and Technology** (FRST) for Enterprise scholarship funding and **Fonterra Co-operative Group Ltd** for funding the project costs.

Lot of thanks goes to the administrative staff of ITE, specially **Joan Brookes, Gayle Leader, Trish O'Grady**, **Alisha Anan** and **John Hayward** for their help and support throughout the project.

Thanks to **Susan Lane** for assisting me with the use of DSC and sample preparation and to Dr. **David Oldfield** and **Chris Ballentyne** for their help during the early stage of the project.

I appreciate **Grant Gilbert** at Whareroa site for his great help and time in conducting experiments at the dairy factory, **Garry Radford** for keeping tons of butter in freezers and then disposing off it, **John Edwards** who was always there for me whenever I needed a hand in experimental work, **Humphrey O'Hagan** for cutting, chopping and drilling my butter, **Bruce Collins** and **Craig Bellhouse** for giving me a hand in understanding data logging equipment.

Huge thanks to **Dr. Tehseen Aslam** and **Muhammad Ali** (my Pakistani friends and colleagues at Massey University) for their support and help during my stay in New Zealand especially **Dr. Zulfiqar Butt** and **Dr. Zaker Hussain**, who always supported me as my real brothers.

I won't be able to forget the support, understanding and encouragement given by the Pakistani community in Palmerston North and Wellington specially **Dr Khalid Sandhu**, **Dr. Razia Sandhu** and **Aunty Salima Bibi** for their moral support and prayers.

A very sincere gratitude to my friends **Misbah Akhar**, **Asifa Butt**, **Shazia Ali**, **Samina Zakir**, **Erum Tariq**, **Nasreen Bhali**, **Rizwana Tehseen** and **Robina Babar** for their help and support that made the last stage of my PhD a bit easier.

I am forever indebted to my father Professor **Abdul Hamid** (late), my mother **Nasim Akhtar,** my father in law **Choudhary Nazir Ahamad** (late) and my mother in law **Khurshid Bibi** for their prayers and support without which I would have never been able to complete this task. Thanks to my brothers **Mumtaz**, **Abbas**, **Ilyas**, **Usman**, and **Suleman**, my sister **Uzma**, my sisters and brothers in law and all other family members for their encouragement.

Lastly my hubby **Tahir**, my daughter **Bazal** and son **Hashim** for their love, understanding, endless patience and encouragement when it was most required.

TABLE OF CONTENTS

CHAPTER 4: HEAT TRANSFER IN BUTTER BLOCKS

CHAPTER 5 - MODELING HEAT TRANSFER IN BUTTER

LIST OF TABLES

LIST OF FIGURES

LIST OF APPENDICES

CHAPTER 1

PROJECT OVERVIEW

1.1 Background and Problem Definition

Fonterra Co-operative Group Ltd is a leading multinational dairy company, owned by 11,600 New Zealand dairy farmers. It is the world's largest exporter of dairy products, exporting 95 percent of its production. A large percentage of its exports consist of milkfat products including butter.

Some initiatives in the NZ Dairy Industry have considered quality (e.g. flavour) or functionality (e.g. hardness) changes during the heating or cooling of bulk butter or milk fat products. The impact of these temperatures changes are of vital importance to day to day operations with regard to butter manufacture and shipping. Bulk butter is generally stored and transported at chilled or frozen temperatures. Frozen storage helps to maximise butter keeping quality due to minimisation of oxidation and microbial spoilage reactions and also increases product rigidity and so avoids pallet instability. In some cases, in order to meet customer requirements, the product is then later raised from frozen to chilled temperatures prior to delivery. Due to manufacturing and handling considerations, a large amount of the heating and cooling of the butter is frequently done on whole pallets of product.

Pallets of butter generally consist of blocks of product (25 kg) wrapped in a polymer liner and placed in corrugated cardboard cartons. Many of these cartons (48 or 56) are then stacked on a pallet. As a result the bulk system contains product, packaging material and air entrapped between the packaging and the butter and between adjacent cartons.

To optimize the temperature conditioning of butter it is important to understand the rate of heat transfer and the temperature distribution throughout the product. This information can then be linked to the functionality of the product and the rates of potential quality related changes that may occur. Specific examples include;

- Dry shipment is the practice which involves shipping the frozen butter in un-refrigerated, insulated containers to export destinations in order to reduce energy and shipping costs. The

warming of palletised, block-stacked butter must be understood to determine the technical feasibility of this practice. The potential quality related problems linked to this (keeping quality and slumping (collapse of pallet due to reduced stability)) need to be balanced against reduced costs of shipment.

- Cartonless butter production depends on assuming sufficient solidification of the milkfat in each block to provide pallet stability. This could be optimised by modeling the heat transfer in individual blocks of butter. This would allow the extent of case hardening (solidification of fat) required in cartonless bulk block butter manufacture to be assessed so that the block can maintain its shape during later pallet based, more complete freezing.
- A modeling tool giving temperature as function of time and position would be useful for giving information regarding thawing/tempering requirements (time, temperature, space allocation) for new customers or customers changing product size/format or allow existing customers and Fonterra to optimise their operations.
- Knowledge of freezing times of the product can help in the optimisation of cool-store management and refrigeration heat loads.
- If the thermal history of the product with respect to its position in the stack is known then the product variability due to temperature related quality deterioration can be minimized.
- A good knowledge of freezing and thawing times of the product can also help in optimising the packaging geometry and strength.

Each of these situations is based upon the same underlying principle: three-dimensional heat transfer with phase change (melting or crystallization of both water and milkfat). The functionality of the product is dependent on the temperature distribution throughout the product and the thermal history it has experienced because the rates of quality changes are dependent on the local temperature within the product.

1.2 Project Objectives

The overall objective was to provide a methodology to the dairy industry to allow prediction of butter thawing and freezing to be made in different situations.

In order to achieve this goal it was necessary to;

- Provide thermophysical property data for a range of butter types over the temperature range used in commercial practice.

- Develop and experimentally validate mathematical models for single homogenous product items that can predict the time temperature relationship as a function of position in butter undergoing freezing and thawing
- Extend the methodologies to allow prediction in multiple product stacks in industrially relevant scenarios.

CHAPTER 2

LITERATURE REVIEW

2.1 Introduction

When modeling the freezing and thawing behavior of butter it is important to understand those properties of butter; which change with temperature or time. It is important to know about the structure and composition of butter, how these are affected by the manufacturing process, how they affect thermal properties of the final product, how the composition of the milkfat changes with season, and how it affects the thermal properties. Approaches that might be appropriate to model the freezing and thawing behavior of butter and which methods are best to solve the heat transfer model also needed to be identified.

2.2 Butter Composition and Structure.

Butter is a water-in-oil emulsion with a continuous phase of both solid (crystalline) fat and liquid fat with aqueous droplets dispersed within it (Alfa Laval, 1980; Boston *et al.*, 2001; Frede, 2002). The size and composition of the water droplets may depend upon the manufacturing process. Most of the physical properties of the butter are governed by the properties of the fat phase but some are also influenced by the moisture dispersion (Boston *et al.*, 2001). In order to model freezing in butter it is important to understand the crystallization behavior of the fat phase as well as the crystallization of the aqueous phase. Because the aqueous phase is an water-in-oil emulsion, the freezing behavior of the droplets is likely to be different from other food products for which water exists as a continuous phase. Similarly, when considering thawing behavior it is important to look at the melting behavior of the milkfat because the melting points of the milkfat triglycerides vary from -40°C to +38°C (Boston *et al.*, 2001). The composition of triglycerides within the butter varies with time of season, making it necessary to characterize the thermophysical properties and the way they change due to storage time, temperature and season.

Standards concerning butter composition are similar in most of countries (Frede, 2002). The principal constituents of a normal butter are fat (80 - 82%), water (15.6 - 17.6%), salt (0 - 3%) as well as lactose, protein, calcium and phosphorous (which total to about 1.2%). Butter also contains

the fat-soluble vitamins A, D and E (Alfa Laval, 1980). Typically New Zealand butter contains no less than 80% fat and no more than 16% moisture (Boston *et al.*, 2001).

The current model of butter structure is a three dimensional network of fat crystals in which there is entrained liquid fat and aqueous droplets (Alfa Laval, 1980; Boston *et al.*, 2001). The fat phase consists of a solid crystalline continuous phase, liquid fat, partially crystalline fat globules and semi- continuous fat crystals. The aqueous phase consists of microscopic droplets that contain salt and milk solids - not - fat (MSNF), (Alfa Laval, 1980; Boston *et al.*, 2001; Frede, 2002). A diagram of this model of butter structure is shown in Figure 2.1.

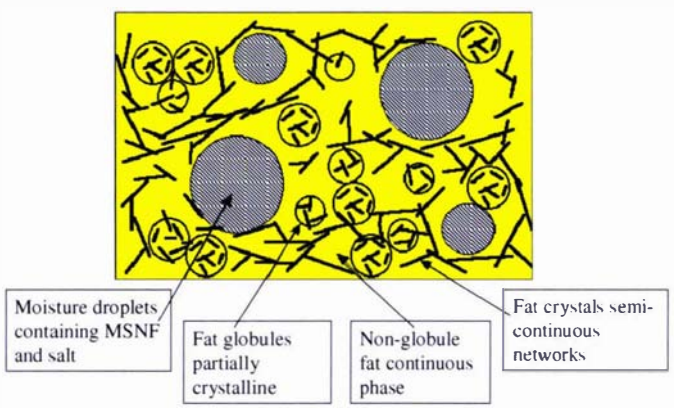

Figure 2.1: Structure of butter (adapted from http://www.foodsci.uoguelph.ca/dairyedu/butter.html)

2.3 Milkfat Composition

Milkfat can be defined as the mixture of lipids and other lipid soluble compounds that are present in the fat or oil phase of milk and cream (Boston *et al.*, 2001). The lipids in butter consist mainly of triglycerides (roughly estimated to be 98% w/w), the rest consists of diglycerides (≈ 0.3%), monoglycerides (traces), phospholipids (≈ 0.3%), sterols (≈ 0.3%), free fatty acids and traces of waxes, squalenes and carotenoids (Boston *et al.*, 2001; Precht, 1988). The composition of milkfat changes with season and this is caused by several factors. Nutritional factors associated with changing availability and quality of pasture through the year, physiological changes associated with the stage of lactation of the cows and pathological factors associated with a changing incidence of mastitis have been identified as playing a significant role (O'Keeffe *et al.*, 1982; Lucey *et al.*, 1992; Kefford *et al.*, 1992; Auldist *et al.*, 1995).

The fatty acids account for approximately 90% of the weight of the triglyceride molecules. Accordingly the fatty acids have a considerable influence on the properties of the triglycerides and thus on the milkfat (Boston *et al.*, 2001; Precht 1988). The factor of importance to this study is the influence of fatty acid composition on the melting points of triglycerides. The melting points of triglycerides increase as the relative molar mass of their fatty acids increase and as the degree of unsaturation of the fatty acids decreases. Table 2.1 shows the fatty acid composition of milkfat triglycerides for spring and summer milkfat.

Table 2.1: Fatty acid composition of spring and summer milkfat (Boston et al. 2001)

Chain length	**Fatty Acid**	**Melting point**	**weight % of total fatty acids**	
		(°C)	**Spring Milkfat**	**Summer Milkfat**
Short chain	4:0 Butyric	-8	4.4	3.9
	6:0 Caproic	-4	2.7	2.4
Medium chain	8:0 Caprylic	17	1.6	1.5
	10:0 Capric	32	3.8	3.2
	12:0 Lauric	44	3.8	3.6
Long Chain	14:0 Myristic	54	10.5	11.5
	16:0 Palmitic	63	24.0	30.0
	18:0 Stearic	70	14.0	11.0
Unsaturated	18:1 Oleic	16	26.1	19.0
	18:2 Linoleic	-5	1.5	1.4
	18:3Linolenic	-10	1.1	0.9

Table 2.1 shows the large melting temperature range of milkfat triglycerides and as a result the bulk milkfat. Spring milkfat has more low melting triglycerides so more melting occurs at low temperatures whereas summer milkfat has more high melting triglycerides and a higher melting point, (melt below 10°C: Spring 9.7% and Summer 8.6%, melt above 20°C: Spring 56.1% and Summer 59.3%). Moreover spring milkfat has higher amounts of Oleic fatty acid as compared with summer milkfat with a melting point of 16°C as shown in Table 2.1. It is expected that this seasonal difference in triglyceride fatty acid composition will result in differences in melting enthalpy as a function of temperature, which will be important in successfully modeling butter freezing and chilling.

2.4 Crystallization of Fat

The melting point of the triglycerides is not only affected by the fatty acid composition as stated above but also due to the subtle changes in the way in which the individual triglycerides pack together to form a crystal (Boston *et al.*, 2001). Clarkson & Malkin (1934) demonstrated that multiple melting points of each triglyceride can occur due to polymorphism. Different polymorphism include the α- form, a form that crystallises from the melt and is the lowest melting polymorph, β' - form is an intermediate melting polymorph and the β- form is the highest melting polymorph (Hagemann, 1988). Numerous reports have been published on the polymorphism of the milkfat but very little is known about the areas where the polymorphic forms are found in butter. This is due to the fact that compared to other naturally occurring fats, milkfat has the most heterogeneous triglyceride composition (Precht, 1988). This wide range of triglyceriods cause more than one triglycerides crystal structure depending on the arrangement of packing of the carbon chains of the fatty acids in the crystal. Boston *et al.* (2001), Precht (1988) and Mulder (1953, 1947) proposed the well-known theory of mixed crystals in the milkfat in which different kinds of molecules incorporate together to form a lattice of a single crystal. It has been assumed that mixed crystals are also found in the fat globules within butter and explain the higher proportion of solid fat in butter fat globules at low temperatures as compared to bulk fat (Mulder & Walstra, 1974). This difference could be associated with the difference in the degree to which the mixed crystals form in fat globules as compared to bulk fat (Mulder, 1953, 1947; van Bersesteyn & Walstra, 1972). Tverdokhleb & Raksti (1957) found both α and β' crystals in butter. Precht (1980) and Frede *et al.* (1978) also detected limited amounts of β and β' crystals in butter. With X-ray diffraction it has been shown that, compared with the orthorhombic β' - form, the relative proportion of the triclinic β phase increased in butter samples with increasing temperature after 12 days storage at 12°C following butter making (Frede *et al.*, 1978). β' crystals exist in the palletized butter after storage at about 12°C after manufacture and setting of butter.

It is possible for the milkfat triglycerides to crystallize in any of these polymorphic forms, depending on the speed of crystallization, which itself depends on the driving force produced by temperature. When milkfat is crystallized at a temperature well below its melting point it crystallizes rapidly and less stable polymorphs, like α, are formed (Boston *et al.*, 2001). Rapid crystallization also plays a role in the inclusion of lower temperature melting triglycerides to form mixed crystals which have lower melting point (Boston *et al.*, 2001), and conversely when the crystallization temperature is close to the melting point the crystals formed will contain a narrow range of triglycerides and thus, have higher melting points and more stable polymorphs.

Milkfat triglycerides can supercool and exist as a liquid well below their melting points. When nucleation occurs in the supercooled milkfat, initial crystal growth rates can be very high and lead to mixed crystals and higher solid fat contents (Boston *et al.*, 2001).

From the above discussion it is quite possible that while freezing the butter, milkfat as well as water may also supercool which will affect the solid fat contents of the butter and hence the enthalpy of butter The enthalpy of cooling of butter could be different from the enthalpy of heating of butter depending on the thermal history of the product. The freezing may affect the proportion of α and β' crystals (due to crystallization and polymorphic transitions) which would affect the enthalpy of butter as the specific heat of α crystals is lower than that of β' crystals.

Figure 2.2 shows the solid fat content (SFC) of summer and spring milkfat as a function of temperature. It can be seen that in the range of 0-10°C there is a small change in the SFC as compared to the change between 10°C to 20°C. The typical range of interest for commercial thawing is from 0 – 12°C. Most of the studies done on modeling the crystallization behavior of milkfat were conducted at temperatures above 10°C. The small change in fat SFC between 0 – 10°C suggests that crystallization behavior of fats is less important then one would initially think in the temperature range of interest.

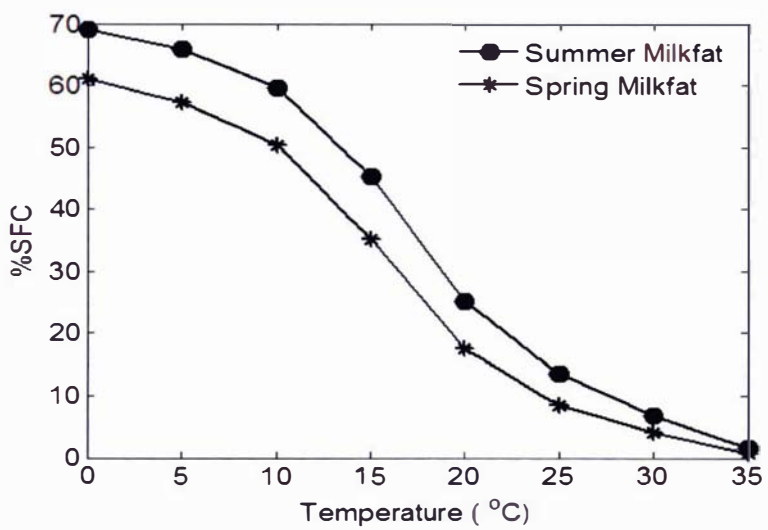

Figure 2.2: Most extreme differences between New Zealand summer and spring milkfat (MacGibbon, 1993)

2.5 Aqueous Phase of Butter

As stated previously, water in butter exists in the form of tiny spherically or ovally shaped droplets embedded in the continuous fat phase. The size of aqueous droplets typically varies from 1.3 to 7.6 μm (Lu, 1999). Various authors mention there are approximately $1 - 3\times10^{10}$ droplets per milliliter in butter (Walstra, 1974; Mulder *et al.*, 1956). Electron microscopy studies showed that the variability between the samples is not large due to the majority of the droplets being very small (Knoop & Wortmann, 1962; Wortmann *et al.*, 1965). In the water droplets, casein micelles of an average diameter of 0.1 μm can be observed (Precht, 1988). It has also been found that the small fat globules of approximately 0.7 to 0.3 μm in diameter are often embedded in the crystalline surface layer, particularly of large water droplets (Precht & Buchheim, 1980). Occasionally, very small (<< 1μm) fat aggregates occur within the aqueous phase (Precht & Buchheim, 1980).

2.6 Crystallization of Aqueous Droplets

In order to model heat transfer in butter in the freezing and thawing temperature range it is extremely important to understand the crystallization behavior of the water phase of butter. The thermal properties of liquid water are significantly different to that of ice. Therefore, the thermal properties of any materials with significant water contents will change significantly as the water freezes.

The heat capacity of the water decreases by 50% if the water freezes but on the other hand if the water is super cooled below 0°C the specific heat curve has no discontinuity (Angell, 1982). A schematic diagram of the freezing of water and a water solution droplet is given in Figure 2.3. The five stages of freezing are distinguished by numbers 1-5.

Stage (1) is the first stage of supercooling of the droplet to many degrees below its initial freezing point until the nucleation occurs. Stage (2) is the nucleation stage where there is enough supercooling for the nucleation to occur. Stage (3) is the release of latent heat due to the crystal growth from the nuclei and this stage continues until the droplet has reached an equilibrium freezing temperature. Stage (4) is the freezing stage where the growth of the solid phase depends on the rate of heat transfer and this stage continues until all the freezable water in the droplet is completely frozen. The last stage (5) is the cooling of the solid droplet to a steady state temperature near to the ambient.

A number of researchers (Butler, 2001; Erickson & Hung, 1997; Macklin & Ryan, 1968; Muhr & Blanshard, 1986) have described that the addition of solutes increases the ice nucleation temperature (stage 1), decreases the crystal growth rate during the recalescence (stage 2) which also decreases the temperature rise and thus progressively depresses the freezing point and introduces freeze concentration during the heat transfer dependent freezing stage (4).

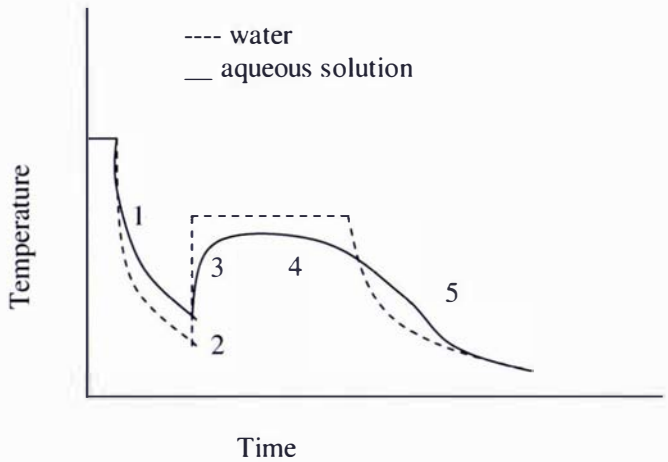

Figure 2.3: The temperature transition during the five stages of freezing for water and aqueous solution

Dumas *et al.* (1994) explained that the freezing and thawing processes for an emulsion droplet are not symmetric due to the supercooling phenomena. During crystallization the release of latent heat is nearly instantaneous as it occurs far from the thermodynamic equilibrium. During melting, the absorption of latent heat is at a fixed melting temperature and its kinetics depends on the rate of heat exchange with the surrounding medium (Dumas *et al.*, 1994).

Through statistical studies on large number of droplets, Skripov (1974) showed that the nucleation process is stochastic in nature. All the droplets do not crystallize at the same time and at the same temperature T. Therefore, for a single droplet at some temperature T lower than its initial freezing point T_{if}, the probability of crystallization $J(T)$ can be defined as a function of time.

Common nucleation theories (Turnball, 1956; Rasmussen *et al.*, 1983) give the function $J(T)$ as:

$$J(T) = a\exp\left(\frac{b}{T.(T - T_{if})^2}\right) \qquad \text{for } T < T_{if} \tag{2-1}$$

Where a ($s^{-1}m^{-3}$) and b (K^3) are constants. The coefficient 'b' represents the characteristics of the undercooled substance (molar volume of the crystal, interfacial tension between liquid and crystal) whereas 'a' depends on the volume of the crystal (Turnball, 1956; Skripov, 1974).

Michelmore and Franks (1982) suggested the use of classical nucleation theory to describe the nucleation kinetics in water-in-oil emulsions and express the nucleation rate in a simpler form as:

$$J(T) = ae^{b\tau_\phi} \tag{2-2}$$

'a' and 'b' are the same constants as in Eq (2-1) and the degree of supercooling (τ_ϕ) is given by:

$$\tau_\phi = \left(\phi^3(1-\phi)^2\right)^{-1} \quad \text{where} \quad \phi = \frac{T + 273.15}{T_{if} + 273.15} \tag{2-3}$$

The Avrami model (Avrami, 1939; 1940; 1941) is extensively used for the analysis of the crystallization kinetics at isothermal temperatures. The model considers the process of both nucleation and growth from a statistical basis (Rogowaski, 2005). The model is given by:

$$F(t) = 1 - e^{Kt^n} \tag{2-4}$$

where $F(t)$ is the fraction of the droplets that are frozen and n is known as the Avrami exponent or the reaction order parameter. The parameter K describes the combined effect of the rate of nucleation (J) and the rate of crystal growth (G) and is given by:

$$K = \frac{\pi}{3} G^3 J \rho^* \tag{2-5}$$

where ρ^* is the relative density.

These theoretical models of the crystallization behavior of water-in-oil emulsions may be suitable to describe nucleation and growth of water droplet freezing in butter.

2.7 Manufacturing Process

The manufacturing process can influence the composition and microstructure of the butter. There are two main butter making processes: Ammix, which is based on scraped surface heat exchanger technology and Fritz, which is based on the traditional cream churning process. Although the butters produced by these methods are nearly the same, there are some subtle differences related to the finer moisture distribution of Ammix butter which affects perceived colour, flavor release, and release of moisture on reworking (Philpott, 1999).

2.7.1 Fritz Buttermaking Process

A simple schematic diagram of the Fritz buttermaking process is given in Figure 2.4

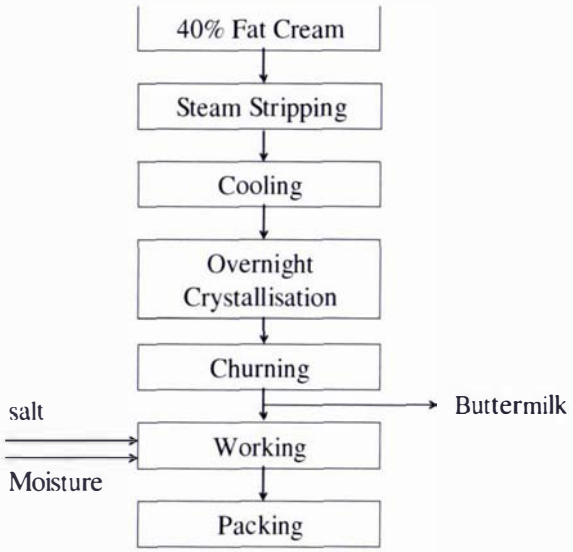

Figure 2.4: The Fritz buttermaking process (Philpott, 1999)

In the Fritz process, milk with approximately 4% fat is concentrated in a centrifugal cream separator into cream of 40% fat. The fat in the cream is contained within globules with a diameter of approximately 1 to 10μm. Cream is pasteurised and, in New Zealand, it is then steam stripped to reduce some of the flavours associated with pastoral feeding (Cant *et al.*, 1997).

After the steam stripping process, the cream is cooled and left overnight to crystallise. During churning of the crystallised cream, phase inversion occurs. The buttermilk is released and is drained

off from the butter which is worked until a stable water in oil emulsion is obtained. The release of butter milk is a concentration step to get a fat content of about 80-84% in the final product (Cant *et al.*, 1997).

In the working stage, the globules are worked into a malleable plastic mass. Excess water is also squeezed to produce a butter texture. The 80% fat within the globules is reduced to 8-30% during the working process. Salt is added at this stage if salted butter is required and the moisture content is standardised. Further working disperses the water into small droplets of less than 10μm diameter. Even moisture dispersion is important for the product quality and prolonged shelf life. The final working process is done under vacuum which removes air and gives a smooth evenly textured butter (Cant *et al*, 1997).

2.7.2 Ammix Buttermaking Process

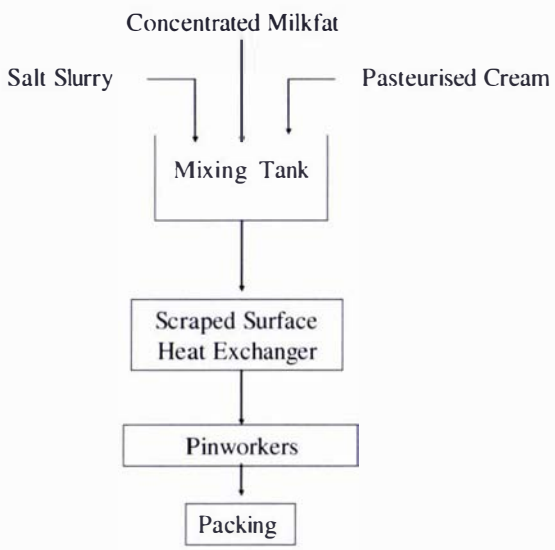

Figure 2.5: Ammix buttermaking process (Philpott, 1999)Figure 2.5: Ammix buttermaking process (Philpott, 1999) Figure 2.5: Ammix buttermaking process

The Ammix style buttermaking system was originally developed in 1950's (Philpott, 1999). In this process the gross composition of the butter including freshly made concentrated milkfat, pasteurised cream and salt slurry is blended together in the mixing tank as shown in Figure 2.5. This mixture is then pumped through a series of scraped surface heat exchangers. These are tubular in construction and use liquid refrigerant as a cooling medium. High rates of heat transfer are possible within the

tubular construction of the heat exchanger which gives small fat crystals by rapid supercooling and nucleation. The scrapping action of the blades provides high shear forces which favour the dispersion of the aqueous phase into small droplets of 10μm or less (Mercer, 1988; Early, 1992) and facilitates the high heat transfer rates by continuously wiping the heat transfer surface.

Most of the crystallisation and the dispersion processes happen in the pinworker units. These units are tubular in construction with some pins fixed to the tube and some mounted on the central rotating shaft. The α polymorph fat crystals can rearrange to form β' crystals in these units. This process releases the latent heat which causes further melting and recrystallisation.

2.7.3 Differences Due to Manufacturing Processes

From the above overview on both the butter making processes it can be seen that there are two steps which could affect the thermal properties of the final product related to this research.

One important difference is the addition of salt slurry at two different steps of manufacturing. In the Ammix butter making process, the salt slurry is added at the beginning of the butter making process which causes a more even concentration of salt and other solid – not – fat compounds. In contrast for butter manufactured by the Fritz process salt slurry is added after churning and water droplets from different sources (some from the undrained butter milk and other from the added moisture and salt slurry) are present in the butter, which may have different salt concentrations and result in different freezing points. This has the potential to directly affect the enthalpy of the butter during thawing and freezing.

2.8 Thermophysical Properties

The modeling of heat transfer in butter requires knowledge of its thermal properties. The key properties of interest are initial freezing point, density, enthalpy and thermal conductivity. The thermophysical properties of butter are needed for different butter compositions and seasonality, over the temperature range of interest (-20°C to +20°C).

During storage at low temperature, butter undergoes the freezing of fats and water which requires the removal of latent heat. The specific heat capacity and thermal conductivity are dependent on the ice fraction at temperatures below the initial freezing point. The thermal properties of the liquid water are considerably different from those of ice and, therefore, the thermal properties of any

material with significant amount of water will change a lot as the water freezes. A schematic diagram of the change in the ice fraction as a function of temperature is given in Figure 2.6.

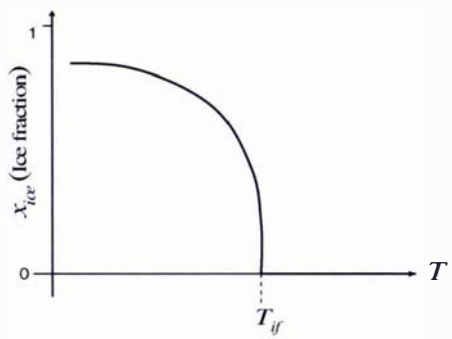

Figure 2.6: Schematic diagram of temperature-ice fraction relationship

2.8.1 Initial Freezing Point

It is very important to be able to estimate the initial freezing point of the water phase in butter as at this point the water latent heat release or absorption begins to limit temperature change within the material undergoing thawing or freezing. The initial freezing point depends on the amount of solutes in the aqueous phase of butter. When the water freezes out of the aqueous phase the other solutes become freeze concentrated resulting in the increased depression of the freezing point as freezing proceeds.

Knowledge of the initial freezing point also potentially allows the estimation of the ice contents of a frozen product at any temperature (Heldman, 1974) and thus other thermal properties like thermal conductivity, enthalpy, density and specific heat, which depend highly on the ice content, can also be determined.

Pham *et al.* (1994) and Lindsay & Lovatt (1994) estimated T_{if} from the intersection of the enthalpy curves below and above the initial freezing point and reported the initial freezing points of butter of varying composition (Table 2.2).

Table 2.2: Composition of butter used by Pham et al. (1994) and Lindsay & Lovatt (1994)

Butter type	Composition (%)						
	Water	Protein	Fat	Ash	Salt	T_{if}	Reference
Salted	10.7	0.4	87.4	0.7	0.7	-4.81	Pham(1994)
Salted	16.7	0.6	80.6	1.7	1.6	-6.25	Lindsay & Lovatt (1994)
Unsalted	15.6	0.8	82.7	0.1	-	-1.94	Pham(1994)
Unsalted	20.4	0.7	78.3	0.1	0.04	-1.12	Lindsay & Lovatt (1994)

Wolfschoon – Pombo & Lima (1983) and Wolfschoon – Pombo (1991) also measured the initial freezing point of salted and unsalted butter using cryoscopy on diluted butter serums (Table 2.3). This method would average out any differences in droplets compositions made during manufacture. According to their procedure 2 ml of the serum phase of the butter were diluted with 10 ml of water and then the sample was mixed thoroughly. The cryoscopy measurements were conducted on 2.5 ml of mixed solution. All the procedure was carried out for butter serums samples before and after the addition of salt to determine the initial freezing points of the samples. The freezing point was then corrected for the dilution of the aqueous extracts.

Table 2.3: Freezing point of salted and unsalted butters

Wolfschoon – Pombo & Lima (1983) and Wolfschoon – Pombo (1991)

Unsalted Butter		Salted Butter			
Water %	Freezing point (°C)	Water%	Salt %	% in Water	Freezing Point (°C)
14.36	-0.611	13.3	0.58	4.36	-3.285
14.56	-0.470	23.6	1.52	6.44	-4.190
14.85	-1.581	17.5	1.72	9.83	-5.975
15.49	-0.656	15.3	1.60	10.45	-6.660
15.75	-0.760	15.5	1.95	12.58	-8.320
15.8	-0.455			salt% measured by	
15.96	-0.581			Mohr's method	

The measured initial freezing point of the salted butter from this source seems to agree with the estimates of Pham *et al.* (1994) and Lindsay & Lovatt (1994) except for the unsalted butter for which the values estimated by Pham *et al.* (1994) and Lindsay & Lovatt (1994) are much lower. It is possible that the amount of solid - not - fat in the unsalted butter used by Pham *et al.*(1994) and Lindsay & Lovatt (1993) was higher than that used by Wolfschoon – Pombo & Lima (1983) and Wolfschoon – Pombo (1991).

Fats do not play a role in water freezing point depression. Tables 2.2 and 2.3 show that the initial freezing point of the butter depends on the concentration of the solutes in the aqueous phase of the butter. At higher concentrations of solutes, more freezing point depression is observed. Thus, the freezing behaviour of the butter depends on both the water fraction in the butter and the solutes concentration in the water. It could also vary with the manufacturing process as mentioned earlier due to addition of water and salt at different stages of the manufacturing process. Because of the variability in the reported data and the sensitivity of the initial freezing point to the composition, a better means of prediction of the initial freezing point of all the butters that are under consideration is needed. It would also be advantageous to develop methods to predict initial freezing point from butter water phase composition along with the measurement methods.

2.8.2 Density

Density data for butter is sparsely available in the literature. A list of the density values reported by different authors is given in Table 2.5. Middleton (1996) reported the density of the butter to be 923 kg m^{-3} on filling into a 25 kg standard carton (butter is normally manufactured at 15°C). Butter density was reported as function of air content and temperature above 0°C by Chubik and Maslov (1965) and Ginzburg *et al.* (1985). It is clear from their results that the density of butter above 0°C is weakly affected by temperature. The density of butter changes from 945 kg m^{-3} to 895 kg m^{-3} when the amount air in the butter increases from 0% to 5%. A 5% increase in air content results in about the same percentage decrease in the density value. There is no data available in the literature for the density of butter below 0°C. Middleton (1996) reported that butter shrinks by 3% when cooled from ambient to -15°C.

The literature density values are quite variable (Figure 2.7 and Table 2.4). Butter manufactured by the continuous churning processing has lower density as compared with the butter made by the batch churning processing. The main reason is the amount of air in the butter. The continuous butter making process includes a vacuum step to remove air, whereas the batch churn butter making process includes no such step and thus butter contains some air in it. If the data given in Table 2.4 is compared, inclusion of about 2.7% percent air in the continuous churning butter gives the same values as those reported value for the batch processed butter.

Table 2.4: Density of butter as a function of temperature and air contents

No	Conditions	Density (kg m^{-3})	Reference
		Formulae	
1	T= 0-5°C (Continuous churn production)	941.7-2.0 T	Ginzburg(1985)
2	T= 5-10°C (Continuous churn production)	951.4-4.0 T	Ginzburg(1985)
3	T = 5-10°C (Batch churn production)	979.4-4.0 T	Ginzburg (1985)
4	T= 0-90°C	949.8-0.7 T	Ginzburg (1985)
5	T= 2-20°C	950.5-0.5 T	Chubik and Maslov (1965)
6	T= 20-35°C	958-0.73 T	Chubik and Maslov (1965)
7	X_{air} = 0-5%	945-10 X_{air}	Ginzburg(1985)
8	X_{air} = 1-10%	950-9.5 X_{air}	Ginzburg(1985)
		Constant value or ranges	
9	T=15°C	923	Middleton (1996)
10	None given	950	Pohlmann (1939)
11	None given	865-870	Winton (1945)

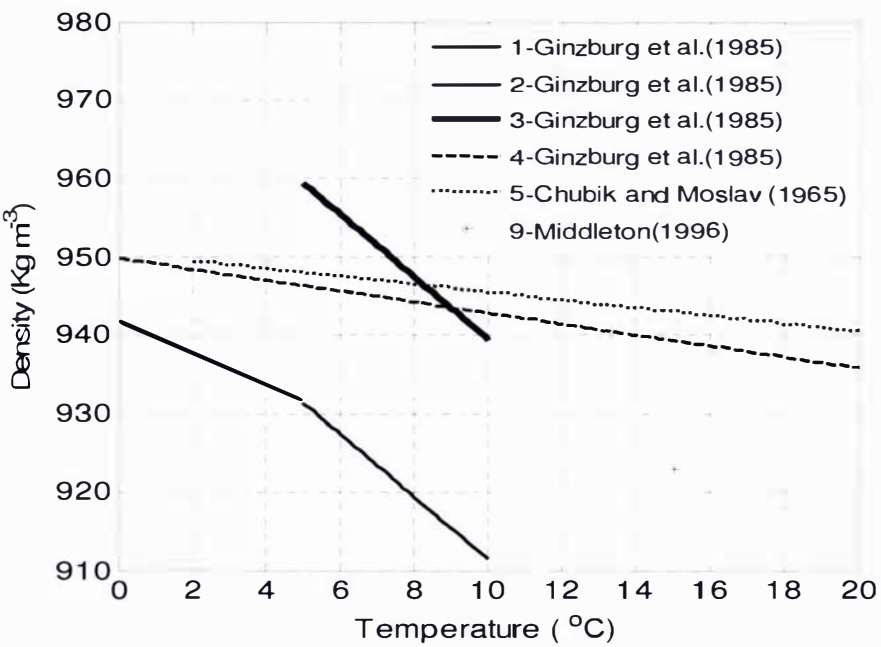

Figure 2.7: Density of butter as a function of temperature as reported in Table 2.5 (the legend corresponds to the numbering in Table 2.5)

As a result of the variability in literature data it is necessary either to measure the density of different kinds of butter or predict it from compositional data by using the weighted sum of the densities of different components of the butter (Rahman, 1995):

$$\frac{1}{\rho} = \sum_{i=1}^{n} \frac{X_i}{\rho_i} \qquad (2\text{-}6)$$

where

ρ = bulk density (kg m^{-3})

ρ_i = density of the i^{th} component (kg m^{-3})

X_i = mass fraction of the i^{th} component.

One of the important components is the fraction of the water frozen as density changes from the density of water which is about 1000 kg m^{-3} to the density of ice which is about 920 kg.m^{-3}. On the other hand, as the butter freezes, it shrinks by 3% which means the density of butter becomes higher due to the change in milkfat density. It is therefore important to look at both these effects (freezing of water and shrinkage of the milkfat) over the whole range of temperature and to consider the sensitivity of the heat transfer predictions to density differences if a constant average value is used within that range. If this error is not significant then use of a constant value of density will greatly simplify the problem.

2.8.3 Thermal Conductivity

The thermal conductivity of butter changes as the butter undergoes freezing mainly due to ice crystallization. At the beginning of the freezing process the fraction of the water that is frozen is zero and as the fraction frozen increases the thermal conductivity of the butter increases due to the large difference in thermal conductivity of ice and water. In many food products the thermal conductivity can be simply related to the composition of the food, ice fraction and the temperature (Pham & Willix, 1989). Willix *et al.* (1998) measured the thermal conductivity of several foods including salted and unsalted butter from the temperature range -40°C to +20°C using a guarded hot plate (Table 2.5).

Table 2.5: Composition of butter and fitted parameters for the thermal conductivity model

Butter type	Composition %					Fitted Parameters				
	Fat	Ash	water	Salt	Protein	T_{if} (°C)	λ_f ($Wm^{-1}K^{-1}$)	$\underline{b}$ ($Wm^{-1}K^{-2}$)	$\underline{c}$ (Wm^{-1})	$\underline{d}$ ($Wm^{-1}K^{-2}$)
Salted	82.4	1.45	14.6	1.32	0.5	-4.81	0.195	1.42×10^{-3}	0.181	9.74×10^{-4}
Unsalted	82.7	0.1	15.2	-	0.7	-1.94	0.178	1.41×10^{-3}	0.092	1.25×10^{-3}

Pham & Willix (1989) fitted equations to the measured data for below and above the initial freezing point respectively:

$$\lambda = \lambda_f + \underline{b}(T - T_{if}) + \underline{c}\left(\frac{1}{T} - \frac{1}{T_{if}}\right) \qquad \text{for} \quad T < T_{if} \tag{2-7}$$

$$\lambda = \lambda_f + \underline{d}(T - T_{if}) \qquad \text{for} \quad T \geq T_{if} \tag{2-8}$$

The fitted constants b, c and d are given in Table 2.5.

Conochie (1964) reported the thermal conductivity of vacuum processed salted butter to be constant at 0.19 W m^{-1} $°C^{-1}$ across the temperature range of -3°C to 12°C although no freezing is likely to occur over this range. Olenew (1959) reported thermal conductivity data over a wide range of temperature and butter types as shown in Table 2.6:

Table 2.6: Thermal conductivity of butter (Olenew, 1959)

	Thermal Conductivity ($Wm^{-1}K^{-1}$)							
Butter Type	17°C	5°C	-5°C	-10°C	-14°C	-18°C	-25°C	-35°C
Batch Churned Unsalted	0.230	0.202	0.279	0.311	0.275	0.275	0.288	0.329
Batch Churned Salted	0.206	0.195	0.268	0.292	0.287	0.284	0.272	0.320
Continuous Churned Salted	0.230	0.195	0.246	0.251	0.232	0.244	0.239	0.273

The data given by Chubik & Maslov (1965) was fitted in the temperature range of -35°C to -5°C by:

$$\lambda = 0.256 - 7.84 \times 10^{-4} T \tag{2-9}$$

Ginzburg *et al.* (1975, 1985) gave the following relationship for the temperature range 5°C to 19°C:

$$\lambda = 0.183 + 0.0025T \tag{2-10}$$

Equation (2-10) accurately represents the data from different independent sources (Houška, 1994). Rahman (1995) reported the thermal conductivity of a butter containing 16.5% water and 80.6% fat at 0°C to be 0.20 $Wm^{-1}K^{-1}$ and at 20°C to be 0. 21 W $m^{-1}K^{-1}$.

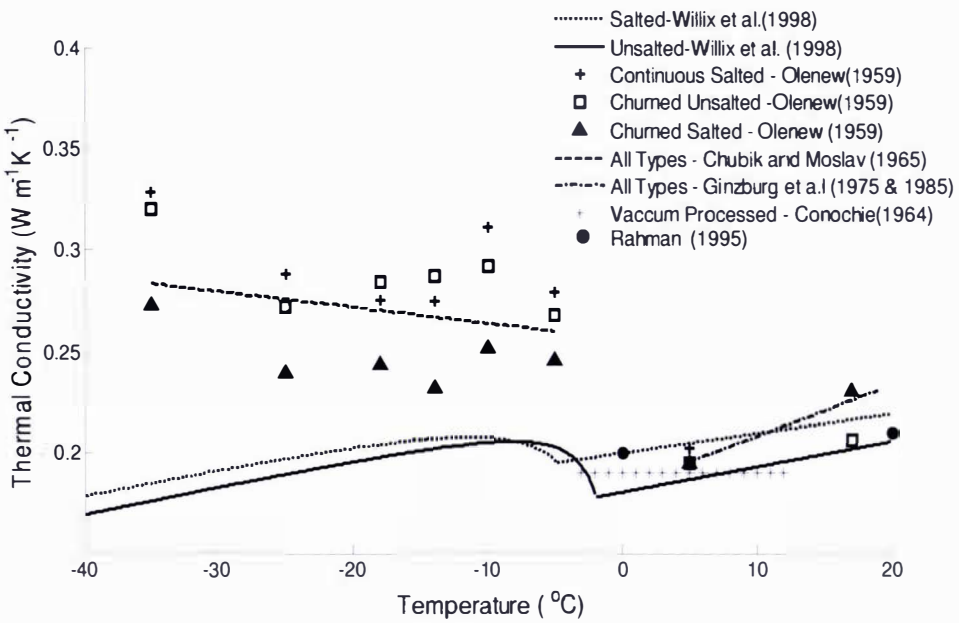

Figure 2.8: Thermal conductivity of butter as function of temperature

Figure 2.8 represents the data from all the sources. The data agree well for the temperatures above the initial freezing point (-2°C or -5°C). The data measured by Willix *et al.* (1998) is different to the other data for the temperatures below the initial freezing point. Their data shows little change in the thermal conductivity above and below the freezing point which is not expected as butter is made of at least 14.6% water and as the water freezes into ice the thermal conductivity should increase as a function of fraction of the water frozen. It is possible that only a small fraction of the water droplets in the butter underwent freezing during the time frame of the experiment and that some of the freezable water remained supercooled during the measurements.

Rahman (1995) reported that various authors claim that the most important factor in the determination of the thermal conductivity is the water content. The other key factor in the determination of the thermal conductivity of the butter is the air content of the butter. It can be seen that batch churned butter has lower thermal conductivity as compared to butter produced by continuous churning processes. This trend is consistent with the reduced density of butter made by the continuous churning process. The butter made at commercial scale is now made solely using the continuous processes and therefore the data for batch churn butter can be disregarded. Salted and unsalted butter made by the same process also have different thermal conductivity. Unsalted butter generally has higher thermal conductivity as compared to salted butter below the initial

freezing point. This is expected as at any temperature below the initial freezing point, a greater fraction of the water in the unsalted butter sample would be frozen.

It can be concluded that the thermal conductivity of butter varies significantly due to the differences in water contents, solute concentration and air contents. Because the butter type and the manufacturing process influence these factors it is desirable to predict it using the theoretical models that exist in the literature or to measure it over the whole range of interest. Prediction of how the thermal conductivity changes with respect to temperature below the initial freezing point is also necessary. If the change within the range is not very high, a constant value could be used for above and below the initial freezing point.

2.8.4 Specific Heat Capacity and Enthalpy

The specific heat capacity observed during freezing includes both sensible heat and latent heat effects and is known as apparent heat capacity. The specific heat capacity of butter is a complex function of temperature due to the crystalline form of triglycerides in the fat (Houška *et al.*, 1994). The specific heat capacity of butter undergoing freezing is affected by the latent heat as these triglycerides undergo phase change. The specific heat capacity of butter for freezing and thawing could be different due to supercooling of fat and water in the butter during rapid cooling.

Table 2.7: Specific heat capacity of butter for different compositions (Houska et al., 1994 (fitted to data from Olenew, 1958))

	Composition	Specific Heat Capacity (kJ $kg^{-1}{}^{o}C^{-1}$)
1	Unsalted Butter $X_w = 15.9\%, X_p = 0.338\%$	$c_p = 2.5 + 2.93\times10^{-2}T + 41.218/\left(1+18.75(T+1.37)^2\right) + 2.13/\left(1+2.88\times10^{-2}(T-15.25)^2\right)$
2	Continuous Production $X_w = 16\%, X_p = 0.515\%$	$c_p = 2 + 1.72\times10^{-2}T + 6.03/\left(1+0.24(T+2.33)^2\right) + 2.85/\left(1+2.57\times10^{-2}(T-16.81)^2\right)$
3	Salted Butter $X_w = 19.2\%, X_p = 0.783\%$	$c_p = 1.81 + 1.06\times10^{-2}T + 6.80/\left(1+0.144(T+2.7)^2\right) + 3.17/\left(1+2.73\times10^{-2}(T-16.5)^2\right)$
4	Salted Butter $X_w = 15.4\%, X_s = 0.815\%, X_p = 0.342\%$	$c_p = 1.61 + 6.11\times10^{-2}T + 6.75/\left(1+0.1(T+6.32)^2\right) + 3.42/\left(1+2.69\times10^{-2}(T-17)^2\right)$

Olenew (1958) measured the specific heat capacity of butter in the range -60 to -25°C. The empirical relations fitted to Olenew's data are given in Table 2.7. The only other data available for specific heat capacity of butter was measured by McDowell (1953) and is given in Table 2.8. This data is in general agreement with the data measured by Olenew (1958).

Table 2.8: Average specific heat capacity of unsalted butter as a function of temperature (McDowell, 1953)

Temperature Range	Average Specific Heat capacity ($kJkg^{-1}°C^{-1}$)
25 to 20°C	4.10
20 to 15°C	5.02
15 to 10°C	4.27
10 to 5°C	3.68
5 to 0°C	3.18
0°C	52.76
0 to -5°C	2.43
-5 to -10°C	2.18

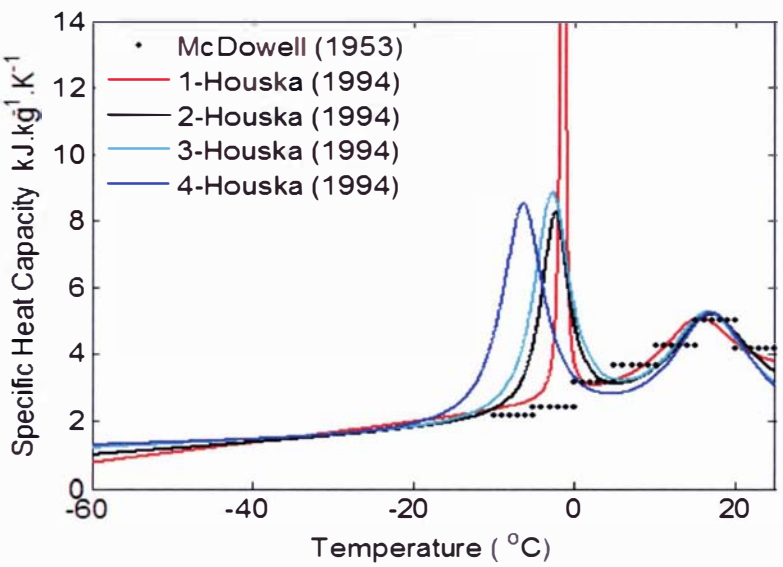

Figure 2.9: Specific heat capacity of butter as a function of temperature

Figure 2.9 shows that all the data agrees well above the initial freezing point and there is little difference in the specific heat capacity value of different butters in this range. The differences

between the butters are large in the phase change region. The temperature for the peak specific heat capacity decreases with increasing salt concentration due to the initial freezing temperature of water in butter being depressed. Rahman (1995) reported the specific heat capacity of butter with water contents from 14% to 15.5% as being 2.05 to 2.134 kJ $kg^{-1}K^{-1}$.

The area under the curves given in Figure 2.9 gives the enthalpy of the butter required for the change in temperature from -60°C to 20°C. The enthalpy of butter as a function of temperature is important for modelling purposes. If the specific heat capacity is used as a function of temperature then, where very large changes occur over narrow temperature ranges, specific heat capacity can easily be over or underestimated during numerical simulations, especially in the phase change region. The enthalpy temperature curve is smoother and makes numerical solution of heat transfer models more stable.

Table 2.9 summarizes the integrated form of the empirical equations for specific heat capacity given in Table 2.9 using -60°C as the reference temperature for $H = 0$ (Houška *et al.* 1994)

Table 2.9: Enthalpy of butter for different compositions Houska et al. (1994)

No	Composition	Enthalpy (H) kJ kg^{-1}
1	Unsalted Butter $X_w = 15.9\%, X_p = 0.338\%$ $T_{ref} = -40°C$	$H = 2.5T + 0.01465T^2 + 9.519\tan^{-1}(4.33(T+1.37))$ $+12.55\tan^{-1}(0.17(T-15.25)) + 130.9 - 21.0622$
2	Continuous Production $X_w = 16\%, X_p = 0.515\%$ $T_{ref} = -40°C$	$H = 2.0T + 0.0086T^2 + 12.31\tan^{-1}(0.49(T+2.33))$ $+17.78\tan^{-1}(0.16(T-16.81)) + 134.4 - 23.5092$
3	Salted Butter $X_w = 19.2\%, X_p = 0.783\%$ $T_{ref} = -40°C$	$H = 1.81T + 0.0053T^2 + 17.92\tan^{-1}(0.38(T+2.7))$ $+19.9\tan^{-1}(0.165(T-16.5)) + 145.5 - 25.5612$
4	Salted Butter $X_w = 15.4\%, X_s = 0.815\%$ $X_p = 0.342\%, T_{ref} = -40°C$	$H = 1.61T + 0.008306T^2 + 21.35\tan^{-1}(0.316(T+6.32))$ $+20.85\tan^{-1}(0.164(T-17)) + 149 - 35.8241$

Lindsay & Lovatt (1994) and Pham *et al.* (1994) measured the enthalpy of butter using an adiabatic calorimeter for the composition of butter given in Table 2.10. The parameters were fitted to the following form of equation proposed by Schwartzberg's (1976) in the range -40°C to +40°C.

$$H(\text{kJ kg}^{-1}) = A + c_f T + B/T \qquad T < T_{if}\,(^{o}C) \qquad (2\text{-}11)$$

$$H(\text{kJ kg}^{-1}) = H_o + c_u T \qquad T \geq T_{if}\,(^{o}C) \qquad (2\text{-}12)$$

where

A = Constant (kJ kg^{-1})

B = Constant (kJ kg^{-1})

c_u = Specific heat capacity of unfrozen butter (kJ kg $^{-1}$K^{-1})

c_f = Specific heat capacity of frozen butter (kJ kg $^{-1}$K^{-1})

H_o= Enthalpy at 0°C (kJ kg $^{-1}$K^{-1})

The fitted parameters are given in Table 2.10

Table 2.10: Parameters fitted to enthalpy equations (2-11) & (2-12) for different compositions of butter

		Composition (%)					Parameters					
No	Butter type	Fat	Ash	water	Salt	Protein	A	c_f	B	c_u	H_o	T_{if}
1	Salted (a)	80.6	1.6	16.7	1.6	0.6	54.7	1.67	-457	3.94	142	-6.25
2	Salted (b)	87.4	0.7	10.7	0.7	0.4	59	1.68	-320	3.97	137	-4.81
3	Unsalted (a)	78.3	0.1	20.4	0.04	0.7	80.4	2.14	-66	4.21	142	-1.12
4	Unsalted(b)	82.7	0.1	15.6	-	0.8	76.0	2.00	-146	4.44	156	-1.94

(a) Lindsay & Lovatt, (1994), (b) Pham *et al.*(1994)

All the enthalpy data is plotted in Figure 2.10 as function of temperature with a datum temperature of -40°C ($H = 0$).

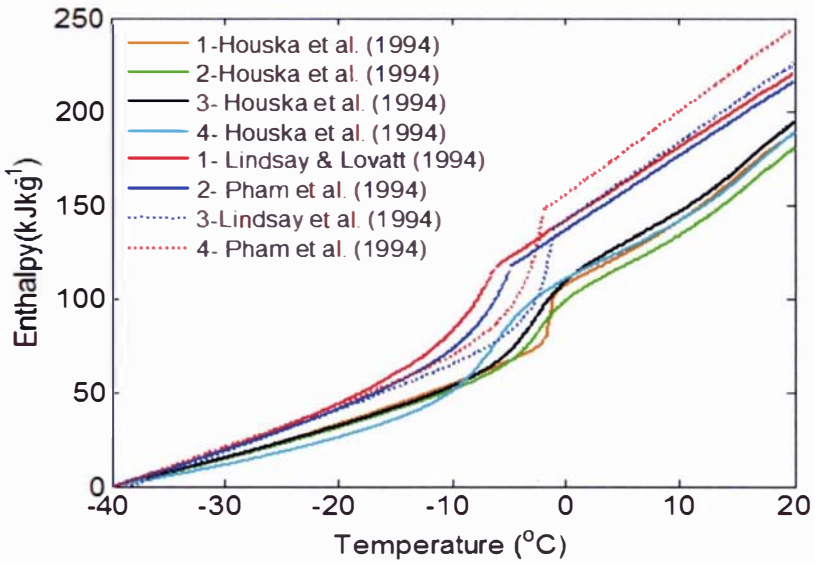

Figure 2.10: Enthalpy of butter a function of temperature

Both sets of data (1-4 in Table 2.9 and 1-4 in Table 2.10) are consistent in the freezing range of below -20°C. In the range above -20°C enthalpy values and the initial freezing point of butter start to differ. There are two reasons for this variation:

- The phase change of ice depends on the concentration of solutes in the aqueous phase of butter. Salted butter has lower freezing point and unsalted butter has higher freezing point and this can be observed in both sets of data. The amount of protein also has some effect in the phase change region. Miles *et al.* (1997) showed that amount of bound water in foods is a function of amount of protein and carbohydrates existing in the food. Bound water directly affects amount of the latent heat as this water cannot under go freezing. A higher protein percentage means higher fraction of bound water and therefore lower total enthalpy change. In addition some of differences could also be due to the difference in the moisture contents of each of the butters.
- The second reason for the variation in the enthalpy in the phase change region is the melting effects of the fat. Approximately 25% of the milkfat triglycerides melt below 5°C (Boston *et al.*, 2001). According to Houška *et al.* (1994) in the temperature range -50°C to 40°C the specific heat capacity of the milkfat is strongly dependent on the composition of milkfat. The composition of milkfat changes with season and lactation as mentioned earlier.

There are also differences above the initial freezing point. Although the data reported in equation (2-12) was fitted by a straight line above the initial freezing point, this is not entirely true as the specific heat capacity of butter is not constant in that range due to the melting of milkfat triglycerides. The more complex enthalpy functions of Houska *et al.* (1994) provide better approximations for the enthalpy in this range.

It can be concluded that the specific heat capacity of butter changes with composition which in turn is a function of season, manufacturing process and the type of butter. To model heat transfer it is required to have accurate data for the specific heat capacity and enthalpy of butter. It was decided that the specific heat and enthalpy should be measured for different kinds of butter from different seasons in order to successfully model the heat transfer in industrial scenarios.

2.9 Heat Transfer Models

The literature review on thermal properties showed that thermal properties are temperature dependent in the range of interest. Temperature dependent properties make the heat transfer models more complicated because analytical approaches may not be possible and a numerical solution might be needed. There are several numerical solutions to the heat transfer models. This section reviews the literature on general heat transfer models and the numerical methods to solve these models to allow selection of appropriate methods for modelling the heat transfer of butter.

2.9.1 General Heat Conduction Equation:

Generally the heat transfer in solid foods is defined either by the Fourier law of conduction or the enthalpy transformed version of Fourier Law. For heat conduction in a solid in three dimensions the equations are:

$$C\frac{\partial T}{\partial t}=\frac{\partial}{\partial x}\left(\lambda\frac{\partial T}{\partial x}\right)+\frac{\partial}{\partial y}\left(\lambda\frac{\partial T}{\partial y}\right)+\frac{\partial}{\partial z}\left(\lambda\frac{\partial T}{\partial z}\right)+q \qquad t>0 \qquad (2\text{-}13)$$

$$\rho\frac{\partial H}{\partial t}=\frac{\partial}{\partial x}\left(\lambda\frac{\partial T}{\partial x}\right)+\frac{\partial}{\partial y}\left(\lambda\frac{\partial T}{\partial y}\right)+\frac{\partial}{\partial z}\left(\lambda\frac{\partial T}{\partial z}\right)+q \qquad t>0 \qquad (2\text{-}14)$$

where the enthalpy H is given by:

$$H=\int_0^T c_p\,dT \qquad (2\text{-}15)$$

For equation (2-13) temperature is the only dependent variable whereas equation (2-14) is based on two dependent variables, enthalpy and temperature. In equation (2-13) the latent heat is incorporated into the apparent specific heat capacity. To accurately model the latent heat in this way a very small time step is required, otherwise in only one time step the local temperature could pass over the range of temperatures at which the freezing/thawing occurred. This could result in the under prediction of the freezing/thawing time due to less latent heat transfer being required. The enthalpy transformation approach (Eq. 2-14) minimizes this problem and is the preferred approach for the phase change problems (Delgado & Sun 2001).

The heat transfer models in equations (2-13) and (2-14) require boundary and initial conditions that describes the surface heat transfer rates and the condition of the product at time zero respectively.

2.9.2 Initial and Boundary Conditions

In the prediction of thawing and freezing in foods many kinds of initial and boundary conditions can be applied. Cleland (1990) categorized boundary conditions as five main types.

First Kind (known surface temperature)

The first kind of boundary condition can be stated as:

$$T = T_a \qquad \text{at the surface,} \quad \text{for } t > 0 \tag{2-16}$$

where T_a is the ambient temperature around the product.

Second Kind (Constant heat flow at the surface)

The second kind of boundary conditions can be stated as:

$$\lambda \; n.\nabla T_{(x,y,z)} = \varphi \qquad \text{at the surface,} \quad \text{for } t > 0 \tag{2-17}$$

where n is the unit vector normal to the surface and φ is the prescribed heat flux from the surface.

Third Kind (Convective and/or radiative heat transfer from the surface)

The third kind of boundary conditions can be stated mathematically as:

$$\lambda \; n.\nabla T_{(x,y,z)} = \varphi_{\text{convective}} + \varphi_{\text{radiative}}$$
$$= h_{\text{convective}} \left(T_{\text{a-convective}} - T \right) + h_{\text{radiative}} \left(T_{\text{a-radiative}} - T \right) \quad \text{at surface, for } t > 0 \tag{2-18}$$

where h is the heat transfer coefficient and T_a is the ambient temperature of the surroundings.

Fourth Kind (variable temperature at the surface)

The fourth kind of boundary conditions assumes variable but known temperature at the surface and can be written as:

$$T = f(t) \qquad \text{at the surface,} \quad \text{for } t > 0 \tag{2-19}$$

Symmetry Boundary Condition

Symmetry boundary conditions can be applied to geometric shapes where there is an axis of planar or rotational symmetry. It is also applied in the case where there is a perfectly insulated surface. The symmetric boundary condition can be written mathematically as:

$$\nabla T(x, y, z) = 0 \qquad \text{at the surface,} \quad \text{for } t > 0 \tag{2-20}$$

The third kind of boundary condition is also known as the Neumann boundary conditions. The first and fourth kinds of boundary conditions are special cases of the third kind where $h \rightarrow \infty$. Practically there is usually significant surface resistance to heat transfer so $h_{\text{convective}}$ cannot be very large therefore the first and fourth kind of boundary conditions are not often the best boundary conditions for industrial problems. The second kind of boundary condition also occurs very rarely and is hardly used even under highly controlled and accurately measured experimental conditions. Cleland (1990) also suggested that the 3rd kind of boundary conditions is the most realistic in modelling thawing and freezing of food processes where phase change occurs.

The initial conditions in the real world could be non uniform depending on the specific application but uniform initial conditions are preferred to avoid any complexity in providing large amounts of input data to the model. Also often the positional temperature profile through the product is unknown. The uniform initial condition is given by:

$$T = T_i \qquad \text{at all places in the object at } t = 0 \tag{2-21}$$

To solve the model given by equations (2-13) or (2-14) and the chosen boundary and initial conditions, the model can be solved by either analytical or numerical methods depending on the accuracy required in the predictions and the assumptions made during the formulation.

2.9.3 Analytical Solutions for Conduction Problems:

Analytical solutions to heat transfer exist for simplified systems with no phase change, constant thermal properties and usually uniform initial conditions (Cleland, 1990). These models are approximations to the complicated real world situations due to the temperature dependence of the thermal properties. The large changes in the thermal properties occur during the phase change period. Because of this complex behaviour it is not possible to derive an exact analytical solution for the freezing time predictions of food for practical situations (Becker & Fricke, 1999). Such limitations of analytical approaches when thermal properties are temperature dependent mean that it is often necessary to use numerical solutions.

Reviews of analytic and other approximate solutions are given by Becker & Fricke (1999) and Delgado & Sun (2001).

2.9.4 Numerical Solutions for Heat Transfer

Cleland *et al.* (1987c) stated that numerical methods are accurate and reliable for freezing and thawing time predictions provided that they are formulated and implemented correctly to reduce any truncation and rounding errors. Due to the availability of fast computers it is now possible to reduce numerical errors by going to very small time and space step sizes to solve the heat transfer equations. The two numerical methods commonly used for freezing and thawing models are the finite element and finite difference methods. For irregular shapes finite element method is the most appropriate and for the regular geometric shapes the finite difference solution scheme is usually preferred (Cleland, 1985).

According to Cleland (1990) the finite difference method can be implemented in several ways including;

- Simple explicit scheme where thermal conductivity and heat capacity are combined and thermal diffusivity is taken as a function of temperature.
- Explicit solution where thermal conductivity and specific heat are taken as separate functions of temperature.

- Explicit difference formulae based on the enthalpy transformation (equation 2-14)
- Fully implicit, multi-time level schemes such as the Crank Nicholson scheme (Crank & Nicholson, 1947); and Lees scheme (Lees, 1966) etc.

Due to the phase change problem in this work the enthalpy approach is the most appropriate. Implicit schemes for the enthalpy transformation involve iterative solutions at each time step, making the solution more complicated but allow greater numerical accuracy and therefore larger time steps. With the availability of fast computers explicit schemes can be used successfully with small time step and are favored because they are easier to implement.

A number of papers reported the application of numerical methods for predicting freezing and thawing of food systems. For example Manpperuma & Singh (1988) used an explicit numerical method involving the enthalpy transformation for one, two and three dimensions with the 1^{st}, 2^{nd} and 3^{rd} kind of boundary conditions to predict thawing and freezing in foods. The predicted results showed good agreement with experiment data for cylindrical, slab shaped and spherical products.

Cleland (1990) reviews numerical methods suitable for predicting freezing and thawing of food products. Most of these methods use equilibrium thermal property data (the process is assumed to be heat transfer limited). However in many food systems freezing involves supercooling (non-equilibrium behavior). Therefore it was decided to review the literature and look at the different approaches available to model the freezing behavior of food systems where supercooling occurs.

2.9.5 Freezing Models for Water–enriched Foods:

The freezing of food is not a simple process and involves the complexity of removal of both latent and sensible heat in the food. This removal of latent heat depends on the structure of food. In some food materials the removal of latent heat occurs once the initial freezing point of the food is reached without any supercooling effects. At the initial freezing point a portion of the water within the food crystallize that makes the remaining solution more concentrated which further decreases the freezing point.

In other kinds of water-enriched foods water supercools to many degrees below its initial freezing point, but as soon as the ice nuclei are formed the crystallisation process begins and starts releasing the latent heat. This process gives a quick rise in temperature until the temperature approaches the initial freezing point.

Cleland *et al.* (1982) observed that high rates of cooling increased the freezing time up to 25% and they postulated that this may be caused by the supercooling throughout the process of ice crystal growth and prior to the initial ice nucleation. Pham (1989) suggested that unless the physical phenomena of ice crystal nucleation and growth are better understood, numerical methods are unlikely to give better predictions than the simple empirical or semi-empirical equations.

Miyawaki (1989) described the freezing process including supercooling:

A typical relationship between the enthalpy – temperature is given in Figure 2.11. Initially the enthalpy during the freezing proceeds along the line a→b→c. The section b→c corresponds to supercooling and heat transfer is simple heat conduction without phase change. Once nucleation occurs the supercooling ceases, and is followed by rapid crystal growth and the enthalpy curve shifts from c→d. This transition happens throughout the sample. The remaining latent heat transfer is limited by the heat removal rates and follows the enthalpy curve from d→e→f until the whole sample is frozen completely. Lastly pure sensible heat transfer occurs following the enthalpy curve follows f→f'.

Pham(1989) used a similar type of step approach to model supercooling followed by dendritic growth of ice crystal in one dimensional meat slab. Pham (1989) used the same enthalpy-temperature relationship given in Figure 2.11 with the inclusion of the process c-d by assuming that the crystallization takes place at a definite nucleation temperature followed by the dendritic growth of crystals.

These models are appropriate in foods in which water is a continuous phase. In such systems nucleation anywhere in the product will initiate ice crystal growth throughout the supercooled water phase. In butter where water is in the form of discontinuous droplets, such models are not likely to be appropriate unless all the droplets begin to freeze at the same level of supercooling. A model combining conductive heat transfer and the nucleation/growth models reported in Section 2.6 is a promising approach to model the freezing behaviour of butter that has not yet been attempted.

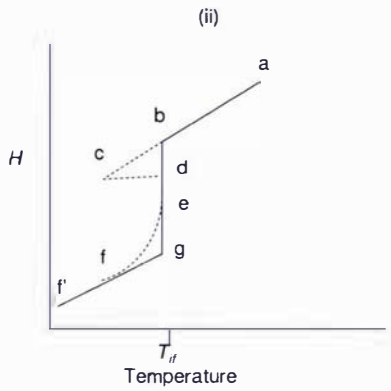

Figure 2.11 Enthalpy – temperature relationship. Pure water: abdgf', water-enriched food without supercooling: abdeff', food with supercooling: abcdegff'.

2.10 Literature Conclusions

From the literature review it was concluded that butter is a water in oil emulsion and freezing and thawing may not be a reversible process like in other food materials where water is a part of continuous phase. Thawing can probably be modeled as conduction only with equilibrium thermal properties. For freezing another approach will probably be required that considers the combined effects of multiple individual droplet freezing events. It is not clear from the literature whether it will be only nucleation limited crystallization of the aqueous phase of butter or whether consideration of growth of crystals is also important in order to model the freezing behavior.

Successful modeling of thawing and freezing of butter requires accurate thermophysical property data. The literature review on the thermophysical properties of butter showed that there are differences in the values of all the thermophysical properties due to seasonal changes and the manufacturing process for different kinds of butter. Therefore it is necessary to either measure the thermophysical properties data for different kinds of butter samples collected from throughout the season or estimate it based on the compositions of the samples under study.

The next chapter comprises the work on collection of samples from throughout the dairy season, compositional analysis of the samples, estimation of the thermophysical properties data and its measurement where good estimation could not be achieved based on composition.

CHAPTER 3

ESTIMATION AND MEASUREMENT OF THE THERMAL PROPERTIES OF BUTTER

3.1 Introduction

Accurate data for the thermal properties of butter is key to the prediction of thermal behavior of food under industrial conditions. The literature review shows that the data available on the thermal properties of butter is highly variable. Some of this variability could be due to the differences in butter types, composition, manufacturing methods or seasonality. For heat transfer models to be useful, it is important to understand how thermophysical properties change because of these variables and to provide appropriate methods for data selection or estimation.

This chapter focuses on estimation and, in the absence of accurate data, the measurement of thermal properties of commercial butter.

3.2 Material

Samples of butter were collected from Fonterra Co-Operative Group Ltd, New Zealand. These butter samples were manufactured from different seasons (spring, summer or autumn), with different compositions and using different manufacturing processes. A code was given to each butter sample and this is used for all the experimental trials in the work. The butters samples can be classified into four different types: salted butter, unsalted butter, high moisture butter and lactic butter. The high moisture butters contained a maximum of 25% of water. The lactic butters had pH in the range 4.3 – 5.0 and contained lactic acid. A list detailing all the butters is given in Table 3.1. These butters include samples selected over a period of four years from two different manufacturing processes.

Samples B15, B16 and B17 were the butters used for the experiments to validate heat transfer models detailed in the thesis, although exact production date were not known. The compositions of all the butters were tested by Fonterra Co-Operative Groups Ltd. Details of the standard methods

used for the composition testing are given in Appendix A-2. Table 3.2 shows the mass fraction (w/w) for each of the measured butter components.

Table: 3.1 Butter samples collected from different seasons

Code	Butter Type	Factory	Production Date	Season	Comment
B1	High moisture	Te Rapa	10-Sep-00	Spring	Ammix
B2	Salted	Whareroa	24-Sep-02	Spring	Fritz
B3	Salted	Whareroa	27-Dec-02	Summer	Fritz
B4	Salted	Whareroa	16-Apr-03	Autumn	Fritz
B5	High moisture	Te Rapa	18-Sep-00	Spring	Ammix
B6	Unsalted	Clandeboye	7-May-03	Autumn	Fritz
B7	Unsalted	Kauri	15-Sep-02	Spring	Ammix
B8	Unsalted	Kauri	21-Dec-02	Summer	Ammix
B9	Unsalted	Kauri	21-Apr-03	Autumn	Ammix
B10	Unsalted	Whareroa	27-Sep-02	Spring	Fritz
B11	Unsalted	Whareroa	23-Dec-02	Summer	Fritz
B12	Unsalted	Whareroa	21-Apr-03	Autumn	Fritz
B13	Unsalted Lactic	Whareroa	23-Sep-02	Spring	Fritz
B14	Unsalted Lactic	Whareroa	8-Oct-01	Spring	Fritz
B15	Salted	Whareroa	2003	Spring	Fritz
B16	Unsalted	Whareroa	2003	Autumn	Fritz
B17	Unsalted Lactic	Whareroa	2003	Summer	Fritz

Table 3.2 shows that except for the high moisture butter (B1; B5), there was very little difference in the moisture contents of all the butters regardless of manufacturing process and the type of butter. The salt contents in the salted butter also varied little. This is because these variables are controlled during butter manufacture. The fat contents in the high moisture butters were lower than that of standard moisture butter as expected. The amount of milk solids not fat (MSNF) (which includes lactate, lactose, non protein nitrogen (NPN), and protein) in the two high moisture butters differs markedly. In all other butters MSNF lay within the range of 1.1% to 1.59%.

This data allows investigation of thermal properties with respect to composition. Selection of salted, unsalted, high/standard moisture and lactic butter samples from different seasons (NZ Autumn, NZ Summer and NZ Spring) and from two different manufacturing processes (Ammix and Fritz) allowed a comparison of the thermal properties of butter caused by these factors. These samples also help in deciding which thermal properties are more affected by these differences and what precision in the thermal data is needed to cover the standard compositional range.

Table 3.2: Composition of butters[a]

Butter	Salt %w/w	Fat %w/w	Moisture %w/w	MSNF %w/w	Lactose %w/w	Lactate %w/w	NPN %w/w	TN-liquid %w/w	Protein %w/w
B1		76.1	21.18	2.33	0.83		0.028	0.155	0.81
B2	1.33	81.5	15.61	1.48	0.64		0.090	0.127	0.24
B3	1.30	81.2	15.68	1.80	0.66		0.052	0.124	0.46
B4	1.26	81.4	15.67	1.51	0.55		0.028	0.132	0.66
B5		78.0	21.41	0.75	0.21	0.04	0.027	0.065	0.24
B6		82.5	15.66	1.59	0.66		0.030	0.147	0.75
B7		83.0	15.50	1.12	0.50		0.034	0.095	0.39
B8		83.2	15.57	1.08	0.45		0.047	0.096	0.31
B9		82.7	15.66	1.50	0.59		0.029	0.128	0.63
B10		82.6	15.66	1.49	0.62		0.045	0.133	0.56
B11		82.6	15.74	1.31	0.53		0.014	0.122	0.69
B12		83.3	15.67	1.22	0.49		0.028	0.126	0.63
B13		82.8	15.67	1.57	0.59	0.07	0.013	0.127	0.73
B14		83.0	15.65	1.42	0.54	0.07	0.037	0.125	0.56
B15	1.23	82.1	15.28	1.45	0.52		0.007	0.115	0.69
B16		83.0	15.38	1.45	0.56		0.005	0.109	0.66
B17		83.0	15.62	1.32	0.81	0.06	0.055	0.117	0.40

(a) MSNF ~ milk solids not fat, NPN ~ non protein nitrogen, TN ~ total nitrogen. Blanks shows that test was not performed for that component

It is expected that the salt and water contents have major effect on the thermal properties of butter. The initial freezing point of salted butter is expected to be lower than the unsalted butter due to the freezing point depression of the salt. It is also expected that salted butter would have lower thermal conductivity than unsalted butter at temperatures below the initial freezing points as in the aqueous phases of these butters in those conditions less water is expected to freeze. The butter with higher moisture contents will have a higher enthalpy change due to the high latent heat and the high heat capacity of water. The amount of protein could affect the amount of bound water during freezing. Butter with a higher amount of bound water would be expected to have a lower enthalpy change on freezing.

Table 3.3 shows the solid fat content (SFC) of the fat extracted from the butters over the temperature range 0 to 35°C as determined by pulsed nuclear magnetic resonance. The SFC is not

normally measured below 0°C as most of the milkfat fractions solidify above 0°C. The sample preparation for the determination of the SFC of milkfat using pulsed nuclear magnetic resonance includes melting the extracted fat, and cooling and crystallizing the fat under constant conditions. This standardized crystallisation enables any contribution from the butter making process to be eliminated and therefore the SFC simply reflects the composition of the original fat when comparing samples prepared in the same way (MacGibbon & McLennan, 1987).

Table 3.3: Solid fat contents of butter at different temperatures

	Solid Fat Contents (%)							
Butter	**0°C**	**5°C**	**10°C**	**15°C**	**20°C**	**25°C**	**30°C**	**35°C**
B1	62.62	59.03	51.51	36.29	19.26	9.94	4.43	0.69
B2	64.31	60.65	52.95	37.35	19.59	10.75	4.17	0.32
B3	69.83	66.43	59.33	44.00	24.39	13.60	6.55	0.71
B4	67.12	63.79	56.91	41.72	23.03	12.62	5.51	0.65
B5	63.47	59.55	52.18	35.67	18.72	10.14	4.32	0.24
B6	65.67	62.33	55.69	40.06	21.64	12.20	5.60	0.45
B7	63.10	59.27	51.93	36.22	18.83	10.20	4.41	0.79
B8	69.63	66.11	59.39	44.47	24.48	14.01	6.88	1.06
B9	66.84	60.56	53.62	38.50	20.74	11.61	5.58	0.89
B10	63.17	59.38	51.26	35.78	18.78	9.77	4.27	0.19
B11	69.64	66.18	58.88	43.51	24.34	13.40	6.38	0.96
B12	66.45	63.10	56.26	41.17	22.44	12.60	5.96	0.80
B13	63.72	59.90	52.36	36.44	19.13	10.01	4.13	0.27
B14	65.31	61.55	53.56	37.46	20.08	10.89	4.49	0.00
B15	67.01	63.34	55.36	38.74	20.85	11.21	4.89	0.00
B16	65.52	62.08	55.21	39.99	21.64	12.55	5.60	0.88
B17	69.83	66.43	59.34	44.64	26.53	14.30	6.74	0.95

As expected, the summer butter (B3; B8; B11) had higher solid fat contents at lower temperatures than the spring butter (B2; B7; B10; B13; B14). The extremes of highest and lowest solid fat contents from the butter samples and a typical autumn milkfat sample are given in Figure 3.1. The SFC of all other butters lay between these extremes.

There was little change in the SFC of the milkfat from the butters between 0 to 10°C. The largest change was in the range 10°C to 20°C. Butter with a higher SFC at any temperature range of interest

is expected to have a higher specific heat capacity over that range and vice versa for butter with lower SFC.

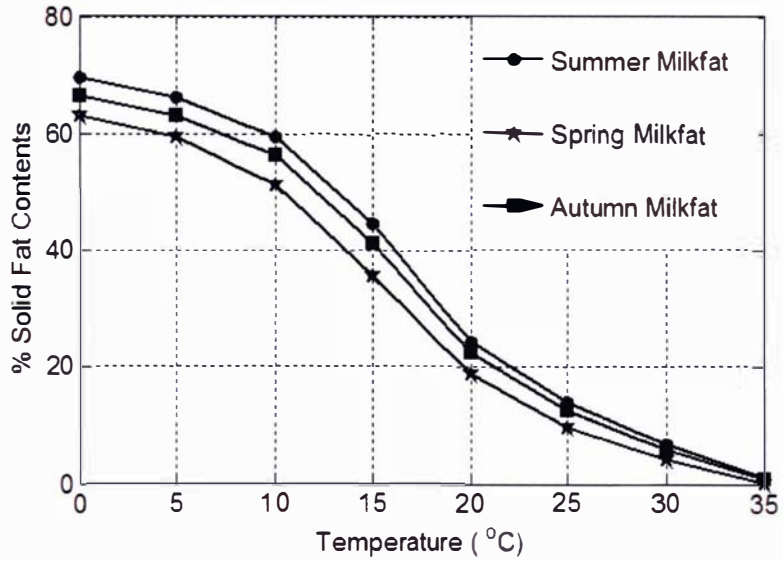

Figure 3.1: Solid fat contents of Summer, Spring and Autumn milk fat

(a) Summer

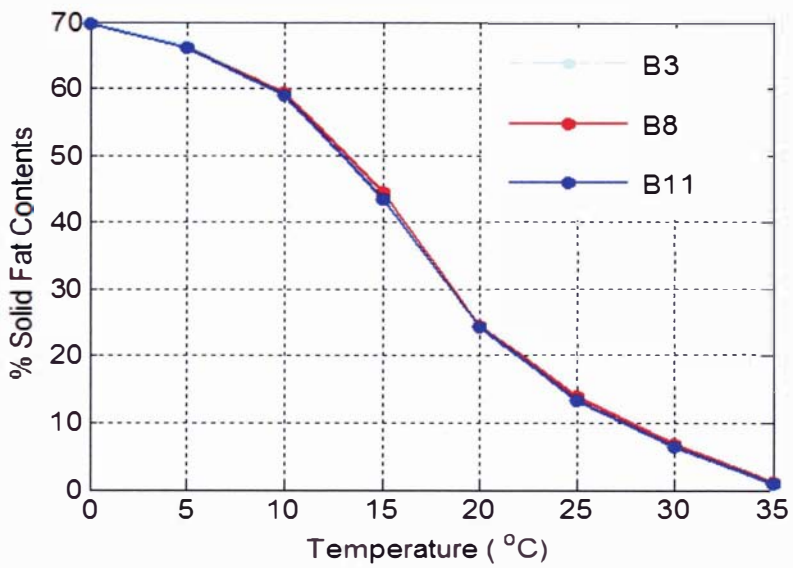

(b) Spring

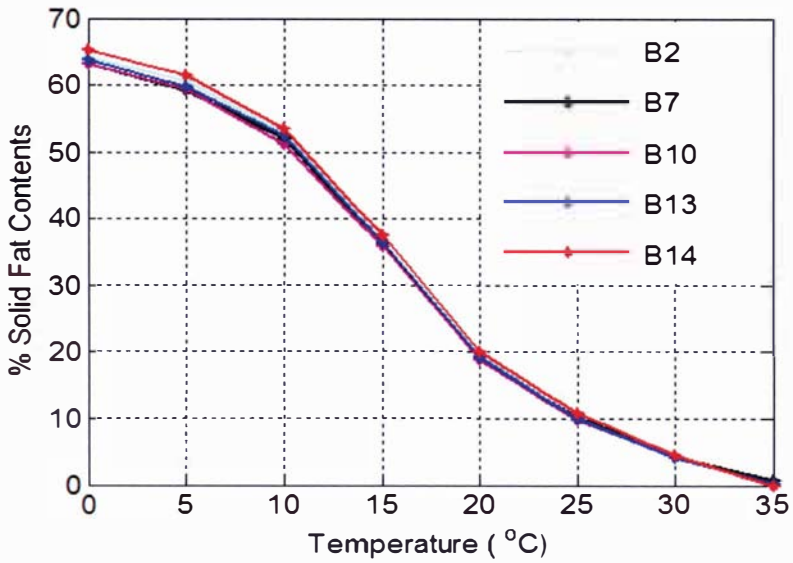

(c) Autumn

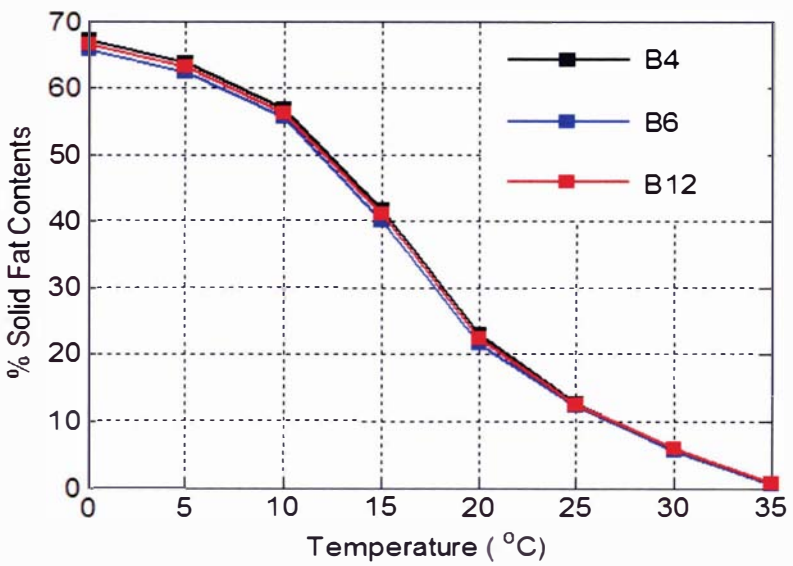

Figure 3.2: Solid fat contents of butter

(a) Summer (b) Spring (C) Autumn

Figure 3.2 shows the SFC as a function of temperature for the each spring, summer and autumn butters. There was very little difference within each season in SFC for three different types (salted,

unsalted and lactic unsalted). Only B 14 deviated from the other spring samples to any extent. This butter was manufactured in October 2001 and this month is in the transition period between spring and summer. This butter was still closer to spring instead of summer with regard to SFC.

Overall, the results show that the SFC of butter varies with season and it is not significantly affected by the manufacturing process or type of butter.

3.3 Initial Freezing point

Due to the variability in the initial freezing points of butter reported in the literature and its dependence on the concentration of solutes in the aqueous phase, the initial freezing points of each butter sample were measured directly.

3.3.1 Measurement Methods

A cryoscope is the main classical instrument used to measure the initial freezing point of food materials (Rahman, 1995). A time - temperature curve is recorded during sample freezing and the initial freezing point is derived from the relatively long plateau which follows supercooling and nucleation on this curve. The thermal history of a sample going through cryoscopy is given in Figure 3.3. The sample is cooled very quickly to 0°C and at that point the cooling rate is slowed to supercool the sample to many degrees below its initial freezing point. When the sample is sufficiently supercooled, a mechanical pulse is applied which induces the sample to freeze and then the heat of fusion warms up the sample asymptotically towards its initial freezing point where it equilibrates. The temperature reading for the initial freezing point is taken after a stable temperature is recorded on the freezing point plateau.

In the case of a pure solvent, the plateau following the nucleation of ice crystals will be horizontal, but in the case of non-ideal solutions, this line will be non-linear due to freeze concentration of the solutes in the aqueous phase. In this case a correction for the freeze concentration can be made using the extrapolation method or by using standard solutions.

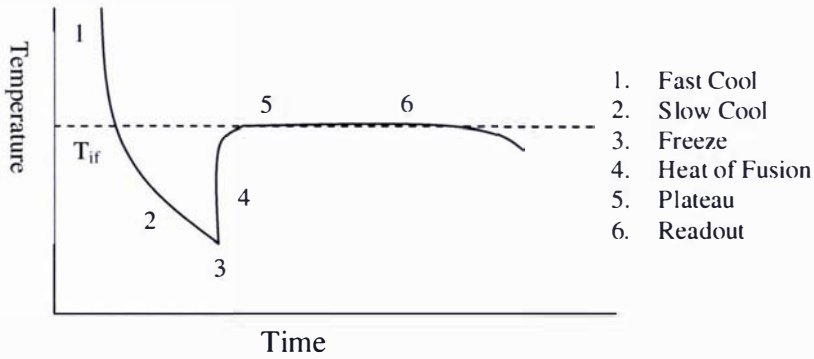

Figure 3.3. Thermal history of a sample during cryoscopy measurements (4C3 cryoscopy manual manufactured by Advanced Instruments Inc)

3.3.1.1 Extrapolation method

The extrapolation method is a simple method of determining the initial freezing point, by extrapolating geometrically the time versus temperature freezing curve. This method is illustrated in Figure 3.4. Detail of this method is given by Fennema *et al.* (1973).

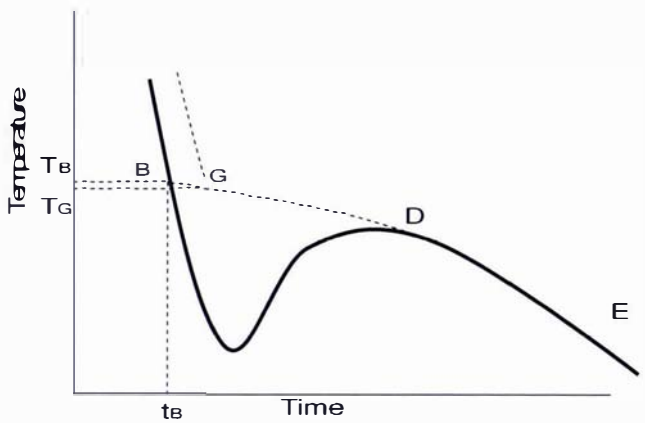

Figure 3.4: Extrapolation method for determining the initial freezing point (adapted from Rahman, (1995))

The line DE is extrapolated backwards to estimate the initial freezing point B whereas the point G is the true freezing point. The error between the points G and B increases with an increase of supercooling and a decrease in the rate of heat removal (Fennema *et al.*, 1973).

3.3.1.2 Calibration with the standard solutions:

The other method to correct the error from freeze concentration is to use standard solutions with known freezing points. Usually two standards are used, one with freezing point slightly above and the other with freezing point slightly below the freezing point of interest. The unknown freezing point can be corrected on the basis of difference between the observed and actual freezing point of the standards. In this case, the same extent of supercooling, same crystallization temperature and the same cooling rate is necessary to get good results (Rahman, 1995).

3.3.2 Measurement of Initial Freezing Point of Butter

Due to the availability of a cryoscope (Model 4c3 manufactured by Advanced Instruments Inc), this method was used to measure the initial freezing point of butter serums.

About 70-100g of butter sample was placed into a glass jar and sealed. The jar was placed in a oven at 60°C until all the butter melted and the water phase could be seen clearly. The aqueous phase (serum) was then transferred into a centrifuge tube and centrifuged for 10 minutes at 20,000 rpm, at room temperature and the aqueous phase sampled from beneath the separated fat. Serums of 17 different samples of butter collected from throughout the manufacturing season (as described above) were prepared in this way. After centrifugation the samples were sent to Fonterra Co-Operative Group Limited laboratory at the Whareroa site to measure the initial freezing point using cryoscopy using the method outlined in section 3.3.1.

Out of the 17 samples, four were salted butters. For the salted butters the serums extracted were too concentrated to freeze in the range of the cryscope and therefore initial freezing point for the salted butter was not measured using this instrument.

Results of Cryoscopy Measurement

Table 3.4 gives the measured initial freezing point of the unsalted butters using cryoscopy.

The measured freezing point data agrees well with the cryoscopy data measured by Wolfschoon (1983) & (1991) whereas it was higher than the values estimated by Pham (1994) and Lindsay & Lovatt (1993) using the Succar and Hayakawa (1990) method.

Table 3.4: Measured initial freezing point of unsalted butters

Butter	T_{if} (°C)	Butter	T_{if} (°C)
B1	-0.443	B11	-0.414
B5	-0.25	B12	-0.408
B6	-0.515	B13	-0.616
B7	-0.397	B14	-0.576
B8	-0.364	B16	-0.52
B9	-0.501	B17	-0.566
B10	-0.481		

The slight variation in the initial freezing points of the butters found was in keeping with the small differences due to composition. Out of four Ammix butters (B5; B7; B8; B9), three had higher initial freezing point as compared with the data for the Fritz butters. The fourth Ammix butter (B9) had a lower initial freezing point than the other Ammix butters (more inline with the data for the Fritz butters) which was probably due to a higher protein concentration which would increase the amount of bound water and therefore depress the initial freezing point.

For Ammix butter, an average value of -0.38°C can be used for the initial freezing point based on the finding that there was not much difference in the composition in all the butters studied in this work (Table 3.2).

For unsalted lactic butter (B13; B14; B17) manufactured by the Fritz process, a value of -0.59°C can be used and for unsalted Fritz butter (B6; B10; B11; B12; B16) a value of -0.47°C is appropriate.

The freezing point of aqueous solutions is depressed with the increase of solutes in it; the amount of carbohydrates and proteins in the aqueous solution increases the amount of bound water, which causes depression of the freezing point. Therefore, an analysis of the initial freezing point as a function of the solute concentration in the aqueous phase of butter (calculated from the solute and moisture fraction given in Table 3.1) was done as shown in Table 3.5.

A clear trend of initial freezing point depression with the increase of total solute concentration can be seen above -0.5°C. Below -0.5°C there is bit of scatter in the data which is probably due to the complicated composition of the water droplets. The amounts of lactose and protein play roles in the amount of bound water that depress the freezing point further and there are some solutes that were

not measured which could also affect the initial freezing point. To understand the contribution of each solute in the determination of the initial freezing point it is necessary to look at the theoretical models in the literature.

Table 3.5: Solute concentration in the aqueous phase of butter compared with the T_{if}

Butter ID	Solute Concentration %	T_{if} (°C)
B5	3.50	-0.25
B8	6.94	-0.36
B7	7.23	-0.40
B12	7.79	-0.41
B11	8.32	-0.41
B17	8.45	-0.57
B14	9.07	-0.58
B16	9.43	-0.52
B10	9.51	-0.48
B9	9.58	-0.50
B13	10.02	-0.62
B6	10.15	-0.52
B1	11.00	-0.44

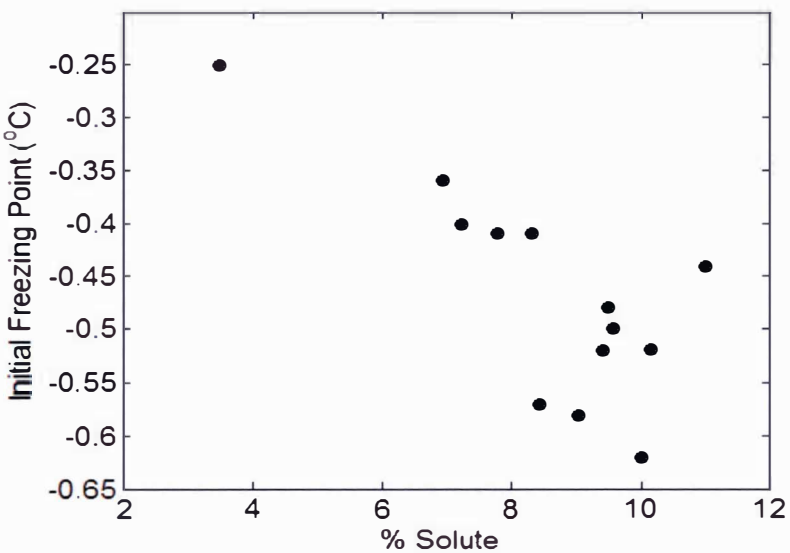

Figure 3.5: Initial freezing point of unsalted butters as a function of solute concentration in the aqueous phase

3.3.3 Alternative Approaches

The salted butter serums didn't freeze using cryoscopy due to the freezing point range being outside the instrument measurement range. Therefore, alternative approaches were sought to estimate the initial freezing point of salted butter.

Butter serum contains considerable amounts of lipid material, proteins (eg α, and β --casein, β-lactoglobulin, α-lactoglobulin) and ionic components such as calcium and phosphate and sodium chloride (McPherson, 1981). Materials with high molecular weight such as fat and protein have a negligible effect on freezing point (Harper, 1981). Thus the freezing point depression of the butter depends primarily on the amount of sodium chloride (NaCl) added during the butter making process.

There are various methods available to predict initial freezing point based on composition. These models can be divided into two main categories; namely empirical curve fitting models and theoretical models.

3.3.3.1 Empirical Curve Fitting Models

Rahman (1995) listed a number of equations various authors (Chang & Tao, 1981; Dickerson, 1968; Reidel, 1951) have developed to estimate the initial freezing point of the food materials as a function of water and salt contents. These authors divided the food into three main groups - meat/fish, Juice and fruit/vegetable. Chen (1986, 1987a) and Chen & Nagy (1987) give a third degree polynomial equation for the freezing point depression of NaCl solutions:

$$T_{if} = -59.278\,S - 7.332\,S^2 - 544.332\,S^3 \qquad (3\text{-}1)$$

Where S is the NaCl content in the aqueous solution. This may be relevant to estimate the initial freezing point of salted butter using the given salt concentration in the aqueous phase of butter.
Potter *et al.* (1978) also measured the initial freezing point of aqueous NaCl solutions with different concentrations. The data reported by Potter *et al.* (1978) can be expressed by the following empirical relationship:

$$T_{if} = -0.0217\,S^2 - 0.3559\,S - 0.772 \qquad (3\text{-}2)$$

Wolfschoon -Pombo (1983) & (1991) measured the initial freezing point of salted butter using cryoscopy on diluted butter serums. The following equation was fitted to the data presented by Wolfschoon (1983, 1991)

$$T_{if} = -0.611S - 0.4361 \tag{3-3}$$

3.3.3.2 Theoretical Models:

Theoretical models exist based on the thermodynamic principles for ideal and non ideal solution systems.

(a) Ideal Solutions

All the theoretical models for estimating freezing point of an ideal solution are derived with the assumptions that all the water is freezable, Raoult's law is valid and insoluble solids do not have any effect on the water activity (Rahman, 1995). These models are based on the Clausius–Clapeyron equation that follows from the first and second law of thermodynamics and is given by:

$$T_{if} = \frac{\beta}{M_w} \ln\left(\frac{1 - X_{si}}{1 - X_{si} + EX_{si}}\right) \tag{3-4}$$

where β is the molar freezing point constant of water (1860 kg K/kg mole), M_w is the molecular weight of the water, X_{si} is the mass fraction of the solute before freezing and E is the molecular weight ratio (molecular weight of the water/molecular weight of the solute). Equation (3-4) holds only if the aqueous solution is very dilute. In butter, due to the presence of protein, it is very likely that all the water does not freeze. Therefore, using equation (3-4) is not appropriate.

(b) Non Ideal Solutions

Most of the solutions in foods do not obey equation (3-4). In real solutions, some water combines with the solutes and acts as non-solvent water. Some water is amorphous in nature (Rahman, 1995) and as such does not contribute to the activity of the solution. Chen and Nagy (1987) explained that the amount of the bound water for any material is a function of temperature and concentration.

Schwartzberg (1976) proposed the following modification of Equation 3-4 for estimating the initial freezing point based on the amount of bound water:

$$T_{if} = \frac{\beta}{M_w} \ln\left(\frac{1 - B'' X_{si}}{1 - B'' X_{si} + E X_{si}}\right) \tag{3-5}$$

where B'' is the amount of water which is bound per unit weight of solids and is unavailable for freezing at any temperature.

Chen and Nagy (1987) proposed the following modification to calculate the freezing point depression:

$$T_{if} = \frac{\beta}{M_w} \ln\left(\frac{1 - X_{si}}{1 - X_{si} + E X_{si}\left(f + c'' X_{si}\right)}\right) \tag{3-6}$$

where f and c'' are empirical constants depending on the concentration of the solutes and can be estimated by regression.

The enthalpy of food as a function of temperature has a sharp change in slope at T_{if}. Succar and Hayakawa (1990) estimated the initial freezing point using the measured enthalpy data of material and then extrapolating it above and below the initial freezing point to determine T_{if} where both the lines intersect as shown in Figure 3.6. This approach was first proposed by Pham (1987) and it needs accurately measured enthalpy data of the material near the freezing point.

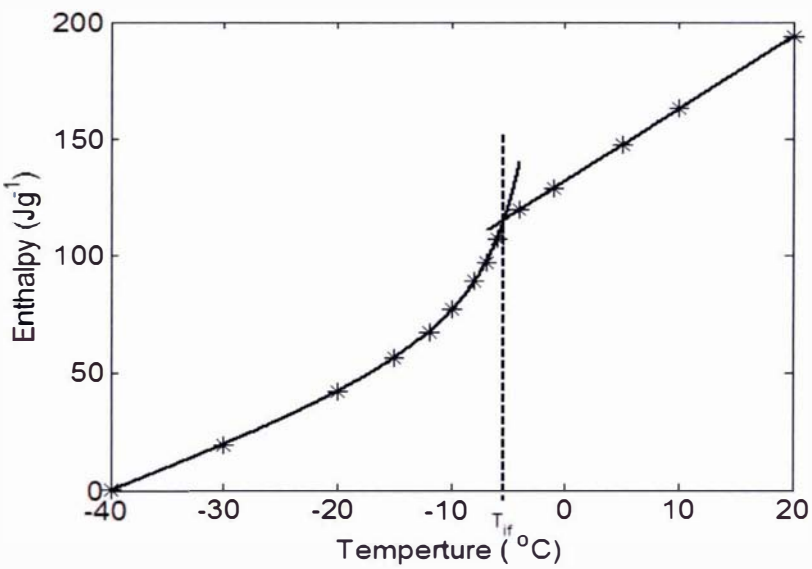

Figure 3.6: Estimation of initial freezing point from measured enthalpy data

Miles *et al* (1997) predicted the initial freezing point of a number of foods depending on the chemical concentration of the foods and explained that the soluble components of food like sugars, ions, acids and soluble proteins contribute to the freezing point depression and the insoluble components such as fats and insoluble proteins do not contribute. The equation for the freezing point depression is:

$$T_{if} = -\frac{RT_o^2 \sum \frac{\tau_i X_i}{M_i}}{\Delta H \left[\frac{X_w - X_{bw}}{M_w} + \sum \frac{\tau_i X_i}{M_i} \right]} \qquad (3\text{-}7)$$

where R is the gas constant, T_o is the temperature (in K) of fusion of pure ice in pure water, ΔH is the molar enthalpy of fusion of ice, X_i is the mass fraction of the ith component , M_i is the molecular mass of the ith component. X_w is the water fraction, and X_{bw} is the bound water. The bound water is given by:

$$X_{bw} = \sum \sigma_r X_r \qquad (3\text{-}8)$$

Where σ_r are component specific constants and X_r is the fraction of specific component that pay a role in bounded water fraction. The values of σ_r for protein and carbohydrates were found to be 0.45 and 0.3 respectively (Miles *et al.* 1997). Three different Fritz butter serums (salted, unsalted, and lactic) were tested for the concentration of a range of elements (Table 3. 6) by induction Coupled Plasmon Spectroscopy (ICP).

Table 3.6: Element analysis of salted, unsalted and lactic butter

Element	Butter ID		
(g m^{-3})	B3 (salted)	B10 (unsalted)	B17(unsalted lactic)
Al	1.6	1.7	3.8
As	<0.5	<0.5	<0.5
B	3.1	3.5	3.8
Ca	804	934	900
Co	<0.03	<0.02	<0.02
Cr	<0.03	<0.02	<0.02
Cu	<0.01	0.12	0.20
Fe	1.0	0.8	1.2

K	1700	1276	1204
Mg	57.4	73.9	92.4
Mn	0.05	0.03	0.05
Mo	<0.03	0.1	0.1
Na	23340	260	333
Ni	<0.1	<0.1	<0.1
P	921	1008	1024
Pb	<0.1	<0.1	<0.1
S	253	288	321
Se	<0.5	<0.5	<0.4
Sn	<0.1	<0.1	<0.1
Sr	0.4	0.4	0.4
Zn	2.3	3.1	3.4

It is clear from the analysis that all other elements except NaCl, have similar concentration and were in small quantity in all the samples and their concentration in the aqueous phase of butter is unlikely to significantly affect the initial freezing point of salted butter.

3.3.4 Estimation on Initial Freezing Point of Salted Butter

Before applying any of the above methods on the butter samples, the methods were tested against two published data for the salted butters (Pham *et al.*, 1994; Lindsay and Lovatt, 1993)

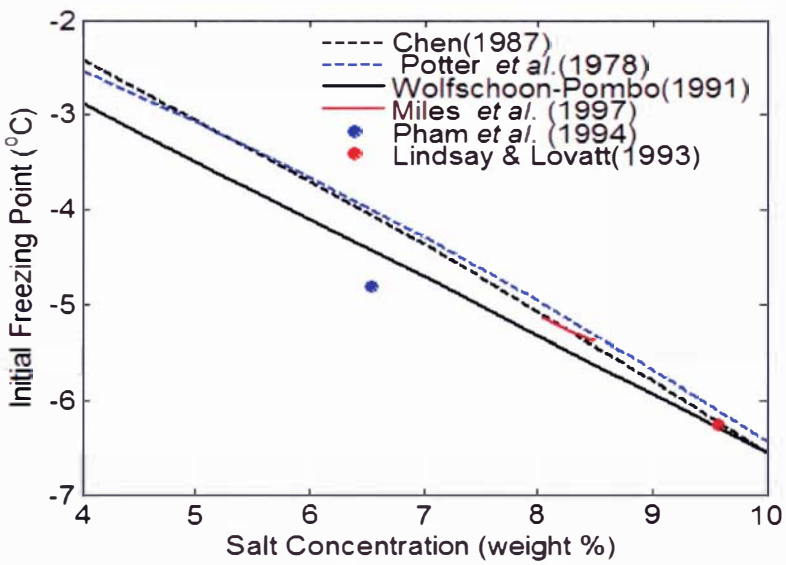

Figure 3.7: Initial freezing point of salt solutions

The initial freezing points of the salted butters available in the literature were calculated using the weight percentage of the NaCl in the aqueous phase of the butter. The results are given in Figure 3.7. The relationship given by Wolfschoon – Pombo (1991) gives a lower initial freezing point than the other three relations and agrees well with the experimental data points. Because these measurements were done on the butter serums and the empirical relations were developed from pure water/NaCl solutions. Equation (3-3) was used to estimate the initial freezing point of salted butters.

The weight percentage of the salt in the water phase of four salted butter (B2; B3; B4; B15) were calculated and equation (3-3) was used to predict the initial freezing point of the butters (Table 3.7).

Overall an average value of -5.5 °C can be used for salted butter with a typical composition of 15.5% water and 1.3% salt.

Table 3.7: Initial freezing point estimated using salt solution and empirical curve fitting

Butter ID	Salt (%w/w)	Moisture (%w/w)	Salt weight (%)	T_{if} (°C) Eq(3-3)
B2	1.33	15.61	8.52	-5.64
B3	1.30	15.68	8.29	-5.50
B 4	1.26	15.67	8.04	-5.35
B15	1.23	15.28	8.05	-5.35

3.4 Density

The literature density values for butter vary with composition and the manufacturing process (which can potentially affect the air content of the butter). The bulk density of any material can be calculated using its component parts (Rahman 1995) from compositional data using the following equation:

$$\frac{1}{\rho} = \sum_{i=1}^{n} \frac{x_i}{\rho_i} \qquad (3\text{-}9)$$

where ρ = bulk density (kg m^{-3})

ρ_i = density of the i^{th} component (kg m^{-3})

x_i = mass fraction of the i^{th} component.

Choi and Okos (1986) give the density of major food components for the temperature range of -40°C to 50°C. Water, air, protein, fat and ash are the major components of butter. New Zealand butter has only 0.1-0.2% air present (Ballentyne, 2003) which would result in only 0.1-0.2% change in the density value. Choi and Okos (1986) show that of the remaining components water is the only component whose density changes significantly in the range -18°C to 10°C. It changes from a value of 997 kg m^{-3} at 10°C to 917 kgm^{-3} at -18°C as the water freezes to ice, which is about a 9% decrease in the density of water. All other components' densities increase by about 1% over this temperature range. If the density is calculated from equation (3-9), assuming constant density values for all the components except water, and varying the density of water from 997 kg m^{-3} to 917 kg m^{-3}, it gave about 1% change in the density of butter showing that water has no significant effect on the density of butter.

Philpott (2001) measured the density of butter at 12°C and 20°C from both the Fritz and Ammix butter making processes. The samples were held at the measurement temperature in the incubator overnight and the measurements were taken the following morning. Three measurements of each sample were taken at both the temperatures for salted, unsalted, Ammix and Fritz butter making processes from different manufacturing sites. The data from Philpott (2001) is given in Tables 3.8 and 3.9.

Table 3.8: Density of butter measured at 12°C (Philpott, 2001)

Butter	Manufacturing site	Density (kg m^{-3})	
Fritz	Te Awamutu	Sample 1	970
		Sample 1	970
		Sample 1	970
Ammix	Te Rapa	Sample 1	970
		Sample 1	970
		Sample 1	970
Ammix	Northland	Sample 1	970
		Sample 1	970
		Sample 1	970
Fritz	Kiwi	Sample 1	970
		Sample 1	970
		Sample 1	970

Table 3.2 shows that all the butters used in this study, except B1 and B5 had nearly the same percentage of water. Thus the density value is not expected to vary significantly for the different butters for the given composition. Middleton (1995) reported that butter shrinks by 3% from ambient to -15°C which results an increase in the density of butter. The increase in density due to the shrinkage of fat is not fully compensated by a decrease in the density of butter due to water freezing. Literature data showed that density of butter increases with temperature but unfortunately there is limited data available below 0°C.

Table 3.9: Density of butter measured at 20°C (Philpott, 2001)

Butter	Manufacturing site	Density (kg m^{-3})	
Summer	Morrinsville	Sample 1	950
		Sample 2	960
Autumn	Morrinsville	Sample 1	950
		Sample 2	950
Summer	Whareroa	Sample 1	950
		Sample 2	960
Autumn	Whareroa	Sample 1	940
		Sample 2	960
Autumn, Ammix	Kauri	Sample 1	960
		Sample 2	960
Autumn, Ammix	Te Rapa	Sample 1	940
		Sample 2	960
Autumn, Ammix	Te Rapa	Sample 1	940
		Sample 2	950
Summer, Ammix	Te Rapa	Sample 1	950
		Sample 2	960
Salted, Spring	Whareroa	Sample 1	960
		Sample 2	960
Unsalted, Spring	Whareroa	Sample 1	950
		Sample 2	950
High Moisture, Spring	Whareroa	Sample 1	960
		Sample 3	650
		Sample 2	950
Salted	West land	Sample 1	960
		Sample 2	970
Unsalted, Spring, Ammix	Te Rapa	Sample 1	950
		Sample 2	950

Salted, Spring, Ammix	Te Rapa	Sample 1	950

The data measured by Philpott (2001) showed that there is little difference in the density of butter due to the manufacturing process. Due to advances in the technology it is unlikely to have any air in the butter. The density measured at 12°C for Ammix and Fritz butter manufactured at four different sites was 970 kg m^{-3}. An average value of 952 kg m^{-3} was found at 20°C. This represents less than 2% change in density from changing temperature from 20°C to 12°C. Combined with the fact that butter shrinks by 3% from ambient to -15°C then it suggests a 2-3% change in the value of density in the range of interest from 10°C to -18°C. An average value over the range of interest was found to be 970 kg m^{-3}. Most of the fat in butter solidifying at about 10°C with its major portion solidifies between 10 – 20°C (Figure 3.1). Therefore the change in the density below that temperature is probably not significant. Thus a constant value of 970 kg m^{-3} for the density of butter was selected to use for freezing and thawing model predictions for butter.

3.5 Specific Heat Capacity and Enthalpy

Specific heat capacity is one the most important properties in modelling heat transfer in butter. In the case of butter in the temperature range of interest (10°C to -20°C) both water, which comprises about 16% of the mass of the butter, and the fat, which makes most of the rest of the butter, undergo phase change. The fat phase change is complicated due to the wide range of triglycerides present in milkfat and the seasonal changes in the composition. Water freezing is complicated by the presence of soluble components which concentrate on freezing and depress freezing point. Therefore, direct measurement was the most sensible approach for providing enthalpy/specific heat capacity data. By carrying out these measurements for a range of butters, the possibility of predicting enthalpy of butter from composition could be investigated.

3.5.1 Measurement Techniques

The specific heat capacity measurement methods can be grouped as: (A) Method of mixture, (B) Comparison method, (C) Adiabatic method, and (D) Differential scanning calorimetry (DSC) (Rahman, 1995).

The ***method of mixtures*** is the most widely used method to measure specific heat due to its simplicity (Rahman, 1995). Mohsenin (1980) explained that in this method the specimen of known mass and temperature is added in a calorimeter of known specific heat capacity containing water or liquid of known temperature and mass. The unknown specific heat then can be computed from a

heat balance between the heat gained or lost by the water or liquid and the calorimeter and that gained by the specimen. The advantage of this method is that it is easy to apply and the apparatus is easy to assemble but there are many sources of error in it including thermal leakage, direct contact with the specimen and the heat exchange medium and problems in mixing due to density differences. Although a number of researchers have made changes in the method to avoid these errors, the system relies on having the fluid in the calorimeter available at the temperature range of interest and to get useful results many experimental trials are required.

The comparison method is usually used to determine the specific heat of liquids. Figure 3.8(a) shows a schematic diagram of comparison calorimeter. While conducting the experiment cup A is filled with distilled water or any other liquid of known specific heat capacity and cup B is filled with the liquid whose specific heat capacity has to be determined. Both cups are heated to same temperature and then placed in the calorimeter to cool. The unknown specific heat capacity is calculated from the cooling curves of both the liquids in cups A and B. If both the cups are of same material, same size, same exterior finish and of identical masses then they can be considered as identical emitters (Mohsenin, 1980). If the two cups have the same initial temperature and the surrounding medium (air or fluid) have nearly constant temperature than the net rate of heat loss through both the cups will be same. The heat balance equation for the cups can be written as (Mohsenin, 1980):

$$\frac{\Delta Q_A}{\Delta t_A} = \frac{\Delta Q_B}{\Delta t_B} \tag{3-10}$$

If the temperature changes in the cooling body are small, the specific heats are constants and the rate of heat loss is equal to rate of temperature change as (Mohsenin, 1980):

$$\begin{aligned} \frac{\Delta Q_A}{\Delta t_A} &= \left(c_A W_A + c_w W_w\right)\frac{\Delta T}{\Delta t_A} \\ \frac{\Delta Q_B}{\Delta t_B} &= \left(c_B W_B + c_{sa} W_{sa}\right)\frac{\Delta T}{\Delta t_B} \end{aligned} \tag{3-11}$$

both of the above equation can be equated by using equation (3-10) and can be rewritten after simplification as:

$$c_{sa} = \frac{(c_A W_A + c_w W_w)\Delta t_B - c_B W_B \Delta t_A}{\Delta t_A W_{sa}} \qquad (3\text{-}12)$$

where

Q = heat rate

ΔT = temperature drop for cups A and B

W = weight of the reference liquid (water) or the sample

Δt_A= time for cup A and contents to drop to ΔT

Δt_B= time for cup B and contents to drop to ΔT

The subscripts *A*, *B*, *W*, and *Sa* denote cup *A*, cup *B*, water and the sample respectively. Typical cooling curves to determine Δt_A and Δt_B are given in Figure 3.8(b) . The specific heat capacity of the sample can be calculated from equation (3-12) (Mohsenin, 1980)

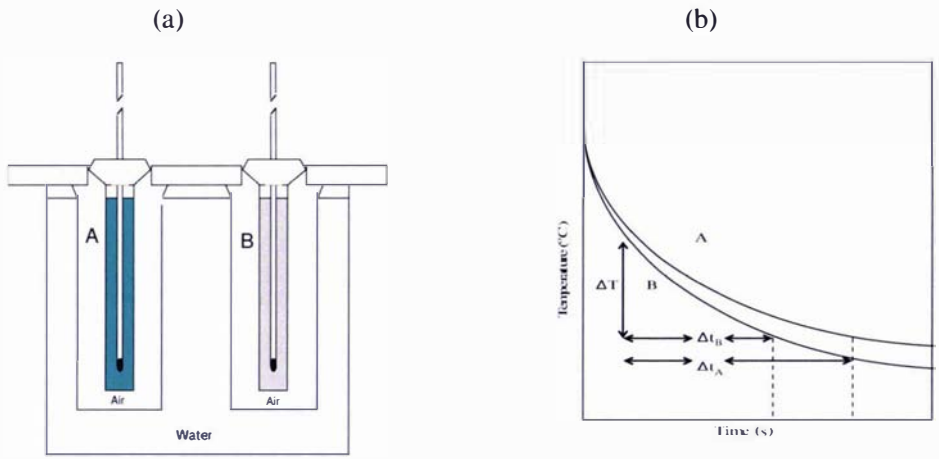

Figure 3.8: (a) Comparison calorimeter, (b) Example of cooling curve for use in method of comparison calorimeter (adapted from Mohsenin, 1980)

Moline *et al.* (1961) proposed a simple and rapid ***adiabatic method*** to measure the specific heat capacity of frozen food materials (Figure 3.9). The apparatus consists of rectangular polystyrene foam with a cylindrical hole in the center to place the aluminum sample container. A polystyrene plug is inserted on the top to minimise the heat transfer to the sample. The sample container is filled with the sample, frozen in liquid nitrogen rapidly till it reaches the equilibrium temperature and then it is transferred quickly to the foam block maintained at room temperature. Moline *et al.* (1961)

measured the heat leakage Q (Js^{-1}) of the calorimeter by using a sample of standard copper material with the known weight and specific heat capacity as:

$$Q = c_{copper} W_{copper} \frac{\Delta T_c}{\Delta t} \tag{3-13}$$

Where c_{copper} and W_{copper} is the specific heat capacity ($J\ kg^{-1}{}^{o}C^{-1}$) and weight (kg) of the copper probe, and $(\Delta T_c/\Delta t)$ is the rate of the core temperature change. Once the rate of heat leakage is determined over the temperature range of interest, the specific heat of any material of identical geometry may be determined, assuming that the rate of heat transfer into the cell will be the same at any given temperature. The specific heat capacity of food sample is then calculated as:

$$c_{sample} = \frac{\dfrac{Q}{\left(\dfrac{\Delta T_c}{\Delta t}\right)} - (c_{aluminum} W_{aluminum})}{W_{sample}} \tag{3-14}$$

Where c_{sample} and W_{sample} are the specific heat ($J\ kg^{-1}{}^{o}C^{-1}$) and weight (kg) of the sample under study. By carrying out these measurements for several temperatures, the change in specific heat with temperature can be determined. This method was used by Moline *et al.* (1961) to measure the specific heat of meat. The main disadvantage of this method is the needed to do measurements at each temperature point.

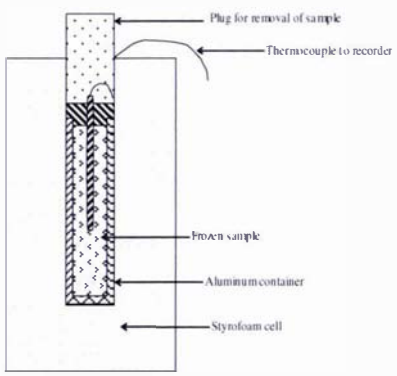

Figure 3.9: Specific heat capacity measurement apparatus for frozen specimen (Moline et al. 1961)

Mohsenin (1980) presented the ***guarded hot plate method*** to measure the specific heat capacity of food and agricultural materials. In this method the specimen is surrounded by electrically heated thermal guards as shown in Figure 3.10. The specimen and the thermal guards are maintained at the same temperature so there is no heat loss from the specimen and the specimen is electrically heated. The specific heat can be calculated by the heat balance as:

Heat gain by the sample = Heat supplied by the electrical heater

$$Q = c_{sample} W_{sample} \left(T_f - T_i\right) = VIt \tag{3-15}$$

$$c_{sample} = \frac{VIt}{W_{sample}\left(T_f - T_i\right)} \tag{3-16}$$

where V and I are the voltage (volt) and current (amp) supplied to the heater during the time $t(s)$, T_i and T_f is the initial and final temperature of the sample (°C). Wright and Porterfield (1970) used this kind of calorimeter to measure the specific heat of peanuts. Their calorimeter consisted of a small cup surrounded by a resistance heating coil and foam insulation. Two thermocouples were used to measure the temperature of the peanut and calorimeter. Time temperature data for heating and cooling curves of the calorimeter with and without the sample were recorded after a constant power was turned on for a specific time. The specific heat was calculated by heat balance on total heat supplied and absorbed, and heat of desorption of water from the sample (Rahman, 1995).

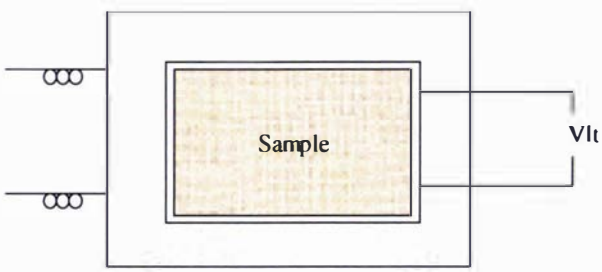

Figure 3.10: The concept of guarded hot plate method for specific heat capacity measurement (Mohsenin, 1980)

Staph (1949) and Clark *et al.* (1946) also proposed alternative calorimeters to measure the specific heat capacity of frozen foods. The detail of these calorimeters is given in Mohsenin (1980).

The ***adiabatic agricultural calorimetry*** was proposed by Riedel (1956, 1957) and the classical work done on food materials is well known. Mohsenin (1980) also used adiabatic agricultural calorimetry to measure the specific heat capacity of agricultural materials. The test chamber is usually designed such that no heat or moisture transfers to/from the chamber. The test chamber is enclosed in another chamber to provide the adiabatic conditions.

Differential Scanning Calorimetry (DSC) is the most versatile thermal analysis technique used for measuring the enthalpy and specific heat capacity of all kind of materials and is regarded as the one of the most quantitative technique (Griffen & Laye, 1992).

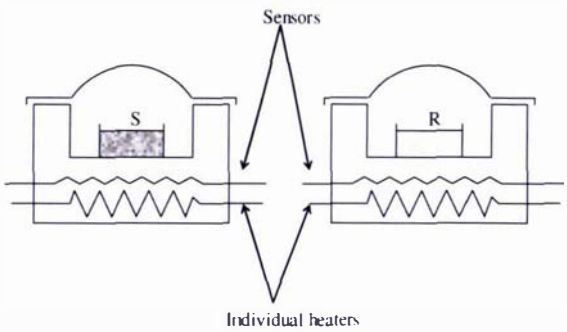

Figure 3.11: Schematic diagram of differential scanning calorimeter (Courtesy of Perkin - Elmer corp.)

A schematic diagram of a DSC is given in Figure 3.11. This method is based on measuring very small thermal effects produced in a thermal process. The recorder in the system produces a thermogram showing any gain or loss of energy as the instrument is scanned at some given rate of temperature rise over a time interval. The area inside the thermogram is proportional to the heat energy released or absorbed by the sample during the cooling or heating process.

The whole system consists of a test sample holder (S), a reference material holder (R), a temperature programmer along with heating or cooling system and a temperature / time recorder. There are two methods to analyse the DSC data. One given by Widman and Riesen (1987) and the other given by Mohsenin (1980).

The specific heat of the sample is calculated from the following relation (Widman and Riesen, 1987):

$$c_p = \frac{\left(dQ/dt\right)}{M_{(SA)}\left(dT/dt\right)} \tag{3-17}$$

where :

$\left(dQ/dt\right)$ is the heat flow rate (Js^{-1})

$\left(dT/dt\right)$ is the heating rate (Ks^{-1})

$M_{(SA)}$ is the mass of the sample (kg)

Mohsenin (1980) presented the following equation for measuring the specific heat capacity of a sample:

$$c_p = \frac{M_{SA}}{M_{REF}} \frac{d_{SA}}{d_{REF}} c_{REF} \tag{3-18}$$

where d is the deflection of the thermogram heat flow (Js^{-1}) as shown in Figure 3.12 and the reference material was sapphire with known weight and specific heat capacity. The behavior of the reference material or pan is compared with that of the sample and its pan. While measuring the specific heat capacity of a sample it is corrected by subtracting the heat capacity of the empty pan.

Specific heat capacity is a fully normalized output of a DSC, i.e. the displacement during a scan is equal to the product of the heat capacity times the sample weight times the scanning rate plus the no-sample baseline. DSC data is sometimes misinterpreted because just one heat flow run is performed. The data from that run may contain the information about the instrument itself such as

the specific heat of the sample holder. This problem can be fixed by performing a baseline run with no sample using the same conditions to be used for the sample. This constitutes the classical two-curve specific heat capacity method.

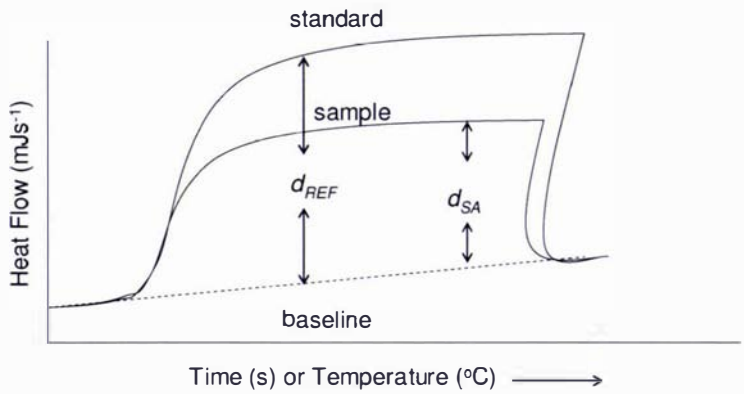

Figure 3.12: Typical specific heat thermogram of food by DSC (adapted from Rahman (1995))

Wendlandt (1986) mentioned sixteen characteristics which influence the shape of thermal analysis curves: some are incorporated in the design of the apparatus; others are available to the operator. Sample mass and preparation, crucible material, heating rate and furnace atmosphere are all known to affect the shape of the results (Wendlandt, 1986). Higher scanning rate moves the DSC peaks (latent heat) towards higher temperatures. Higher rates mean easily measured heat flows because the total latent heat change will occur over a smaller time interval, but it is less likely to have uniform temperature in the sample as assumed in the DSC analysis and so the sample appears to melt at higher temperatures.

DSC can be used to observe both melting and freezing phenomena in the sample. It has the advantage of covering the whole range of the temperature of interest in one analysis.

A Micro- Calorimeter method is suggested by Ohlsson (1983) as an alternative to DSC where the reference material is not available. Thermopiles are placed around the sample and around an empty

reference cell. Specific heat capacity is calculated from the difference between the heat flows into the sample and the reference cell.

Since DSC was the only apparatus available to use in the research, it was used to measure the specific heat of butter. Construction of other specific heat capacity measurement instruments like the adiabatic calorimeter was a time taking process. Moreover these calorimeter instruments require measurement at each temperature rather giving specific heat capacity as a continuous function of temperature.

3.5.2 Measurement of Specific Heat Capacity and Enthalpy

To model thawing and freezing of butter and in an attempt to improve the existing knowledge on the thermal properties of butter over the range of interest, a power compensated Perkin Elmer 7 DSC 7 was used to measure the specific heat capacity and enthalpy of butter. It was important to develop a robust DSC measurement methodology and to demonstrate accuracy. Factors that must be considered in DSC methodology and operation include:

- Measurement technique
- Scanning rate
- Phase separation
- Sample homogeneity
- Variation in frozen water contents
- Equilibrium melting compared with supercooling of the water phase
- Equilibrium melting compared with supercooling of the bulk fat phase
- Hysteresis effects brought about by microstructural changes.

Before investigating each of these effects, a generic methodology is needed for sample preparation and calibration of the DSC.

3.5.2.1 Generic Methodology

Sample preparation: Aluminum volatile sample pans and lids were pre weighed before preparing the sample and placing in a labeled vial. The sample pans used for determination of specific heat capacity were of approximately the same weight as the reference pan to avoid error due to the sample pan weights. The samples of all butters were prepared in a cold room at approximately 4°C. A cork borer with a diameter approximately equal to the base of the aluminum pan (3.5 mm) was used to collect the sample of the butter. By pushing a cylindrical sample from the cork borer a slice

of about 1 mm thickness was cut and placed in the sample pan. It was ensured that the samples sat flat in the sample pan for good thermal contact and that the top of the sample did not protrude above the base of the sample pan. If the sample is too high it may contact the lid of the sample pan and uneven heating during the DSC run would distort the results. The sample pans were sealed using the sample closure tool (PE 0219-0061). The sample was then put in the vial again and left in the cold room. All the samples were weighed before and after the DSC run to check for any weight loss due to moisture loss via a bad seal which could contribute to higher specific heat capacity values.

Calibration: To minimize the measurement error, the DSC should ideally be calibrated with the standards having a melting onset within the temperature range of interest. The DSC was calibrated with octadecane and n-decane according to the manufacture's specification for the onset temperatures and enthalpies of fusion given in Table 3.10 (Perkin Elmer DSC manual).

Table 3.10: Calibration standards for the DSC

Standard	Onset (^{o}C)	ΔH (kJkg^{-1})
n-decane	-29.66	202.09
Octadecane	28.24	241.42

Operation: After calibrating the DSC it was set to 0^{o}C. To analyze a butter sample the DSC dry box purge gas flow was set to high. The sample was loaded into the DSC sample holder very quickly and smoothly to ensure that sample did not get warm to avoid any phase separation. The purge gas flow was then set to normal low flow. The sample was then cooled down to the required temperature immediately.

3.5.2.2 Measurement Technique

As described earlier there are two methods to determine the specific heat of a material using DSC (Widman & Riesen, 1987 and Mohsenin, 1980). Mohsenin's method is considered to be the most reliable and is recommended by the ASTM (method 1269E, 2005), but it is more time consuming due to an extra run being required using the sapphire standard as compared with the Widman & Riesen method. Both methods have been used by a number of researchers successfully. Tang *et al.* (1991) and Yang *et al* (1997) both used the Widman and Riesen method to determine the specific heat capacity of lentil and borage seeds respectively.

The measurement method of Mohsenin (1980) was tested by determining the specific heat of sapphire using the DSC method and comparing it with the well-known relationship given by Sarge *et al.* (1994):

$$c_p(T) = A + BT + CT^2 + DT^3 + ET^4 + FT^5 + GT^6 + HT^7$$

where the values of A to H are given in the Table 3.11 for two temperature (K) ranges.

Table 3.11: Constants for the specific heat capacity of sapphire (Sarge et al. 1994)

Constant	T = 70 – 300K	T = 290 – 2250K
A	3.63245×10^{-2}	-5.81126×10^{-1}
B	-1.11472×10^{-3}	8.25981×10^{-3}
C	-5.38683×10^{-6}	-1.76767×10^{-6}
D	5.96137×10^{-7}	2.17663×10^{-8}
E	-4.92923×10^{-9}	-1.60541×10^{-11}
F	1.83001×10^{-11}	7.01732×10^{-15}
G	-3.36754×10^{-14}	-1.67621×10^{-18}
H	2.50251×10^{-17}	1.68486×10^{-22}

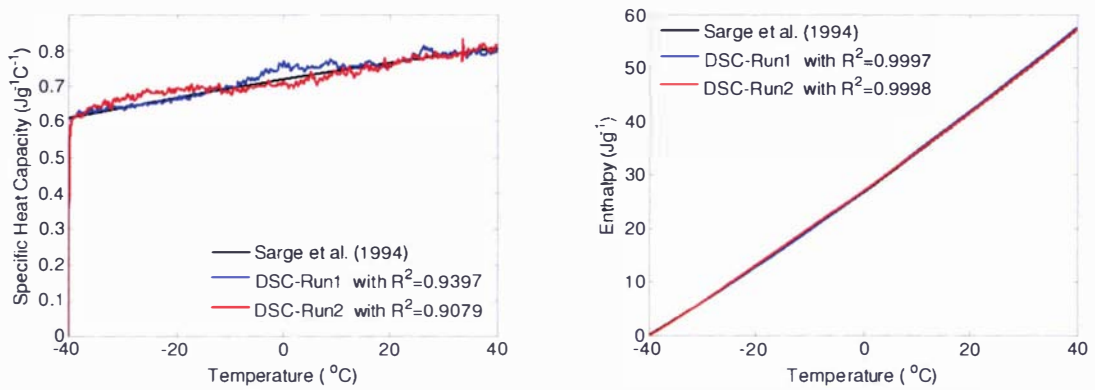

Figure 3.13: Measured specific heat capacity and enthalpy of sapphire compared with literature data

In the current work a base line with the empty pans was determined first for better precision. The empty pan run was performed by cooling the pans to -40°C at a rate of 10°C per minute from 0°C, holding for 10 minutes and then heating it up at a rate of 1°C per minute. The sapphire sample was

also run in exactly the same way. The specific heat capacity was determined by the software Pyris 1 DSC using the two curve method. Two independent runs were done on the sapphire. The results thus obtained are given in Figure 3.13. There is little difference in the results and they agree well with the literature values for the specific heat capacity and the enthalpy of sapphire.

To check the DSC method for butter the specific heat capacity of a sample of butter was determined in the same way and the results were compared with the specific heat determined by Mohsenin's method (ASTM standard 1269E, 2005) using sapphire as a standard using a scanning rate of 1 $^{o}Cmin^{-1}$. The results obtained are given in Figure 3.14.

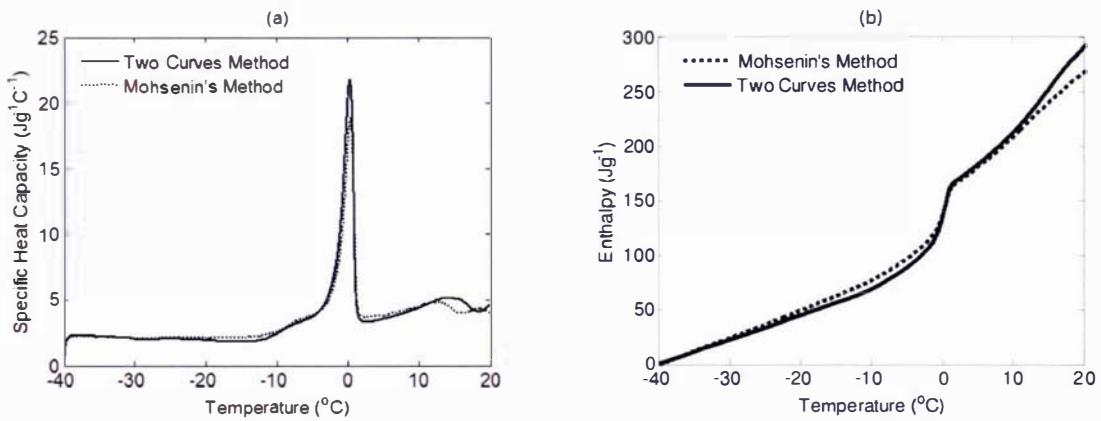

Figure 3.14: (a) Specific heat capacity (b) Enthalpy of unsalted butter (B17) with two curve method compared with Mohsenin's Method (scanning rate 1 $^{o}Cmin^{-1}$)

There was little difference between the results given by the two methods. The most important differences in enthalpy between the two methods were at the higher temperature (above 10°C) as the differences in the specific heat capacity accumulate throughout the heating process.

From the above experiments it was concluded that the two curves method is reliable to use for measuring specific heat capacity of butter. This method saves time as it requires only two runs, one for the base line with empty pan and the other for the sample.

The butter (B17) used for this measurement was an unsalted butter. The specific heat capacity in the temperature range of -40°C to about -10°C remained constant at about 2 kJ $kg^{-1}{}^{o}C^{-1}$. There was an increase in the specific heat capacity above -10°C due to the melting of triglycerides and at about 0°C there is a large peak of water melting. There is some difference in the height of both the peaks which could be due to slightly different moisture content in the two samples of the same butter. The

butter seemed to be still melting above 0°C which is probably due to the thermal lag within the sample because of the temperature gradient between the bottom of the sample pan and the sample. If the scanning rate is very slow then this problem can be overcome to some extent. Above 0°C the specific heat capacity of butter is not constant and is a very complicated function due to melting of the triglycerides that varies with season, time of lactation etc.

3.5.2.3 Scanning Rate

Scanning rate has a large effect on the measurement of the specific heat capacity, especially in the phase change region which could shift the specific heat capacity or enthalpy curve to the right (high temperature) with increasing heating rate. The reason is the assumption that during the test, the temperature in the sample and sample pan is uniform. Tang *et al.* (1991) mentioned that due to the low thermal diffusivity of biological materials, thermal lag within the sample may introduce significant error in the measured value of the specific heat capacity value. Therefore, it was, necessary to choose an appropriate scanning rate. Scanning rates of 1 °Cmin^{-1}, 5 °Cmin^{-1} and 10 °Cmin^{-1} were used on samples of butter to see the differences. The DSC was calibrated at each rate before performing each experiment. The results for the specific heat capacity and enthalpy at the three different rates are given in Figure 3.15

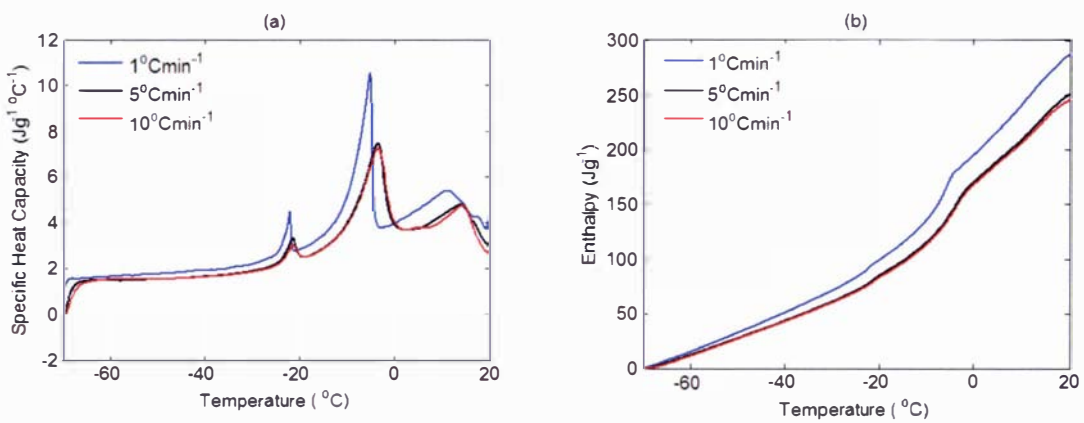

Figure 3.15: (a) Specific heat capacity (b)Enthalpy of salted butter (B15) at different scanning rates

Higher scanning rates shifted the specific heat curve to the right. There was little difference in the runs with scanning rates at 5 °Cmin^{-1} and 10 °Cmin^{-1} but a large difference relative to 1 °Cmin^{-1} data. The specific heat capacity of the butter was nearly constant below -30°C. Two distinct water

melting peaks can be seen in this butter. One peak is at about -22°C and the other is at about -5°C. The butter (B15) in this run was salted and, therefore, had salt in the water phase which caused the initial freezing point to be depressed. The two peaks are probably due to variation in salt concentration. In Fritz butter a small population of droplets has a higher concentration of salt in them compared with the bulk of the moisture droplets which caused them to melt at about -22°C, while more of the population has some lower concentration of salt (<8 %) so they melt at about -5°C as anticipated. The difference in water peaks could be due to differences in different moisture contents in the two samples of same butter. The shift of the curve to the right for higher scanning rates gives a significant difference in the initial freezing point of the butter.

It is expected that there could be differences if a scanning rate lower that $1^{\circ}Cmin^{-1}$ was used. To go lower than $1^{\circ}Cmin^{-1}$ was not a practical option due to a large amount of time involved in testing each sample. Therefore a scanning rate of $1^{\circ}Cmin^{-1}$ was used for the measurement of specific heat and enthalpy, but subsequent corrections around the ice melting region were investigated (detail later in the thesis).

3.5.2.4 Phase Separation

When butter is heated to relatively high temperature, there is a potential for phase separation (water droplet co-alescence) to occur. To investigate if this phenomenon would affect specific heat capacity measurements a sample of salted butter was heated up at a rate of $1^{\circ}Cmin^{-1}$ from -40°C to 40°C and then cooled down to -70°C at a rate of $10^{\circ}C\ min^{-1}$ to repeat the measurements. The results obtained are given in Figure 3.16.

The results were surprising. Although the enthalpies at 5°C of the two runs were identical, the repeated run showed two distinct melting peaks. The reverse behavior was expected, as in Fritz buttermaking process two different water droplets distributions are present. Some were originating from the butter milk and some originating from the added salt slurry. In this situation two melting peaks might be observed. If droplets co-alescence occurs then it follows that salt concentration in the different droplet distributions might converge giving a single melting peak.

The observation of two melting peaks after heating to 40°C where previously there had been one was also observed in other salted butter samples. The reason for this is not clear. Possibly salt crystals trapped in the fat fraction of butter dissolve in some water droplets, upon heating to 40°C, thereby reducing the initial freezing point of these droplets.

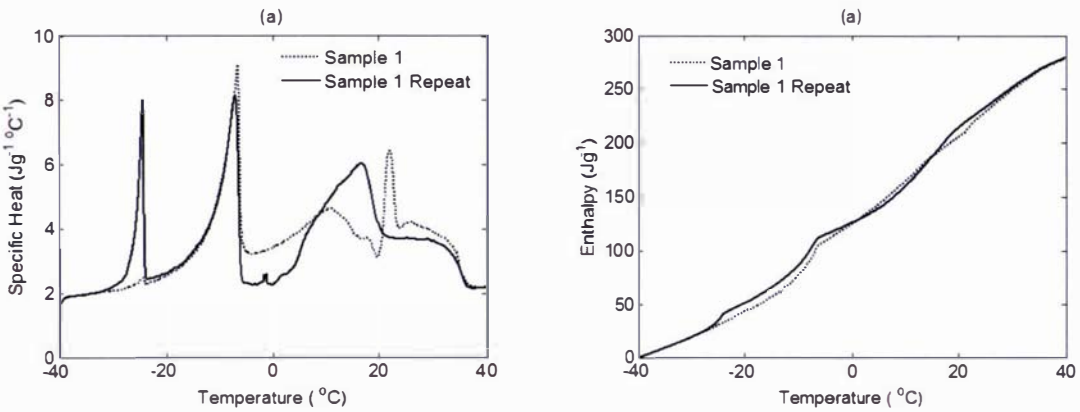

Figure 3.16: (a) Specific heat capacity (b)Enthalpy from repeated DSC trial with the same sample of butter (B15)

Based on this observation it was decided that duplicate measurements for the same sample would not be used. Any duplicate experiment on the same butter was performed on a new sample of butter.

3.5.2.5 Sample Homogeneity

Because only small samples are used in the DSC technique (5-15mg) it was important to demonstrate repeatability by using replicate samples from the same butter. Two samples of the same butter were chosen from a block of butter (B17).

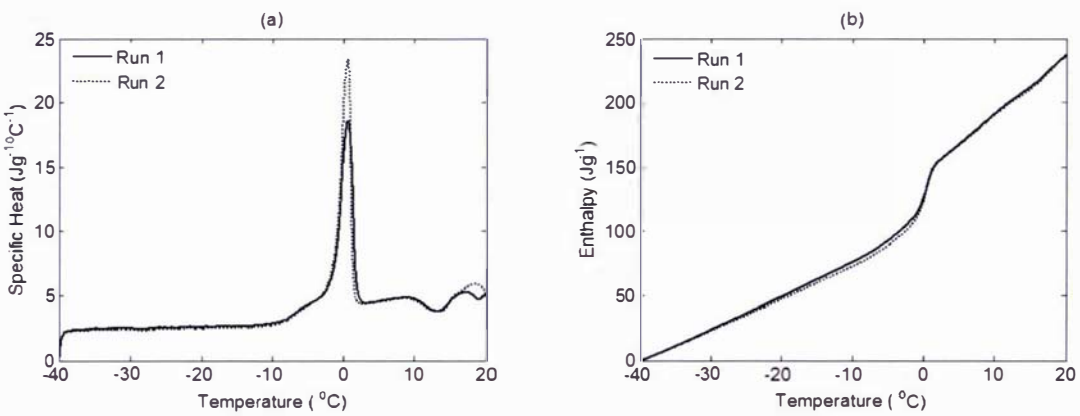

Figure 3.17: (a) Specific heat capacity (b) Enthalpy of the same kind of butter (B17) for two samples done on the same day.

Figure 3.17 shows the specific heat capacity and enthalpy of duplicate butter samples of one unsalted butter (B17) done on the same day. Both the samples are very consistent apart from the water melting peak near 0°C being slightly higher for run 2. This was probably due to slightly higher water contents compared with the Run-1 sample. Overall there was little change in the total enthalpy change.

3.5.2.6 Variation in Frozen Water Contents

Values for the specific heat capacity and enthalpy of butter are required in the range of -20°C to 10°C for modelling work but the water in the butter could supercool and may not freeze at -20°C and this is likely to differ for salted and unsalted butter. It was therefore required to investigate the freezing DSC behavior for both the unsalted and salted butters.

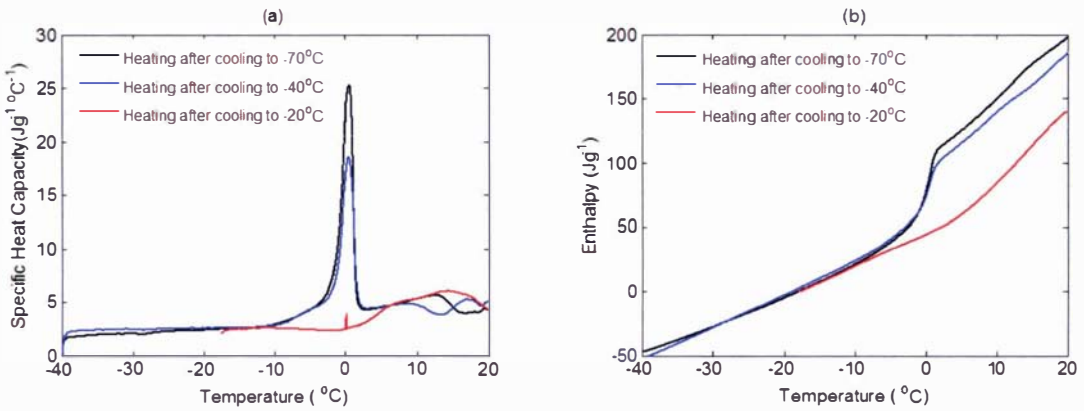

Figure 3.18: (a) Specific heat capacity and (b) Enthalpy of unsalted butter (B17)frozen to different temperatures

Figure 3.18 shows the specific heat capacity and enthalpy of the unsalted butter frozen to -70°C, -40°C and -20°C and held for 10 minutes prior to heating DSC run. The butter did not fully freeze after 10 minutes at -20°C and only a tiny peak can be seen at approximately 0°C. Most of the water in the butter froze at -40°C and the butter was more completely frozen when cooled down to -70°C. The water in the butter would supercool rather than freeze and it was observed (although not recorded) from the DSC thermogram for cooling that the butter sample froze just below -40°C.

The same procedure was repeated on salted butter. Figure 3.19 shows that the salted butter did not fully freeze even after cooling to -40°C due to the salt concentration reducing the initial freezing point and allowing even greater supercooling. The water in salted butter appears to supercool to a

lower temperature as compared with unsalted butter. From the cooling DSC thermogram for salted butter it was observed that the butter froze below -50°C (Figure 3.20).

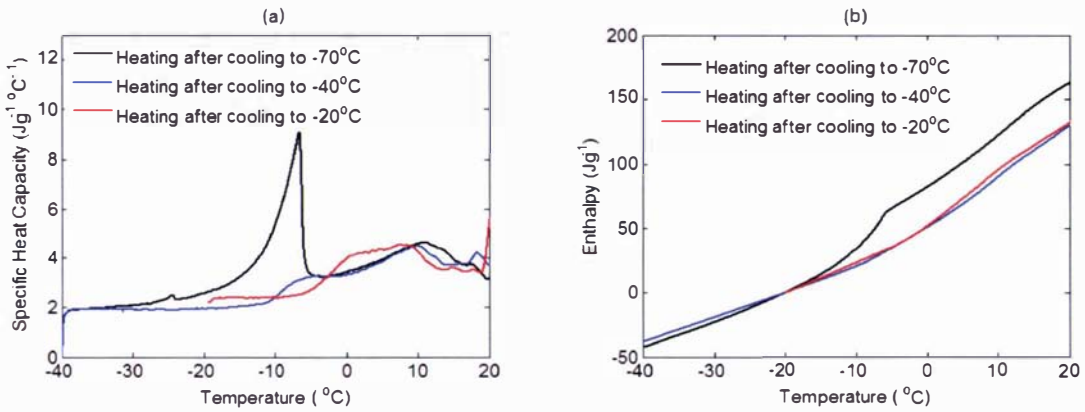

Figure 3.19: (a) Specific heat (b) Enthalpy of salted butter (B15) measured by heating runs after cooling to -20°C, -40°C and at -70°C

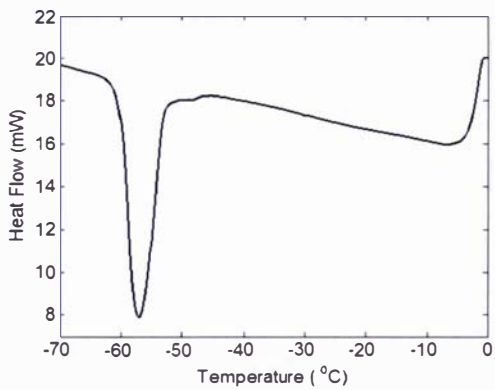

Figure 3.20: Cooling of a salted butter sample (B15) at a rate of 10°Cmin^{-1} to avoid the water supercooling problem

As a result of these findings it was decided that the butter sample should be cooled to -70°C to ensure complete freezing, heated up to -40°C at a rate of 10 °Cmin^{-1} prior to each heating DSC measurement at a rate of 1°Cmin^{-1}.

3.5.2.7 Equilibrium Versus Supercooling of the Water Phase

Since the water in the butter supercools during cooling runs, the specific heat capacity of water will not change until the water starts to freeze. Some of the milkfat fraction may also freeze or could

supercool over the temperature range of interest. This means that the specific heat capacity measured during DSC heating of butter might not be appropriate for modeling the freezing process. Therefore the difference between the specific heat capacity during cooling and heating was measured. A sample of unsalted butter (B12) and a sample of salted butter (B15) were cooled down from 10°C to -70°C at a rate of 1°C min^{-1} and then heated to 10°C. Measurements were taken during both the heating and cooling stages. The process was repeated three times using the same sample without removing it from DSC. Since it was heated up to just 10°C, no separation of the phases was likely.

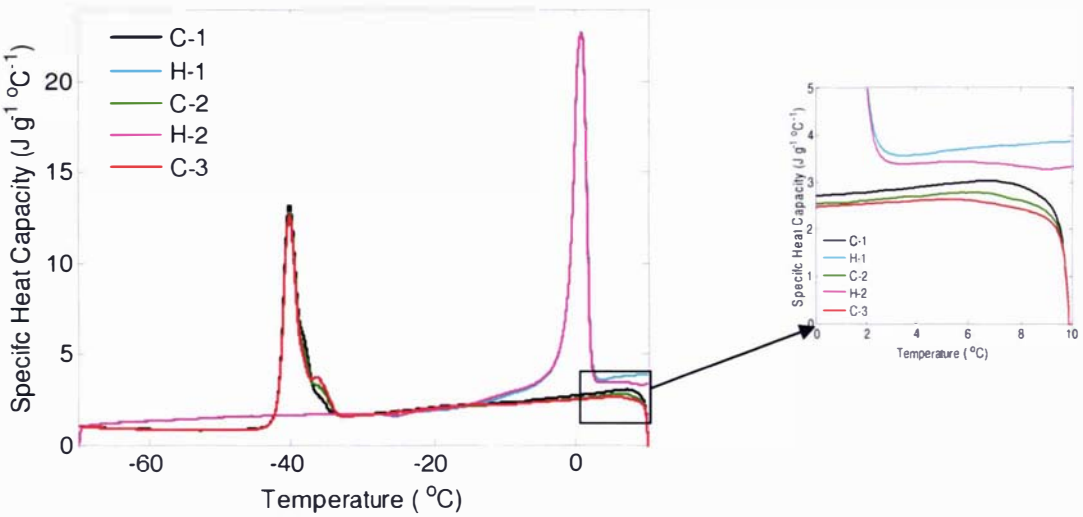

Figure 3.21: Specific heat capacity from repeated heating and cooling of a unsalted butter sample (B12)

The results for the unsalted butter are shown in Figure 3.21. H-1 and H-2 are the 1st and 2nd time heating specific heat capacity and C-1, C-2 and C-3 are the cooling specific heat capacities. The peak at about 0°C in the heating curves is the water melting at equilibrium temperature, whereas the peak at -40°C in the cooling curves is the non – equilibrium freezing due to super cooling. The specific heat capacity of the 2nd run was slightly lower than the 1st run for both cooling and heating at temperatures above 0°C (see inset in Figure 3.20), while the 3rd run was only slightly lower than that of 2nd run. The reason is likely to be the complex structure of the fat crystallization. Before performing the 1st run, the butter was heated up from 0°C to 10°C at a rate of 10°C min^{-1} and was held there for 10 minutes. Whereas in the 2nd run the butter was heated up from -70°C to 10°C at a rate of 1°Cmin^{-1} and held there for 10 minutes before starting the 2nd cooling run. This change in the cooling and heating rate could affect the crystallization of fat. Recrystallisation of the fat could alter

the composition and therefore the melting points of the crystals. In particular this treatment is likely to reduce the amount of α crystals than the β crystal in the fat. α crystals have higher specific heat capacity and therefore the overall measured value will reduce.

The specific heat capacity from heating and cooling runs above -10°C was also found to be quite different. This is probably due to the significant supercooling and crystallization of the fat fraction in the butter at temperatures well below the equilibrium phase change temperature during cooling. In this case supercooling is caused by the time delay required for crystallization (triglycerides take time to move to the surface of the fat crystals) rather than a lack of crystal nuclei. During heating, as the melting occurs at equilibrium phase change temperature, the apparent specific heat capacity above T_{if} includes a fat latent heat component. The specific heat capacity of supercooled butter remains relatively constant, dropping from 2.5 kJ $kg^{-1}{}^{o}C^{-1}$ to 1.8 kJ $kg^{-1}{}^{o}C^{-1}$ over the range T_{if} down to -45°C.

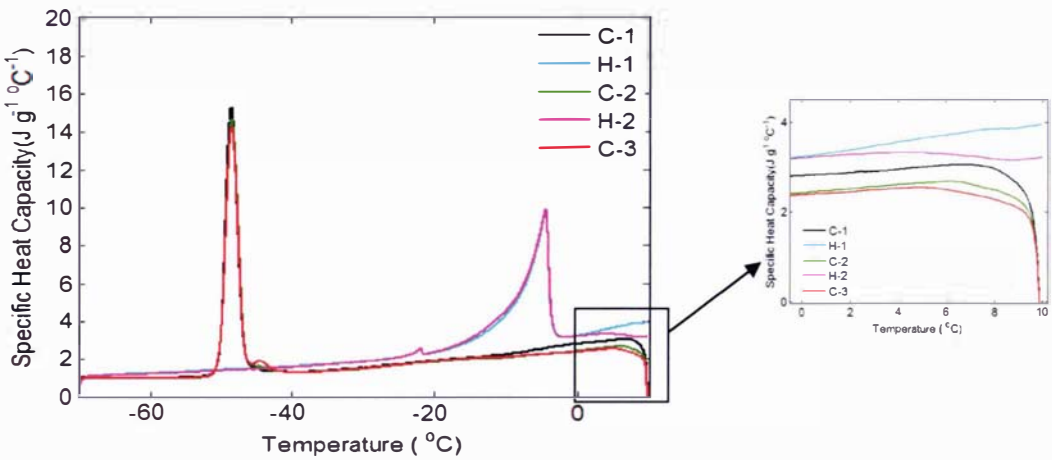

Figure 3.22: Specific heat capacity measured from repeated heating and cooling DSC runs for one salted butter sample (B15)

Figure 3.22 shows the measured specific heat capacity of cooling and heating for a salted butter (B15). The trends for unsalted butter can also be observed for salted butter. The water fraction of the butter froze at about -50°C, after supercooling well below its initial freezing point. The cooling and heating specific heat capacity profiles are significantly different. Again the repeated sample measurement had lower specific heat capacity above -5°C. This suggests that some changes in the fat crystal network occur upon repeated heating and cooling.

In salted and unsalted butter the average specific heat capacity for cooling was 3.1 kJ $kg^{-1}{}^{o}C^{-1}$ and 3.2 kJ $kg^{-1}\,{}^{o}C^{-1}$ respectively above the initial freezing point.

3.5.2.8 Equilibrium Versus Supercooling of the Bulk Fat Phase

It is believed that the difference in the specific heat capacity above 0°C observed in butter between heating and cooling DSC run is due to milkfat supercooling caused by the time taken for fat crystallization and that the reduction observed in repeated temperature cycling is due to the milkfat crystal modification. To test this hypothesis, fat was separated from the unsalted butter (B12) by heating 250 g of butter to about 100°C in an oven and then separating it from the serum. The specific heat capacity and enthalpy of the milkfat was then measured using DSC. The DSC runs were carried out in exactly the same way as for the butter samples to see the differences between the specific heats.

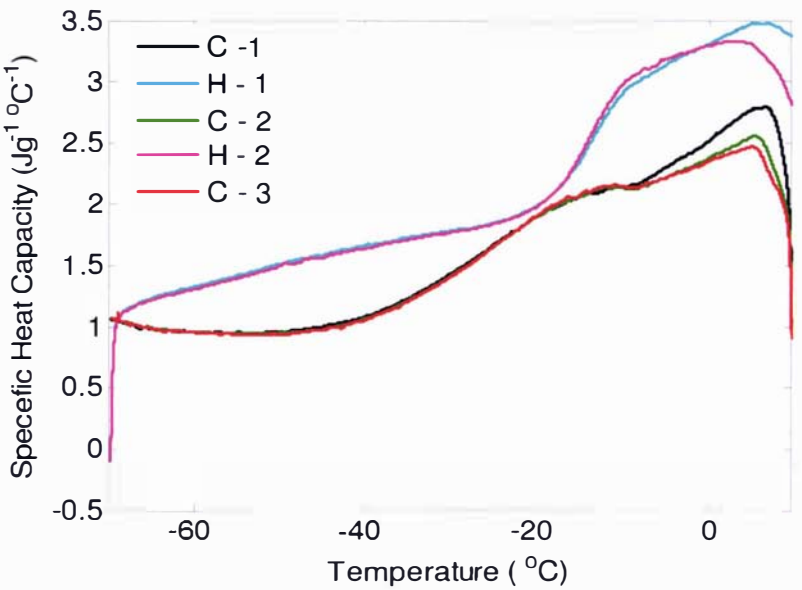

Figure 3.23: Specific heat capacity of repeated heating and cooling of separated milkfat

The results of these experiments are given in Figure 3.23. The cooling and heating specific heat capacity of the butter fat is clearly different over the whole range of temperature, with much greater heat being required to melt the milkfat than required to cool it. This is consistent with milkfat supercooling and the observation made for the whole butter (Figures 3.21, 3.22). The specific heat

capacity of the repeated runs also decreases exactly as that observed in butter. This is evidence to support the hypothesis that repeated heating and cooling result in differences in crystal structure of the fat phase in the butter.

Middleton (1998) explained that if milkfat is heated above its melting point and then cooled rapidly then the specific heat capacity is initially low but rises gradually to a steady level over the following 4-5 hours. This increase is due to a gradual rise in the rate of fat crystallization.

Figure 3.24 shows the heating specific heat capacity and enthalpy of milkfat compared with the specific heat capacity and enthalpy of the salted butter frozen to -40°C and unsalted butter frozen to -20°C. The total enthalpy change of milkfat and the unfrozen butters in the temperature range -40°C to 10°C is approximately the same. In the temperature range from -10°C to +10°C the average specific heat capacity of milk fat is 3.2 kJ $kg^{-1}°C^{-1}$ and if it is combined with the 15% of water (cp = 4.18 kJ $kg^{-1}°C$) and 85% of fat an average specific heat capacity of 3.4 kJ $kg^{-1}°C^{-1}$ can be estimated for butter. It is clear that in this range the apparent specific heat capacity is dominated by the crystallisation of the fat fraction of butter which in turn depends on the triglyceride composition in the fat.

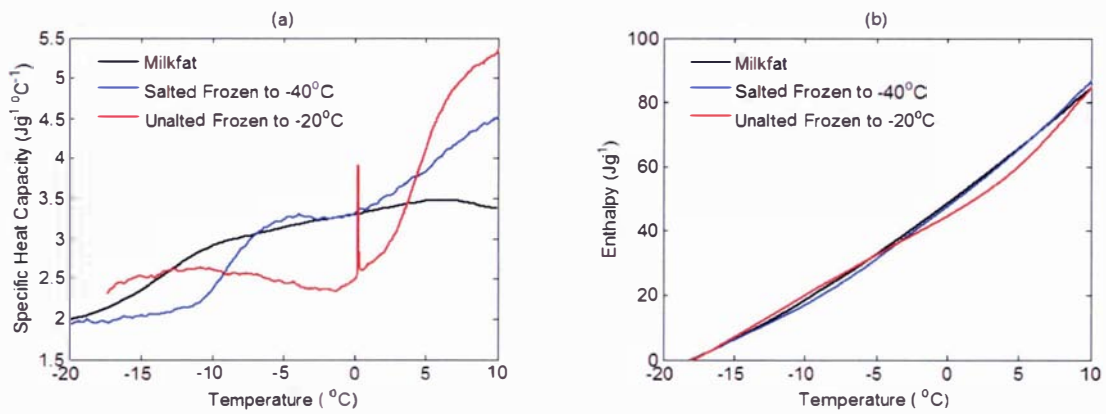

Figure 3.24: Specific heat capacity and enthalpy of milkfat compared with the specific heat and enthalpy of salted butter frozen to -40°C and unsalted butter frozen to -20°C

3.5.2.9 Hysteresis Effects Brought About by Microstructure

It was observed in DSC runs that repeated thawing and freezing gave a lower value of specific heat capacity. To check whether this change is observed when bulk butter is repeatedly thawed and

frozen, samples were taken from salted and an unsalted butter blocks 8 months apart and the specific heat capacity was measured using DSC. During the eight months the butter blocks were thawed and frozen many times. Figure 3.25 gives the cooling specific heat capacity of the two samples of salted and unsalted butter measured eight months apart. Interestingly in the first run, two water freezing peaks were observed. This was probably due to the presence of two distinctly different water droplet distributions with different salt concentration. One was derived from the cream in the Fritz butter making process. The second was due to the addition of standardization water and salt slurry. Because of a difference in solute concentration in these different droplets, they freeze/melt at different temperatures. In the second run, there is only one distinct freezing peak indicating that the water droplets now are more homogenous in concentration as compared to the earlier run. Possibly the repeated thawing of the butter block has facilitated diffusion of the salt and other solutes through the fat phase of butter or perhaps co-alescence of adjacent droplets.

This phenomenon had no significant effect on the heating enthalpy values or the initial freezing point of the water phase but would affect the crystallization process.

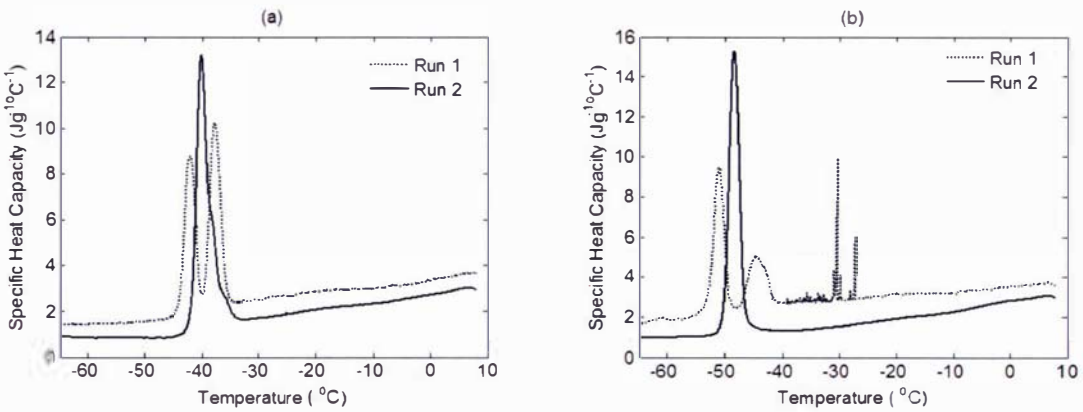

Figure 3.25: Specific heat capacity
(a) unsalted butter (B18)
(b) salted butter (B15) measured by cooling DSC runs
Run 2 measured eight months later than Run 1

3.5.2.10 Method Summary

From these preliminary experiments a number of phenomena were identified which influence the appropriateness and the quality of the DSC derived enthalpy and specific heat capacity data. The

impact of the scanning rate, phase separation, sample homogeneity and the variation in fraction of frozen water as a function of temperature were observed. Differences were observed between the cooling and thawing enthalpy of butter due to supercooling of the water and fat phase during cooling and equilibrium thawing during heating of butter.

From those observations the following DSC methodology was carried out on the full range of butter samples (Table 3.1) to identify the effects of composition and season on the enthalpy curves.

1. The samples were prepared and loaded at 0°C into the DSC (see Sections 3.6.2.1 and 3.6.2.3) after calibrating the DSC with two standards (octadecane and n-decane see Section 3.6.2.2)
2. An iso-thermal step of ten minutes at both ends of the run was used to ensure the samples were homogenous in temperature and to get better temperature control in the DSC.
3. The sample was cooled to -70°C from 0°C at a rate of 10°C per minute to achieve complete freezing.
4. A scanning rate of 1°C min^{-1} was used to minimise the occurrence of temperature gradients in the samples.
5. The temperature range for the specific heat capacity measurement was -40°C to +40°C.
6. The specific heat capacity and enthalpy was determined using the built in software (Pyris specific heat capacity software) that incorporated the baseline and the sample compensation and were saved separately as text files for further analysis and comparison.

3.5.2.11 Results and Discussion

The specific heat and enthalpy for all 17 butter samples (Table 3.2) were measured by the above method. For ease of interpretation, the results were divided into two main classes by butter type, namely salted and unsalted butter, as they have significant differences in the initial freezing point. The unsalted butter was further divided into lactic and standard unsalted butter. Figure 3.26(a) shows the enthalpy results for the salted butters. The measurements are consistent below -20°C.

Variation in enthalpy results above the initial freezing point is due to the different composition of triglycerides in the fat fraction and the moisture content of the butter. Table 3.12 compares the initial freezing point of salted butter estimated from the salt concentration in the aqueous phase (Eq. 3-3) with the DSC derived initial freezing point.

The initial freezing points (Table 3.4 and 3.7) of the butters are considerably higher than estimated initial freezing points (intersection of enthalpy curve above and below the initial freezing point). This difference is due to the temperature lag of the DSC which is still significant at a rate of scanning rate of 1°C min^{-1} (Wendlandt, 1986).

Table 3.12: Comparison of estimated (Eq. 3-3) and DSC measured initial freezing point

Butter ID	T_{if} (estimated) (°C)	T_{if} (DSC) (°C)
B2	-5.64	-5.4
B3	-5.5	-5.1
B4	-5.35	-5.0
B15	-5.35	-4.8

(a)

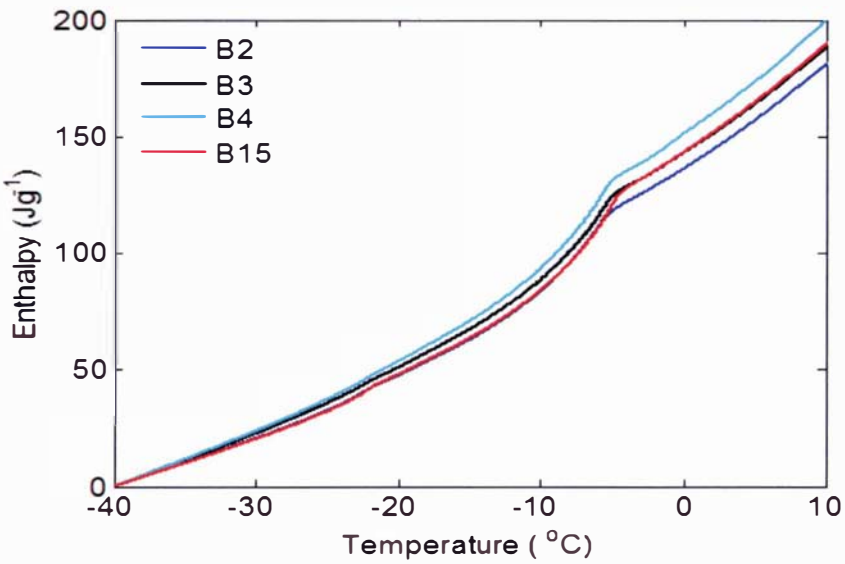

(b)

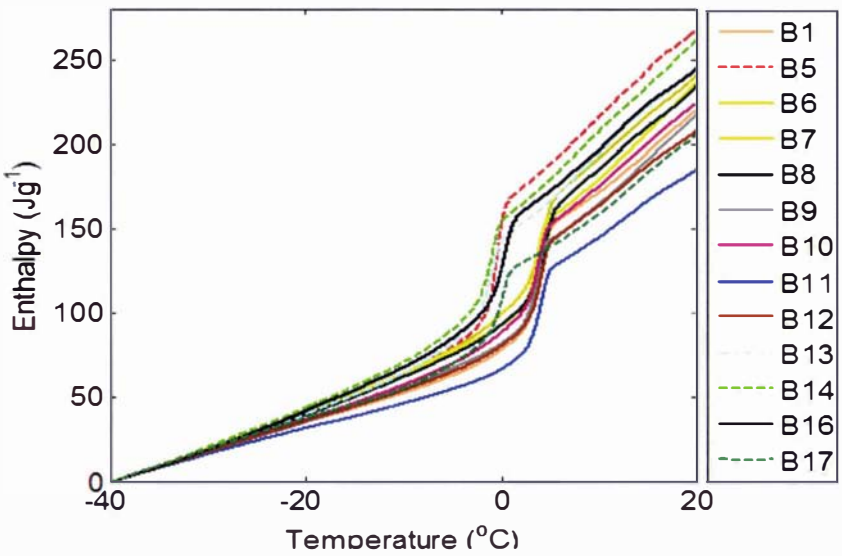

Figure 3.26: Measured enthalpy for (a)Salted butter (b) Unsalted butter using DSC

Figure 3.26 (b) shows the measured enthalpy of unsalted butters. The apparent initial freezing point was above 0°C for all the butters. Differently sized samples were used for the measurements of enthalpy as it was not possible to control this precisely. A typical sample size between 5-10 mg was used. Small sizes samples gave less temperature lag in comparison with larger size samples which confirms that thermal lag is a significant problem.

To use these data to model heat transfer in butter it was required to adjust enthalpy data to take account of the thermal lag of DSC.

3.5.2.12 Adjusting and Modeling the Measured Data

To use the data in subsequent heat transfer models, a simple equation for enthalpy as a function of temperature was required. Although the measurements were done over a temperature range of -40°C to +40°C, the models were fitted from -40°C to 10°C as this is the range of importance in industry. Above 10°C, the specific heat capacity of butter changes significantly due to the melting of fat which, in turn, strongly depends on milkfat composition

Schwartzberg (1976) gave the following equation for the enthalpy of water enriched foods:

$$H = A + c_f T + B/T \qquad T < T_{if} \tag{3-21}$$

$$H = H_o + c_u T \qquad T \geq T_{if} \tag{3-22}$$

where

A = Constant (kJ kg^{-1})

B = Constant (kJ K kg^{-1})

c_u = Specific heat capacity of unfrozen food (kJ $kg^{-1}K^{-1}$)

c_f = Specific heat of capacity frozen food (kJ $kg^{-1}K^{-1}$)

H_o= Enthalpy at 0°C (kJ $kg^{-1}K^{-1}$)

Below the initial freezing point the enthalpy-temperature curve is represented as the sum of a straight line and a hyperbola. The component c_fT is the sensible heat component, $-B/T$ is the latent heat component and A is integration constant depending on the datum temperature. Above freezing, the curve is the sum of component enthalpies and can be represented as a straight line as phase change is negligible or uniform.

There is a lag in the measured DSC temperature due to temperature gradients in the sample and this distorts the DSC derived enthalpy curve and initial freezing point so it is appears higher than it is in reality. This phenomenon is most significant when greater heat flows are required such as when there is significant melting of ice. As such, in the regions of the curve where only sensible heat is required, the DSC result are reliable (e.g. below -20°C). This means the onsets of the melting peak are at the correct temperature but the peak and the completion temperature are shifted to higher temperatures. How much they are shifted depends on the size of the sample, the amount of the latent heat required and the heating rate. To deal with this problem a modelling approach was taken to curve fit the data using the following adjustment procedure:

- -40°C was used for the enthalpy datum;
- the total enthalpy change from –40 to +10°C from the heating DSC run was maintained because this was the accumulated heat flow over the experiment and the sample temperatures were well controlled at each end of the curve;
- T_{if} was specified by the cryoscopy measurement for the unsalted butter (Table 3.4) or estimated from salt concentration for salted butter (Table 3.7);

- the specific heat capacity was set constant from 10°C down until the phase change occurred;
- Constant specific heat capacity was also used from –40 to –20°C;
- For the enthalpy above freezing Equation (3-22) was fitted to the DSC data and the straight line was then extrapolated down to the initial freezing point of the butter;
- Below the initial freezing point, three points were fixed, the enthalpy at -40°C, the enthalpy at -20°C and enthalpy at the initial freezing point as shown in the Figure 3.26. Equation (3-21) was fitted to these three points to give the adjusted shape of the curve in the phase change region.

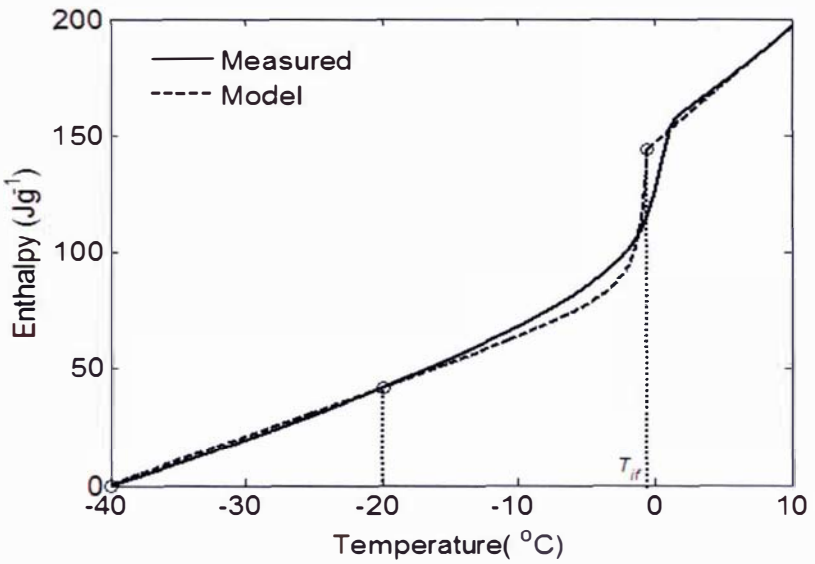

Figure 3.27: Measured and modeled enthalpy of butter

Figure 3.27 shows the measured and modeled enthalpy profile for butter sample B16 from -40°C to 10°C. The same procedure was repeated for all the measured butter data. Table 3.13 gives the curve fitted parameters calculated for each butter.

Table 3.13: Enthalpy equations parameters for all butters

Code	A (kJ kg^{-1})	c_f (kJ kg^{-1}K^{-1})	B (kJ K kg^{-1})	Ho (kJ kg^{-1})	c_u (kJ kg^{-1}K^{-1})	T_{if} (°C)
B1	68.77	1.73	-25.01	130.17	4.18	-0.44
B2	71.79	1.99	-308.72	139.07	4.21	-5.64
B3	79.23	2.17	-304.33	146.00	4.25	-5.5
B4	83.61	2.29	-312.93	154.17	4.54	-5.35
B5	79.81	2.01	-20.33	161.93	5.34	-0.25
B6	78.07	1.97	-32.24	142.18	4.91	-0.52
B7	79.63	2.00	-20.78	132.99	4.58	-0.40
B8	77.31	1.95	-20.99	136.04	4.91	-0.36
B9	68.54	1.73	-25.69	121.14	4.33	-0.50
B10	72.11	1.82	-26.98	129.50	4.54	-0.48
B11	62.42	1.57	-17.37	105.40	4.02	-0.41
B12	70.08	1.76	-20.38	121.04	4.25	-0.41
B13	77.02	1.95	40.87	142.17	5.06	-0.62
B14	84.39	2.14	-40.24	153.03	5.38	-0.58
B15	64.04	1.77	-275.55	125.85	3.69	-5.35
B16	81.03	2.05	-33.31	146.66	5.01	-0.52
B17	73.30	1.85	-26.77	121.60	3.62	-0.57

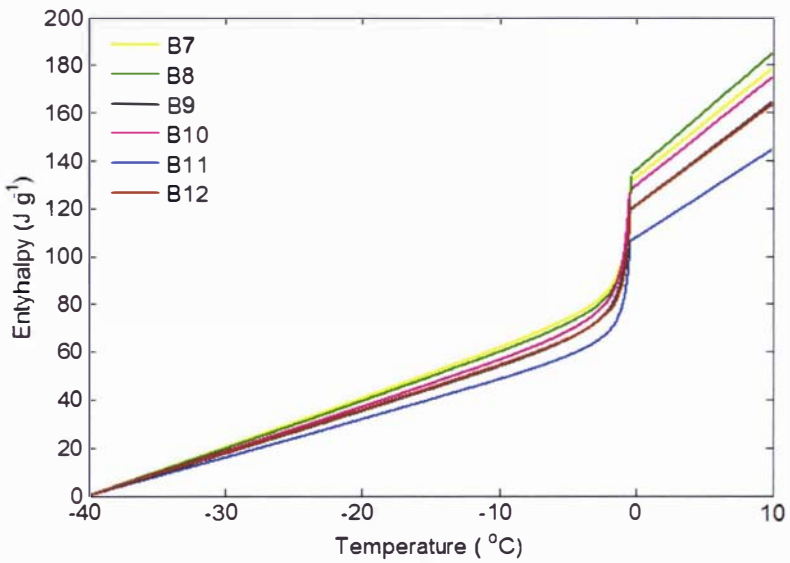

Figure 3.28 Modeled data for unsalted butters

Figure 3.28 shows the adjusted data for each of the unsalted standard butters. The total enthalpy change is clearly different for all the unsalted butters. The maximum value was found for B8 and a minimum value was found for B11. The enthalpy of butters B9 and B12, and butters B7 and B10 were produced at the same time in the season from different manufacturing process but were nearly the same. Butters B8 and B11 from the same season but from different manufacturing sites and processes showed a large difference in the enthalpy both above and below the initial freezing point. It was postulated that the difference were explained by compositional differences.

Figure 3.29 gives the measured solid fat contents of butters B7, B8, B9, B10, B11, and B12 as a function of temperature. Samples B7 and B10 are spring butters whereas samples B8 and B11 are summer butters and samples B9 and B12 are autumn butters.

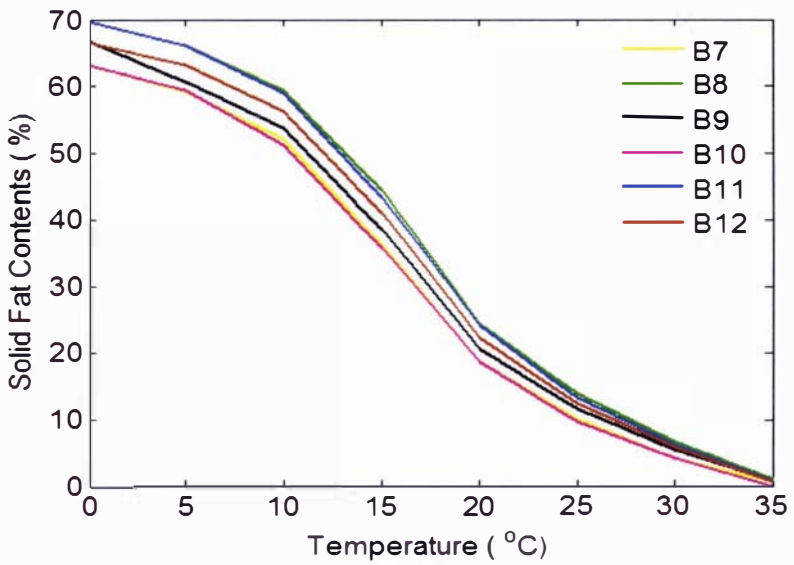

Figure 3.29: Solid fat contents of butters at different temperatures

The solid fat contents in samples B7 and B10 are same and the solid fat contents in samples B8 and B10 are same. The pair B7 and B10 has low solid fat contents being spring butter and samples B10 and B11 had higher solid fat contents at the given temperature range being summer butter. Butter with higher SFC should have lower specific heat capacity and vice versa. This is true for the salted butter. Sample B2 being spring butter has a value of 1.69 kJ $kg^{-1}{}^{o}C^{-1}$ and 3.42 kJ $kg^{-1}{}^{o}C^{-1}$ for the frozen and unfrozen range respectively as compared to the specific heat capacity of 1.56 kJ $kg^{-1}{}^{o}C^{-1}$ and 3.03 kJ $kg^{-1}{}^{o}C^{-1}$ for sample B3 which is a summer butter produced in the same year and with same manufacturing process.

The same observation can be found for samples B10 and B11 for both the frozen and unfrozen range whereas for samples B7 and B8 (spring butter) have higher specific heat capacity in the frozen range but not in the unfrozen range.

(a)

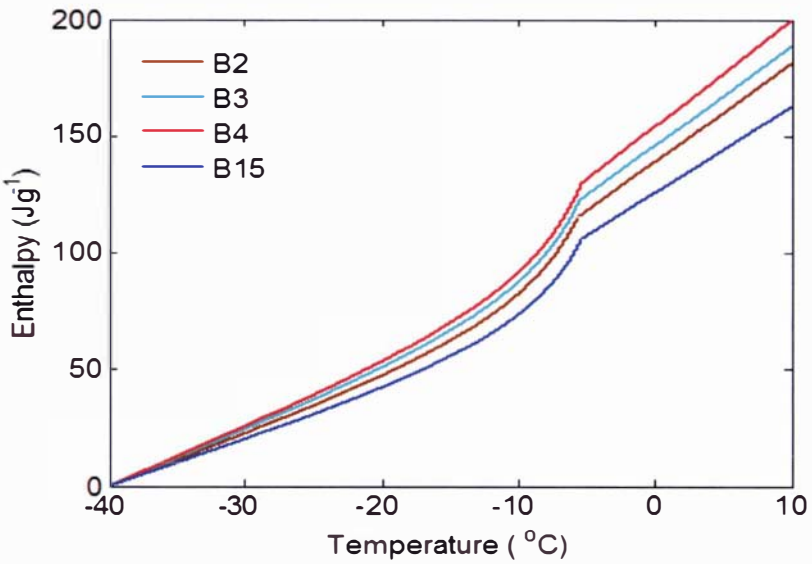

(b)

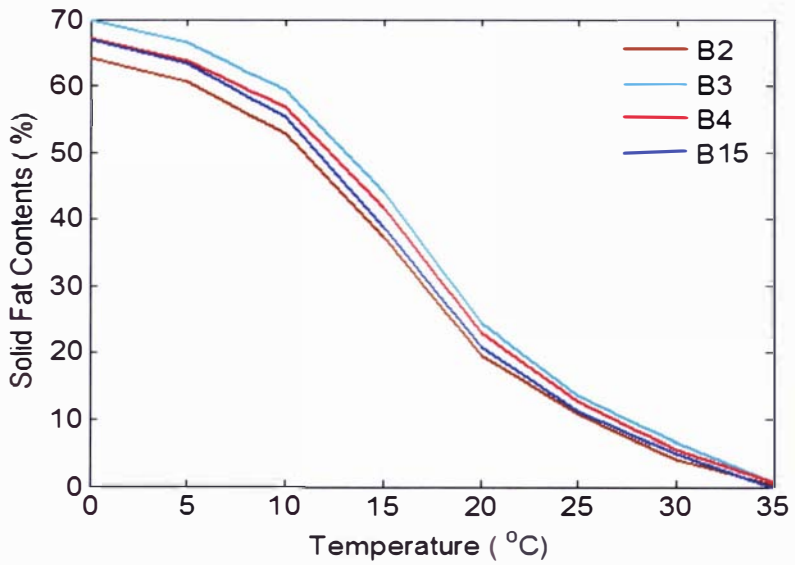

Figure 3.30: (a) Adjusted enthalpy for salted butters (b) Solid fat contents for salted butters

Figure 3.30(a) gives the adjusted enthalpy for all the salted butters and Figure 3.30(b) shows the solid fat contents as a function of temperature for all the salted butters. From the compositional data

it can be seen that the moisture contents in all the salted butters were nearly the same except for B15 which was bit lower than others, contributing to the lower total enthalpy change. B2 and B3 were spring and summer butter respectively whereas B4 and B15 were autumn butters. There was little difference in the specific heat capacity of all the butters in the frozen and unfrozen range. Although B15 is an autumn butter, it has the lowest values of specific heat capacity for both frozen and unfrozen range as the moisture content effect is dominant. Similarly B4 is also an autumn butter but had the highest values of specific heat capacity for both the frozen and unfrozen ranges.

(a)

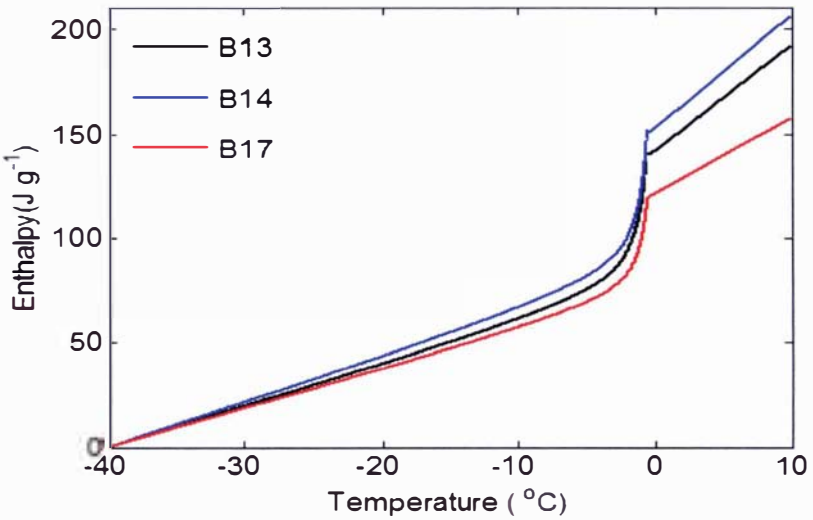

(b)

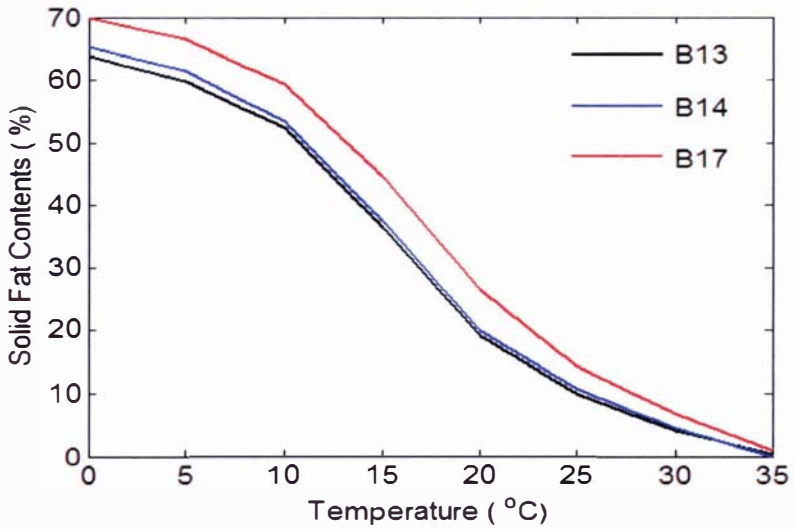

Figure 3.31: (a) Adjusted enthalpy of lactic butters (b)Solid fat contents of lactic butters

Figure 3.31 (a) shows the adjusted enthalpy for all the lactic butters from Table 3.1 and Figure 3.31(b) shows the measured solid fat contents for the lactic butter. There were very small compositional differences in these three butters. Figure 3.31(b) shows the milkfat fractions of the butters B13 and B14 are very similar at any temperature. The higher SFC at 0°C in butter B17 could explain the lower specific heat capacity in the fully frozen region of the enthalpy curve as less milkfat would undergo phase change below 0°C. The lower enthalpy of water freezing in B17 is probably due to the higher lactic content of that sample.

3.5.2.13 Comparison with Literature Data

Adjusted data was compared with the data from the literature. Figure 3.32 compares the adjusted data for salted butters with the data measured for salted butters by Olenew (1959), Lindsay & Lovatt (1994) and Pham *et al.* (1994).

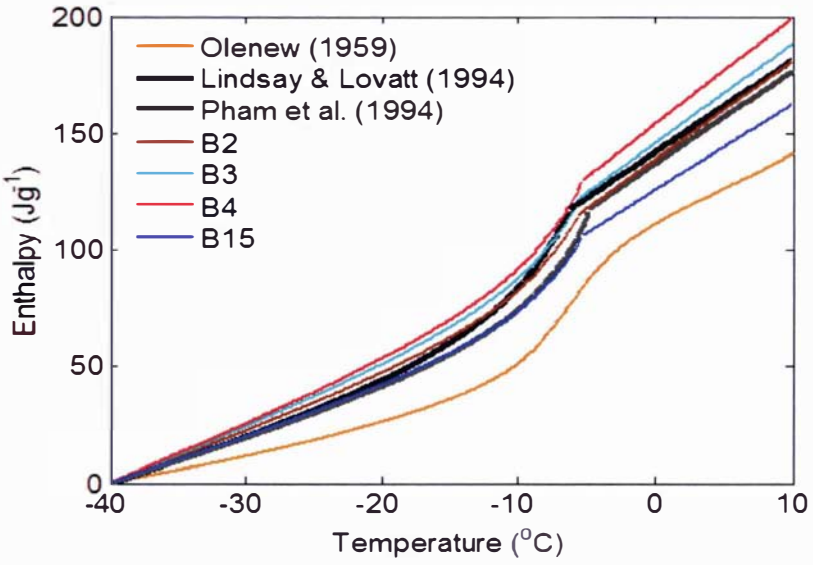

Figure 3.32: Comparison of measured enthalpy data with the literature data

The data from Pham *et al.* (1994) and Lindsay & Lovatt (1994) is intermediate to the measured enthalpy data for four salted butters by DSC over the whole temperature range. The data from Olenew (1959) is much lower than any of the measured data. There was little information on the butter used by Olenew (1959) regarding the season and manufacturing process. Although the composition of the butter used by Olenew (1959) was not very different from the butter used in this research (Table 2.9).

The total enthalpy change in B15 was lower and for B2 was higher than that measured by Lindsay & Lovatt (1994) and Pham *et al.* (1994). The butter used by Lindsay & Lovatt (1994) had 80.6% fat and 16.7% moisture content and the butter used by Pham *et al.* (1994) has 87.4% fat and 10.7% moisture contents, which explains some of the differences in the measured enthalpy changes. There was no information available on the seasonality and the manufacturing process of the butter; moreover Lindsay & Lovatt (1994) and Pham *et al.* (1994) used an adiabatic calorimeter to measure specific heat capacity of the butter. Some of the differences can be attributed to the different measurement techniques.

Overall, the measured enthalpy data agreed well with the other measured data in the literature.

3.5.3 Conclusions

From the discussion above, the following conclusions can be made for the enthalpy and specific heat capacity of butter in the range -40°C to 10°C:

- Salted butter has lower specific heat capacity compared with unsalted butter in both the completely frozen (below -20°C) and unfrozen (above T_{if}) temperature ranges.
- Spring salted butter has about 15% higher total enthalpy change between -40°C and 10°C as compared with summer butter.
- Spring butter has higher specific heat capacity value for both the frozen and unfrozen temperature ranges for both salted and unsalted butters.
- There is little difference in the enthalpy of butter produced by different manufacturing processes in the same season.

3.6 Thermal Conductivity

The data in the literature was discussed in the second chapter. The data measured from different sources agree well above the initial freezing point, but there are significant differences below the initial freezing point. A constant value can be used above the initial freezing point but it was still necessary to check the other estimation methods to see which data are more reliable and if independent measurement of thermal conductivity for different kinds of butter is required.

In food products the thermal conductivity can be estimated from the volume fraction of its components and their thermal conductivities. One method to obtain the thermal conductivity data is to apply the empirical relations given by a number of authors using the composition of butter.

Rahman (1995) quoted a number of studies suggesting the thermal conductivity of the foods is affected mostly by moisture content. Rahman (1995) and Miles (1983) gave empirical relations for the thermal conductivity of basic food components as a function of temperature. Rahman (1995) reported a series of theoretical model to use depending on the structure of food and the direction of heat transfer through the material. The basic models are given below:

Series Model

In the series model, the phases are thermally in series with respect to the direction of heat flow. This model gives the minimum value of thermal conductivity and is given by the weighted harmonic mean of the continuous and discontinuous phase conductivities:

$$\frac{1}{\lambda} = \sum_{i=1}^{n} \frac{V_i}{\lambda_i} \tag{3-9}$$

where :

λ = Thermal conductivity of the material under study ($Wm^{-1}K^{-1}$)

λ_i = Thermal conductivity of the i^{th} component ($Wm^{-1}K^{-1}$)

V_i = Volume fraction of the i^{th} component (m^3. m^{-3})

n = Number of the components

Parallel Model

In the parallel model the direction of heat transfer is considered to be acting as parallel to components of the material. This gives the maximum value of the thermal conductivity and is given by the weighted arithmetic mean of the thermal conductivities of the components:

$$\lambda = \sum_{i=1}^{n} V_i \lambda_i \tag{3-10}$$

All other models predict the value of the thermal conductivity of the material between the limits given by the series and parallel model.

Effective Medium Theory

This theory assumes that the system is a simple homogenous mixture of components and each part has a known thermal conductivity. The thermal conductivity using the medium effective theory for mixtures can be calculated as:

$$\sum_{i=1}^{n} V_i \left(\frac{\lambda - \lambda_i}{\lambda_i - 2\lambda} \right) = 0 \qquad (3\text{-}11)$$

Maxwell- Eucken Model

The Maxwell – Eucken Model was derived on the basis of randomly distributed discontinuous spheres in a continuous medium and assumes that the discontinuous spheres are far enough apart that they do not interact. This equation is strictly only applicable where the volume fraction of the discontinuous phase is very small:

$$\lambda = \lambda_1 \left[\frac{\lambda_2 + 2\lambda_1 - 2V_2(\lambda_1 - \lambda_2)}{\lambda_2 + 2\lambda_1 + V_2(\lambda_1 - \lambda_2)} \right] \qquad (3\text{-}12)$$

where:

λ_1 = Thermal conductivity of the continuous phase ($Wm^{-1}K^{-1}$)

λ_2 = Thermal conductivity of the discrete phase ($Wm^{-1}K^{-1}$)

V_2 = Volume fraction of the discrete phase. ($m^3.m^{-3}$)

If component 2 is continuous then equation (3-12) can be written as:

$$\lambda = \lambda_2 \left[\frac{\lambda_1 + 2\lambda_2 - 2V_2(\lambda_1 - \lambda_2)(1 - V_2)}{\lambda_1 + 2\lambda_2 + V_2(\lambda_1 - \lambda_2)(1 - V_2)} \right] \qquad (3\text{-}13)$$

Levy Model

Levy (1981) modified the Mawell-Eucken model to avoid the decisions which of the Maxwell – Eucken equations should be used as both the equations give different answers. The Levy model is given as:

$$\lambda = \lambda_1 \frac{2\lambda_1 + \lambda_2 - 2(\lambda_1 - \lambda_2) f}{2\lambda_1 + \lambda_2 + (\lambda_1 - \lambda_2) f} \tag{3-14}$$

where

$$f = \frac{1}{2}\left[2/g - 1 + 2V_2 - \sqrt{(2/g - 1 + 2V_2)^2 - 8V_2/g} \right] \tag{3-15}$$

and

$$g = \frac{(\lambda_1 - \lambda_2)^2}{(\lambda_1 + \lambda_2)^2 + \lambda_1 \lambda_2 / 2} \tag{3-16}$$

The Levy model was obtained initially on a mathematical basis rather than a physical basis and despite often giving the best predictions researchers were hesitant to recommend the use of this model. Recently, Wang *et al* (2006) showed that the Levy model is the combination of the two Maxwell – Eucken models and hence provides a physical meaning to the Levy model.

Other Models

Wang *et al* (2006) gave a new procedure for modelling complex materials as composites of the five basic models given above using the combinatory rules.

3.6.1 Estimation of Thermal conductivity of Butter

The thermal conductivity of butter was estimated using the composition of the butter from different theoretical models. The composition of the butters studied did not differ much except for B1 and B5, which had higher water contents and as a result would have higher thermal conductivity value. The other significant difference might be between salted and unsalted butters. For all other butters the thermal conductivity is not expected to differ significantly.

Water, fat, protein, ash and other MSNF (including lactose and salt) are the major components of butter. Some butter contains air, which could affect the thermal conductivity significantly. Since NZ butter has negligible amounts of air, air was not considered as a component. Protein and ash form

parts of aqueous phase and the volume fraction of these two components is very small. The major components are thus fat and water/ice. Water or ice makes on average 15.7% of the volume of butter and most of the remaining 84.3% is fat. For butters B1 and B5 (high moisture) 20.7% was water.

In the freezing range, the difference in thermal conductivity is mostly due to the water freezing. It was decided to estimate two values for thermal conductivity: one for the freezing range (below T_{if}) and the other for the unfrozen range (above T_{if}). The value for the freezing range was estimated for fully frozen butter because intermediate thermal conductivity can be estimated from the estimates of the fraction of frozen water using enthalpy diagram for partially frozen butter.

For temperatures above T_{if} the thermal conductivities of the fat, ash, protein and water were calculated using the empirical models of Choi & Okos (1986) at a temperature of 5°C as shown in table 3.14. Then the effective thermal conductivity (using parallel model) of the remaining components was combined with that of the water using the Levy model. An average value for the thermal conductivity of butters B1 and B5 was found to be 0.20 $Wm^{-1}K^{-1}$. For all other kinds of butter the value was 0.18 $Wm^{-1}K^{-1}$. This is in good agreement with the data reported in Table (2.6) at 5°C (0.20 $Wm^{-1}K^{-1}$ for unsalted and 0.19 $Wm^{-1}K^{-1}$ for salted).

Table 3.14: thermal conductivity of butter components in frozen and unfrozen range using Chio & Okos (1986) models

Temperature	λ_{fat}	λ_{water} or λ_{ice}	λ_{ash}	$\lambda_{protien}$
5.00	0.17	0.58	0.34	0.18
-30.00	0.26	2.50	0.29	0.14

For the fully frozen temperature range, the same procedure was applied using a temperature of -30°C, but instead of using 15.7% of water, 15.7% of ice was used. A value of 0.34$Wm^{-1}K^{-1}$was estimated for B1 and B5. For all other butters a value of 0.29 $Wm^{-1}K^{-1}$ was estimated. This agrees very well with the values reported in Figure 2.5.

The same approach was taken to calculate the thermal conductivity of partially frozen butter using the Levy model with the fraction of water frozen. It was found that the thermal conductivity of butter lies within the range of 0.212 $Wm^{-1}K^{-1}$ to 0.290 $Wm^{-1}K^{-1}$ when the water fraction frozen changes from 0 to 1.

It can be concluded that the data reported in Table 2.7 is more reliable than the data measured by Willix *et al.* (1998), probably because the water was not frozen completely for the samples of Willix *et al.* At temperatures above T_{if}, thermal conductivity values of 0.20 $Wm^{-1}K^{-1}$ and 0.22 $Wm^{-1}K^{-1}$ can be used for salted and unsalted butter respectively. At temperatures below T_{if}, thermal conductivity values of 0.28 $Wm^{-2}K^{-1}$ and 0.29 $Wm^{-2}K^{-1}$ can be used for salted and unsalted butter respectively. Intermediate values of thermal conductivity can be calculated using weighted averages of the frozen and unfrozen values based on the ice fraction of the water in the butter.

3.7 Conclusions

For modelling heat transfer in butter thermal properties data was defined through a mixture of literature data and measurements.

The density of butter does not change significantly over the temperature range of interest and therefore a constant value of density can be used.

A constant value of thermal conductivity for the frozen temperature range (below T_{if}) and a constant value for the unfrozen temperature range (above T_{if}) can be used.

Measured values for the enthalpy of butter will be used. It was observed that during cooling, supercooling is important and, therefore, a lower value of the specific heat capacity and a value for the unfrozen range for thermal conductivity should be used for predicting freezing processes than for thawing processes.

CHAPTER 4

HEAT TRANSFER IN BUTTER BLOCKS

4.1 Introduction:

The investigation of enthalpy changes in butter during heating and cooling using DSC showed that the butter samples supercool below the initial freezing point before freezing. Even when the cooling rates in the DSC were slowed to one degree per minute, this rate is still much faster than the cooling rates expected during the freezing of bulk butter. During cooling of butter pats and blocks it is thought that, due to the slow rates, the butter may not show the supercooling behavior observed in the DSC. Before developing a mathematical model, thermal history data for bulk butter was collected on blocks of butter during freezing and thawing to investigate the freezing and thawing behavior of bulk butter. A number of experiments were conducted on pats and blocks of both salted and unsalted butter.

4.2 Material and Method:

This section describes the geometry and type of the butter samples used for the freezing and thawing trials, along with the experimental design for each trial.

4.2.1 Butter:

Two 500 g butter pats (one salted and one unsalted) were bought from a local super market. Similarly, two 25 kg cartons of butter were sourced from Fonterra Co-operative Ltd. The geometry of each butter type used in the cooling/heating trials are summarised in Table 4.1:

Table 4.1: Dimensions and type of butter used in block experiments (without packaging)

Butter Type and Code	Weight (kg)	Length (mm)	Width (mm)	Height (mm)
Salted Pat (B18)	0.5	116	64	60
Unsalted Pat (B16)	0.5	116	64	60
Salted Block (B15)	25	377	242	264
Unsalted Block (B19)	25	367.5	236.5	273.1

All the butter samples were manufactured using the Fritz butter making process. Analysis of composition and initial freezing point was carried out as described in Chapter 3 on the unsalted pat (B16) and the salted (B15) block samples. The salted pat (B18) and the unsalted block (B19) were not tested due to the small differences already observed in Chapter 3 for a number of salted and unsalted butters. Enthalpy and the specific heat capacity characterisation were carried out on four types of butters using DSC.

The cartons in which the butter blocks were packed were made of corrugated cardboard and the blocks had a single layer (4 mm) of cardboard on each face and two layers on the top and bottom. The butter inside the cartons was wrapped in 0.85 mm thick polyethylene liners. The mass of the carton was 514 g and the mass of the liner was 37.8 g. The weight of the butter block with the packaging was found to be approximately 25.6 kg. Butter pats were wrapped in a parchment paper packaging of about 0.011 mm thickness.

4.2.2 Temperature Measurements

Type – T thermocouple wire (copper/constantan) with a gauge of 1 mm was used to measure the temperature of the butter. All the thermocouples were calibrated at 0°C using an ice-water slurry. Three types of data loggers were used to record the temperature profiles within the butter. These data loggers were a Grant Squirrel (series 1000) data logger, a Data taker (series 600) and a Campbell (CR10) data logger which had data accuracies of ±1 °C, ±1°C and < ±0.1°C respectively. A data collection time interval of 2 minutes was used for the heating and cooling runs of butter pats and an interval of 5 or 10 minutes was used for the butter blocks.

4.2.3 Position of Thermocouples

Thermocouples were positioned in the butter by first freezing the butter at about -24 °C for about 2-3 weeks and then drilling holes with a 1 mm drill in the desired location. The thermocouples were then positioned within these holes. For butter pats a short drill was used to bore into the frozen butter pat. For blocks a short drill was used first to drill the hole and then a longer drill was used to extend the hole to the required position. To minimize the error due to the heat transfer through the thermocouple wire, the thermocouple junction was positioned such that the wire entered from the farthest surface of the butter.

4.2.3.1 Salted Pat (B18)

Figure 4.1 shows the positions of the thermocouples in the salted butter pat.

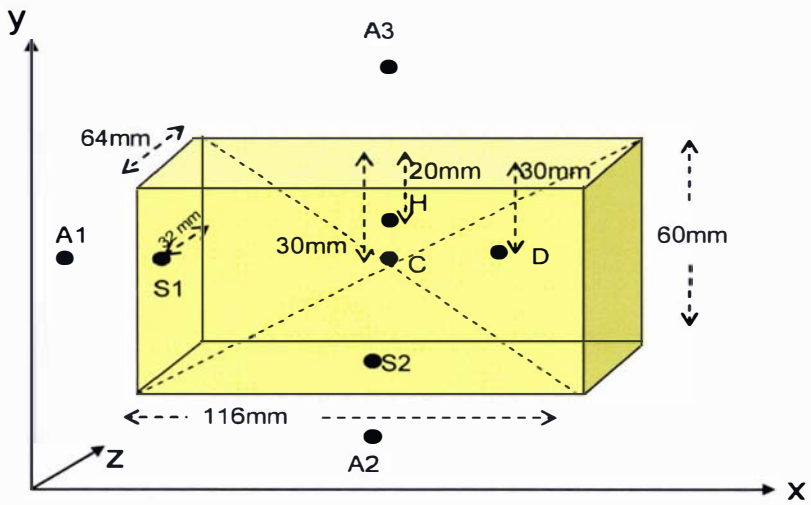

Figure 4.1: Position of thermocouples in the salted butter pat (B18)

Three thermocouples were positioned inside the butter pat at different positions relative to the origin of the x, y and z axis (positioned at the lower, left hand corner) as follows. One was placed in the geometric centre C (58, 30, 32 mm) of the butter pat, which is the position in the pat that is likely to be slowest in changing temperature. One thermocouple was positioned at point D (87, 30, 16 mm), half way from center to the corner of the pat but vertically centered. The third thermocouple H (58, 40, 32mm) was positioned 20 mm from the top in the center of the butter pat. Two thermocouples were attached to the surfaces of the pat (S1 and S2) and three thermocouples were positioned in the air to measure the air temperature around the butter pat (A1 to A3). The tips of the thermocouples in the air were wrapped with foil to minimize the any error in thermocouple readings due to heat transfer by radiation. The thermocouples were positioned in such a way that they can give an overall trend for the heat transfer in the butter from top to bottom as well as from one side to the other.

4.2.3.2 Unsalted Pat (B16)

Figure 4.2 shows the positions of the thermocouple in the unsalted pat. Three thermocouples were positioned inside the butter to observe the thawing and freezing behavior of butter across the diagonal of the butter pat. The positions of the thermocouples were C (58, 30, 32 mm), D (87, 45, 48 mm), and Q (102, 52.5, 56 mm) in x, y and z directions of the butter pat. Three thermocouples

were positioned outside the pat for recording ambient temperatures (A1 to A3) and one on the surface of the butter pat (S1).

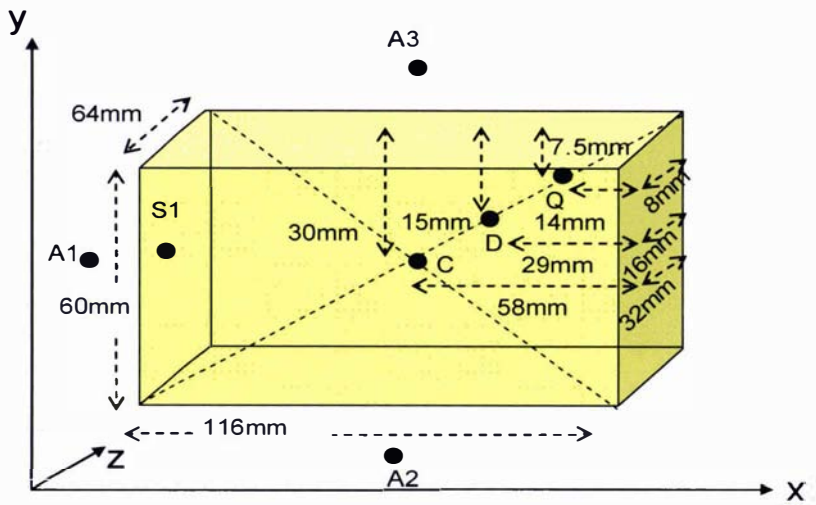

Figure 4.2 Position of thermocouples on the unsalted butter pat (B16)

4.2.3.3 Salted Block (B15)

Thermocouples positions inside and outside the butter block are given in Figure 4.3 and Table 4.2.

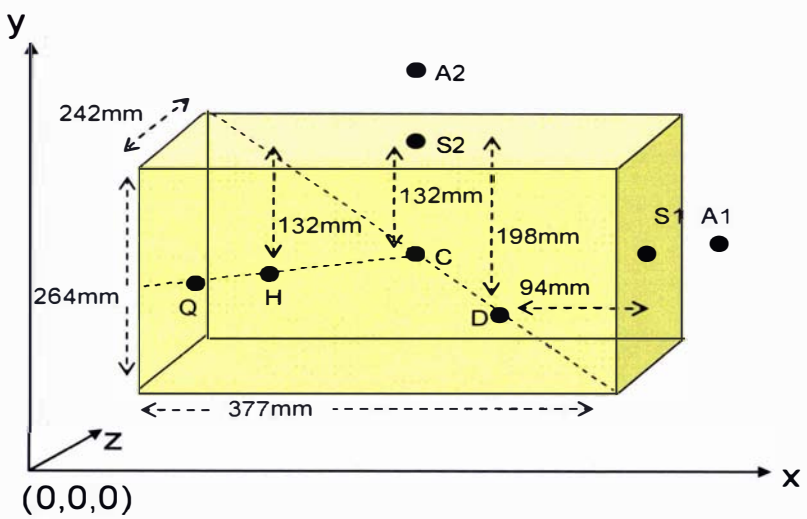

Figure 4.3: Position of the thermocouples in the salted butter block (B15)

Table 4.2: Thermocouples position in the salted butter block (B15) related to the origin as shown in Figure 4.3

Thermocouples	Position
C	Thermal centre (188.5,132,121 mm)
D	(282.75, 66,60.5 mm)
H	(94,132,60.5 mm)
Q	(47,132,30.25 mm)
S1	Face $x=X$ (377,132,121 mm)
S2	Face $y=Y$ (188.5,242,121 mm)
S3	Face $z=Z$(188.5,132,264 mm)
A1	Adjacent to S1
A2	Adjacent to S2

4.2.3.4 Unsalted Block (B19)

Figure 4.4 shows the position of the thermocouples in the plan view of the block. Three thermocouples were placed inside the butter, two on the surface of the block (S1to S3) and two outside the packaging (A1 to A2) to measure ambient temperatures as shown in the Figure 4.4.

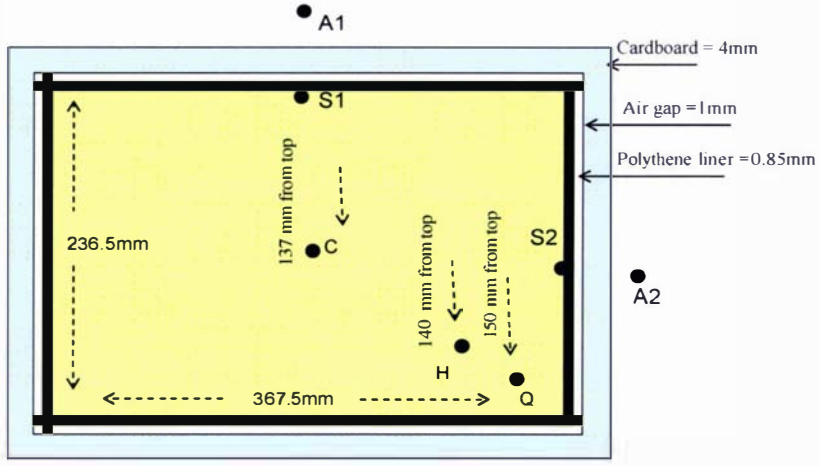

Figure 4.4: Position of thermocouples in the plan view of unsalted block. (B19)

C(183.7, 137, 118), H(275.6, 140, 61),Q (321.5, 150, 30.6)

4.2.4 Initial and Ambient Conditions

All the trials were conducted at Massey University laboratory. Before starting each experiment, the butter was held at the initial temperature in a controlled temperature walk - in room long enough to ensure a uniform initial temperature. The samples were then transferred to another room and held at

the desired air temperatures. To minimise the temperature variations in the initial temperature during transfer, the butter pats were transferred in an insulated container. Once installed in the new temperature environment the thermocouples were connected to the data logger. Thus, a lag time of several minutes was observed due to the time spent in connecting the thermocouples with the data loggers. During this time the data could not be recorded but the conditions to which the butter was exposed were held constant. Table 4.3 summarizes the initial and ambient conditions used for all the trials along with the preconditioning of each butter sample.

Table4.3: Experimental conditions for the trials on butter pats and blocks

Butter Type	Code[1]	Initial Temperature (T_i)	Ambient Temperature (T_a)	Preconditioning Time (t_p)
Salted Pat	SPC-1	10°C	-24°C	10 hours
(B18)	SPH-1	-24°C	10°C	13 hours
	SPC-2	10°C	-24°C	10 hours
	SPH-2	-24°C	10°C	60 hours
Unsalted Pat	UPC-1	15°C	-15°C	10 hours
(B16)	UPH-1	-15°C	20°C	12 hours
	UPC-2	20°C	-70°C	10 hours
	UPH-2	-70°C	20°C	12 hours
	UPH-3	-15°C	20°C	12 hours (-70°C)
Salted Block	SBC-1a	4°C	-18°C	3 days
(B15)	SBC[2]-1b	4°C	-18°C	3 days
	SBH-1a	-18°C	2°C	3 days
	SBH[2]-1b	-18°C	2°C	3 days
	SBH-2a	-10°C	10°C	1 year
	SBH-2b	-10°C	10°C	1 year
Unsalted Block	UBH-1a	-10°C	10°C	6 months
(B19)	UBH-1b	-10°C	10°C	6 months
	UBC-1a	10°C	-23°C	3 weeks
	UBC-1b	10°C	-23°C	3 weeks
	UBC-2	10°C	-10°C	3 weeks

[1] 'S' – Salted, 'U'- Unsalted, 'P' – Pat, 'B' – Block, 'C' – Cooling, 'H' – Heating, [2] without cardboard packaging

4.3 Results and Discussion

This section describes the results from all the above trials. A comparison of heat transfer for different types of butter under the same environmental conditions is also given. All the data is also included in the accompanying CD as text files.

4.3.1 Heat Transfer in Salted Butter Pats:

Figure 4.5(a) shows the temperature profile of the butter pat undergoing cooling with an air temperature of approximately -24°C for 10 hours. The water droplets in the butter did not appear to freeze and, therefore, the butter did not exhibit a typical freezing plateau. As such the water droplets appeared to have been supercooled to many degrees below the nominal initial freezing point of the butter. There was little difference in the air temperature measured on the three sides of the butter measured, suggesting even air flow and, hence, even cooling around the sample. Similarly there was not much difference in the heat transfer through different sides of the butter as the surface temperature was nearly the same on the two different sides of the butter pat measured. As a result, as expected, the geometric center of the pat was found to be the slowest point to cool.

(a)

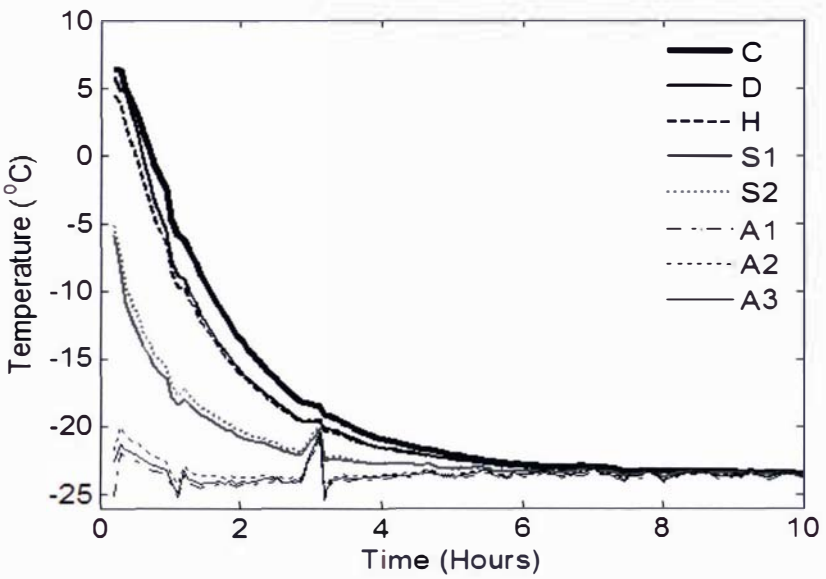

(b)

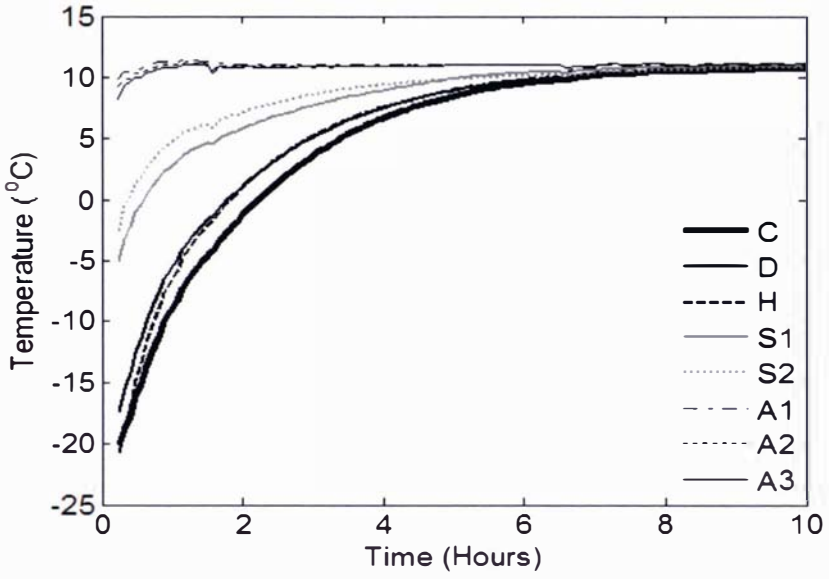

Figure 4.5:Heat transfer in salted butter pat (B18)

(a) Cooling (SPC – 1) with: T_i =10°C, T_a = -24°C, t_p=10h

(b) Heating (SPH – 1)with: T_i =-24°C, T_a = 10°C, t_p=13h

Figure 4.5 (b) shows the temperature profile of the same butter pat during heating in an air temperature of about 10°C after freezing for about 13 hours at -24°C. There is some data missing for first few minutes due to the time taken to connect the thermocouples to the data logger. The air temperatures were relatively consistent on the different sides of the pat measured. The surface temperatures show that the heat transfer through the different sides of the pat were not completely uniform which is likely to be due to differences in the air flows around the butter pat.

The most important observation in this thawing trial is the absence of the expected plateau at the freezing point of the water phase, which shows that the water in the butter did not freeze at all during the cooling experiment and subsequent storage at -24°C for 13 hours. This behaviour was very consistent with the observation made from the DSC runs where the water in salted butter did not freeze until the temperature decreased to about -50°C. Walstra (2003) explains that super-cooling can occur in water in oil (W/O) emulsions due to the dividing of the water phase into such small droplets that nucleation origins are not present in most of the droplets. This finding has important implications for rapid cooling of butter blocks during butter manufacture and storage. The rates of cooling and, therefore, milkfat solidification are faster than might be expected.

(a)

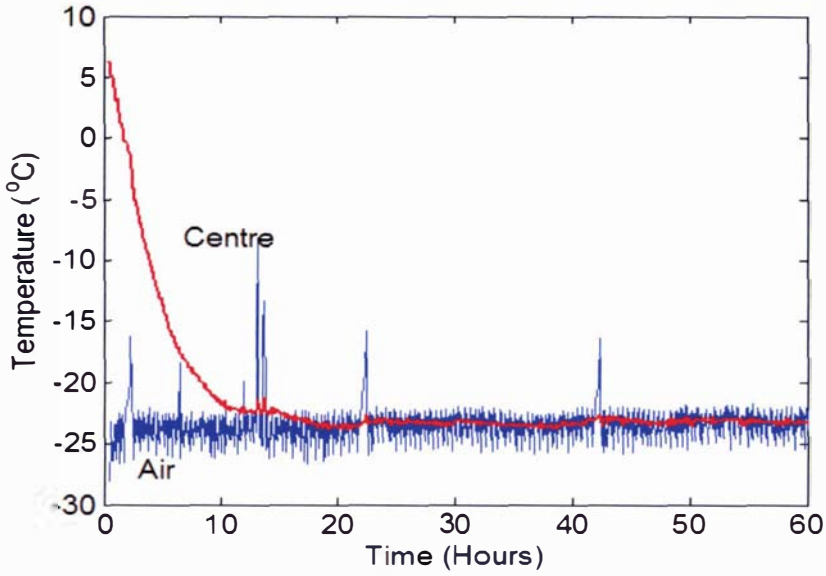

(b)

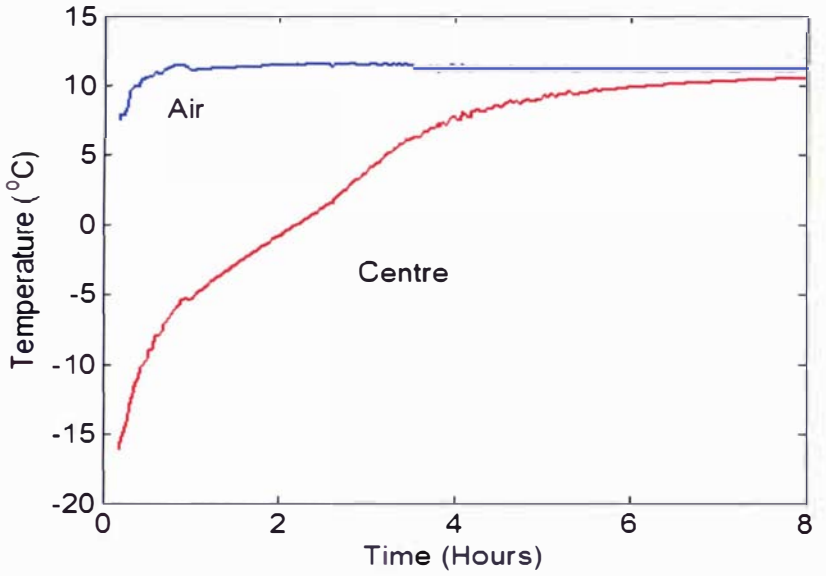

Figure 4.6:Heat transfer in salted butter pat (B18)

(a) Cooling (SPC – 2) for 60 hours

(b): Thawing (SPH – 2)after cooling at -25°C for 60 hours

A temperature profile for an experiment conducted on a salted butter pat (B18) for extended period of time is given in Figure 4.6 (a). The temperature rise after 13 hours is likely due to the change in

ambient temperature rather than release of latent heat of freezing. It seems that the pat might not exactly have equilibrated with the air temperature but remained at a slightly elevated temperature. This could be consistent with gradual water crystallisation releasing latent heat slowly over time. However, the precision of the temperature measured and the control of the air temperature mean that any such elevation in temperature is not certain. When the pat was thawed immediately after the 60 hours of cooling (Figure 4.6(b)), there was a slight latent heat plateau just below the initial freezing point of the butter however; it is clear from its small size that not all the water in the butter had frozen. To observe any latent heat release in small scale experiments, it appears that very careful experiments are needed in a very well temperature controlled room. In industrial situations butter pats are normally packed together to form a bigger block. Therefore, as they were not very useful for the practical industrial situations and accurate measurement of latent heat release was unlikely, no further experiments on butter pats for extended period of time were attempted.

4.3.2 Heat Transfer in Unsalted Butter Pats

The above experiment was repeated for the unsalted butter and apart from higher freezing point depression; the same supercooling behavior was expected.

Figure 4.7(a) shows the cooling temperature profile of the butter pat with an air temperature of about -15°C. The three ambient temperatures were quite consistent (less than 1°C different) so an average air temperature is shown. The same supercooling behavior observed for salted butter pats was observed in these data as well. In addition, the butter temperature asymptote was clearly about a degree higher than the ambient even after 12 hours. This difference in the temperatures was greater than the measurement and temperature control uncertainty. The difference could be due to the slow release of the water latent heat as water droplet freezing occurs slowly, i.e. the water droplets did freeze but very slowly and well below the initial freezing point.

Figure 4.7(b) shows the heating temperature profile of the butter pat with an air temperature of about 20°C after storage at -15°C for about 12 hours. The air temperature was not well controlled but the temperature on all the sides of the butter pat was relatively uniform. A latent heat absorption plateau was missing from the data, which suggests that, even though the butter was unsalted, the water in it did not freeze significantly during storage at -15°C for 12 hours. This behavior is again consistent with the DSC results for which the moisture in unsalted butter did not freeze at -20°C, even when it was kept there for 10 minutes.

(a)

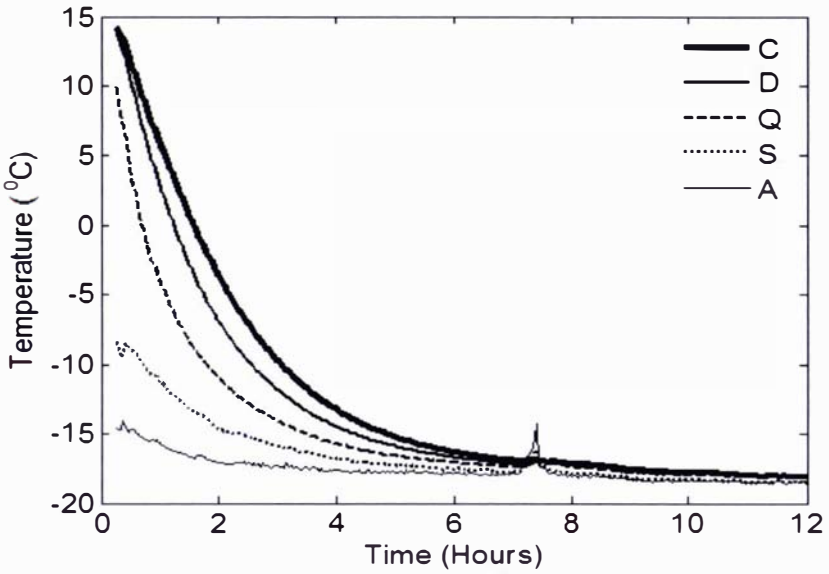

(b)

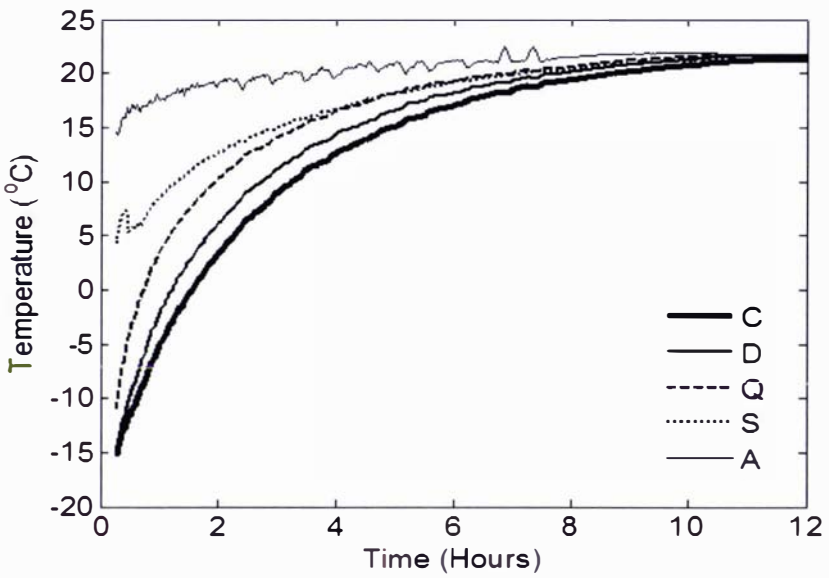

Figure 4.7: Heat transfer in unsalted butter pat (B16)

(a) Cooling (UPC – 1) with: T_i = 15°C, T_a = -15°C, t_p= 10h

(b) Heating(UPH – 1) with: T_i = -15°C, T_a = 20°C, t_p= 12h

The DSC showed that the moisture in unsalted butter froze at about -40°C when cooled at a rate of 10°C per minute from 10°C to -70°C. To see whether butter pats show the same behavior, the

unsalted pat was monitored while cooling with an air temperature at about -70°C (Figure 4.8a). Even though this was a much lower air temperature than previously used, it should be noted that the rate of cooling of the butter pat was much slower than that experienced by the DSC sample. The water in the butter froze at about -40°C and the release of latent heat of water gave a distinct plateau in temperature especially at the centre of the pat (Figure 4.8a). This is consistent with what was observed in the DSC run.

(a)

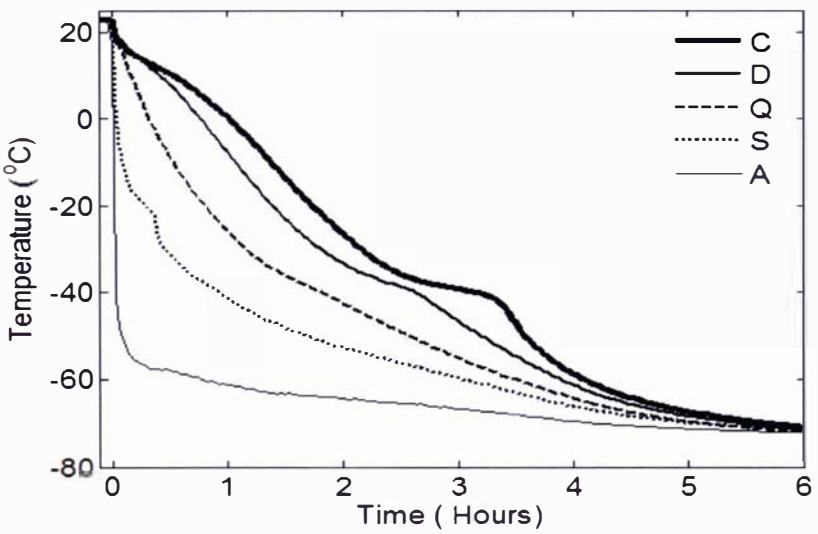

(b)

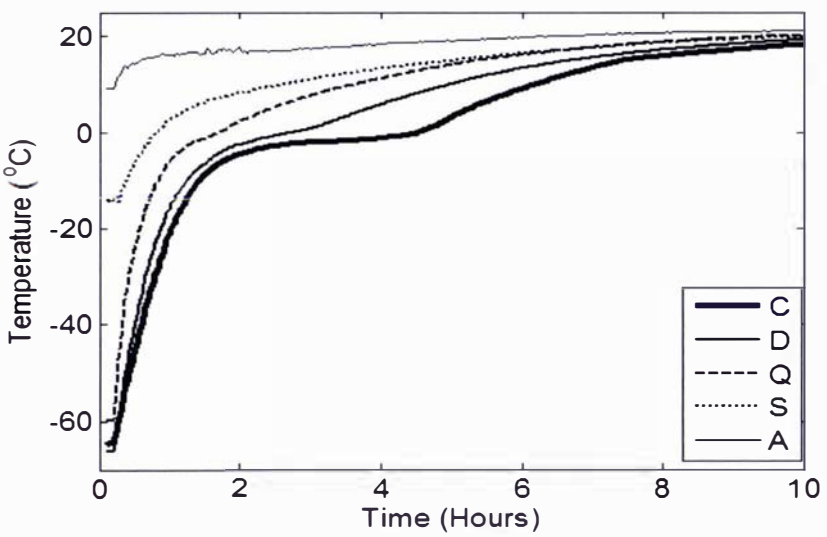

Figure 4.8: Heat transfer in unsalted butter pat (B16)

(a) Cooling (UPC – 2) with: $T_i = 20^oC$, $T_a = -70^oC$, $t_p = 10h$

(b) Heating (UPH – 2) with: $T_i = -70^oC$, $T_a = 20^oC$, $t_p = 12h$

The butter was kept at -70°C for about 12 hours and no change in the temperature was observed after 6 hours. Figure 4.8(b) shows the temperature profile of the thawing of this pat with an air temperature of about 20°C. The butter heated up just below the initial freezing point quite quickly due to the higher thermal conductivity of the frozen butter. A clear plateau can be seen just below the initial freezing point, after which the butter slowly approached the ambient temperature. Since the air temperature was not well controlled, and kept on rising very slowly, the butter centre temperature took a long time to finally approach the ambient temperature. However it clearly took longer to thaw a pat of fully frozen butter as compared to butter with supercooled water due to the need to provide the latent heat necessary for melting the ice. Direct comparison of this trial with Figure 4.7(b) is not possible due to the dramatically different initial temperatures, and hence heat transfer rates, in the experiments.

Another experiment was conducted on the butter pat by freezing it to -70°C and then heating it to approximately -15°C. The butter was equilibrated at -15°C and then it was again heated with air at about 20°C. This was done to allow direct comparison of the heating of butter with and without fully frozen water. Figure 4.9 shows the measured data.

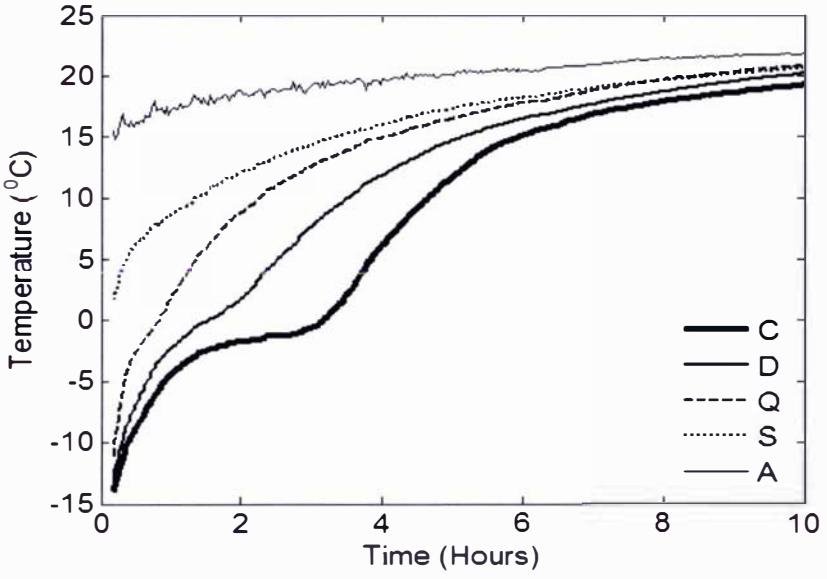

Figure 4.9: Heating of unsalted butter pat (UPH – 3) with: T_i = -15°C, T_a = 20°C, t_p= 12h

A plateau for the center of the butter pat can be seen just below the initial freezing point. The other

two points in the butter (D & Q) also showed some ice melting below the initial freezing point. A comparison of the thawing time for this pat when the water phase is frozen and unfrozen is given in Figure 4.10 which confirms the slower thawing rate of butter in which the water phase is fully frozen due to the extra latent heat. There was not much difference in the temperature profile below the initial freezing point. However, there was a two hour difference in the time required to reach 5°C between the "frozen" and "unfrozen" butter pat.

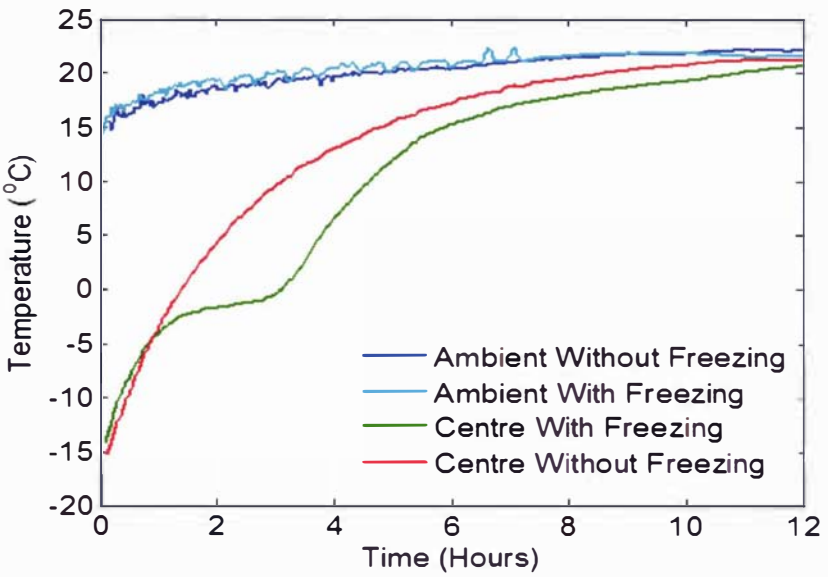

Figure 4.10: Comparison of thawing time for an unsalted pat with (UPH – 3) and without (UPH – 1) complete prior water freezing

Overall, the data collected for the butter pats were consistent with those collected during the DSC measurement. The water in butter pats did not fully freeze after 12 to 13 hours under normal commercial storage conditions. It is expected that crystallisation of the water phase would occur slowly if longer storage conditions are applied.

From an industry point of view, most of the butter used for thawing and freezing purposes is in form of 25 kg blocks packed in corrugated card board carton, either individually, or as a part of pallet. The rates of cooling in blocks are expected to be much slower than that for a 0.5 kg butter pat. Whether the freezing shows non equilibrium behavior as was observed in butter pats experiments was investigated as this has more commercial relevance.

4.3.3 Heat Transfer in Salted Butter Blocks

The results of the 25 kg salted butter block cooling trial are given in Figure 4.11(a). Although the rates of cooling were much slower than that of the DSC trials, the water droplets in the butter supercooled and did not fully freeze even after the storage at about -18°C for more than 60 hours. There was little difference in the air temperature on two sides of the box. The heat transfer from the face $y=Y$ was slower compared to two other sides which could be due to less air flow on that side of the carton. The temperature at all the positions in the butter block leveled out a few degrees higher than the ambient temperature. This was consistent to what was observed for the butter pat experiments and can be attributed to progressive but slow freezing of the water droplets.

Butter was kept at -18°C for sufficient time to equilibrate the temperature before starting the heating trial. Figure 4.11(b) shows the temperature profiles in the butter carton during heating with air at approximately 2°C. An ice melting plateau is missing, even though the butter was kept for 60 hours in the freezer at -18°C. This observation confirms that even though the rates of cooling were much slower than that were used in DSC, significant amounts of water in the butter did not freeze at all.

(a)

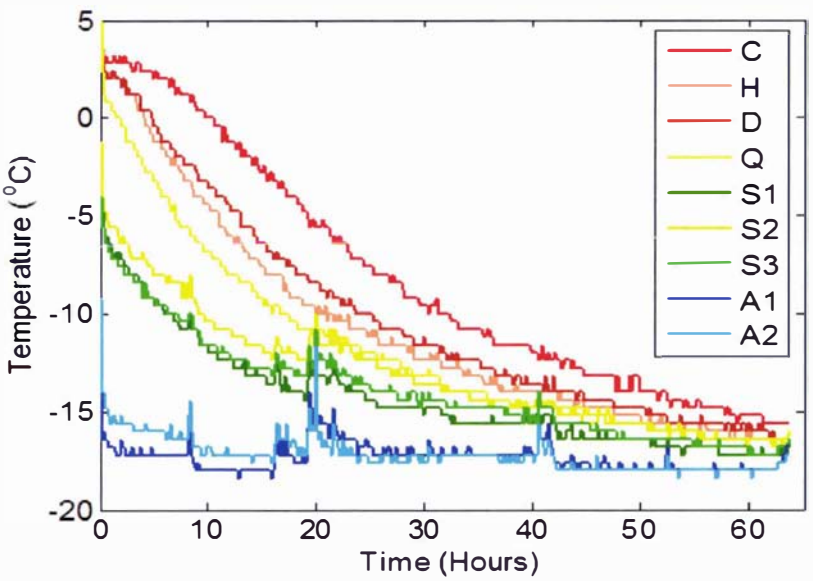

(b)

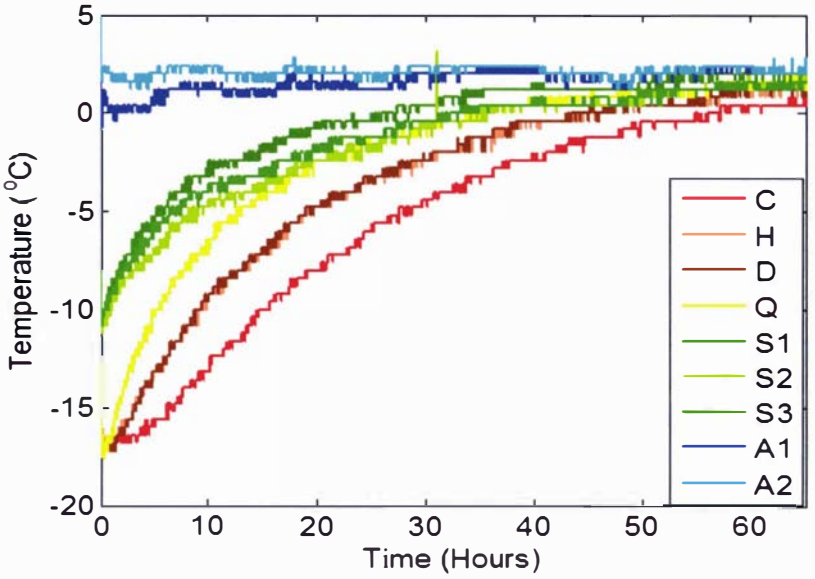

Figure 4.11: Heat transfer in butter block (B15) with cardboard packaging.

(a) Cooling (SBC – 1a) with: $T_i = 4^oC$, $T_a = -18^oC$, $t_p = 3days$

(b) Heating (SBH – 1a) with: $T_i = -18^oC$, $T_a = 2^oC$, $t_p = 3days$

To show the effect of the heat transfer resistance due to the packaging the above experiments were repeated with the same ambient conditions and butter blocks, but without the corrugated card board packaging. A faster cooling and heating was expected in this case.

The result of the cooling and heating trial without packaging is given in Figure 4.12 and a comparison of with and without packaging is given in Figure 4.13. The air temperatures in both the cooling and heating trails were similar to those for blocks in cartons (Figure 4.11). The slower heat transfer rates are obvious. The slow heat transfer rates had no obvious effect on the rate of water droplet freezing.

(a)

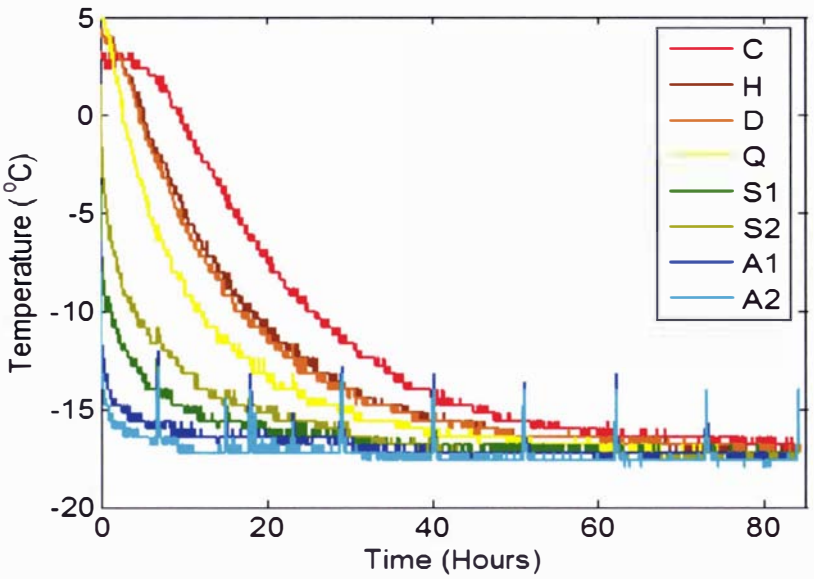

(b)

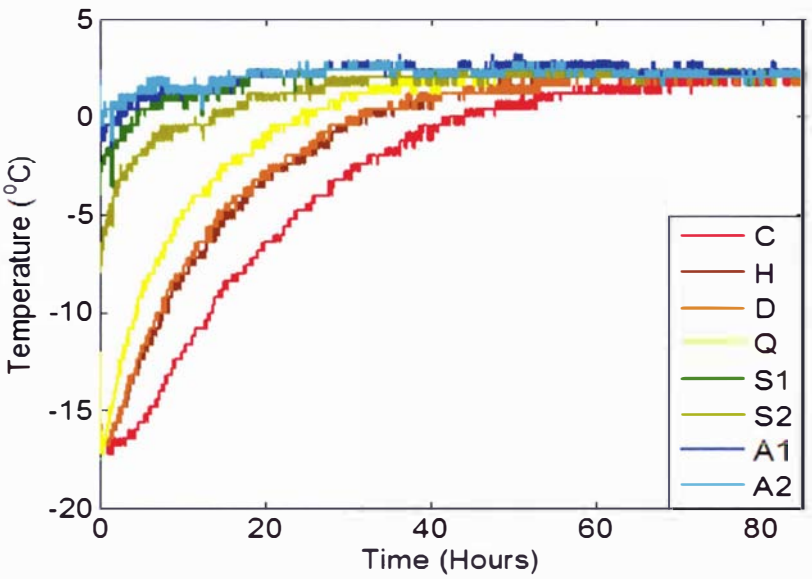

Figure 4.12: Heat transfer in butter block (B15) without cardboard packaging.

(a) Cooling (SBC – 1b) with: $T_i = 4^oC$, $T_a = -18^oC$, $t_p = 3days$

(b) Heating (SBH – 2b) with: $T_i = -18^oC$, $T_a = 2^oC$, $t_p = 3days$

(a)

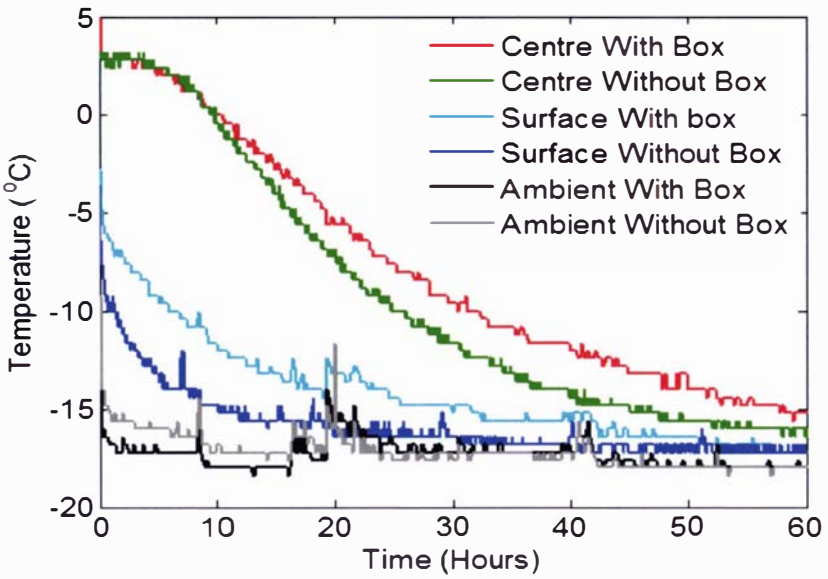

(b)

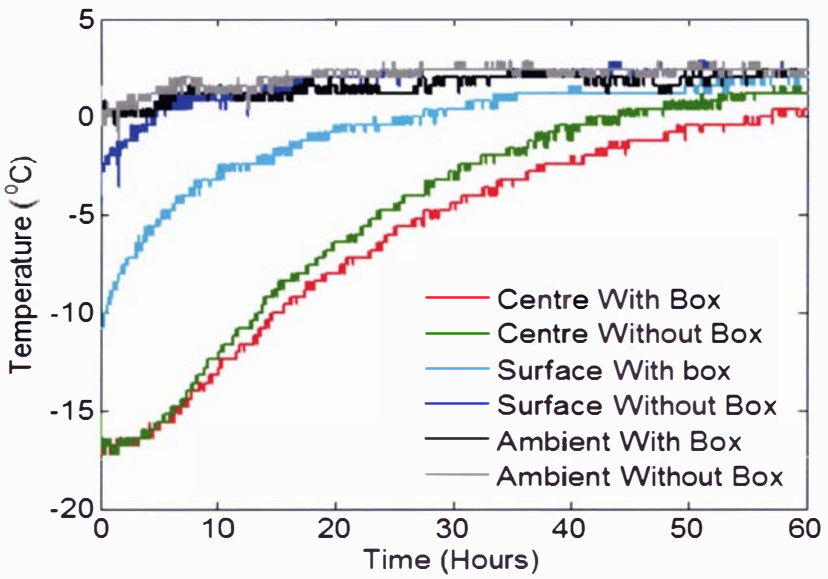

Figure 4.13: Comparison of with box and without packaging trails for salted butter (B15) (a) Cooling (b) Heating

In all the experiments conducted on the salted pats and blocks it was observed that the salted butter did not freeze even after storage at quite low temperatures for many days. Further heating trials were conducted on two salted butter blocks which had been in -10°C for more than a year. The

purpose of this trial was to see whether the water in the butter eventually freezes at normal industrial storage conditions or remained undercooled during that period of time. The position of the thermocouples in the plan view of block 1 is given in Figure 4.14. The positions were similar in block 2.

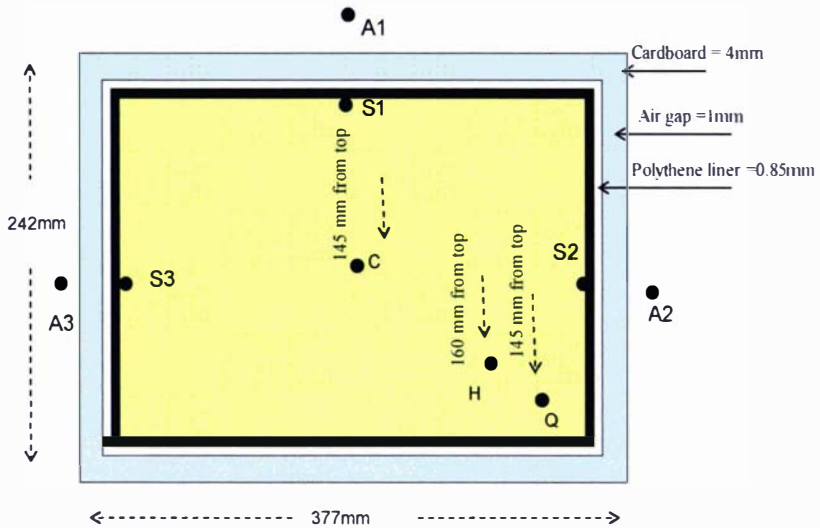

Figure 4.14: Position of the thermocouples in the plan view of frozen salted block (B15)

C(192.5, 145, 125 mm), H(96, 160, 62.5 mm), Q(48, 145, 31 mm)

The temperatures for one of the blocks are given in Figure 4.15. The heat transfer through different sides of the block was uniform. Position C in the butter clearly shows some ice melting. There is change in the rate of temperature change around -4°C at point C due to the change in the thermal conductivity and the moisture in butter changing from frozen to unfrozen states and the requirement to provide latent heat to melt the ice. Point C was 13 millimeters away from the thermal center of the block so the phase change plateau was shifted and a temperature bit higher than would be expected for the thermal center of the block.

Overall the absence of a clear latent heat plateau is probably because the initial temperature was quite close to the initial freezing point. Therefore even if equilibrium was reached the ice fraction might not be large and latent heat release would be less noticeable.

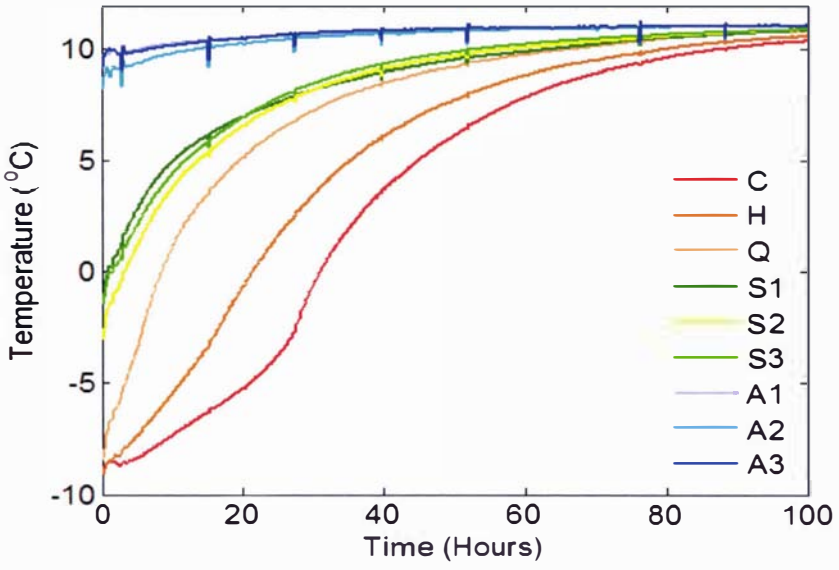

Figure 4.15: Thawing of frozen salted butter block (SBH – 2a) with:
T_i = -10°C, T_a = 10°C, t_p= 1 year

Figure 4.16 compares the results for the two replicate blocks of but er. The average air, surface and center temperatures were very consistent between both the experiments. The rates of temperature change at the positions H and Q were slightly slower in block 2, which is probably due to some differences in positioning of the thermocouples in the blocks. In block 2, all the thermocouples were positioned at a depth of 140 mm from the top rather than 145 mm as for block 1. Overall the thawing behavior was found to be repeatable.

These experiments demonstrate that while short term storage at industrially relevant temperatures does not result in significant water fraction freezing, the water does freeze after long term storage. In salted but er, the difference in time scale between cooling (days) and water droplet freezing (perhaps months) mean that from a modelling perspective cooling might be accurately predicted by ignoring the latent heat effects for the water phase. Thawing predictions however will depend on how long the sample has been stored for and at what temperature. For long storage times the fraction of water frozen would need to be predicted.

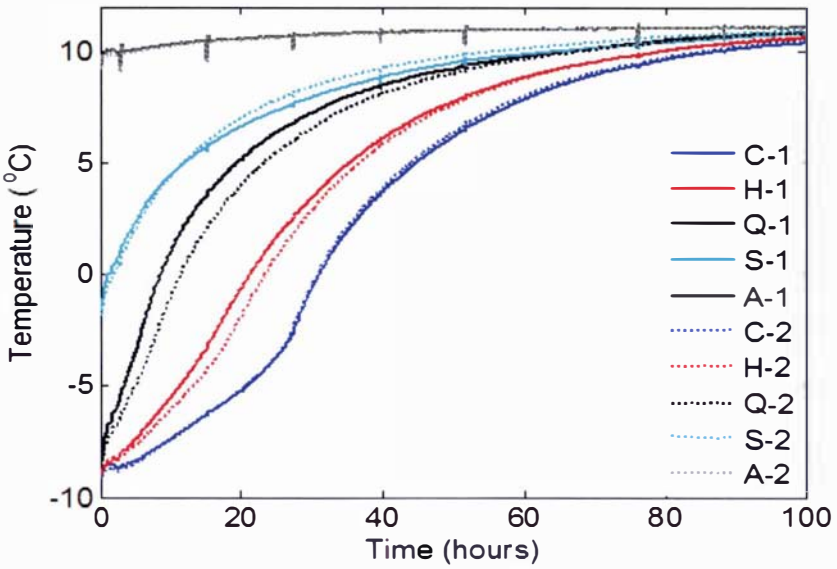

Figure 4.16: Comparison of two independent thawing trials (SBH – 2a) and (SBH – 2b) of salted butter blocks (B15) with:

T_i = -10°C, T_a = 10°C, t_p= 1 year

In contrast to salted butter, unsalted butter would be expected to experience greater supercooling, and hence greater driving forces for ice nucleation would exist at commercial storage temperatures due to less freezing point depression. Therefore, it is possible that the time scales for heat transfer and water freezing might converge for unsalted butter.

4.3.4 Heat Transfer in Unsalted Butter Blocks

The last two experiments conducted for the salted butter were repeated for unsalted butter. Figure 4.17 shows the temperature profile of the butter thawed with an ambient temperature of about 10°C after storage for 6 months at -10°C temperature. A clear plateau can be seen just below the initial freezing point of the butter, which shows that a significant fraction of the water in the butter froze during the few months in which the butter block was kept at -10°C. Both the surface temperatures were consistent, as were the air temperatures, which show that the heat transfer through different sides of the block was uniform. Positions H and Q also demonstrate a clear phase change just below the initial freezing point. The central temperature C quickly reached about -2°C, influenced by the higher thermal conductivity value of frozen butter, and then plateau for nearly 40 hours due to the absorption of latent heat required for ice melting. Once all the ice melted, the temperature increased to approach the ambient temperature.

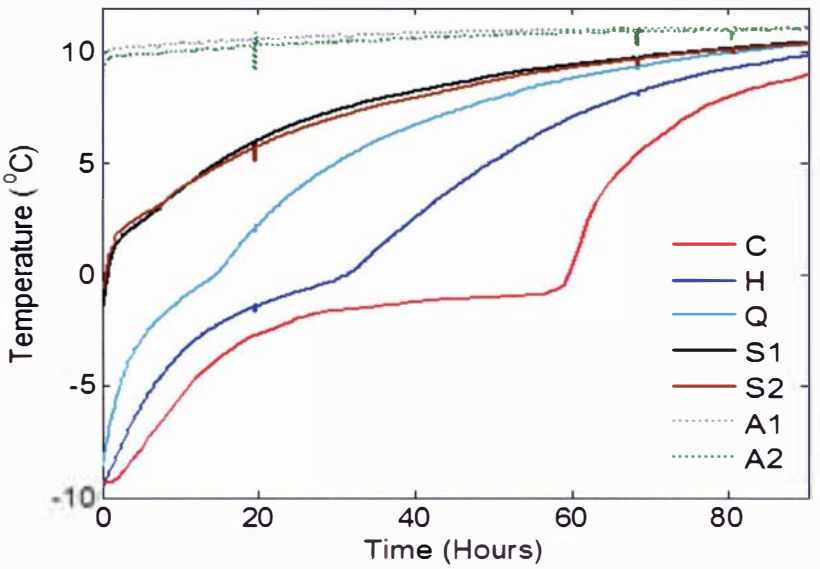

Figure 4.17: Heating of a frozen unsalted butter block (UBH – 1a) with: T_i = -10°C, T_a = 10°C, t_p= 6 months

A comparison of the experimental data collected for frozen (i.e. the water was frozen) salted and unsalted butter is given in Figure 4.18. The salted butter requires less time to thaw compared with unsalted butter. Since the thermal conductivity of the salted butter is lower than that of unsalted butter, below the initial freezing point, the unsalted butter temperature rises more quickly as compared with the salted butter. The phase change for salted butter occurs at a much lower temperature compared with unsalted butter and probably required less latent heat due to less complete freezing due to the greater salt concentration, greater freezing point depression and hence a lower equilibrium ice fraction at -10°C. Overall, even with lower thermal conductivity, the salted butter took about 22 hours less to heat from -10°C to 4°C with a 10°C ambient temperature due to the lesser amount of ice that needed to be thawed.

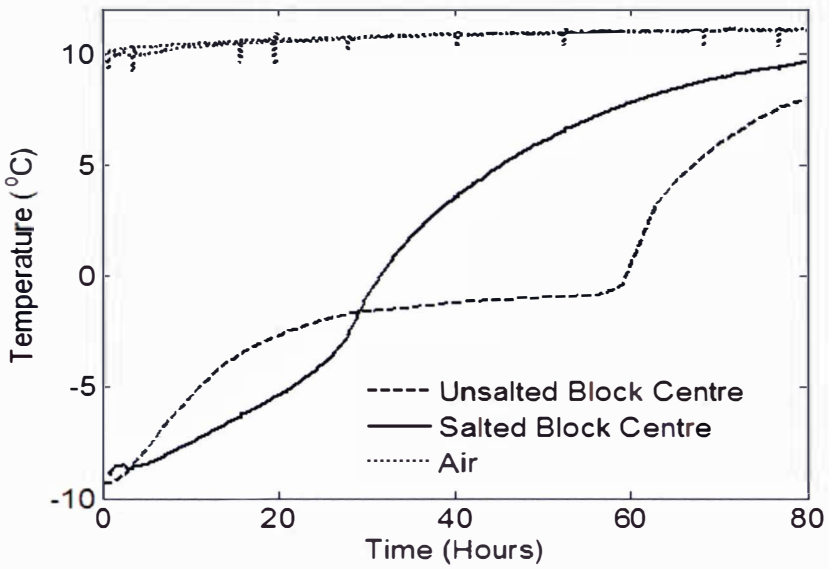

Figure 4.18: Comparison of heating times for salted (SBH – 2a) and unsalted (UBH – 1a) butter blocks

The data for unsalted block showed that most of the water in the butter was frozen if it was kept for 6 months at -10°C. Therefore, it was decided to observe the effect of different ambient temperatures on the freezing time.

A cooling experiment was carried out on the same block of unsalted butter in a room at about -23°C. The block had previously been kept at 10°C long enough to obtain a uniform initial temperature. Figure 4.19 shows the observed temperature profile. The water droplets in the butter were supercooled to many degrees below the initial freezing temperature. After approximately 60 hours, the crystallization process in the water droplets began releasing latent heat faster than it could be removed by conduction, giving a temperature rebound in most of the butter block. As the cooling was ongoing and the crystallisation was not instantaneous, the temperature of the system slowly increased towards the equilibrium freezing point. However, it started to decrease again before the initial freezing point was reached. This is because a large fraction of the water that could freeze had frozen and freeze concentration of the solutes in the water droplet had lowered the freezing point, thereby reducing the driving force for further crystallisation. An alternative explanation is that overall the rate of crystallisation has reduced to a point where the rate of heat removal was greater than the rate of latent heat release.

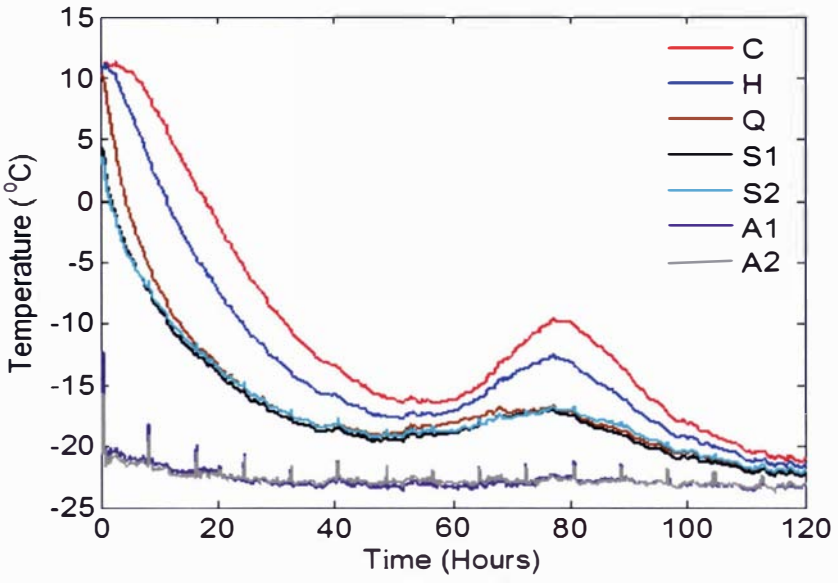

Figure 4.19: Cooling of unsalted butter block (UBC – 1a) with: T_i = 10°C, T_a = -23°C, t_p= 3 weeks

The freezing behavior of butter is apparently very different from other food products where water is present as a continuous phase. To check this behavior was repeatable, the butter block was thawed to 10°C and when a uniform initial temperature was achieved, the block was again cooled under the same conditions. Figure 4.20 shows the comparison of the results of the replicate trials. In the supercooled region the temperature profile of both the runs was nearly identical, but, although cooling conditions were nearly identical, the rebounds in two runs differed by about 20 hours. This suggests that the crystallization processes is stochastic in nature. The nucleation event in a water droplet does not necessary trigger nucleation and ice crystal growth in the other droplets and, thus, the crystallization in each droplet may not be independent. Given the high number of droplets with significantly different droplet size, solute concentration and temperature differences, it is not surprising if nucleation is stochastic in nature.

The repeated experiment showed that the butter freezing behavior was not observed by chance and it is a repeatable process with the exception of the difference in timing of the release of latent heat due to the water crystallization process.

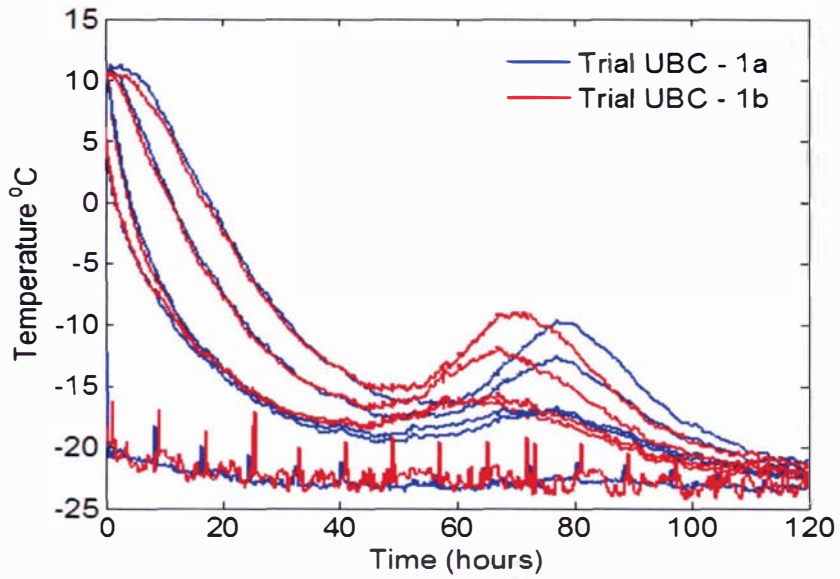

Figure 4.20: Comparison of two cooling trial in the same unsalted butter block (B 19) under identical cooling conditions as:

T_i = 10°C, T_a = -23°C, t_p= 3 weeks

Finally, another experiment was conducted on the same block under different cooling conditions. This time an ambient temperature of about -10°C rather then -23°C was chosen because this is a commonly used industrial storage temperature but the experiment was continued for much longer period of time. Figure 4.21 shows the freezing temperature profile of the butter block. It was observed that butter supercooled to a temperature about 1.5°C above the air temperature and settled there for about 20 hours after which the crystallisation process releasing latent heat very slowly and steadily. Only the centre temperature rebounded to any significant extent, presumably because the rate of cooling achieved was lower (and therefore the rate of crystallisation was lower) at warmer ambient temperature than at -23°C. The extent of the rebound seems to be a delicate balance between the rate of crystallisation of water and the rate of cooling affected by both air temperature and size of the butter block.

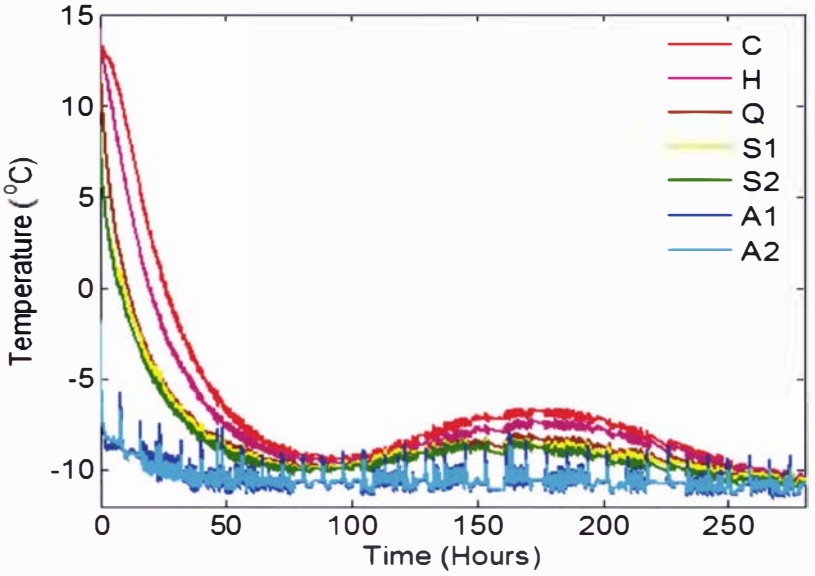

Figure 4.21: Cooling of unsalted butter block (UBC – 2) with: T_i = 10°C, T_a = -10°C, t_p= 3 weeks

4.4 Conclusions

The experiments conducted on salted and unsalted pats and blocks indicated that release of latent heat during freezing is controlled as much by the rate of crystallisation of water in each of the water droplets as by the rate of heat transfer. This is due to the water droplets behaving independently due to the water in oil emulsion structure of but er. Experiments on butter freezing showed that the release of water latent heat depended on the degree of super-cooling, which in turn depended on cooling medium temperature, size of the butter item, packaging, and the type of butter. The crystallization process appears stochastic in nature and, therefore, under the same cooling conditions, water in the same butter may release its latent heat with different timing during the cooling process.

Based on these observations the following conclusions can be made with respect to modelling of heat transfer in butter:

1. The thawing behavior of fully frozen butter might be accurately modeled using a conduction only model with equilibrium thermal properties.
2. The heating behavior of frozen butter depends on the storage temperature history of the butter (how long and at what temperature was it stored at), and therefore the fraction of frozen water. If the fraction frozen is low then might be accurately modeled with a sensible heat model. If the fraction frozen is high then a model that takes account of the latent heat

effect is needed.

3. The freezing of butter is not solely a heat transfer controlled process and probably needs to be modeled using appropriate ice nucleation or both ice nucleation and crystal growth models.

CHAPTER 5

MODELING HEAT TRANSFER IN BUTTER

5.1 Introduction

From the experimental data collected in chapter 4 it was observed that the heat transfer during thawing of frozen butter appeared to be an equilibrium process. That is, the melting of ice and release of latent heat occurs at the temperature representing equilibrium between the frozen and unfrozen phases in the butter. As such it should be able to be accurately modeled using a conduction only model with equilibrium thermal properties. Unfortunately the freezing process probably cannot be accurately modeled in this way due to considerable amount of super cooling and release of latent heat at a lower temperature instead of at the equilibrium freezing point.

This chapter explains the formulation, implementation and validation of a conduction only mathematical model for predicting the heating and cooling behavior of butter.

5.2 Model Formulation

This section describes the development and mathematical formulation of a model in order to predict the temperature of butter as a function of time and position.

5.2.1 Conceptual Model

Figure 5.1 illustrates the physical situation of a block of butter being heated or cooled. The physical basis and assumptions of the model can be summarized as:

- Butter is a homogenous medium of milkfat and dispersed water and ice.
- Three dimensional conduction heat transfer through a homogenous rectangular block of butter of any size depending on the particular application (e.g. pat, carton etc).
- The butter box has symmetric cuboid geometry.
- Initially the block has a constant temperature.

- The heat transfer from the surface of the block to the ambient is by convection to the surrounding medium temperature.
- Radiation and evaporative heat transfer at the surface are either negligible or can be modeled as pseudo-convection.
- Different sides of the carton may experience different air temperatures and different air flow rate (surface heat transfer coefficients).
- Butter has constant density
- The corrugated card board case and the polyethylene liner affect the effective surface heat transfer coefficient but their thermal mass is negligible.
- There is no internal heat generation
- The enthalpy and thermal conductivity of butter follow the temperature dependent relationships determined in chapter 3.
- Enthalpy changes follow equilibrium conditions and thus there is no supercooling.

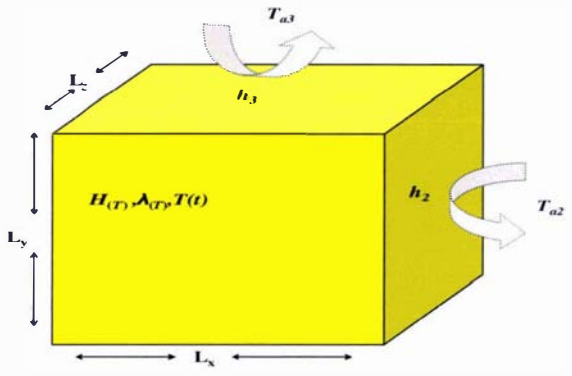

Figure 5.1: A block of butter

5.2.2 Validity of Assumptions

Philpott (2001) measured the density of different types of butter and found less than 1% difference in the density of butter. He found a decrease in density due to temperature increase. The density varied from 960 kg m^{-3} at 12 °C to 952 kg m^{-3} at 20°C which gives < 1% change in this range. Butter shrinks during cooling due to the fat shrinkage and thus increases its density upon freezing. An average value of 970 kg m^{-3} gives about 1% error. Upon thawing, butter increases its volume which would cause the model to underestimate the volumetric heat capacity and over estimate the

thermal conductivity also by about 1%. Thus from these considerations it seems reasonable to assume the density is constant.

From the physical structure of butter explained in chapter 2 it is reasonable to consider butter as homogenous medium of fat with water dispersed in it in the form of tiny droplets.

The packaging used for the butter includes two types. One is corrugated cardboard and other is a polythene liner. The corrugated cardboard has a thermal conductivity of about 0.061 $Wm^{-1}K^{-1}$ and the polyethylene liner has a thermal conductivity of 0.29 $Wm^{-1}K^{-1}$ (ASHRAE 1989). The thermal resistance at the surface includes that caused by the cardboard and any trapped air, so these resistances were included in the effective heat transfer coefficient using equation (5-1). The air-side heat transfer coefficient h_a was estimated from the measured air velocities in the freezer rooms using the relationship given by Cleland *et al.* (2005) which takes account of convection and radiation effects.

$$\frac{1}{h} = \frac{1}{h_a} + \sum \frac{d_p}{\lambda_p} + \frac{d_a}{\lambda_a} \tag{5-1}$$

$$h_a = 7.3 v_a^{0.8} \tag{5-2}$$

For a typical 25 kg block of butter the butter thermal mass is 62.5 kJ $°C^{-1}$ while the thermal mass of the packaging is 0.83 $kJ°C^{-1}$ (< 2 %). So it is reasonable to assume negligible thermal mass of the packaging. Jamieson *et al.*, (1993) successfully used a similar conceptual approach to model freezing in cheese.

Butter is normally manufactured in the form of pats or blocks. Some deformation of the shape at the edges was observed but that gives less than ±5mm error on each axis. This corresponds to less than 1% difference in the volume. Therefore modelling the system as a regular shape was reasonable.

In the product storage rooms it was observed that air velocity varies with position. Although the heat transfer to each surface was found to be reasonably uniform, temperatures on different faces were observed to be different depending on the position of the block in the cool store. If an item was placed near the block then this could affect the air flow and hence the heat transfers through

that face of the block. Therefore different heat transfer coefficients and air temperatures were used for different sides of the block.

Uniform initial temperature was observed in industrial measurements. The temperature data collected from different blocks of a pallet from an industrial production facility differ by less than 0.5°C.

Microbial growth or chemical oxidative reactions can happen in butter at high temperatures but at a very slow rate. These normally do not generate a large amount of heat and have negligible affect on heat transfer.

The butter is tightly wrapped in a polyethylene liner and then packed into corrugated cardboard cases so it is unlikely that there will be any evaporation from the butter surface.

Data collected using cryoscopy for the unsalted butter and estimated for the salted butter showed that the initial freezing point of the butter varies with its composition. Thus thermal conductivity will also be a function of composition.

Data collected in the chapter 3 shows that heat capacity of the butter changes with temperature so it was necessary to use temperature dependent enthalpy relationship.

5.2.3 Mathematical Formulation

Heat conduction in a solid with phase change is governed by the three dimensional partial differential equation:

$$C\frac{\partial T}{\partial t}=\frac{\partial}{\partial x}\left(\lambda_{(T)}\frac{\partial T}{\partial x}\right)+\frac{\partial}{\partial y}\left(\lambda_{(T)}\frac{\partial T}{\partial y}\right)+\frac{\partial}{\partial z}\left(\lambda_{(T)}\frac{\partial T}{\partial z}\right) \text{ for } t>0 \text{ and } 0>x,y,z>L_x,L_y,L_z \tag{5-3}$$

If the enthalpy transformation of Eyres *et al* (1946) is used then (5-3) becomes:

$$\rho\frac{\partial H}{\partial t}=\frac{\partial}{\partial x}\left(\lambda_{(T)}\frac{\partial T}{\partial x}\right)+\frac{\partial}{\partial y}\left(\lambda_{(T)}\frac{\partial T}{\partial y}\right)+\frac{\partial}{\partial z}\left(\lambda_{(T)}\frac{\partial T}{\partial z}\right) \quad \text{for } t>0 \text{ and } 0>x,y,z>L_x,L_y,L_z \tag{5-4}$$

where $H = \int_0^T c_p dT$ (5-5)

and $H(T) = \begin{cases} A + c_f T + B/T & T < T_{if} \\ H_o + c_u T & T \geq T_{if} \end{cases}$ (5-6)

Equation (5-5) can be rearranged to get an inverse relation for T as a function of H given by:

$$T(H) = \begin{cases} \dfrac{-(A-H) - \sqrt{(A-H)^2 - 4c_f B}}{2c_f} & H < H(T_{if}) \\ \dfrac{H - H_o}{c_u} & H \geq H(T_{if}) \end{cases} \quad (5\text{-}7)$$

The thermal conductivity is defined as a function of

$$\lambda(T) = \begin{cases} \lambda_f & T < T_{if} \\ \lambda_u & T \geq T_{if} \end{cases} \quad (5\text{-}8)$$

The convective boundary conditions are given by:

$$\begin{aligned}
h_1(T_{a1} - T) &= -\lambda_{(T)} \frac{\partial T}{\partial x} \quad at \quad x = 0 \;\; \& \;\; t > 0 \\
h_3(T_{a3} - T) &= -\lambda_{(T)} \frac{\partial T}{\partial y} \quad at \quad y = 0 \;\; \& \;\; t > 0 \\
h_5(T_{a5} - T) &= -\lambda_{(T)} \frac{\partial T}{\partial z} \quad at \quad z = 0 \;\; \& \;\; t > 0 \\
h_2(T_{a2} - T) &= \lambda_{(T)} \frac{\partial T}{\partial x} \quad at \quad x = L_x \;\; \& \;\; t > 0 \\
h_4(T_{a4} - T) &= \lambda_{(T)} \frac{\partial T}{\partial y} \quad at \quad y = L_y \;\; \& \;\; t > 0 \\
h_6(T_{a6} - T) &= \lambda_{(T)} \frac{\partial T}{\partial z} \quad at \quad z = L_z \;\; \& \;\; t > 0
\end{aligned} \quad (5\text{-}9)$$

Heat transfer coefficients on all the faces were calculated using equation (5-1).

The uniform initial conditions are given by:

$$T = T_{initial} \quad \text{at} \quad t = 0 \quad \text{and} \quad 0 < x < L_x, \quad 0 < y < L_y, \quad 0 < z < L_z \tag{5-10}$$

5.3 System Input Parameters

The model developed above requires input data for thermal properties and other parameters. The equations describing thermophyscial properties of butter are discussed in chapter 3, dimensions and initial conditions for each experimental trial are discussed in chapter 4 on data collection.

5.4 Numerical Solution of the Heat Transfer Model

The model is too complex to be solved by analytical methods, due to the non-linear relationship between variables and temperature. Moreover with the advancement in the computing technology and facilities available, the model was best solved numerically.

As mentioned in chapter 2 there are a number of commonly used numerical solution methods for partial differential equations, including finite element methods as well as explicit and implicit finite difference schemes.

Finite element methods are used especially where the geometry of the object under study is not regular and simulation software packages are available. However many finite element packages have limited ability to incorporate temperature variable thermal properties.

Explicit finite difference schemes are the easiest to use because the temperature predictions are based on the known values from the past time step. This method has the disadvantage of instability when there are fast changes in the dependent variables (temperature and enthalpy). Implicit finite difference schemes have the advantage of unconditional stability but require additional complexity to solve the simultaneous non linear equations for the past and future values of the dependent variables.

In the case of thawing, the butter pats and blocks of rectangular geometry, and the changes in the temperature are relatively slow apart from at the surfaces, thus the explicit method was used in this study. It was expected that small time steps might be needed to ensure numerical approximation uncertainty was acceptably small and to ensure a stable solution.

A rectangular grid of nodes with p, m and n nodes in the x, y and z direction was used as shown in Appendix A3.1.Thus the continuous system for each block was changed into a discrete system of small similar sized blocks.

The partial differential heat equations that describe the heat transfer for each node were approximated using the Taylor series. Boundary conditions were also approximated using standard finite difference methods. The whole set of equations were generated such that one equation was used for the internal nodes, 8 equations for the 8 corners, 12 equations for 12 edges and 6 equations were used for the 6 faces. These equations along with the initial conditions and thermal property relationships were solved using MATLAB. The detail of the formulation of finite difference scheme can be found in Appendix A3.1-A3.3. Separate function files were used for each of the thermal properties for ease of debugging. The other advantage of separate function files is that for the enthalpy approach, the temperature of the next step must be calculated from the enthalpy at the end of previous time step. One function gave the enthalpy at the given temperature and the other gives the temperature at a given enthalpy. The time domain was solved using Euler's method. A copy of the MATLAB code is given in Appendix A3.4

5.5 Maths Checking

Once the model was solved numerically, it was necessary to perform maths checking to ensure no errors were included in the coding. This included checks of the model against existing validated numerical solutions and checks for any numerical error due to the time step and number of nodes used in the model.

5.5.1 Numerical Error Checking

Significant error in the numerical solution solved by finite difference explicit scheme could occur if the time or space step is too large. For explicit finite difference methods the stability criterion is:

$$\Delta t \leq \frac{\rho c_p}{2\lambda\left(\frac{1}{\Delta x^2}+\frac{1}{\Delta y^2}+\frac{1}{\Delta z^2}\right)} \tag{5-11}$$

Generally if the space sub-division tends towards infinity and time step tends towards zero the model will closely model a continuous system but this requires considerable simulation time.

Numerical solutions also introduce rounding error which keeps on increasing as the simulation time increases. Therefore a study to determine the appropriate space and time steps that could give both stability and accuracy was performed.

A series of simulations were run using typical input data for a block of butter by choosing a grid of 10×10×10 nodes in all the directions. This grid has a maximum time step of 1750 seconds using equation 5-11. Simulations with time step of 875 seconds and 1750 seconds were compared for thawing a typical butter block. The results had a difference of less than 0.026°C from each other over the entire 70 hour period of simulation for the centre temperature of the block. It took 37seconds on a 1.67GHz computer to complete the simulation with the time step of 1750 seconds and halving the time step doubled the simulation time.

Another simulation was run by increasing the nodes to 20×20×20 in each direction. This gives a maximum time step of 486 seconds using the stability criteria. It took 947 seconds to complete the same simulation and the results showed less than 0.07°C difference in the temperature of the centre of the block compared with the 10×10×10 block. These results indicated that the numerical errors were not significant if an appropriate time step is selected using the stability criteria.

Equation (5-11) is a function of density, thermal conductivity and specific heat capacity. Density is assumed to be constant but thermal conductivity and specific heat capacity are functions of temperature. Therefore while using temperature dependent properties minimum values of specific heat capacity and maximum values of thermal conductivity should be used to find the appropriate time step.

5.5.2 Checks Against Previously Validated Solutions

The numerical solution was checked against two existing and validated solutions. A comparison was made against a previously validated finite difference model RADS developed by Cleland and Cleland (1991) for heat conduction in a solid with convective boundary conditions and uniform initial conditions. The comparison was made for a 1m × 1m × 1m cuboid with constant thermal properties (ρ = 923 kg m^{-3}, $\lambda = 0.19 Wm^{-1}K^{-1}$, c_p = 3.6 kJ kg^{-1} $^oC^{-1}$) being heated from 4°C to 12°C. A maximum difference of less than 0. 01°C was found for the centre of the block for a 250 hour simulation with 10×10×10 nodes in each direction.

The other check was made against the analytical solution (Carslaw and Jaeger, 1959). For heat conduction in a block with uniform initial conditions (T_i = 4°C, T_a=12°C) and convective boundary conditions (h =11.4Wm^{-2}K^{-1}). When the analytical solution was compared with the model predictions the maximum temperature difference for the centre of the block temperature was found to be less than 0.03°C.

5.6 Evaluation of Mathematical Model

In this section a sensitivity analysis was done on all the input data to the model and then the model was validated against the experimental data.

5.6.1 Sensitivity Analysis

Once the model was rigorously checked for numerical errors and validated against already existing models, a sensitivity analysis was performed to see how sensitive the model predictions were to each of the input parameters data including density, thermal conductivity, enthalpy, heat transfer coefficient, dimensions, initial freezing point, ambient temperature and initial butter temperature.

The best estimates of the above input data was taken and applied to a 25kg block of butter being heated up from an initial temperature of -9.5°C to an ambient temperature of 11°C. Simulations were run for both completely frozen and unfrozen unsalted butter.

Table 5.1 gives the upper and lower bounds for the predictions for defined % errors in each corresponding input. The percentage error was different for different inputs and was selected from the measured data to reflect the uncertainty in each value.

The density of butter does not change significantly within the temperature range of interest. Sensitivity analysis shows a negligible change in the predictions with 1% density change. So using a constant value for modeling heat transfer in butter is appropriate. Uncertainty in thermal conductivity of the butter was estimated to vary by about 10% below T_{if} and about 5% above T_{if}. Sensitivity analysis on the thermal conductivity shows that it has negligible effect on predicted temperature in the freezing range but gave some differences in the final thawing time. Thus using an appropriate value for thermal conductivity for the thawing and freezing range is important. Uncertainty of ±10% in the enthalpy of the butter had large effects on the thawing time predictions as shown in Table 5.1. Lower specific heat capacity predicts shorter thawing time and higher

specific heat capacity predicts longer thawing times. Heat transfer coefficients are a function of the air flows and the packaging material. The overall resistance is dominated by the packaging and the air gaps. The effect of the resistance due to convection and radiation is not significant as shown in the Table 5.1. Dimensions have significant effect on the thawing time predictions. So accurate determination of the dimensions is very important. Ambient temperature also affects the thawing time significantly. In storage rooms the ambient temperature changes with time due to the incoming and outgoing of the load traffic and imprecise refrigeration system controls. If the measured ambient temperature has large changes, it is important to use time - variable ambient temperature for the model input. The initial temperature of the product is also necessary, although it has negligible effect on the final thawing time predicted.

Table 5.1: Sensitivity analysis of the thawing model to changes in input variables

Input property data	Prediction band (---- + x%, ——— – x %)	
	With Freezing	Without Freezing
Density ρ = 970 ± 1%	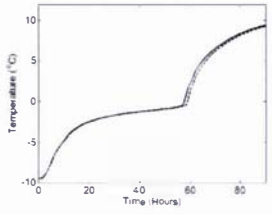	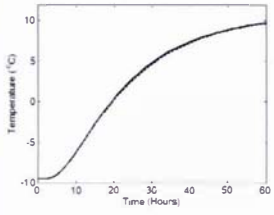
Thermal conductivity λ_f = 0.29 ± 10% λ_u = 0.22 ± 5%	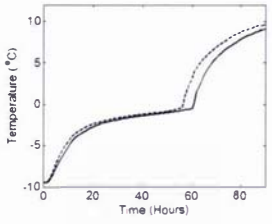	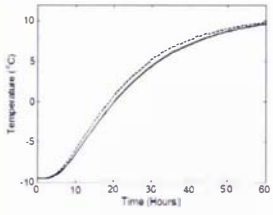
Enthalpy /specific heat H = Eq (5.4) ± 10% c_p =3.2 ±10%	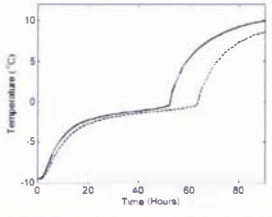	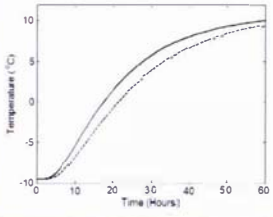
Heat Transfer coefficient h_a = 4.3 ± 30%	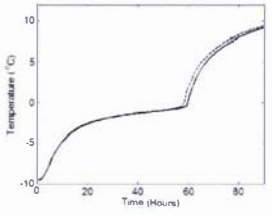	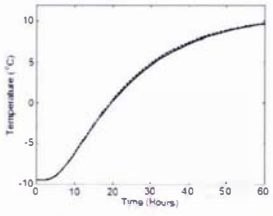

Dimensions $V = \pm 5\%$	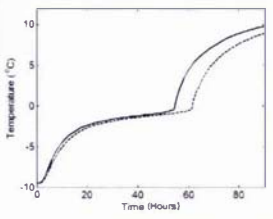	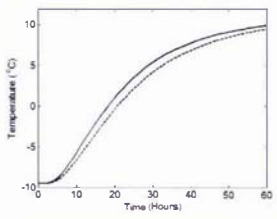
Ambient Temperature $T_a = \pm 2^{\circ}C$	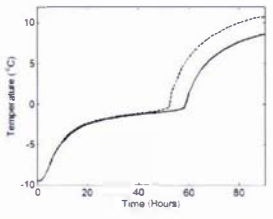	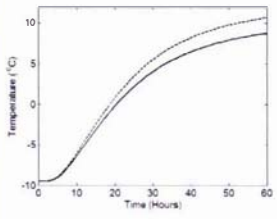
Initial Temperature $T_i = \pm 2^{\circ}C$	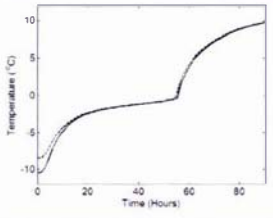	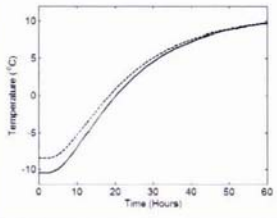

5.6.2 Model Predictions - Thawing

In chapter 4, the experimental data collected for thawing and freezing of butter pats and blocks was summarized. Using the guidelines developed for the number of nodes and the time step in section 5.5 and the thermal properties data determined in chapter 3, the model predictions were compared against the measured data for thawing butter pats and blocks. Two modeling approaches were taken to model the thawing behavior of butter.

The first approach (Equilibrium Properties -Model - 1) assumed equilibrium thawing behavior where the latent heat is absorbed over a range of temperatures up to the initial freezing point. This data is given in Table 3.13. Thus in this case the temperature of the butter will not rise above T_{if} until all the latent heat is absorbed at that position.

The second approach (Sensible Heat Only – Model - 2) was taken by using a temperature dependent enthalpy relationship measured in chapter 3 where the butter was frozen only to -20°C before thawing and no significant water freezing was observed. This was done to approximate the thawing of butter that had not fully frozen prior to thawing.

5.6.2.1 Predicting Thawing of Pats

5.6.2.1.1 Salted Butter Pat (B18, SPH – 1)

From the measured data for the freezing and thawing of butter pats it was observed that the water in butter pat did not freeze unless it was frozen to -70°C. The salted butter pat thawing was predicted with both modeling approaches. Table 5.2 gives the input data used for the predictions.

Table 5.2: Input data for salted butter pat (B18) heat transfer predictions (Trial SPH – 1)

Lx (m)	0.116
Ly (m)	0.060
Lz (m)	0.064
v_a (ms^{-1})	2.5
h ($Wm^{-2}K^{-1}$)	14.9
ρ ($kg\ m^{-3}$)	970
T_i (°C)	-20
$\lambda_f\left(Wm^{-1}K^{-1}\right)=0.29$, $\lambda_u\left(Wm^{-1}K^{-1}\right)=0.22$	Equilibrium Properties Model
$\lambda_f\left(Wm^{-1}K^{-1}\right)=0.22$, $\lambda_u\left(Wm^{-1}K^{-1}\right)=0.22$	Sensible Heat Only Model
$H(kJ\ kg^{-1})=\begin{cases}64.04+1.77T-275.55/T & T<T_{if}\\ 125.85+3.69T & T\geq T_{if}\end{cases}$	(Equilibrium Properties Model)
$H\left(kJ\ kg^{-1}\right)=\begin{cases}2.3T+45.7 & T<-6.8^{o}C\\ 0.06T^{2}+3.6T+51.4 & T\geq -6.8^{o}C\end{cases}$	(Sensible Heat Only Model)
$T_a\left(°C\right)=\begin{cases}-0.98(t/3600)^2+3.1(t/3600)+8.6 & 0\leq t<7200\\ 10 & t\geq 7200\end{cases}$	

For Model -1 the measured enthalpy data given in Table 5.2 measured by DSC was used. For Model - 2 the enthalpy data given in Figure 3.18(b) was used. This data does not include the water latent heat but does include the change in specific heat capacity due to melting of different fat fractions of butter.

The heat transfer coefficient was calculated using equation (5-1) for a pat with 0.011 millimeter thick wax paper in which the butter was wrapped ($\lambda_{paper} = 0.07$ $Wm^{-1}K^{-1}$ Robertson *et al.*, 1998) and assuming no air gap. Equation (5-9) was used to calculate h_a.

The model was run for a grid of 20 ×10×10 nodes in x,y and z directions respectively.

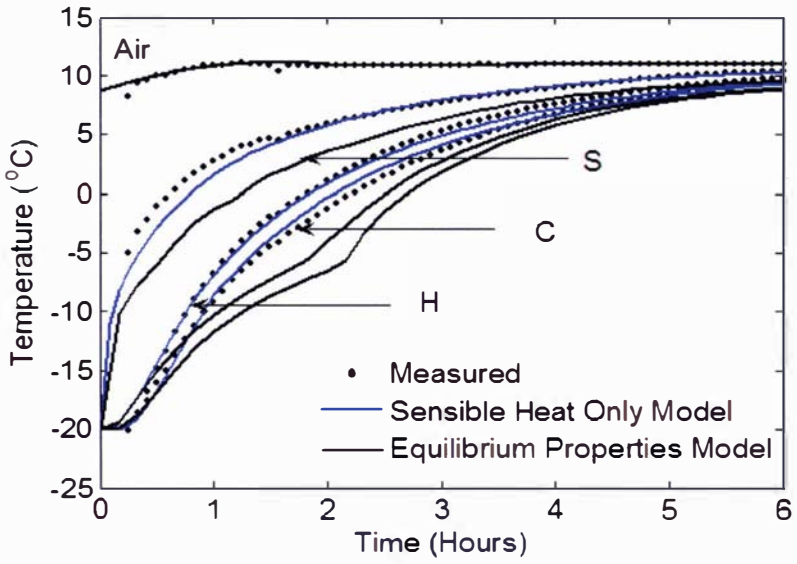

Figure 5.2: Comparison of measured data for thawing of salted butter pat (B18, Trial SPH -1, t_p=13 hours at -20°C) with equilibrium property model and sensible heat only model predictions (S- surface, C-centre, H-20mm from the top) (R^2=0.9956 for the position C)

Figure 5.2 shows the predictions compared with the measured thawing data for B18. Equilibrium thermal properties model closely predicted the experimental data in the very early stages due to the good estimation of the specific heat capacity value used in those ranges but the measured data did not have the predicted latent heat plateau. Thus the equilibrium property model cannot predict the thawing behavior of salted butter pat unless it was completely frozen prior to thawing.

The Model - 2 predictions given in Figure 5.2 agree closely with the experimental data at the centre point (C) (with $R^2 = 0.9956$) and the point (H) which is 20 mm in from the top at the centre of the block (see Fig 4.1). The surface predictions (S) do not match well at the beginning of the thawing process; however these predictions are very sensitive to the location of the thermocouple, ambient

conditions and heat transfer coefficient estimates. The small deviation in the surface would not significantly affect the predictions at the centre of the pat.

There was no experimental data where the salted pat was completely frozen and showed signs of ice melting when thawed.

5.6.2.1.2 Unsalted Butter Pat (Unfrozen, B16, Trial UPH - 1)

For the unsalted butter pats the same approach as used for the salted butter was taken. Both the equilibrium property data (Table 3.13) and the measured enthalpy data for unfrozen unsalted butter given in Figure 3.12(a) were used. Table 5.3 gives the input data used in both the models.

Table 5.3: Input data for unsalted butter pat (B16) heat transfer predictions (Trial UPH – 1)

Lx (m)	0.116
Ly (m)	0.060
Lz (m)	0.064
v_a (m s^{-1})	2.5
h (Wm^{-2}K^{-1})	14.9
ρ (kg m^{-3})	970
T_{if}(°C)	-0.52
T_i(°C)	-15
$\lambda_f\left(\mathrm{Wm^{-1}K^{-1}}\right)=0.29$, $\lambda_u\left(\mathrm{Wm^{-1}K^{-1}}\right)=0.22$	Equilibrium Properties Model
$\lambda_f\left(\mathrm{Wm^{-1}K^{-1}}\right)=0.22$, $\lambda_u\left(\mathrm{Wm^{-1}K^{-1}}\right)=0.22$	Sensible Heat Only Model
$H(\mathrm{kJ\ kg^{-1}})=\begin{cases}81.03+2.05T-33.31/T & T<T_{if}\\ 146.66+5.01T & T\geq T_{if}\end{cases}$	(Equilibrium Properties Model)
$H\left(\mathrm{kJ\ kg^{-1}}\right)=0.07T^2+3.4T+44.9$	for all T (Sensible Heat Only Model)
$T_a\left(^{\circ}\mathrm{C}\right)=\begin{cases}-0.12(t/3600)^2+4.5(t/3600)+14.6 & 0\leq t<7200\\ -0.03(t/3600)^2+0.7(t/3600)+17.8 & t\geq 7200\end{cases}$	

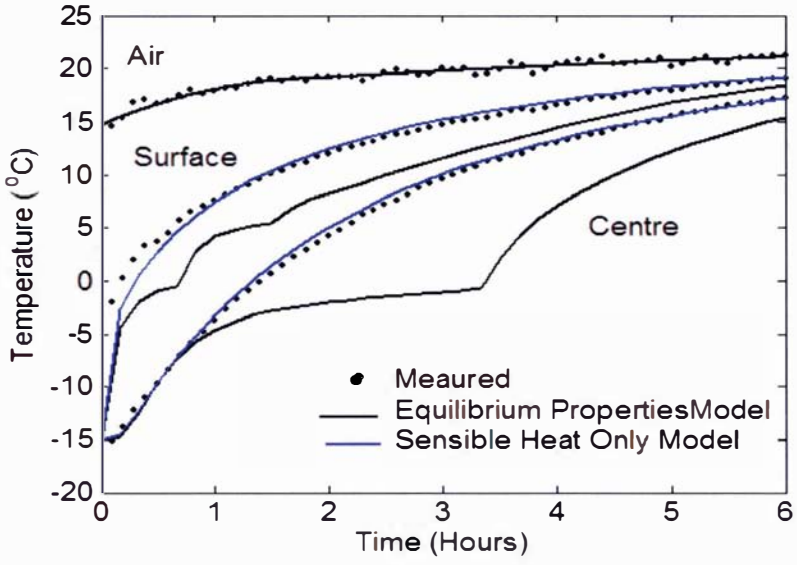

Figure 5.3: Comparison of measured data for thawing of unsalted butter pat (B16, Trial UPH -1, t_p=12 hours at -15°C) with equilibrium properties model and sensible heat only Model predictions for centre and surface of pat

Figure 5.3 shows the predictions compared with the experimental data for the surface and the centre of the block. The results of both model predictions gave the same trends as for the salted butter pat. The Equilibrium properties model showed a long plateau before the initial freezing point is approached, consistent with the absorption of the latent heat of water. This gives a large difference in predicted and actual thawing time.

Figure 5.4 shows the results of sensible heat only predictions for all the positions in the pat. The predictions match very well with the measured data at all points in the unsalted pat.

From both salted and unsalted pat predictions it can be concluded that the equilibrium properties model cannot predict the thawing behavior of butter very well if the water in the pat is not fully frozen. It is necessary to use the temperature dependent enthalpy data excluding water latent heat effects for accurate predictions for the unfrozen butter.

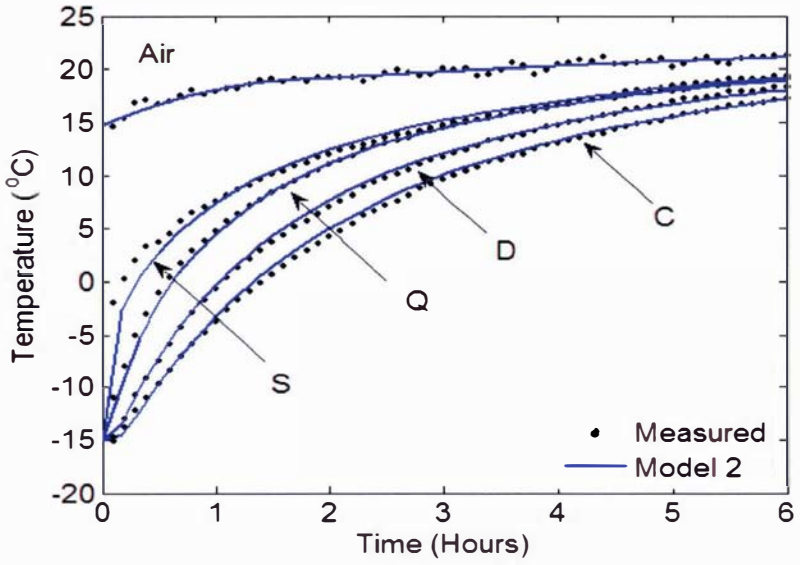

Figure 5.4: Comparison of measured data for unsalted butter pat (B16, Trial UPH -1) with sensible heat only model using temperature dependent specific heat capacity (position of thermocouples position are given in Figure 4.2) (R^2=0.9986 for position C)

5.6.2.1.3 Unsalted Butter Pat (Frozen, B16, Trial UPH – 3):

Trial UPH -3 was the butter which had been previously cooled to -70°C to ensure that all the water had been frozen. The non availability of the thermal properties below -40°C meant that the pat was warmed approximately to -14°C and was kept there for long enough (7 hours) to achieve uniform temperature before thawing it in air at about 20°C.

From the predictions of the salted and unsalted butter pats using both the models it can easily be seen that the equilibrium properties model would be the most realistic in this case. Sensible heat only model predictions were not performed. The input data in Table 5.4 was used in the model to predict the thawing of completely frozen pats.

The predictions of the model are given in Figure 5.5. It can be seen that equilibrium properties model predicts the experimental data well with a coefficient of determination of 0.99 for the centre of the pat. The model under predicts the temperature at the centre of the pat slightly but the prediction for an adjacent node close to the centre of the block has very good fit. The difference

between measured and predicted temperatures can be explained by uncertainty in the position of the thermocouple.

Table 5.4: Input data for unsalted butter pat (B16) heat transfer predictions (Trial UPH – 3)

Lx (m)	0.116
Ly (m)	0.060
Lz (m)	0.064
v_a (ms^{-1})	2.5
h ($Wm^{-2}K^{-1}$)	15
ρ ($kg\ m^{-3}$)	970
T_{if}(°C)	-0.52
T_i(°C)	-14
λ_f ($Wm^{-1}K^{-1}$)	0.29
λ_u ($Wm^{-1}K^{-1}$)	0.22
$H(Jg^{-1}) = \begin{cases} 81.03 + 2.05T - 33.31/T & T < T_{if} \\ 146.66 + 5.01T & T \geq T_{if} \end{cases}$	
$T_a(^{o}C) = \{-0.05(t/3600)^2 + 1.03(t/3600) + 16.32 \quad t \geq 0$	

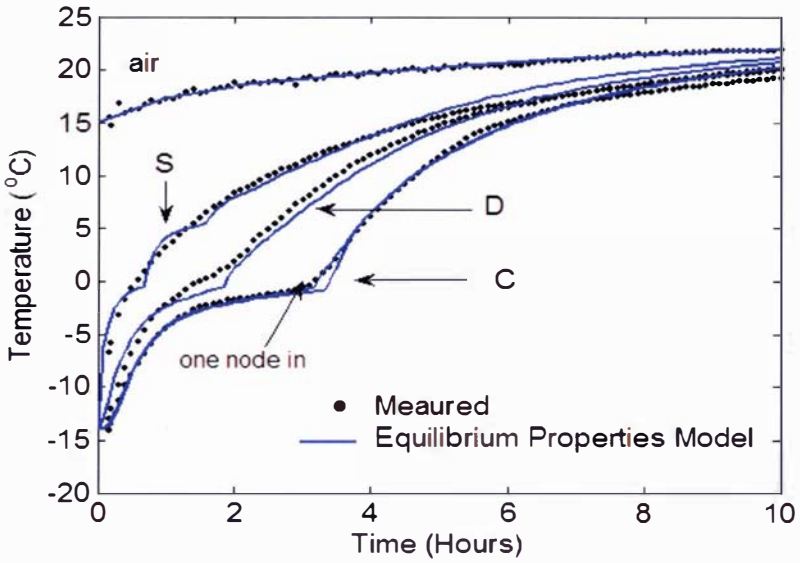

Figure 5.5: Comparison of thawing data of a fully frozen butter pat (B16, Trial UPH – 3, t_p=12 hours at -70°C) with equilibrium properties model (position of the thermocouples are given in Figure 4.2) (R^2=0.9975 for position C)

5.6.2.2 Predicting Thawing of Blocks

Butter is normally packed in 25 kg cartons after manufacturing for the purpose of storage and later on transporting them in the form of pallets to export to other countries. In this section the predictions using either equilibrium thermal properties model or sensible heat only model depending on the extent of water freezing are compared with the thawing data collected for the salted butter blocks with and without packaging and for an unsalted butter block.

5.6.2.2.1 Salted Block (unfrozen with corrugated card board packaging, B15, Trial SBH – 1a)

To predict heat transfer during thawing of 25 kg blocks of butter both the models were used. The input data given in Table 5.5 was used in the models to predict the thawing behavior of salted butter blocks.

Table 5.5: Input data for unsalted butter pat (B15) heat transfer predictions (Trial SBH – 1a)

Lx (m)	0.377
Ly (m)	0.264
Lz (m)	0.242
v_a (ms^{-1})	2.5
h ($Wm^{-2}K^{-1}$)	[4.2, 4.2, 3.3, 3.3, 4.2, 4.2]
ρ ($kg\,m^{-3}$)	970
T_{if} (°C)	-5.35
T_i (°C)	-16.5
$\lambda_f\left(Wm^{-1}K^{-1}\right)=0.29$, $\lambda_u\left(Wm^{-1}K^{-1}\right)=0.22$	Equilibrium Properties Model
$\lambda_f\left(Wm^{-1}K^{-1}\right)=0.22$, $\lambda_u\left(Wm^{-1}K^{-1}\right)=0.22$	Sensible Heat Only Model
$H(kJ\,kg^{-1}) = \begin{cases} 64.04+1.77T-275.55/T & T<T_{if} \\ 125.85+3.69T & T\geq T_{if} \end{cases}$	(Equilibrium Properties Model)
$H(kJ\,kg^{-1}) = 0.02T^2+3.2T+92.4$ for all T	(Sensible Heat Only Model)
$T_a\left(°C\right) = 0.12(t/3600) + 1.48$ $t \geq 0$	

The measured enthalpy data for butter (B15) was used for equilibrium properties model (Table 3.13). For sensible heat only model the data measured and reported in Figure 3.18 (b) was used as an input.

For all models the effective surface heat transfer coefficient (h) was estimated assuming convection from the packaging surface, with the inclusion of the additional resistance to heat transfer caused by the corrugated cardboard carton and the polyethylene liner, and air gaps between the butter and the packaging using equation (5-1). The airside heat transfer coefficient h_a was estimated to be 8 W m^{-2} K^{-1} from the measured air velocities in the freezer rooms using equation (5-2).

Taking $\lambda_a = 0.024$ W m^{-1} K^{-1}, $\lambda_c = 0.061$ W m^{-1} K^{-1} and $\lambda_p = 0.290$ W m^{-1} K^{-1}, and assuming a 1 mm air gap between the cardboard and the liner, gave an overall heat transfer coefficient of 4.2 W $m^{-2}K^{-1}$ for the four vertical side faces (single layer of cardboard) and 3.3 W m^{-2} K^{-1} for the top and bottom surfaces of the carton (due to the double layer of cardboard).

Figure 5.6(a) gives both the model predictions along with the measured data for the salted block of butter with packaging. Predictions using equilibrium properties model were poor due to the absence of the plateau below the initial freezing point in the measured data and therefore over prediction of the time to reach the ambient temperature. The predictions agree very well with the measured data for all the points in the butter block using sensible heat only model with measured temperature dependent heat capacity of butter when butter was froze to -40°C prior to DSC measurements.

Figure 5.7 (b) shows the sensible heat only model predictions for all the positions in the butter block. There was some lack of fit for positions 'D' and 'H' probably due to the actual thermocouple position not exactly matching with the position in the model for the defined grid. A better prediction could be achieved either by increasing the number of nodes in each direction or by using a weighed average method to predict the temperature at the actual position of the thermocouple location.

(a)

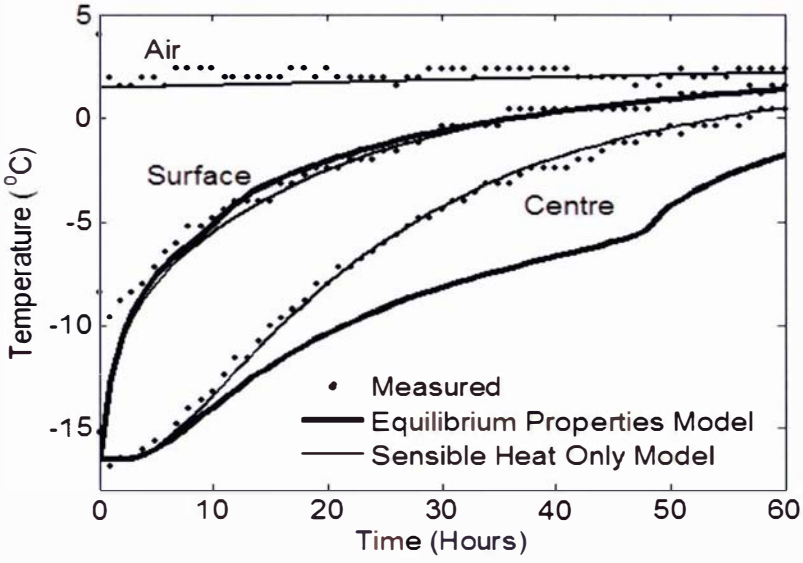

(b)

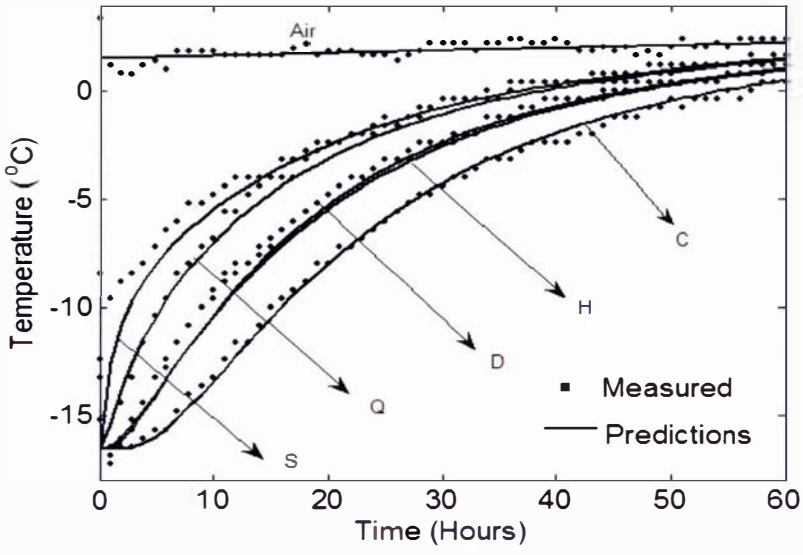

Figure 5.6: (a) Comparison of the measured data for the salted block (B15, Trial SBH-1a, t_p= 3days at -18°C) with equilibrium property model and sensible heat only predictions for surface and centre.

(b) Comparison of the measured data for the salted block using equilibrium properties model predictions for all the positions.

(position of the thermocouples is given in Figure 4.14) (R^2=0.9965 for position C)

5.6.2.2.2 Salted Block (unfrozen without corrugated card board box, B15, Trial SBH – 1b)

To predict the thawing behavior of butter block without corrugated cardboard packaging material, the heat transfer coefficient value was estimated using the equation (5-1) by deleting the cardboard and air gap terms. The value was found to be 7.8 W m^{-2} K^{-1} for all the faces. An average ambient temperature for the model was used as given by equation (5-15). All other input data was the same as used in Table 5.5 for the prediction of the salted block with packaging.

$$T_a\left(^{\circ}\mathrm{C}\right)=\begin{cases}-0.004(t/3600)^2+0.17(t/3600)+0.33 & 0\le t<7200\\ -0.0002(t/3600)^2+0.016(t/3600)+2.08 & t\ge 7200\end{cases} \quad (5\text{-}15)$$

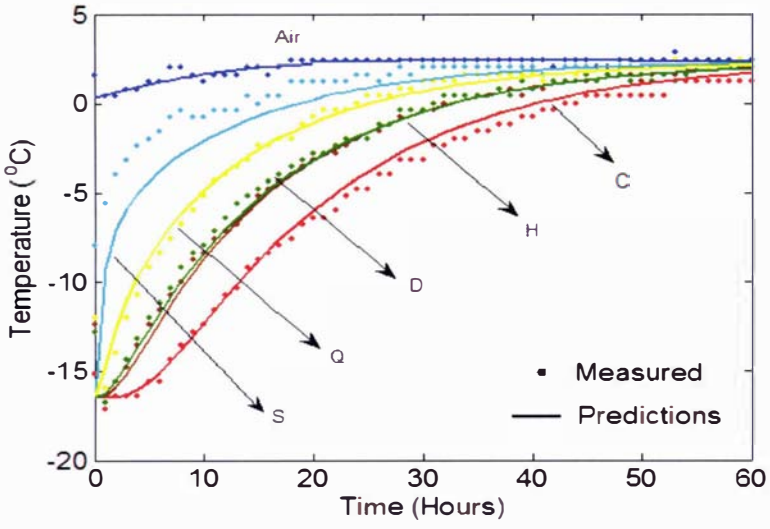

Figure 5.7: Comparison of measured data for salted butter block without packaging (B15, Trial SBH – 1b, t_p= 3 days at -18°C) with predictions using sensible heat only model predictions with temperature dependent heat capacity. (positions of the thermocouples are given in Figure 4.14)

Figure 5.7 shows the measured temperature profiles and the sensible heat only model predictions for the block of salted butter without the packaging effect of the corrugated cardboard. The predictions agree well with the experimental data except for the surface of the block. The poor agreement for the surface temperature probably reflects variation in air temperatures and air velocities on different sides of the block due to its position in the storage room. When packaging is present, the dependence of the overall heat transfer coefficient on air velocities is much less.

5.6.2.2.3 Salted Block (Fully frozen, B18, SBH – 2a)

When a salted butter box of the same type (B15) as the unfrozen ones was thawed after 1 year at about -10°C, it was observed that the water in the butter had fully frozen during that time. In this situation the predictions using the equilibrium properties model were expected to be the most appropriate.

The input data in Table 5.6 was used for the model. The equilibrium enthalpy data from Table 3.12 for butter B15 was used.

Table 5.6: Input data for unsalted butter pat (B15) heat transfer predictions (Trial SBH – 2a)

Lx (m)	0.377
Ly (m)	0.264
Lz (m)	0.242
v_a (ms^{-1})	2.5
h ($Wm^{-2}K^{-1}$)	[4.2, 4.2, 3.3, 3.3, 4.2, 4.2]
ρ (kg m^{-3})	970
T_{if}(°C)	-5.35
T_i(°C)	-8.5
λ_f ($Wm^{-1}K^{-1}$)	0.28
λ_u ($Wm^{-1}K^{-1}$)	0.20
$H(\text{kJ kg}^{-1}) = \begin{cases} 64.04 + 1.77T - 275.55/T & T < T_{if} \\ 125.85 + 3.69T & T \geq T_{if} \end{cases}$	
$T_a\left(^{\circ}\text{C}\right) = 2\times10^{-5}(t/3600)^2 + 0.035(t/3600) + 9.74 \qquad t > 0$	

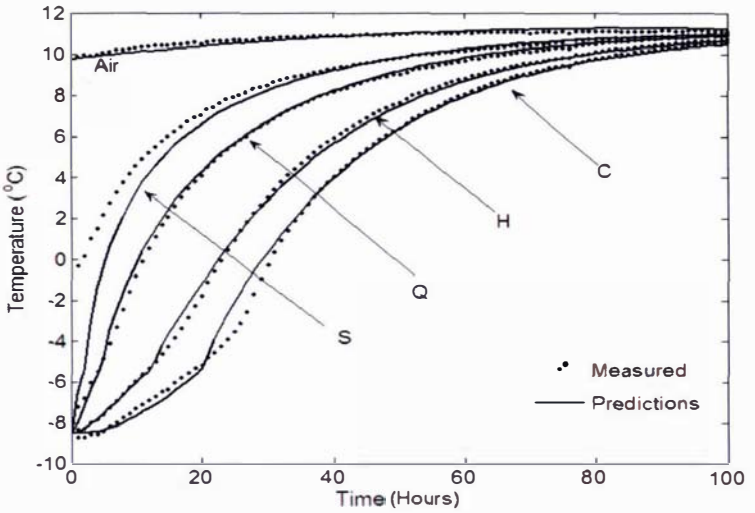

Figure 5.8: Measured data for thawing of fully frozen salted butter block (B 15, Trial SBH – 2a, t_p=1 year at -10°C) compared with the equilibrium thermal properties model predictions (positions of the thermocouple are given in Figure 4.14) (R^2=0.9898 for position C)

Figure 5.8 shows that the model predictions compared well with the experimental data over the whole range except for the centre of the butter in the phase change region (R^2= 0.9898). The estimated initial freezing point appears lower than that observed in the data suggesting that uncertainty in the enthalpy data may have caused the lack of fit in that region. In addition, the method used to model the data to correct the temperature shift in DSC may have led to increase uncertainty for the enthalpy data in this temperature range.

5.6.2.2.4 Unsalted Block (Fully Frozen, B19, Trial UBH – 1a)

An unsalted butter block was also kept for a long time at about -10°C before thawing it. The recorded thawing data showed a very clear plateau just below the initial freezing point. Therefore only the equilibrium property model was used to predict the thawing behavior. The enthalpy data given in Table 5.7 measured by DSC was used. The other input data used is given in Table 5.7. The model was run with 20 x 20 x 20 nodes in each direction to more closely match the exact positions of the thermocouple.

Table 5.7: Input data for unsalted butter block (B19) heat transfer predictions (Trial UBH – 1a)

Lx (m)	0.3675
Ly (m)	0.2731
Lz (m)	0.2365
v_a (ms^{-1})	>4.5
h ($Wm^{-2}K^{-1}$)	[6.8, 6.8, 4.7, 4.7, 6.8, 6.8]
ρ ($kg\ m^{-3}$)	970
T_{if}(°C)	-0.41
T_i(°C)	-9.3
λ_f ($Wm^{-1}K^{-1}$)	0.29
λ_u ($Wm^{-1}K^{-1}$)	0.22
$T_a\left(^{\circ}\mathrm{C}\right) = 2\times10^{-5}(t/3600)^2 + 0.04(t/3600) + 9.37 \qquad t \geq 0$	
$H\left(\mathrm{kJ\ kg^{-1}}\right) = 71.08 + 1.8T - \frac{27.75}{T} \qquad T \leq T_{if}$ $H\left(\mathrm{kJ\ kg^{-1}}\right) = 139.98 + 3.96T \qquad T > T_{if}$	

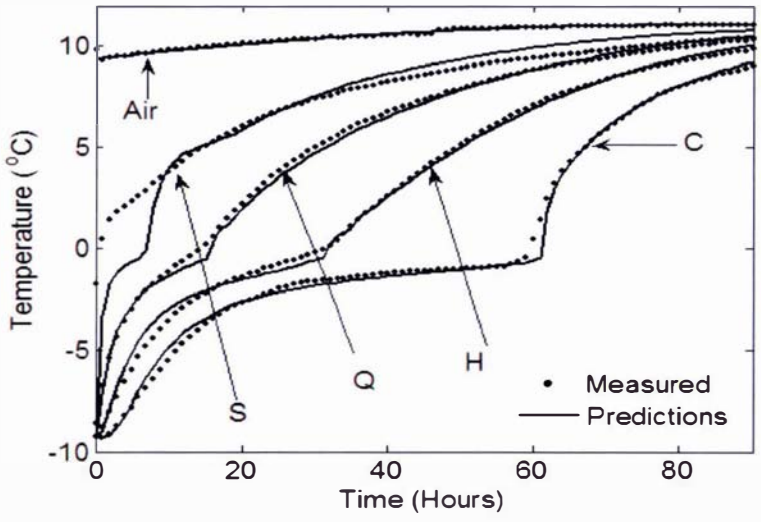

Figure 5.9: Measured data for thawing of fully frozen unsalted butter block (B 19, Trial UBH – 1a, t_p= 6 months at -10°C) compared with the equilibrium thermal properties model predictions (positions of the thermocouple are given in Figure 4.4) (R^2=0.9963 for position C)

Figure 5.9 shows the model predictions along with the experimental data. It can be seen that the equilibrium property model agrees well with the experimental data for all the positions in the butter block. The surface temperature also agreed well except below T_{if} where the model predictions show a distinct plateau that was not observed in the measured data.

5.6.2.3 Summary

The above sections show that the model performance for the thawing behavior of blocks was similar to that found for the pats although the thawing rates were slower. The equilibrium thermal property model was needed to model the thawing behavior of butter blocks where the blocks are fully frozen. For unfrozen blocks, the measured temperature dependent enthalpy relation for the unfrozen butter was needed to get accurate predictions.

5.6.3 Model Predictions – Freezing

Like thawing, two modeling approaches were taken for predicting freezing in butter. In the Model -1, **equilibrium thermal properties** were used. For the equilibrium thermal properties model the measured enthalpy data from chapter 3 was used (Table 3.13) along with temperature dependent thermal conductivity values.

In Model -2, **sensible heat only** thermal properties data was used (Figure 3.21, Figure 3.22)

5.6.3.1 Predicting Freezing of Pats

The experimental data collected for the butter pats showed that the water in the butter super cooled and did not freeze even if it was held at a lower temperature for long period of time. The unsalted pat did completely freeze when an experiment was conducted in a -70°C freezer.

5.6.3.1.1 Salted Pat

The system inputs in Table 5.8 were used to model the freezing behavior of a salted pat. Figure 5.10 compares the model predictions with the measured data for the surface and the centre of the salted butter pat (Trial SPC -1). The experimental data for the ambient conditions varied significantly at the third hour after the start of the experiment due to the opening of freezer doors. It can be seen that the sensible heat only model (Model - 2) predicted the measured data very well over the whole of the temperature range. The equilibrium thermal properties model (Model – 1) showed a plateau at the initial freezing point and as soon as all the latent heat had been removed the temperature

approached the ambient temperature gradually. Although both models reached the ambient temperature at the same time there was a large difference in predictions in the phase change region. It is clear that the best approach modeling freezing in butter pats is by Model -2 and neglecting water droplet freezing.

Table 5.8: Input data for salted butter pat (B18) heat transfer predictions (Trial SPC – 1)

Lx (m)	0.116
Ly (m)	0.060
Lz (m)	0.064
v_a (m s^{-1})	2.5
h ($Wm^{-2}K^{-1}$)	[4.2, 4.2, 3.3, 3.3, 4.2, 4.2]
ρ (kg m^{-3})	970
T_{if}(°C)	-5.35
T_i(°C)	2
c_p (k $Jkg^{-1}°C^{-1}$)	3.1 (Sensible Heat Only Model)
$\lambda_f\left(Wm^{-1}K^{-1}\right)=0.29$, $\lambda_u\left(Wm^{-1}K^{-1}\right)=0.22$	Equilibrium Properties Model
$\lambda_f\left(Wm^{-1}K^{-1}\right)=0.22$, $\lambda_u\left(Wm^{-1}K^{-1}\right)=0.22$	Sensible Heat Only Model
$H(\text{kJ kg}^{-1}) = \begin{cases} 64.04+1.77T-275.55/T & T<T_{if} \\ 125.85+3.69T & T\geq T_{if} \end{cases}$	(Equilibrium Properties Model)
$T_a(°\text{C}) = \begin{cases} 0.83(t/3600)^2 - 2.96(t/3600) - 21.52 & 0\leq t<10080 \\ -0.02(t/3600) - 23.41 & t\geq 10080 \end{cases}$	

(a)

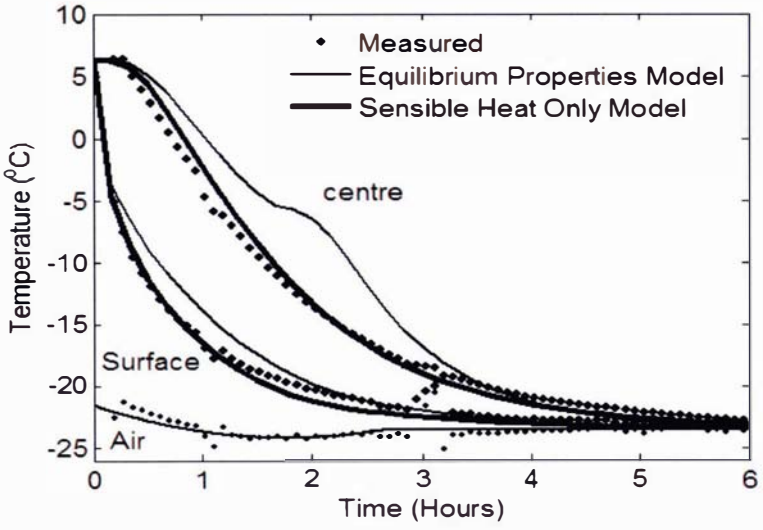

(b)

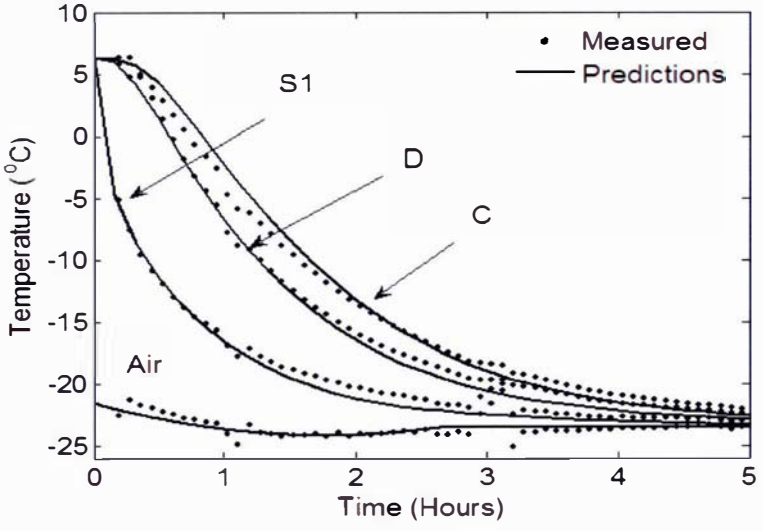

Figure 5.10(a): Comparison of measured data for the freezing of the salted pat (B18, Trial SPC - 1) with Equilibrium thermal properties model predictions and the sensible heat only model predictions

(b) Measured data for the salted pat(B18) with the sensible heat only model for all the positions (positions of the thermocouple are given in Figure 4.1)

5.6.3.1.2 Unsalted Pat (B16, Trial UPC -1)

The data measured in Chapter 4 for the unsalted butter showed that the water in the butter supercooled to many degrees below the initial freezing point of the butter and the centre temperature remained a degree higher than the ambient temperature for a while. Both the modeling approaches were used to compare with the experimental results. The input data given in Table 5.9 was used to model the freezing of unsalted butter pats:

Table 5.9: Input data for unsalted butter block (B16) heat transfer predictions (Trial UPC – 1)

Lx (m)	0.116
Ly (m)	0.060
Lz (m)	0.064
v_a (ms^{-1})	2.5
h ($Wm^{-2}K^{-1}$)	15
ρ ($kg\ m^{-3}$)	970
T_{if} (°C)	-0.41
T_i (°C)	14.5
c_p ($Jg^{-1o}C^{-1}$)	3.2 (Sensible Heat Only Model)
$\lambda_f\left(Wm^{-1}K^{-1}\right)=0.29$, $\lambda_u\left(Wm^{-1}K^{-1}\right)=0.22$	Equilibrium Properties Model
$\lambda_f\left(Wm^{-1}K^{-1}\right)=0.22$, $\lambda_u\left(Wm^{-1}K^{-1}\right)=0.22$	Sensible Heat Only Model
$H\left(kJ\ kg^{-1}\right)=62.42+1.578T-\frac{17.37}{T}$ $H\left(kJ\ kg^{-1}\right)=105.40+4.02T$	$T \le T_{if}$ $T > T_{if}$ (Equilibrium Properties Model)
$T_a\left(^{\circ}C\right)=\begin{cases}-0.47(t/3600)^2 - 2.56(t/3600)-13.69 & 0 \le t < 10080 \\ -0.15(t/3600)-16.97 & t \ge 10080\end{cases}$	

Figure 5.11 shows the predictions using both models compared with the experimental data. As expected the equilibrium property model predicted a plateau at the initial freezing point after which the temperature approached the ambient temperature quickly. Again the sensible heat only model predicted the measured temperature accurately but due to absence of any heat removal the predicted temperature continuously cooled and reached the ambient temperature slightly faster than the actual measured data.

Figure 5.11(b) shows the predictions for the sensible heat only model for all the measured positions in the butter pat. The model predicted well for all positions. There was some difference in the surface temperature prediction that suggested some uncertainties in the input data or the thermocouple positions.

(a)

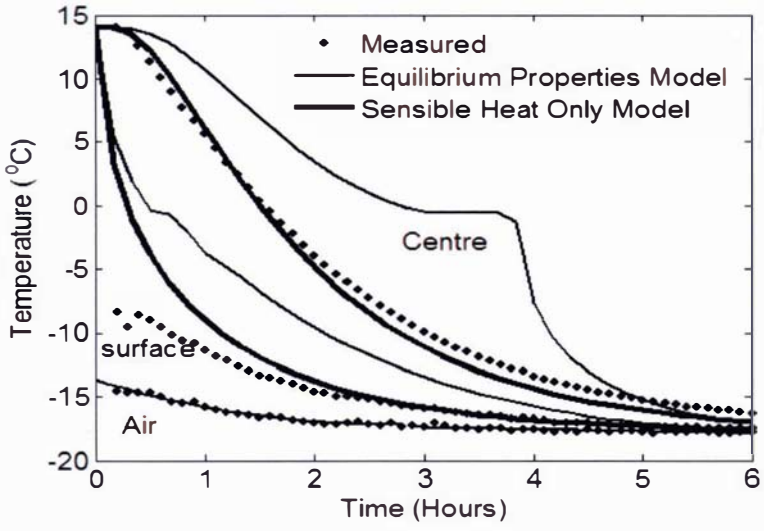

(b)

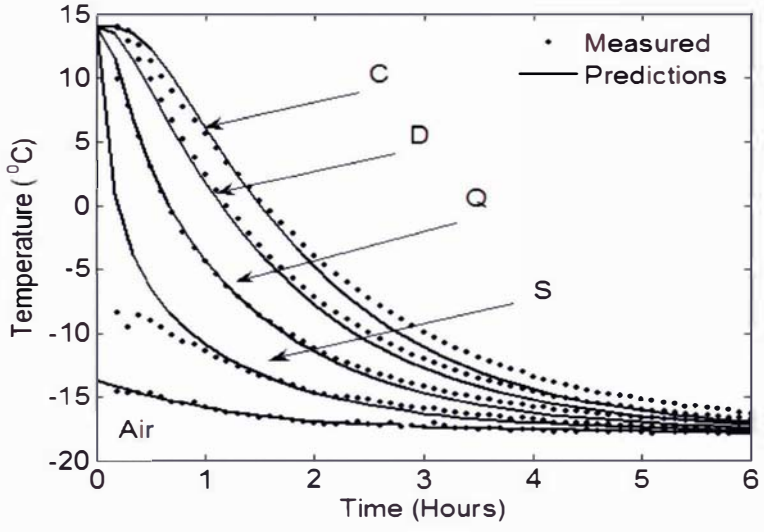

Figure 5.11: (a) Measured data for the unsalted butter pat (B16, Trial UPC – 1) compared with the sensible heat only model and the equilibrium property model predictions
(b) Measured data compared with the sensible heat only model predictions for all the position in the pat (positions of the thermocouples are given in Figure 4.3)

Overall in both salted and unsalted butter pats, the sensible heat only model predicted the data better than the equilibrium property model. For both the pat predictions equilibrium property model used a specific heat capacity above the T_{if} that was higher than that used for the sensible heat only model which gave significant differences in the predictions above T_{if}. It was observed in the DSC measurement that the heating and cooling specific heat capacity of butter was different due to the supercooling of the fat fraction and the fat fraction phase change.

5.6.3.2 Predicting Freezing of Blocks

Both the models were also used to predict freezing in 25 kg salted and unsalted butter blocks in the same manner to that described for freezing of pats.

5.6.3.2.1 Salted Blocks (B15, SBC – 1a)

Chapter 4 showed that during freezing of salted butter blocks the water in the butter did not freeze when the block were held for about 60 hours in a -18°C room. Therefore it was expected that a sensible heat only model would give the best predictions. The experimental data for the ambient conditions varied significantly during the experiment due to the opening of freezer doors. Ambient temperature has a large effect on the model predictions and accurate input data is necessary for the model. The ambient temperature was approximated by breaking it into four regions. Table 5.10 shows the input data used:

Figure 5.12 (a) shows the predictions for the salted block frozen to a temperature of about -18°C using both the models. The prediction trends were exactly the same as for the freezing of butter pats. It was thought that due to the slow rates of cooling in butter as compared with the pats, the equilibrium property model might give better predictions compared with the sensible heat only model but this was not the case. Figure 5.12 (b) shows that the sensible heat only model predicted the measured data at all the positions very well.

Table 5.10: Input data for salted butter block (B15) heat transfer predictions (Trial SBC – 1a)

Lx (m)	0.377
Ly (m)	0.264
Lz (m)	0.242
v_a (m s^{-1})	2.5
h (Wm^{-2}K^{-1})	[4.2, 4.2, 3.3, 3.3, 4.2, 4.2]
ρ (kg m^{-3})	970
T_{if} (°C)	-5.35
T_i (°C)	2
c_p(kJ kg^{-1}°C)	3.1 (Sensible Heat Only Model)

$$\left.\begin{aligned}\lambda_f\left(\mathrm{Wm^{-1}K^{-1}}\right)&=0.29\\ \lambda_u\left(\mathrm{Wm^{-1}K^{-1}}\right)&=0.22\end{aligned}\right\}\ \text{Equilibrium Properties Model}$$

$$\left.\begin{aligned}\lambda_f\left(\mathrm{Wm^{-1}K^{-1}}\right)&=0.22\\ \lambda_u\left(\mathrm{Wm^{-1}K^{-1}}\right)&=0.22\end{aligned}\right\}\ \text{Sensible Heat Only Model}$$

$$H\left(\mathrm{kJ\ kg^{-1}}\right)=\begin{cases}64.04+1.77T-275.55/T & T<T_{if}\\ 125.85+3.69T & T\geq T_{if}\end{cases}\quad\text{(Equilibrium Properties Model)}$$

$$\begin{aligned}T_a\left(^{\circ}\mathrm{C}\right)&=-0.13(t/3600)-16.03 && 0\leq t<54000\\ T_a\left(^{\circ}\mathrm{C}\right)&=\ \ 1.45(t/3600)-39.75 && 54000\leq t<68400\\ T_a\left(^{\circ}\mathrm{C}\right)&=-1.25(t/3600)+11.55 && 68400\leq t<82800\\ T_a\left(^{\circ}\mathrm{C}\right)&=-0.03(t/3600)-16.43 && t\geq 82800\end{aligned}$$

(a)

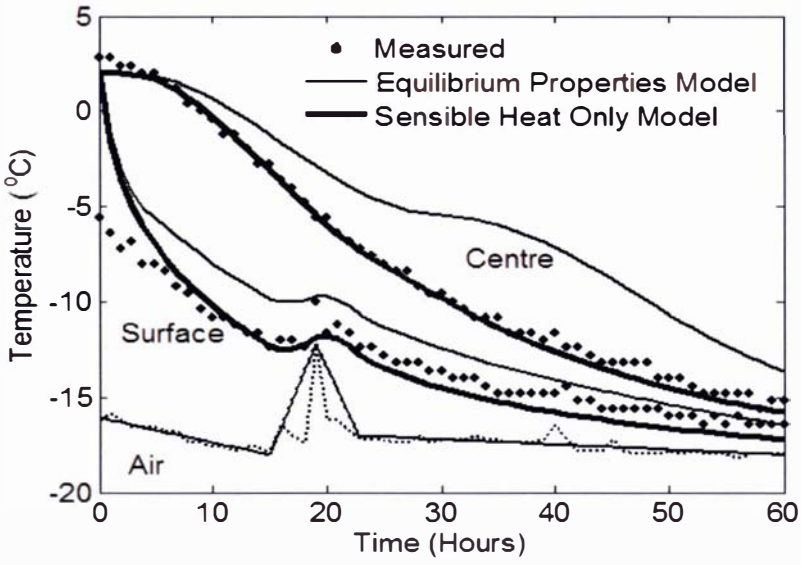

(b)

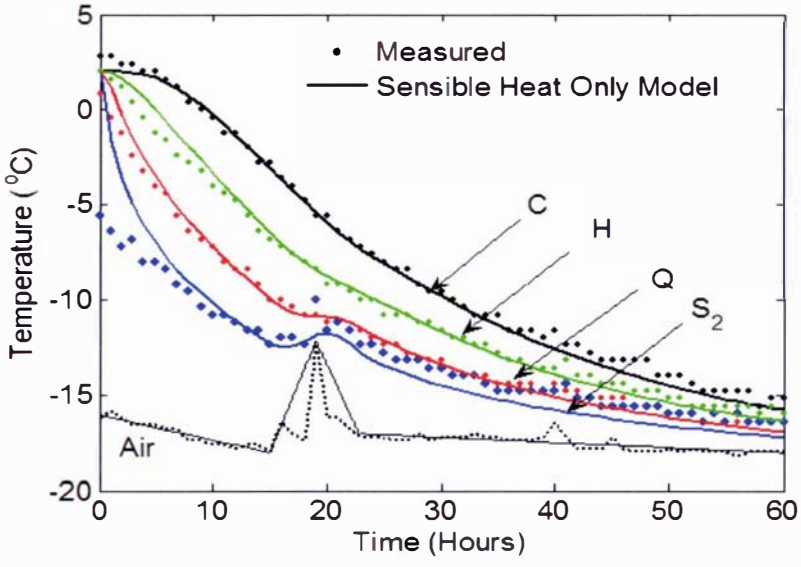

Figure 5.12: (a) Measured data for the salted butter block (B15, Trial SBC – 1a) compared with the sensible heat only model and the equilibrium property model predictions (b) Measured data with the sensible heat only model for all the positions in the salted block (positions of the thermocouples given in Figure 4.3)

Figure 5.13 shows the predictions for the salted block without packaging using the sensible heat only model. The predictions and measured data agree very well for all the positions in the block. For this model a higher heat transfer coefficients value (7.2 $Wm^{-2o}C^{-1}$) was estimated from equation (5-1) because the resistance due to the cardboard packaging was not present.

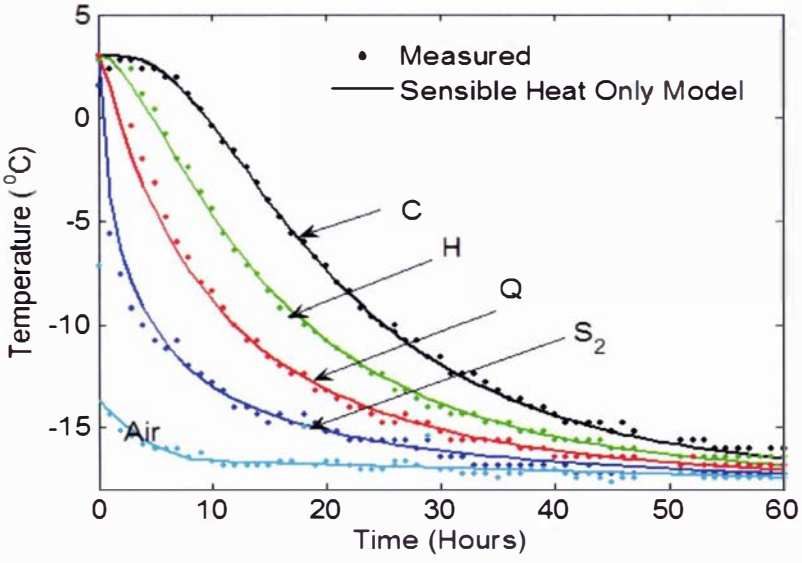

Figure 5.13: Measured data for the salted butter block (B15, Trial SBC – 1b) compared with the sensible heat only model for all the positions in the salted block (positions of the thermocouples given in Figure 4.3)

5.6.3.2.2 Unsalted Block (B18, UBC – 1a)

In chapter 4 the measured data for the unsalted butter showed that the water in the butter supercooled and then a temperature rebound was observed in the whole block when the block was frozen with an air temperature of about -23°C. The same phenomenon was observed when the same block was frozen in a -10°C room. It took quite a long time (300 hours) to freeze the butter completely in a -10°C room as compared to the -23°C room (120 hours).

Both sensible heat only and the equilibrium properties model were used to predict the freezing behavior in this case as well, although neither model would ever predict a temperature rebound as observed experimentally. The input data in Table 5.11 was used:

Table 5.11: Input data for unsalted butter block (B18) heat transfer predictions (Trial UBC – 1a)

Lx (m)	0.3675
Ly (m)	0.2731
Lz (m)	0.2365
v_a (m s^{-1})	2.5
h (Wm^{-2}K^{-1})	[4.2, 4.2, 3.3, 3.3, 4.2, 4.2]
ρ (kg m^{-3})	970
T_{if}(°C)	-0.41
T_i(°C) for -23°C Ambient	11
T_i(°C) for -10°C Ambient	13
c_p(kJ kg^{-1}°C)	3.2 (Sensible Heat Only Model)
$\lambda_f\left(\mathrm{Wm^{-1}K^{-1}}\right)=0.29$, $\lambda_u\left(\mathrm{Wm^{-1}K^{-1}}\right)=0.22$	Equilibrium Properties Model
$\lambda_f\left(\mathrm{Wm^{-1}K^{-1}}\right)=0.22$, $\lambda_u\left(\mathrm{Wm^{-1}K^{-1}}\right)=0.22$	Sensible Heat Only Model
For -23°C room: $T_a(^\circ\mathrm{C})=\begin{cases}-0.1\left(t/3600\right)-20 & 0\le t\le 118800\\ -23.2 & t>118800\end{cases}$	
For -210°C room: $T_a(^\circ\mathrm{C})=\begin{cases}-0.5\left(t/3600\right)-8.7 & 0\le t\le 140400\\ -10.7 & t>140400\end{cases}$	
$H\left(\mathrm{kJ\ kg^{-1}}\right)=71.08+1.8T-\frac{27.75}{T}$ $H\left(\mathrm{kJ\ kg^{-1}}\right)=139.98+3.96T$	$T\le T_{if}$ (Equilibrium Property Model) $T>T_{if}$

Figure 5.14 compares the predictions for both the models with measured data for the centre and a surface of the block of butter The "sensible-heat-only" model predicted the experimental data very well for the whole of the supercooled region (down to about –10 °C) but because of the absence of latent heat removal, the predicted centre and surface temperatures continued to decrease to the ambient temperature without any freezing plateau or rebound. As expected, the equilibrium thermal properties model gave a temperature plateau just below the initial freezing point. After all the latent heat had been released, the temperature decreased rapidly to the ambient temperature because of the removal of sensible heat only. However, because the latent heat was removed at a higher temperature on average compared with the experimental data, the overall predicted rate of freezing

was too fast. These results suggest that if freezing predictions of butter cartons is required, more complex models of water freezing kinetics must be included in the model.

(a)

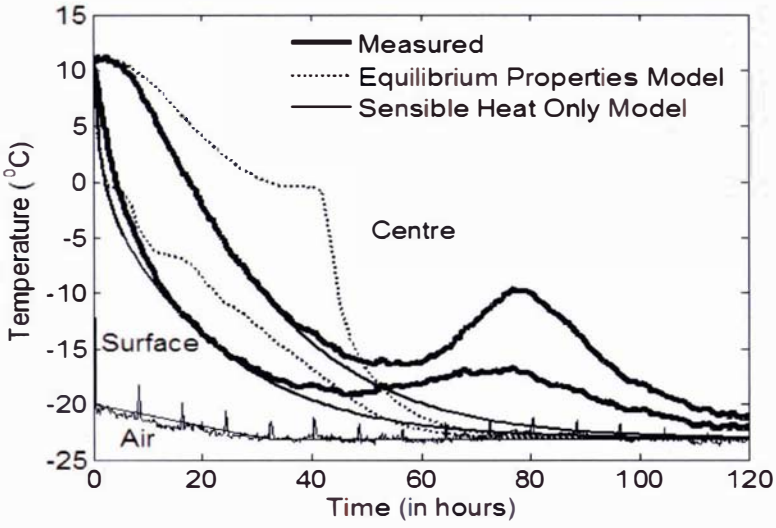

(b)

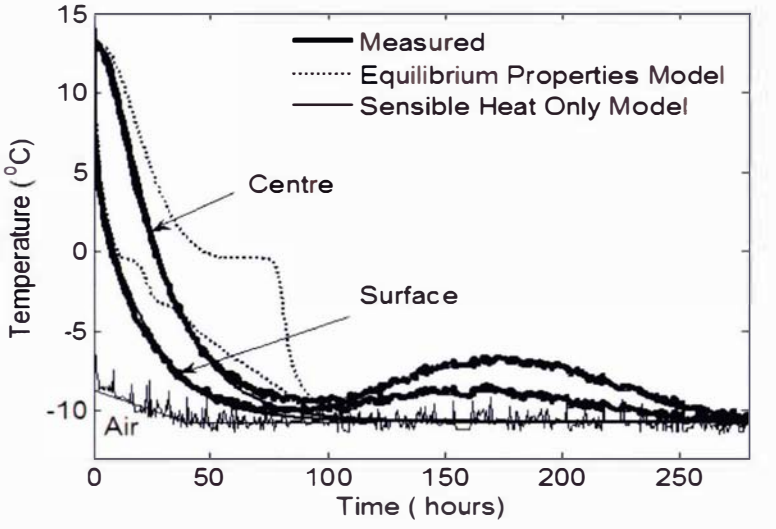

Figure 5.14: Measured data for the unsalted butter block (B19) compared with the sensible heat only model and the equilibrium property model predictions

(a) Freezing with an air temperature of -23°C (UBC-1a)

(b) Freezing with an air temperature of -10°C (UBC-2)

5.7 Conclusions

In light of the observations made in Chapter 4 and Chapter 5 the following conclusion can be drawn:

5.1.1 Thawing of Butter

- The equilibrium thermal properties model (Model 1) predicted the thawing behavior of butter pats and blocks well when the water in the butter was completely frozen before thawing.
- The modeled equilibrium thermal properties model could not predict the thawing behavior of butter when the water in butter was not previously fully frozen due to the absence of the plateau around the initial freezing point of the butter.
- Using the measured temperature dependent specific heat capacity data for unfrozen butter including melting of some of the fat fraction gave accurate predictions.

5.7.2 Freezing of Butter

- The equilibrium thermal properties model gave poor predictions of the freezing of butter pats or butter blocks.
- The simplified model with sensible heat only predicted the freezing behavior accurately for butter pats and the salted blocks of butter during the supercooling period only.
- For butter blocks the sensible heat only model predicts the measured data accurately until the water droplet freezing occurs, releasing latent heat and giving a rebound in the temperature of the block.
- Modeling the freezing of butter is not trivial. The rebound in the temperature occurred for same block of butter at two different places in time in replicate experiments; suggest that freezing in butter is not limited by the rate of heat transfer but also by nucleation and growth of ice crystals. To model this behavior a model taking account of nucleation and /or growth in water in oil emulsions is needed.

The next chapter comprises the modification of the heat transfer model developed in this chapter to take account of nucleation and growth of the water droplets in butter.

CHAPTER 6

MODELLING FREEZING OF BUTTER

6.1 Introduction

Butter is a water in oil emulsion so its behavior during freezing is very different from that of most of the food products, in which water forms the continuous phase. Measurements of the freezing of butter in Chapter 4 showed that the release of latent heat from the freezing water depends on the degree of supercooling which, in turns depends on the cooling medium temperature, the size of the butter item, the packaging and the type of butter. It was postulated that the nucleation of water within butter is the rate limiting process because they are present in the form of tiny droplets, which supercool below the initial freezing point of the water in the bulk form. The nucleation in each droplet would be unlikely to trigger nucleation and ice growth throughout the rest of the butter because the droplets probably nucleate and freeze independently of each other. Franks (1985) and Walstra (2003) explained that significant supercooling can occur in water in oil emulsions because of the division of the water phase into such small droplets that nucleation sites (e.g. impurities) are not present in most of the particles. Therefore, in butter the release of latent heat during freezing may be controlled as much by the rate of crystallization of water in each droplet as by the rate of heat transfer.

A conduction only heat transfer model with convective heat transfer at the surfaces using the enthalpy transformation and equilibrium thermal properties was developed in Chapter 5. For freezing, it was shown that such an equilibrium thermal properties model predicted a temperature plateau near the initial freezing point of the butter in a manner that was inconsistent with the measured data. A sensible heat only model accurately predicted the butter temperature until temperatures were reached at which the water freezing became significant.

As stated in the literature review, Pham (1989) modeled nucleation as a function of supercooling, but assumed that the thermal equilibrium was restored after the initial nucleation (i.e. once the nucleation occurred, crystal growth was instantaneous). This approach had a significant effect on the predicted freezing times for situations where ice forms as dendrites with low nucleation

temperatures and low freezing medium temperature. Miyawaki *et al.* (1989) took the same approach to model the freezing behavior of water enriched foods when supercooling occurs. This approach may not work in predicting freezing of butter as the nucleation temperature of the water in butter is unknown and, as observed in the experimental data under different experimental conditions, the nucleation temperature was quite different. In the modeling approaches taken by Pham (1989) and Miyawaki *et al.* (1989), it was assumed that, as soon as the nucleation started, the crystal growth was instantaneous, leading to the release of latent heat which raised the temperature of the product to its equilibrium freezing temperature instantaneously. In contrast, in butter freezing experiments it was found that the increase in temperature during the release of latent heat was very slow. These results suggest that the introduction of a crystallisation rate term in the heat transfer model is needed.

This chapter describes the modification of the conduction only model developed in Chapter 5 into a more universal freezing model so that the effects of the rates of nucleation and growth on butter freezing can be predicted more accurately.

6.2 Model Formulation

Using the same assumptions stated in Chapter 5 for the conduction only model, the general equation for heat transfer by conduction in three dimensions was used, incorporating a term that accounts for the release of latent heat at a rate that is dependent on the kinetics of ice crystallization.

$$C\frac{\partial T}{\partial t}=\frac{\partial}{\partial x}\left(\lambda_{(T)}\frac{\partial T}{\partial x}\right)+\frac{\partial}{\partial y}\left(\lambda_{(T)}\frac{\partial T}{\partial y}\right)+\frac{\partial}{\partial z}\left(\lambda_{(T)}\frac{\partial T}{\partial z}\right)+M\frac{\partial F}{\partial t} \qquad (6\text{-}1)$$

for $t > 0$ and $0 < x < L_x$, $0 < y < L_y$, $0 < z < L_z$

The convective boundary conditions are given by:

$$\left.\begin{aligned}
h_1(T_{a1}-T) &= -\lambda_{(T)}\frac{\partial T}{\partial x} \quad at \quad x=0 \;\; \& \;\; t>0 \\
h_3(T_{a3}-T) &= -\lambda_{(T)}\frac{\partial T}{\partial y} \quad at \quad y=0 \;\; \& \;\; t>0 \\
h_5(T_{a5}-T) &= -\lambda_{(T)}\frac{\partial T}{\partial z} \quad at \quad z=0 \;\; \& \;\; t>0 \\
h_2(T_{a2}-T) &= \lambda_{(T)}\frac{\partial T}{\partial x} \quad at \quad x=L_x \;\; \& \;\; t>0 \\
h_4(T_{a4}-T) &= \lambda_{(T)}\frac{\partial T}{\partial y} \quad at \quad y=L_y \;\; \& \;\; t>0 \\
h_6(T_{a6}-T) &= \lambda_{(T)}\frac{\partial T}{\partial z} \quad at \quad z=L_z \;\; \& \;\; t>0
\end{aligned}\right\} \qquad (6\text{-}2)$$

and the uniform initial conditions are given by:

$$T = T_{initial} \quad \text{at} \;\; t=0 \;\; \text{and} \;\; 0<x<L_x, \;\; 0<y<L_y, \;\; 0<z<L_z \qquad (6\text{-}3)$$

Equation (6-1) can be transferred into the sensible heat only model by simply substituting:

$$M=0 \qquad F=0 \qquad C=\rho c_u \qquad (6\text{-}4)$$

This assumes that the water in the butter supercooled but never freezes, so that no water latent heat is removed from the butter and the specific heat capacity is constant and equals the unfrozen value.

Equation (6-1) can also be transferred to the equilibrium thermal properties model where the rate of the latent heat removal is heat transfer limited rather than mass transfer (nucleation and crystal growth) by substituting:

$$M=0 \qquad C=\rho\frac{\partial H}{\partial T} \qquad (6\text{-}5)$$

Because the sensible heat only model worked well for the situations where the supercooling occurs and water in the butter never freezes and the equilibrium thermal properties model did not adequately model the freezing behavior of butter, a new model is required that estimates the freezing rate of water droplets during freezing (that is estimation of $\partial F/\partial t$ in Equation (6-1)).

6.3 Modeling Freezing Kinetics

Nucleation Only Kinetics

One approach is to assume that ice crystal growth is rapid once ice nuclei have formed. Therefore, the overall freezing is controlled by the rate of nucleation.

Nucleation is a process by which embryos (nuclei) of the new phase are formed in a phase transition from a pure metastable (parent) phase to a more stable (daughter) phase (Abraham, 1974; Oxtoby, 1992). The onset of the nucleation occurs as a result of fluctuations in time and space of temperature and density. In vapor to liquid water nucleation, the nucleation event occurs only if a critical supersaturation of the vapor (dependent in time) is exceeded. Similarly, in liquid to solid nucleation the nucleation event occurs only if supercooling of the water exceeds the critical limit (Pruppacher and Klett, 1997).

The process of nucleation is said to be homogenous (spontaneous) when no foreign particulates or surfaces take part in the nuclei formation and said to be heterogeneous if a foreign particulate is involved as a nucleation site.

The theory of homogenous nucleation considers the energetic and kinetics of the growth and decay of molecular clusters due to random density fluctuations and their ability to act as nuclei for the crystallization process (Turnbull & Fisher, 1949; Dufour & Defay, 1963; Hobbs, 1974). This theory is currently under review because of several alleged shortcomings (Katz & Spaepen, 1978; Rasmussen, 1982; Franks *et al.*, 1984).

To get an expression for the nucleation rate a small spherical volume V is considered in a supercooled liquid at temperature T, corresponding to a degree of supercooling:

$$\Delta\theta = \theta_{if} - \theta \qquad (\theta = T + 273.15) \tag{6-6}$$

If the molecules which make up the spherical cluster are assumed to be in ice like configuration, then the free energy of condensation is given by:

$$\Delta G_c = R\theta \ln\left(p_{ice} / p_{liquid} \right) \tag{6-7}$$

where p_{ice} and p_{liquid} are the vapor pressure of ice and the vapor pressure of the supercooled liquid respectively. At subzero temperatures ice is a stable phase so $p_{ice} < p_{liquid}$, and thus $\Delta G_c < 0$.

ΔG_c is the free energy change that accompanies the transfer of a mole of water from supercooled liquid to the interior of the solid-like cluster.

Equation (6-7) can be approximated as:

$$\Delta G_c = -\frac{\theta \Delta H_f \Delta \theta}{(\theta_{if})^2} \tag{6-8}$$

where ΔH_f is the molar latent heat of crystallization. For a cluster of radius *r* the net free energy accompanying the liquid solid condensation is given by Equation (6-9)

$$\Delta G_{l \to s} = 4\pi r^2 \sigma - \left(\frac{4}{3}\right)\pi r^3 \Delta G_c \tag{6-9}$$

σ being the interfacial free energy of the cluster. To estimate the value of *r* when $\Delta G_{l \to s}$ becomes negative, Equation (6-9) can be differentiated w.r.t. 'r' and then equated to zero to get the critical points.

This gives $r^* = -\frac{2\sigma}{\Delta G_c}$ and $\Delta G^* = \frac{16\pi r^3}{3(\Delta G_c)^2}$ as the critical values.

The number of critical clusters $n_o(r^*)$ in a given volume of water at a given temperature is estimated by assuming the Boltzmann distribution:

$$n_o(r^*) = n_1 \exp\left(-\frac{\Delta G^*}{k\theta}\right) \tag{6-10}$$

Where n_1 is the number of molecules per unit volume in the liquid phase.

Apart from the estimation of the number of critical clusters under the varying conditions it is also important to get an expression for the kinetics of nucleation. This gives the rate of the generation of

the critical clusters in the body of the supercooled water. The nucleation rate J, the number of nuclei formed per second and per unit volume is commonly written as:

$$J \cong \frac{n_1 k\theta}{H} \underbrace{\exp\left(\frac{-\Delta G_*^*}{k\theta}\right)}_{\text{Kinetic Tenn}} \underbrace{\exp\left(\frac{-\Delta G^*}{k\theta}\right)}_{\text{Boltzmann distribution}} \tag{6-11}$$

The term G_*^* is taken to be the free energy of activation of self diffusion. The kinetic term depends on the mechanism by which the clusters are formed.

By making various substitutions for ΔG^* in Equation (6-11), it can be written in a simple form as (Franks, 1985) assuming that kinetic term is not limiting:

$$J(\mathrm{s}^{-1}\mathrm{m}^{-3}) = ae^{b\tau} \tag{6-12}$$

Where τ is the quantity containing all the θ terms from Equation (6-11) and is given as:

$$\tau = \left[\theta^3 (\Delta\theta)^2\right]^{-1} \tag{6-13}$$

Michelmore and Franks (1982) expressed τ in a more useful form of reduced temperatures (supercooling) as:

$$\phi = \frac{\theta}{\theta_{if}} \quad \text{and} \quad \Delta\phi = \frac{(\theta_{if} - \theta)}{\theta_{if}} = 1 - \phi \tag{6-14}$$

which upon substitution in Eq (6-12) gives:

$$J = ae^{b\tau_\phi} \tag{6-15}$$

$$\text{where } \tau_\phi = \left[\phi^3 (\Delta\phi)^2\right]^{-1} \tag{6-16}$$

This substitution makes it possible to compare different solutions and liquids which freeze at different temperatures. A plot of $\ln J$ against τ_φ should be linear. The constant 'a' depends on the volume of the crystal and the other parameter 'b' is a characteristic of the supercooled substance, molar volume of the crystal and interfacial tension of the liquid crystal; (Skripov, 1974; Turnbull, 1956).

Equation (6-15) describes the rate of nucleation and, therefore, the rate of water freezing can be calculated, if crystal growth from a nucleus is rapid, by:

$$\frac{\partial F}{\partial t} = JV(1-F) \tag{6-17}$$

where V is the volume of droplet and F is the fraction of the freezable water which is frozen and can be calculated by integrating Equation (6-17). The unknowns a and b are the kinetic constants which needed to be measured or estimated as an input to the nucleation model.

The definition of nucleation rate J is completed by setting $J = 0$ for $\theta \geq \theta_{if}$

Combined Nucleation and Crystal Growth Kinetics (Avrami Model):

An alternative model to describe crystallization rate is the theory known as the Johnson, Mehl, Avrami, and Kolmogorov (JMAK) Model (Kolmogorov, 1937; Johnson & Mehl, 1939; Avrami 1939, 1940 & 1941) or as the Avrami Model, which considers both nucleation and crystal growth kinetics. The equation for isothermal conditions is:

$$F(t) = 1 - \exp(-Kt^n) \tag{6-18}$$

This model is used extensively for the analysis of crystallization kinetics at isothermal temperatures and considers the processes of nucleation and growth from a statistical basis (Rogowski, 2005). The amount of crystallisation is clearly time-dependent. According to Yinnon & Uhlmann (1983) and Christian (1965), the power n is a reaction-order parameter, which is expected to be dependent on the morphology of the growing crystal (needles, plates, dendrites, spherulites, etc). Van Krevelen (1990) gives the theoretical values of 'n' and 'K' according to the form of growth and type of nucleation (Table 6.1). To apply the Avrami Equation to the freezing of butter it was assumed that,

since nucleation type is not predetermined (no nuclei to start with), nucleation will be spontaneous and the form of growth will be spherical. Hence the Avrami exponent has a value of $n = 4$ that accounts for the three dimensional linear growth of the spheres and a constant nucleation rate.

Table 6.1: Theoretical values of Avrami constants (Van Krevelen, 1990)

Form of growth	Type of nucleation			
	Predetermined (constant number of nuclei per cm^3)		Spontaneous (sporadic) (constant nucleation rate)	
	n	K	n	K
Spherulitic (spheres)	3	$\frac{4}{3}\pi G^3 N \rho^*$	4	$\frac{4\pi}{3} G^3 J \rho^*$
Discoid (platelets)	2	$\pi b G^2 N \rho^*$	3	$\frac{4}{3} b G^2 J \rho^*$
Fibrillar (rodlets)	1	$f G N \rho^*$	2	$\frac{f}{2} G J \rho^*$

f = cross section rodlets, b= thickness of platelet, N = number of nuclei per unit volume, J = rate of nucleation per unit volume, G = rate of crystal growth. ρ^* = relative density

The parameter K describes the combined effect of the nucleation rate (J) and the rate of crystal growth (G) and is defined as:

$$K = \frac{\pi}{3} G^3 J \rho^* \tag{6-19}$$

Where J is the nucleation rate as defined by Equation (6-15).

The relationship between the crystal growth rate and the supercooling is often written in the simple form as (Muller, 2004; Jackson, 2004):

$$G = g\left(T_m - T\right) \tag{6-20}$$

Where g is a kinetic constant and T_m is the equilibrium freezing temperature of the liquid phase within the droplet, which changes as a function of F as a result of freeze concentration of the solutes.

For non isothermal applications, the differential form of the Equation (6-18) should be used. Differentiating Equation (6-18) gives:

$$\frac{\partial F}{\partial t} = nKt^{n-1}e^{-Kt^n} = nKt^{n-1}(1-F) \tag{6-21}$$

the time term can be eliminated by substituting Equation (6-18) into Equation (6-21) to give:

$$\frac{\partial F}{\partial t} = nK^{1/n}(1-F)\left(-\ln(1-F)\right)^{(1-1/n)} \tag{6-22}$$

By combining the Equations (6-15), (6-19), (6-20), and (6-21) the overall rate of crystallization is given by:

$$\frac{\partial F}{\partial t} = U(T_m - T)^{3/4}\left(\exp(b\tau_\phi)\right)^{1/4}(1-F)\left(-\ln(1-F)\right)^{3/4} \tag{6-23}$$

where $U = 4\left(\frac{\pi}{3}ag^3\rho^*\right)^{1/4}$ is a constant. (6-24)

The two parameters U and b in Equation (6-23) are the rate constants which need to be estimated to use the model.

The main difference between Equations (6-15) and (6-18) is that ice crystal formation is now dependent on time as well as supercooling i.e. the more time spent at a certain temperature, the greater the extent of crystallisation. Normally the Avrami model divides crystallisation into nucleation and growth. However in practice the mechanisms may not be easily separated. Hence, overall, the model represented by Equation (6-18) was considered as modelling the whole crystallisation process and the subdivision between the nucleation and growth was ignored.

6.4 Measurement and Estimation of Model Input Data

The crystallisation models represented by Equation (6-1), Equation (6-15) and Equation (6-23) needed additional input data in order to run the simulation. The methodology required for data measurement and estimation to obtain these variables is given in this section.

6.4.1 Measurement of Nucleation Rate

The function $J(T)$ given in Equation (6-15) has been determined using differential scanning calorimetry by many authors for water and water in oil emulsions using isothermal experiments (Wood & Walton 1970; Michelmore & Franks, 1982; Franks *et al*, 1983; Bronshteyn & Steponkus, 1995). However isothermal experiments are very time consuming and require very precise control of experimental conditions. Rasmussen and Looper (1971) described how DSC can be used in either isothermal or scanning mode to measure the nucleation rates in metallic systems. Michelmore and Franks (1982) conducted DSC experiments in scanning mode to measure nucleation rates of ice in supercooled water and aqueous solutions of polyethylene glycol by adapting the method given by Rasmussen and Looper (1971).

The method used by Michelmore and Franks (1982) was used to measure the nucleation rate of water droplets in butter. The same Perkin Elmer DSC 7 that was used to measure the specific heat capacity of butter was also used for nucleation rate measurement after calibration. This method is based on the graphical integration of the power-time contour of a scanning rate cooling experiment. Samples of the unsalted butter were cooled at a rate of 1.25°C min^{-1} (a very low rate) until the freezing was complete. Figure 6.1 gives the cooling results for the two unsalted butters (Fritz (B19), Ammix (B8)) cooled at a rate of 1.25°C min^{-1} for the determination of the nucleation kinetics.

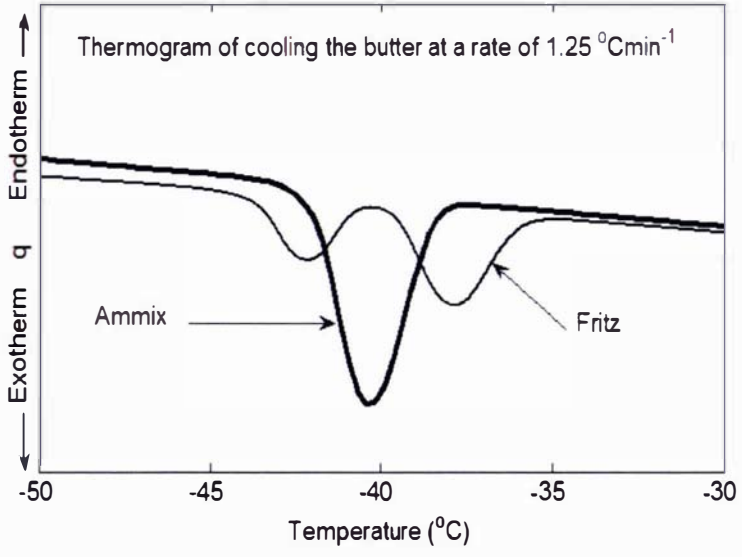

Figure 6.1: DSC thermogram for Fritz and Ammix butter

Two distinct peaks can be observed in the butter manufactured by the Fritz process, probably due to two populations of water droplets having different concentrations of solutes (as discussed in Chapter 3). The kinetic constants for both the peaks were analyzed using the method given by Rasmussen & Loper (1971). Ammix butter shows only one peak, probably due to a more uniform solutes concentration in all the water droplets.

The power-time curve was then divided into equal time intervals with Δt = 11.25 sec, which was equal to the time interval between the successive heat time measurements output by the DSC. The temperature at each time interval was known. The corresponding areas under the curve were evaluated and J was estimated (Rasmussen and Looper, 1971):

$$J = -\frac{1}{V\Delta t}\ln\left(\frac{A_{(t_1+\Delta t)}}{A_{t_1}}\right) \qquad (6\text{-}25)$$

Where A_{t_1} is the area after time t_1 which is directly proportional to the fraction of the droplets which has frozen and V is the volume of the droplet. The volume of the water droplets for Ammix (1.55×10^{-16} m^3) and Fritz butter (1.1×10^{-17}m^3) were taken to be those measured by Lu (1999).

The results found in this way for J as a function of T were then fitted to the linearised version of Equation (6-26) to determine the kinetic constants 'a' and 'b' :

$$\ln J = \ln a + b\tau_\phi \qquad (6\text{-}26)$$

Figure 6.2 shows the DSC thermogram for Fritz butter from which the temperature dependence of the nucleation rate was calculated using the Equation (6-25). Figure 6.3 gives ln J as a function of τ_ϕ.

For the Fritz unsalted butter, the analysis gave a value of a = exp (66.392) s^{-1}m^{-3} and b = -0.364 for the larger peak, and a = exp (91.062) s^{-1}m^{-3} and b = -0.7751 for the smaller peak. For Ammix butter, this analysis gave: a = exp (101.788) s^{-1}m^{-3} and b = -1.223.

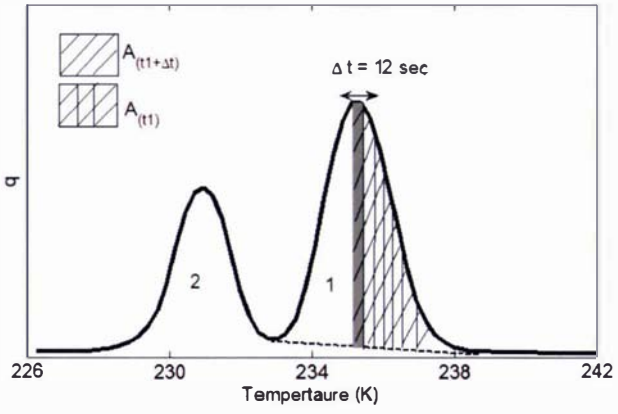

Figure 6.2: DSC thermogram for the Fritz unsalted butter with cooling rate of 1.25°C min^{-1}

Table 6.2: Measured kinetic constants 'a' and 'b' for different emulsions

Solution	a ($s^{-1}m^{-3}$)	b	V (m^{-3})	Reference
Pure water	3×10^{50}	-1.010	3.40×10^{-17}	Michelmore and Franks (1982)
16.7% PEG[1]	5×10^{46}	-1.025	1.53×10^{-17}	Michelmore and Franks (1982)
23.0% PEG	3×10^{44}	-1.030	1.53×10^{-17}	Michelmore and Franks (1982)
Erthrocytes	1×10^{54}	-1.13	6.5×10^{-17}	Franks *et al.* (1983)
Erthrocytes	1×10^{54}	-1.12	6.5×10^{-17}	Franks *et al.* (1983)
Saline Solution	6×10^{57}	-1.24	5.8×10^{-18}	Franks *et al.* (1983)
Saline Solution	4×10^{58}	-1.26	5.8×10^{-18}	Franks *et al.* (1983)
Glycine max cells	4×10^{16}	-0.11	1.8×10^{-14}	Franks *et al.* (1983)
Glycine max cells	6×10^{14}	-0.07	1.8×10^{-14}	Franks *et al.* (1983)
Ammix Butter	1.59×10^{44}	-1.223	1.55×10^{-16}	Current research
Fritz butter (Peak 1)	6.82×10^{28}	-0.364	1.1×10^{-17}	Current research
Fritz butter (Peak 2)	3.53×10^{39}	-0.775	1.1×10^{-17}	Current research

[1]PEG polyethylene Glycol

A comparison of kinetic constant values with other literature values for water in oil emulsions is given in Table 6.2. The literature measurements were performed for pure water in oil binary solution whereas, the water droplets in butter are not pure water but contained other solutes. The values found in this research were found intermediate to the literature values of *a* and *b*.

The calculated nucleation rate *J* as a function supercooling is given in Figure 6.3. Figure 6.4 shows the nucleation rate as function of temperature for the two Fritz and Ammix butters. In all three cases, the temperature range relevant for most of the freezing experiments has a *J* of zero which means that $\partial F/\partial t$ is also close to zero. Use of this nucleation data would predict that each droplet will just supercool and will take a very long time to freeze which does not seems consistent with the observed freezing behavior.

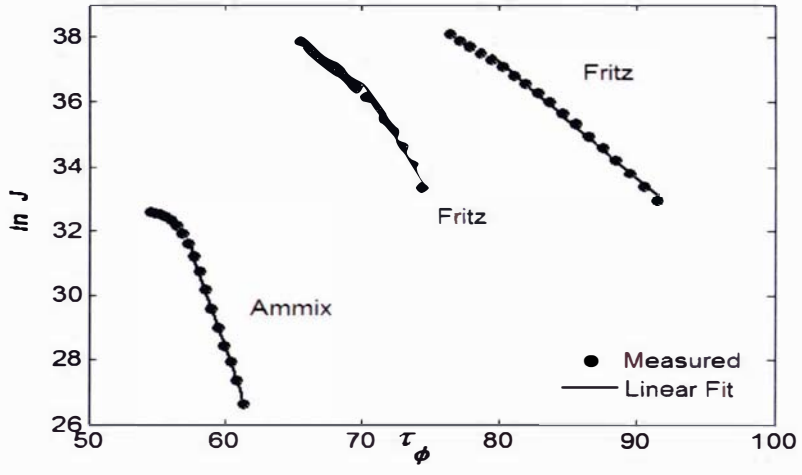

Figure 6.3: lnJ as a function of super cooling for both Fritz butter and the Ammix butter

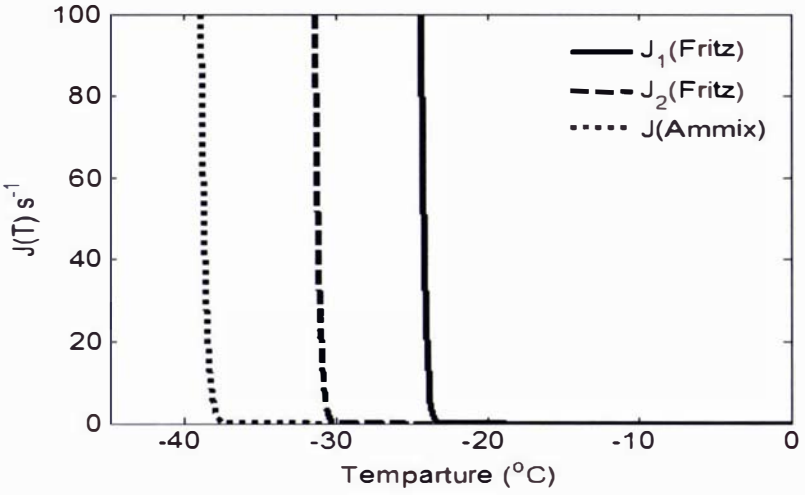

Figure 6.4: Nucleation rate as a function of temperature for the Fritz and Ammix butters

Most of the data used in the measurement of nucleation rate using DSC is for temperatures less than -35°C (Figure 6.1). However the temperature used in the freezing experiments was never below -25°C and industry freezing temperatures of -18 and -9°C are common. Therefore, application of the DSC kinetics rates to the experimental conditions requires significant extrapolation which is likely to add considerable uncertainty.

Therefore an alternative approach was taken; the nucleation kinetic values were back-calculated from the experimental data collected for different sizes and types of butter. J was calculated from different sets of freezing data for butter pats and blocks using the following integrated form of Equation (6-17) for periods where the temperature was relatively constant.

$$J = -\frac{\ln(1-F)}{Vt} \tag{6-27}$$

For each set of data, this calculation was performed for the centre and the surface of the butter pat or block, assuming that, between the start and end temperatures of the crystallisation process about 95% of the water in the butter had frozen (that is F=0.95). The data thus obtained is given in Table 6.3. A plot of all the resulting data (Table 6.3) and the nucleation rates calculated by the DSC analysis is given in Figure 6.5:

Table 6.3: Calculation of the nucleation rate J from the experimental data

Butter	Position	Nucleation Temperature (°C)		τ_φ	t (hours)	ln$J$
Pat (B16, UPC – 2)	Surface	undetectable				
@ -70°C	Centre	Start at	-35	92.11		
		End at	-42	69.92	0.9	32.07
Block 1 (B19, UBC – 1a)	Surface	Start at	-19.5	246.26		
@ -25°C		End at	-21.5	207.33	55	27.96
	Centre	Start at	-16	351.52		
		End at	-19.2	253.14	55	27.96
Block 2 (B19, UBC – 2)	Surface	Start at	-10	900.36		
@ -11°C		End at	-10.5	768.99	170	26.83
	Centre	Start at	-9	1030.89		
		End at	-9.5	929.86	170	26.83

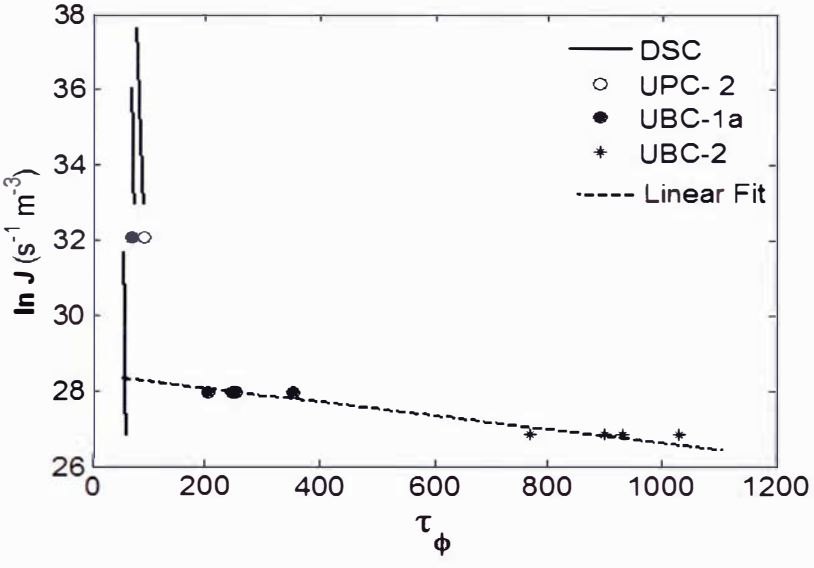

Figure 6.5: ln$J$ *as a function of super cooling calculated from the experimental freezing data and the DSC measurements*

Figure 6.5 confirms that extrapolation of the DSC results to model the freezing of butter in the temperature range -25°C to -10°C is unlikely to be accurate. Therefore, it was decided to find the nucleation rate kinetic values '*a*' and '*b*' from experimental data for the unsalted block of butter under two different ambient conditions. The time taken for nucleation at the surface of the butter block and at the centre was the same but there was no unique temperature of nucleation. An average temperature for both the data sets was taken and the values of '*a*' and '*b*' were found by linear fit to those two points. These values were: $a = \exp(28.423)\ s^{-1}m^{-3}$ and $b = -0.0018$.

Figure 6.6 gives the function $J(T)$ and shows that the probability of the droplets nucleating starts to increase at about -5°C contrary to the nucleation rates measured using the DSC which gave values of nearly zero above -25°C.

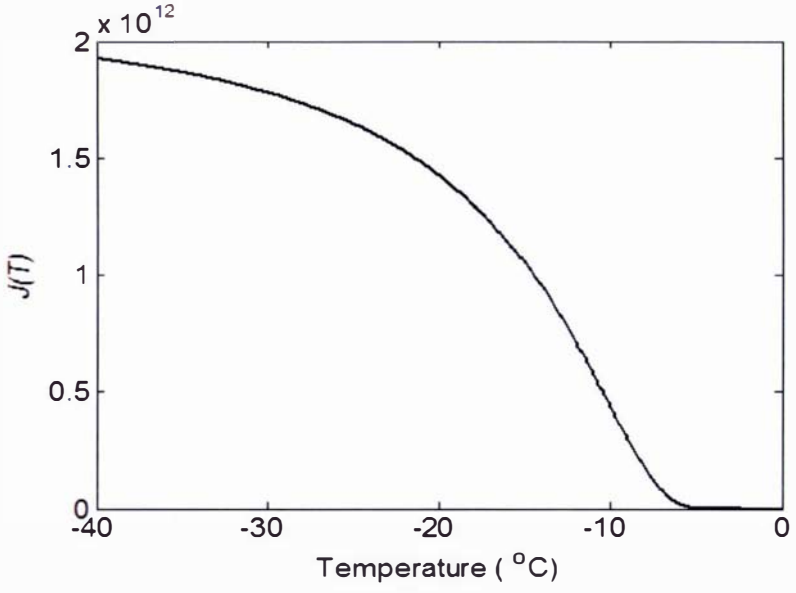

Figure 6.6: Nucleation rate J as a function of temperature calculated from two freezing experiments on a butter block (B19)

The kinetic constants for the Avrami Model have been measured by number of researchers using isothermal experiments assuming n and K as constants. In this study K is a function of $(T_m\text{-}T)$ (Equation 6-23) and is not constant. It is a function of the fraction frozen which in turn is a function of temperature. It was decided to use the same value of '*b*' for the Avrami model as for the Classical Nucleation model. The other constant '*U*' could then be found by curve fitting to one set of experimental data. Fitting the data for a block of butter (B19) at -25°C gave a value of $U = 0.014$.

Using only one set of data to fit the constant means that the other sets of data can be used to validate the kinetics modeling.

6.4.2 Specific Heat Capacity

To model freezing, the specific heat capacity during cooling of butter is required for both the frozen and unfrozen ranges.

As explained in Chapter 3, the specific heat capacity of the butter was measured using a DSC (Perkin Elmer DSC 7). Samples were frozen to –70 °C at a rate of 1.25 °C min^{-1} and then heated at the same rate to calculate the specific heat capacity and the enthalpy for both heating and cooling (Figure 6.7). The average specific heat capacity for fully frozen butter (c_f) was found to be 1.8 kJ kg^{-1} K^{-1} for both heating and cooling measurements.
The specific heat capacity of the thawed butter (ie. the water phase was not frozen) in the range from T_{if} to 10 °C was higher when heating than during cooling. It was postulated that this was due to the significant supercooling and crystallization of the fat fraction in the butter at temperatures well below the equilibrium fat phase change temperature.

During heating, as the fat melting is at equilibrium temperature, the apparent specific heat capacity above T_{if} includes a fat latent heat component. Figure 6.7 shows that the apparent specific heat capacity of supercooled butter in DSC cooling mode measurements remained relatively constant from 10 °C down to about –35°C, below which water latent heat started to be removed. As any fat supercooling and phase change effect would also occur during a butter freezing trial, the value measured in the DSC cooling mode (c_u = 3.2 kJ kg^{-1} K^{-1}) was used for unsalted butters and a value of 3.1 kJ kg^{-1} K^{-1} was used for all the salted butter samples.

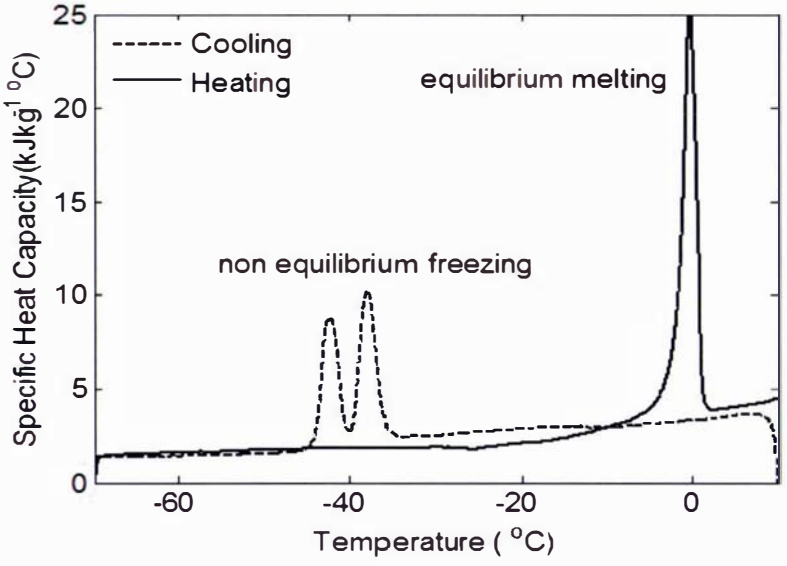

Figure 6.7: Specific heat capacity of butter (B19) measured by DSC in heating and cooling modes

The equilibrium freezing model requires an apparent heat capacity that includes latent heat effects. The thawing specific heat capacity curve was used in this case, except that the unfrozen heat capacity was taken to be the apparent value measured during the cooling run.

The heating enthalpy data were adjusted by:

- using –40 °C for the enthalpy datum.
- using constant fully frozen specific heat capacity from –40 to –20 °C.
- keeping the enthalpy change from –40 to +10 °C the same as for the heating differential scanning calorimetry run.
- keeping T_{if} at the measured initial freezing point.
- holding the specific heat capacity constant at c_f from 10°C until T_{if}.
- adjusting the value of H_{if} to meet the above criteria.

Table 6.4: Enthalpy equation parameters for experimental butters

Code	A' (kJ kg^{-1})	c'_f (kJ kg^{-1}K^{-1})	B' (kJ K kg^{-1})	H'_o (kJ kg^{-1})	c'_u (kJ kg^{-1}K^{-1})	T_{if} (°C)	dH_{if} (J kg^{-1})
B15	58.28	1.68	-354.12	131.97	3.1	-5.35	57.34
B16	91.66	2.32	-39.25	167.35	3.2	-0.52	74.25
B19	70.8	1.8	-31.6	148.4	3.2	-0.41	76.17

Equation (6-28) was fitted to the measured data using the above adjustments for all the experimental butter. The parameters for the butters used in the experiments are given in Table 6.4.

$$\left.\begin{aligned} H(kJ/kg) &= A' + c'_u\, T - \frac{B'}{T} && 0 < T < T_{if} \\ H(kJ/kg) &= H'_o + c'_f\, T && T \geq T_{if} \end{aligned}\right\} \tag{6-28}$$

Essentially, this procedure means that any fat melting related latent heat not included in the sensible heat between T_{if} and 10°C, was added to the equilibrium water latent heat peak as the fat freezing would occur at similar temperatures to ice freezing behavior.

For the classical nucleation and Avrami crystallisation models for partially frozen butter, the volumetric heat capacity C was taken to be a pro rata function of the fraction of frozen water and given by:

$$C = \rho\left(Fc'_f + (1-F)c'_u\right) \tag{6-29}$$

6.4.3 Equilibrium Freezing Temperature

The equilibrium freezing temperature (T_m) is required by the crystallization model Equation (6-22). It was calculated from the adjusted equilibrium enthalpy (Figure 6.8(b)).

For any point below T_{if} on the enthalpy diagram (Figure 6.8(b)), H can be calculated from the values of T and F using:

$$H = H_{if} - F\left(dH_{if} + c'_f\left(T_{if} - T\right)\right) - c'_u\left(1-F\right)\left(T_{if} - T\right) \tag{6-30}$$

By substituting this value of H into Equation (6-28) with T replaced by T_m and using the constants in Table 6.4 results in a quadratic Equation for T_m as a function of F:

$$T_m = \frac{-A_2 + \sqrt{A_2^2 + 4\times 31.6 A_1}}{2A_1} \tag{6-3}$$

where

$$A_1 = \left(c'_u - c'_f\right)(1-F) \tag{6-32}$$

$$A_2 = \left(70.8 + H_{if} - FdH_{if} - T_{if}\left(A_1 + c_f'\right)\right) \tag{6-33}$$

This allows the equilibrium melting point to be calculated from the instantaneous frozen fraction (F) and used to calculate the driving force for crystallization.

(a)

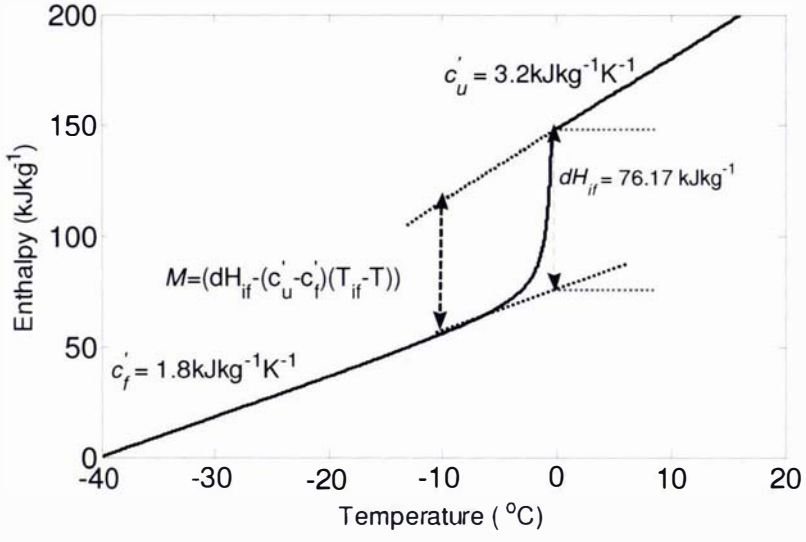

(b)

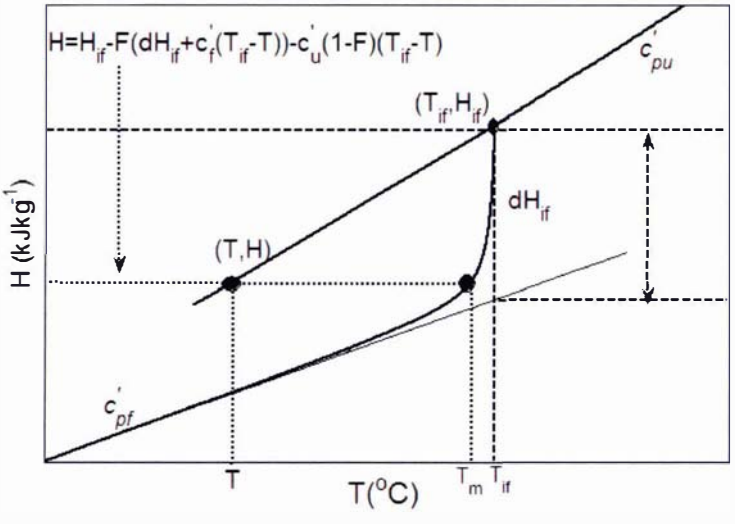

Figure 6.8: (a) Equilibrium enthalpy-temperature diagram for butter (B19) showing specific heat capacity values used for different temperature ranges.

(b) Enthalpy-temperature diagram for the calculation of equilibrium freezing temperature

6.4.4 Latent Heat

For the nucleation and crystallization models, the latent heat released as a function of temperature is given by the vertical distance between the unfrozen sensible heat line and the frozen sensible heat line in Figure 6.8(b).

$$M = \rho\left(dH_{if} - (c_u' - c_f')(T_{if} - T)\right) \tag{6-34}$$

6.4.5 Thermal Conductivity

Values of the thermal conductivity of butter were calculated from the data reported by Middleton (1995) for the completely frozen and unfrozen temperature ranges. In the freezing range, the thermal conductivity was interpolated between these values using the predicted local estimate of the fraction of frozen water (F) using the parallel model:

$$\lambda = \lambda_u(1 - F) + \lambda_f F \tag{6-35}$$

As the difference between the fully frozen and fully unfrozen thermal conductivities was small, more sophisticated models were not justified (Wang *et al.* 2005).

6.4.6 Model Solution

The model was solved using the input data for Nucleation Only Model and the Avrami Model for butter pats and blocks. A detail of the MATLAB code is given in Appendix A4.

6.5 Nucleation Only Model Predictions

Using the input data discussed in Section 6.3, the model was run using the DSC derived and experimental data derived values for '*a*' and '*b*' to compare the model predictions with the experimental data for the centre and the surface of the butter block.

The predictions of the Nucleation Only model using the kinetics constants measured using the DSC are given in Figure 6.9. As expected the water in the butter supercooled and did not freeze at all because the DSC nucleation rate was too low at temperature above -20°C. Thus, this model behaves like the sensible heat only model discussed in the previous chapter.

(a)

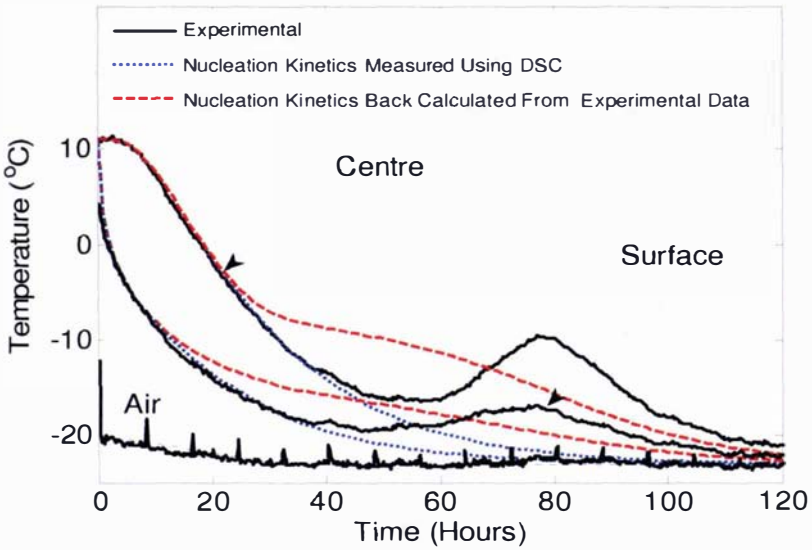

(b)

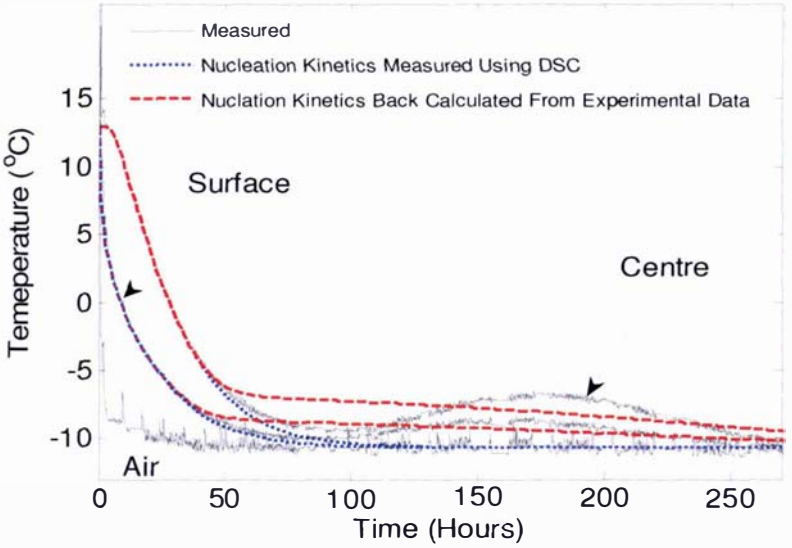

Figure 6.9: Comparison of the measured data (B19) with the prediction using the nucleation-only model. (a) Freezing of butter block (UBC – 1a) with an ambient temperature of -23°C. (b) Freezing of butter block (UBC – 2) with an ambient temperature of -11°C.

The predictions in Figure 6.9 for the nucleation-only model using the kinetics constants calculated from the experimental data matched those for the sensible heat only model until ice nucleation

began to occur at about –5 °C. As the predicted fraction of frozen water increased, the temperature decline slowed because of the release of latent heat. No increase in temperature (rebound) was predicted. Once all the freezing had occurred, the temperature decreased rapidly to the ambient temperature, as expected. Although more realistic than the equilibrium thermal properties model, the differences between the predictions and the measurements suggest that the mechanism of nucleation and ice crystal growth is more complicated than that modeled by nucleation only. In particular, the measured data at –11 °C showed a temperature rebound at the centre of the butter despite the degree of supercooling being less than 10 °C.

The temperature rebound suggests that water phase crystallization in butter has time dependence as well as temperature dependence, similar to that observed by Broto and Clausse (1976). It can be shown that supercooling-driven nucleation only will not predict a rise in temperature, because, if the temperature rises, the nucleation rate will drop and the rate of latent heat release will no longer exceed the rate of cooling. In addition, the nucleation-only model assumes that, once a nucleus has formed, ice crystal growth is instantaneous. Finite rates of ice crystal propagation and interdependence between droplets may explain some of the rebound phenomenon.

6.6 Avrami Model Predictions

6.6.1 Unsalted Butter Block (B19)

Figure 6.10 shows the predictions for the centre and one surface positions of the block of butter for the Avrami model (Equation 6-23). Figure 6.10(a) shows the model predictions compared with the measured data for the block frozen with –23 °C air with a coefficient of determination of 0.99. The model had very good agreement with the measured data with the exception that the model did not rebound to as high a temperature as the experimental data and the rebound occurred slightly later in time than observed for one of the trials (UBC -1b)

Figure 6.11(b) shows the model prediction using the same values for the crystallization kinetics constants (U and b) for the freezing trial at –11 °C. The model predicted the data very well for the first 80 hours and predicted a rebound at the centre of the butter with a coefficient of determination of 0.99. The crystallization process appeared to be slightly faster in the model than for the experimental data, however the freezing completion time was the same. The difference in the positions of the rebounds for the two experiments at –23 °C suggests a stochastic nature for the crystallization process. It is likely that the values of U and b are not the same for each droplet in the

butter and may vary randomly for essentially the same cooling conditions. The Avrami model appears to accurately predict the mechanism apart from the time of the rebound and its magnitude.

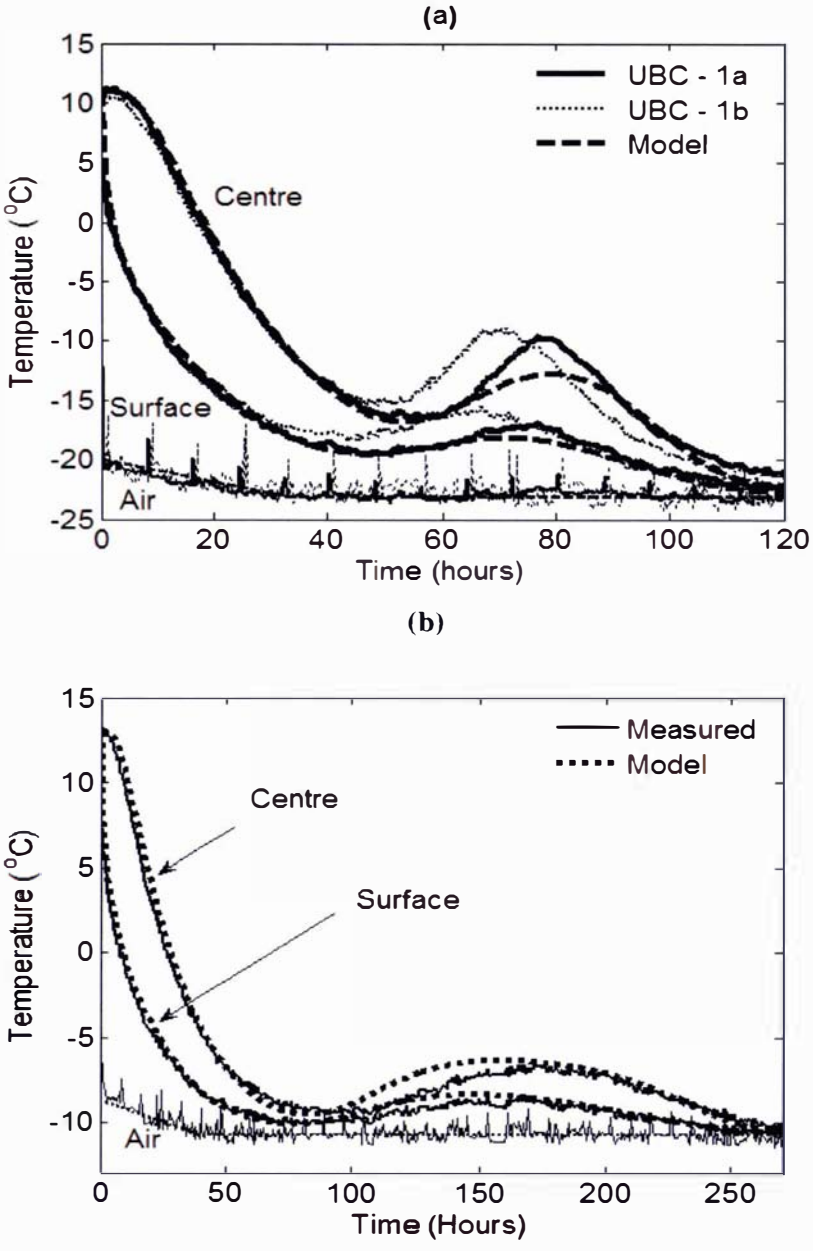

Figure 6.10: Comparison of the measured data for unsalted butter (B19) with the predictions using the Avrami model.

(a) Freezing with an ambient of -23°C (UBC – 1a,UBC – 1b), R^2=0.9865 for centre

(b)Freezing with an ambient of -11°C (UBC – 2), R^2=0.9873 for centre

6.6.2 Sensitivity Analysis

Figure 6.11 shows the predictions for the data collected for the freezing trial at -11°C with a slightly lower value of U (U = 0.012, 10% lower). The model predicted the data very accurately (R^2 = 0.99), which suggests that the lack of fit in Figure 6.11 was due to the uncertainty in the kinetics data or variation in the samples of butter rather than the model being conceptually inappropriate.

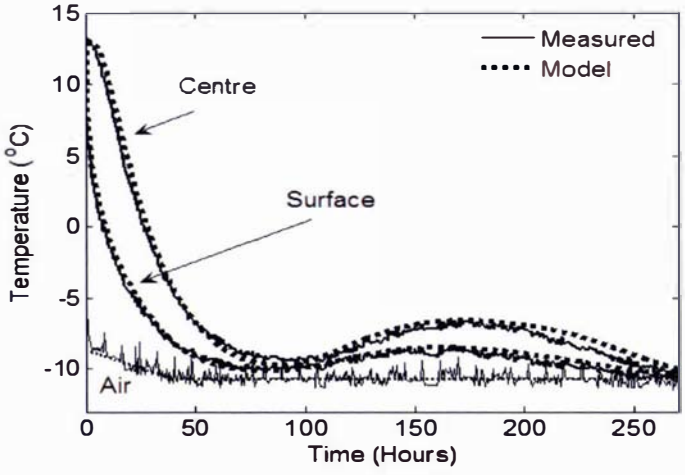

Figure 6.11: Comparison of the measured data (UBC – 2) for unsalted butter (B19) with the Avrami model using a U value of 0.012 rather than 0.014, R^2 = 0.9922 for centre

A further sensitivity analysis was performed on the values of kinetics constants 'b' and 'U' to see how sensitive the model predictions are to these values.

Figure 6.12 shows the model predictions with ± 10% change in U and ±50% change in b. It was observed that a 10% change in U gives nearly the same variation in predictions as the 50% change in b value. It can be seen that higher values of U or b shift the rebound to the left (earlier in time) and lower values shift the rebound to the later in time. This happens because the higher value of b or U means the nucleation starts with less supercooling.

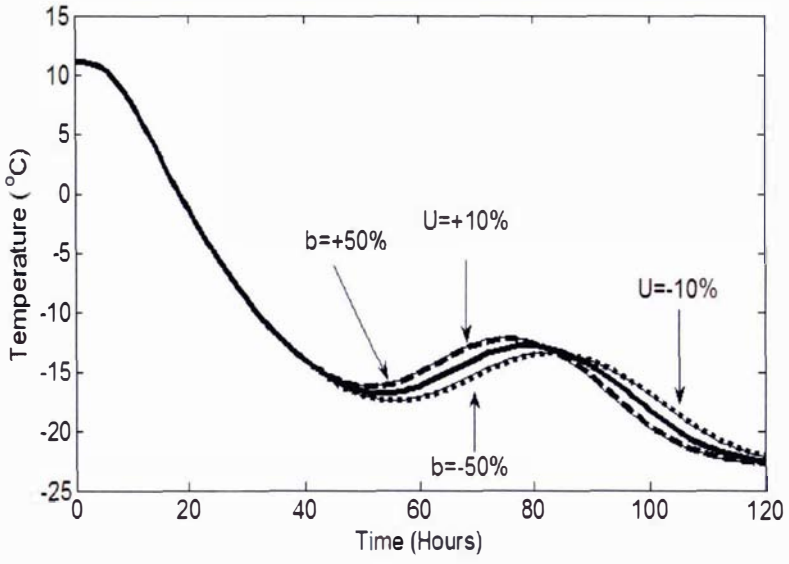

Figure 6.12: Effect of U and b values on the model prediction using the Avrami Model with T_a= -23°C, T_i= 11°C, U =0.014, b = -0.0018

6.6.3 Salted and Unsalted Pats

The Avrami model was applied to the freezing of salted and unsalted butter pats where no release of latent heat was observed and the water in the butter was observed to super cool and did not freeze over a long period on time. In these situations the sensible heat only model worked very well as explained in the previous chapter.

6.6.3.1 Salted Pats (B 18)

Figure 6.13 compares the prediction using the sensible heat only model, Nucleation only model and Avrami model with the experimental data (SPC -1) for the salted pat (B18).

There was very little difference between the models for the first 10-15 hours. However the simulation with the Avrami Model predicted a very small rebound between 30 hours 70 hours as shown in Figure 6.13 (b). The temperature difference between the centre of the butter and the ambient was <0.03°C before the start of temperature rebound. The maximum temperature rebound was found about 0.5°C which is the same order of magnitude as the experimental temperature measurement uncertainty and, therefore, this effect is likely to have been too small to have been

detectable in the experimental data. As expected the Nucleation model and the sensible heat only models did not predict any rebound in the temperature.

(a)

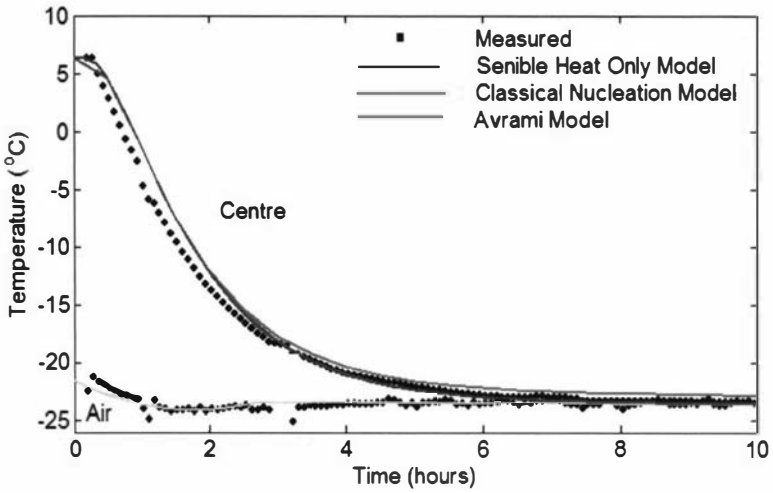

(b)

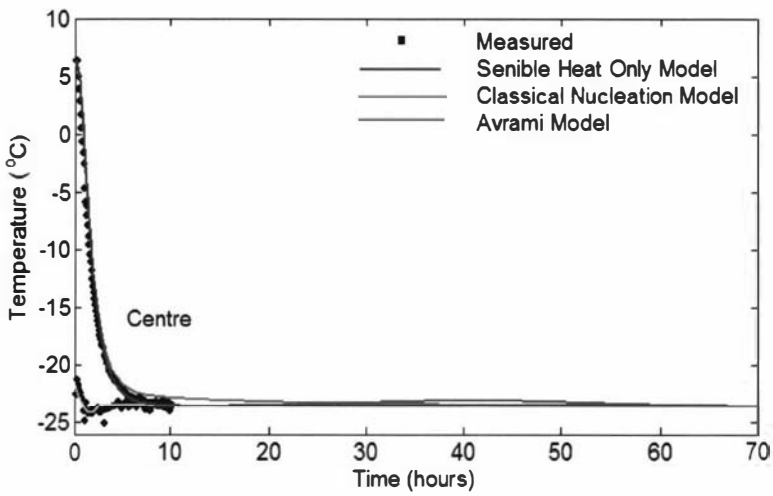

Figure 6.13: Comparison of the measured data (SPC – 1) for the salted butter pat (B18) with the prediction using various freezing models
(a) For 10 Hours (b) For 70 hours

Comparison of the model predictions with a temperature profile for a freezing experiment (SPC-2) conducted on a salted butter pat (B18) for an extended period of time is given in Figure 6.14 (a). A predicted rebound in temperature can be observed between 30 to 60 hours. The fraction of the water shows that 80% of water would be frozen after 60 hours. This seemed to be more than what was observed. When the pat was thawed immediately after the 60 hours of cooling a slight latent heat

plateau just below the initial freezing point of the butter was observed showing not all the water in the butter had frozen. This could be due to the model not taking account of the change in the air temperature that occurred during the experiment.

A comparison of the measured thawing data (SPH-2) with both the thawing models is given in Figure 6.14(b). The measured data clearly lies within the prediction band.

(a)

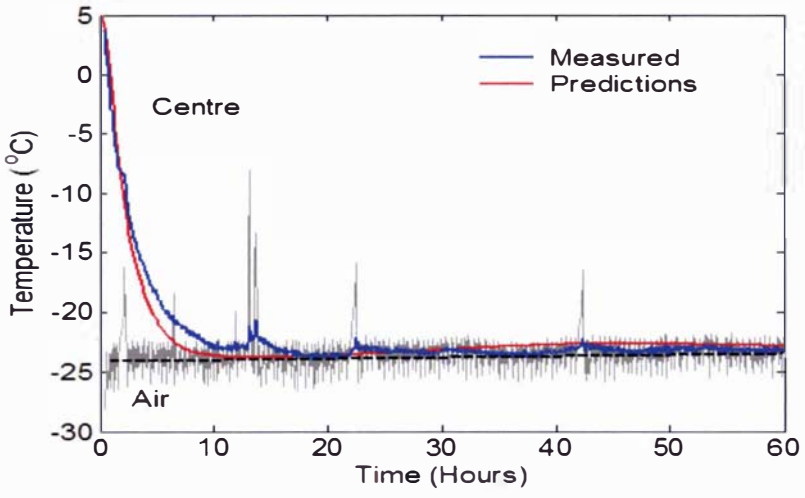

(b)

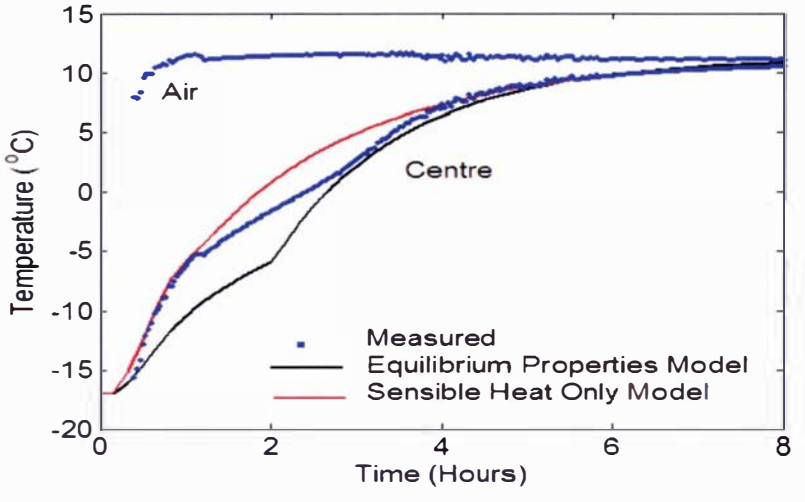

Figure 6.14(a): Comparison of the measured data(SPC-2) for the salted butter pat (B18))with the prediction using Avrami Model predictions for longer period of time

(b) Comparison of measured data (SPH-2) for the thawing of salted butter pat (B18)with the equilibrium properties models and sensible heat only model predictions after cooling at -25°C for 60 hours

6.6.3.2 **Unsalted Pat (B16, UPC - 1)**

(a)

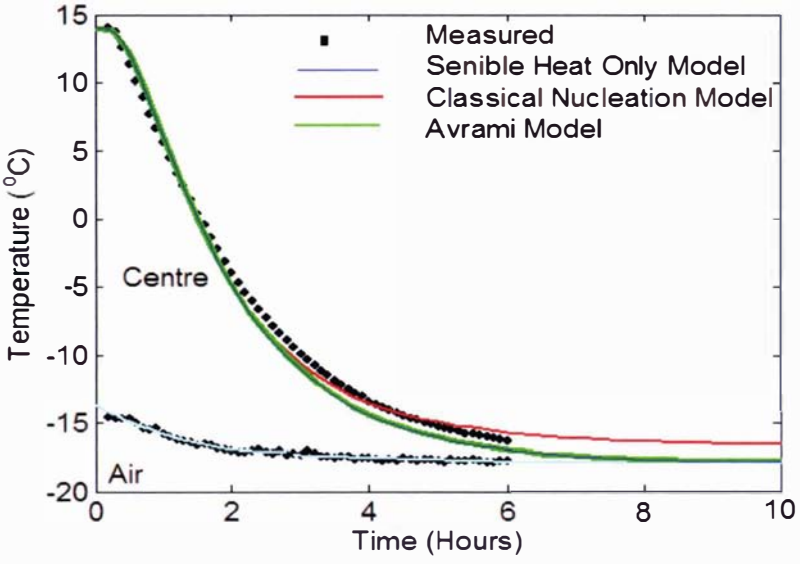

(b)

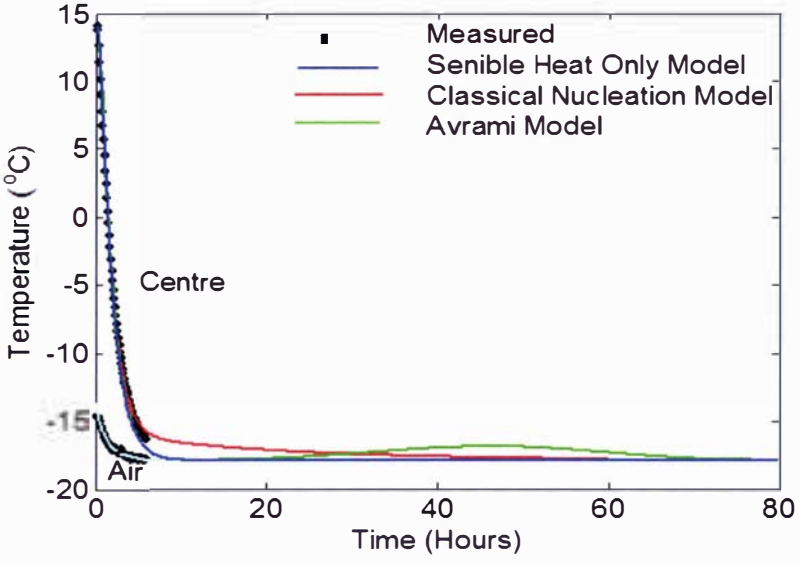

Figure 6.15: Comparison of the measured data (UPC – 1) for the unsalted butter pat (B 16)with the prediction using various freezing models predictions (a) For 10 hours (b) For 80 hours

Figure 6.15 gives the comparison of the measured data with various freezing models. The predictions with the Avrami Model were not significantly different from the sensible heat only model for the first 10 hours of cooling. The Nucleation model predicted slightly higher temperatures than other models. The sensible heat only model and the Avrami Model started to differ after about 20 hours with a temperature rebound for the Avrami Model. The sensible heat only model quickly approached the ambient temperature after 10 hours. A small rebound (<1°C) over a long period of time (65 hours) was observed for the Avrami model. The Nucleation model remained higher than the measured data and approaches the ambient after about 60 hours (Figure 6.15b).

Overall, the trends for the models were exactly the same as in the salted butter pat predictions and unsalted butter block trial predictions. The size of the predicted rebound was sufficiently small that it would be difficult to detect in the measured data.

6.6.4 Predictions for the Salted Block (B15, SBC – 1a)

The Avrami model was validated against the data collected for a 25 kg salted butter which was cooled at an approximately -18°C (B15) for abut 60 hours. No rebound was observed during the experiment. Figure 6.16 (a) compares the model predictions against the experimental data for the centre of the salted butter block. As observed for the unsalted pat, there was no difference between the model predictions for the sensible heat only model and the Avrami model for first cooling period (70 hours in this case). The temperatures for the nucleation model remained higher than the other model predictions. A rebound was predicted after about 115 hours (after data measurement was terminated) for the Avrami Model. Unfortunately, time constraints precluded repeating this experiment for a longer period of time to experimentally confirm this behaviour, but similar observation were observed in the whole pallet trials for salted butter described in the next chapter.

(a)

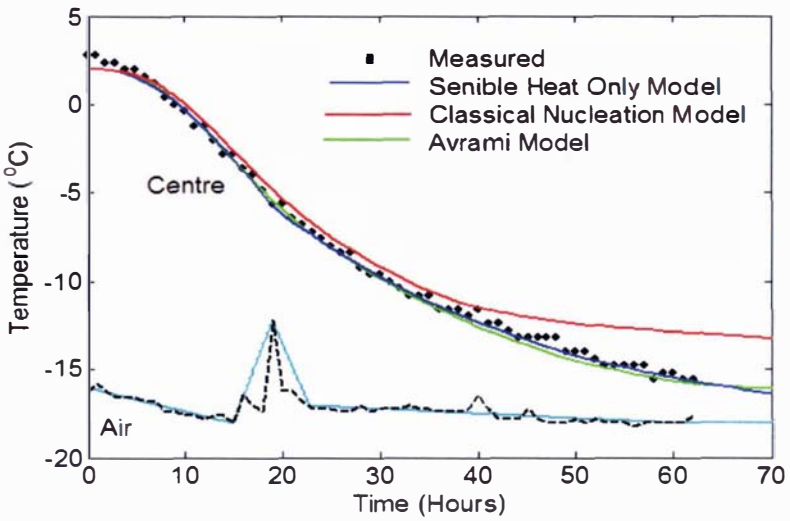

(b)

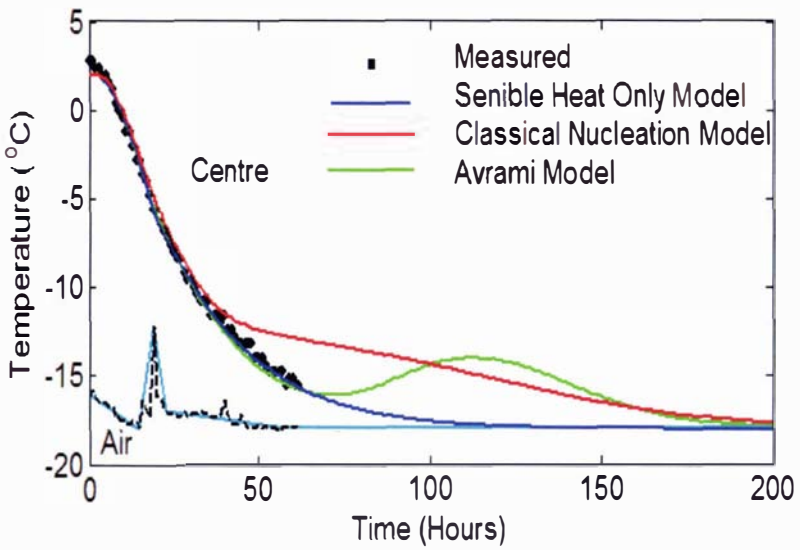

Figure 6.16: Comparison of the measured data (SBC -1a) for the salted butter block(B 15) with the prediction using various freezing models

(a) For 70 hours (b) For 200 hours

6.7 Conclusions

A graphical summary of the freezing models used in Chapter 5 and in this chapter is given in Figure 6.17. It can be concluded that the "sensible-heat-only" model predicted the experimental data very

well for the whole of the supercooled region but, because of the absence of latent heat removal, the predicted centre and surface temperatures continued to decrease to the ambient temperature without any freezing plateau or rebound. The equilibrium thermal properties model gave a temperature plateau just below the initial freezing point followed by a rapid drop to the ambient temperature. However, because the latent heat was removed at a higher temperature on average compared with the experimental data, the overall predicted rate of freezing was too fast and the temperature predictions were generally poor.

The Classical Nucleation Model was an attempt to model the interesting behavior of a temperature rebound repeatedly observed during freezing of butter blocks. The model assumed the nucleation rate was just a function of super-cooling using the classical nucleation theory for water in oil emulsions. It was clear that this mechanism alone will never give the rebound in the temperature as observed in the experimental data.

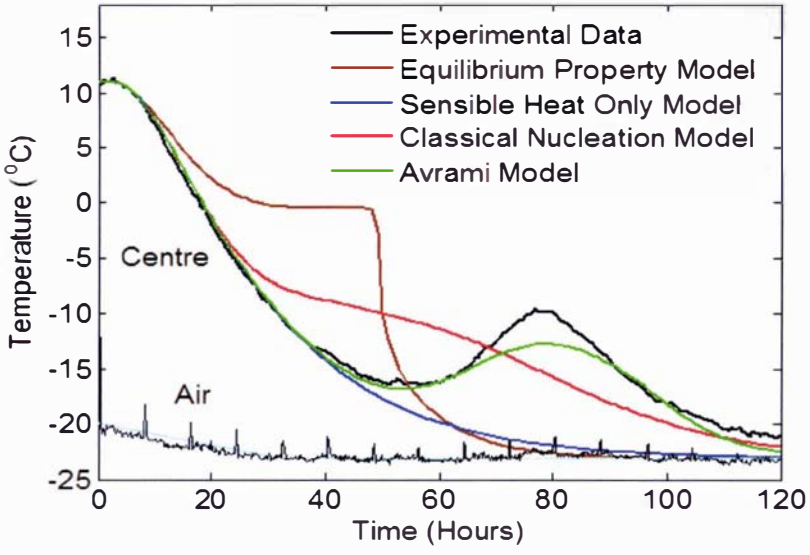

Figure 6.17: Comparison of the measured data for the salted block freeze to -23°C with all the freezing models

A differential form of the Avrami Equation, used for modelling the kinetics of crystallization, predicted the measured data for the freezing of butter very well using the fitted kinetics parameters. It not only predicted the temperature rebound observed in unsalted blocks of butter at two different temperatures but also predicted small rebounds for butter pats and salted butter blocks. A more detailed independent study to determine the nucleation and growth kinetics constants for the

Avrami Equation by means of isothermal experiments is needed to improve the predictions under all cooling conditions. A population balance modelling approach for the freezing process may be appropriate to predict the fluctuations in the position of the temperature rebound observed in nearly identical experimental trials.

In summary, the freezing behavior of the butter was modeled successfully in this chapter. Both freezing and thawing models were validated against the experimental data collected for the 0.5kg pats and 25kg blocks of butter.

In commercial stores, the butter blocks are stacked in the form of a pallet containing 48 or 56 blocks. These pallets are either stretched wrapped or stacked without the wrap which creates air gaps in between the adjacent blocks. The collection of data on wrapped and unwrapped pallets and a new approach to model the situation where there are potential of air flows in between the blocks is the subject of the next Chapter.

CHAPTER 7

HEAT TRANSFER IN PALLETISED BUTTER

7.1 Introduction

In Chapter 5 a heat transfer model of thawing or cooling of blocks of butter was developed and validated against experimental data collected for regular 25kg blocks and ½ kg pats of butter. In Chapter 6 this model was extended to include ice crystallization kinetics for freezing. These models were developed for regular shaped homogenous blocks of the product. In commercial stores butter blocks are generally wrapped in a plastic liner and placed in corrugated cardboard cartons. These cartons (48 to 56) are then stacked on a pallet base. The pallets are usually stretch wrapped to maintain the shape of the pallet. As a result the bulk system contains product, packaging material and air entrapped between the packaging and butter and between adjacent cartons. In the case of unwrapped pallets there is potential for air flows between the cartons on the pallet that can accelerate the thawing and freezing rates.

This chapter experimentally characterizes the freezing and thawing behaviour of wrapped or unwrapped butter pallets. By understanding how the pallet configuration influences the rates of air infiltration into the pallet and the rates of heat transfer into the butter blocks, approaches to adapt the individual block heat transfer models to palletised butter could be identified.

7.2 Data Collection

In order to identify typical pallet scenarios and realistic external conditions for experimental trials the configurations used in industrial practice were surveyed.

Figure 7.1 gives a pallet configuration used commercially for butter. In the New Zealand dairy industry a pallet is made up of 6 or 7 layers of 25 kg cartons with 8 cartons in each layer. The cartons are placed in an interlocking pattern in order to maintain the stability of the stack during transport and storage. Normally the pallet is constructed in last stage of the manufacturing process of butter. Butter is manufactured at about 15°C to 17°C and packed in pre lined cardboard cartons. At the time of manufacturing the butter has a paste like structure and it flows into the cardboard

carton easily. After filling, the cartons are stacked on a pallet base using a palletizing machine. Since the butter is usually soft enough to deform at this stage, the butter blocks becomes tightly packed and have no significant gaps between adjacent blocks. The butter pallet is then stored in freezer rooms with or without stretch wrapping around it. The solidification of the butter provides enough strength to the pallet stack to avoid slumping. If the butter is not cooled fast enough or is subsequently heated, the cartons can slump and bulge at the sides making close packing difficult, resulting in air gaps between cartons within the pallet stack.

During transportation from one store to another, the pallets without wrap can be significantly disrupted. The jolts received during fork lift transport can jostle the block positions and this deformation creates air gaps between the adjacent blocks. If these gaps are such that air can flow through them then it can have significant impact on the thawing and freezing times. Therefore experiments needs to consider both tightly packed pallets (wrapped or unwrapped) and pallets where there are significant air flows between the cartons.

A total of 7 pallet trials were conducted. Two of these (Trial 1 and 2) were thawing and freezing of full sized pallets under industrial conditions in a commercial storage facility (Fonterra, Whareroa site, Hawera, NZ). To support this data, and to, achieve better control of ambient conditions it was decided to conduct extra experiments in a Massey University frozen storage facility. Due to limited height in the freezing facility, the number of layers in the pallet was reduced to include only the middle three layers in a half pallet.

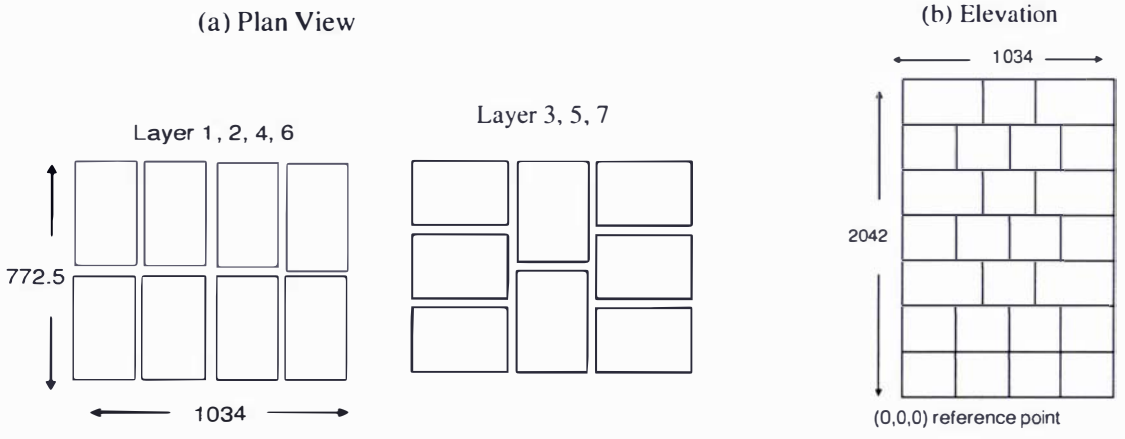

Figure 7.1: Plan and elevation view of the full butter pallet configuration (approximate outer dimensions in mm)

Thawing and freezing experiments were conducted on the half pallets for three different scenarios. The first (Trial 3) was the freezing and thawing of a fully wrapped half pallet. The second (Trial 4) consisted of thawing and freezing an unwrapped tightly stacked half pallet. The third (Trial 5) investigated the freezing and thawing of unwrapped loosely stacked layers to identify how significant the air flows between adjacent cartons might be. Table 7.1 gives the code number, average ambient and initial conditions, and the thermocouple positioning plan for each trial. More complete details of ambient conditions are given in the results section below. The following sections provide the details of the experiments for two full pallet and three half pallet trials.

Table 7.1: Experiment plan for half and full pallet trials

Code		Type	Configuration	T_i (°C)	T_a(°C)	Thermocouple positions
Trial 1	PC – 1	Full pallet	Wrapped tightly stacked	10	-11	Appendix (A5.1)
	PH – 1	Full pallet	Wrapped tightly stacked	-11	10.4	Appendix (A5.1)
Trial 2	PC – 2	Full pallet	Unwrapped tightly stacked	10	-11	Appendix (A5.1)
	PH – 2	Full pallet	Unwrapped tightly stacked	-11	10	Appendix (A5.2)
Trial 3	PC – 3	Half pallet	Wrapped loose stacked	20	-25	Figure (7.5, 7.6)
	PH – 3	Half pallet	Wrapped loose stacked	-25	20	Figure (7.5, 7.6)
Trial 4	PC – 4	Half pallet	Unwrapped tightly stacked	20	-25	Figure (7.5, 7.6)
	PH – 4	Half pallet	Unwrapped tightly stacked	-25	20	Figure (7.5, 7.6)
Trial 5	PC – 5a	Half pallet	Unwrapped loose stacked	10	-25	Figure (7.5, 7.6)
	PC – 5b	Half pallet	Unwrapped loose stacked	20	-25	Figure (7.5, 7.6)
	PH – 5	Half pallet	Unwrapped loose stacked	-25	20	Figure (7.5, 7.6)

7.2.1 Full Pallet Trials

The first trial was performed on a full pallet of butter. Figure 7.2 shows the actual wrapped pallet on which the experiments were performed. The configuration of the pallet is also given in Figure 7.1. The pallet was selected from pallets of freshly made butter at Fonterra, Whareroa, Hawera and then stored for about six weeks in a cheese store at 10°C. The cartons were re-stacked on the pallet after placing 45 thermocouples at different positions inside and outside the butter cartons. The thermocouples inside the butter were placed using a needle, nylon thread and a guide to ensure accurate placement of the thermocouple to the required positions. The thermocouples were then

connected to a Grant Squirrel data logger (1000 series) and a Campbell data logger (CR10X) to record the temperatures profiles throughout the pallet. The whole pallet was then tightly wrapped in polyethylene stretch-wrap.

All the thermocouples inside the butter and outside the cartons were positioned at the vertical centre of the blocks at different positions along the width and length of the blocks, except for along the diagonal of the pallet for which the thermocouples were positioned in approximate position of the diagonal. Altogether there were 46 thermocouples positioned in and outside the pallet. The thermocouples were positioned throughout the pallet in such a way that it could give maximum information not only on the general trend of heat transfer in the pallet but also on how the air gaps affect the heat transfer in different layers.

Before starting the trial (PC – 1), the pallet was held at 10°C for another month to ensure uniform initial temperatures. The pallet was then shifted to a freezer store at approximately -11°C. Temperature readings were recorded every hour for 28 days. The pallet was kept in the freezer store for another 30 days before beginning the thawing trial (PH – 1). At this time uniform initial temperatures were achieved and the pallet was shifted to a cheese store at about10°C where the readings were monitored for a further 28 days.

The pallet used in Trial 1 was again used for Trial 2 but the stretch wrap was removed. It was expected that there would be more chance of air flow to occur through the channels between the cartons. These gaps occurred due to the loosing of the pallet stacking caused by repeated movement of the pallet between freezers and cheese stores in the previous experiments. To give some pallet stability, the top and the fourth layers were strapped. This resulted in these two layers being more closely stacked as compared to others as shown in Figure7.3.

The pallet was frozen and thawed (PC – 2 & PH – 2) under the similar conditions as for Trial 1. To more closely follow what was happening around the slowest cooling block and to observe the heat transfer in the single inner block of a commercial pallet, the thermocouples were repositioned in Blocks 31 & 38 and the air channels around them. Block 31 was in layer 4 which was the middle layer with direct paths for the air to reach all the faces of the block whereas the Block 38 was in layer 5 which had direct path for the air to reach only two of the side faces of the block but an indirect path to reach the inner faces of the block. These boxes were selected to identify how the air movement in the pallet could be affected by the different block layout of the layers.

Figure 7.2: Wrapped full pallet used for Trial 1(PC – 1, PH – 1)

Front Back

Figure 7.3: Unwrapped full pallet used for Trial 2 (PC – 2, PH – 2)

The repositioned thermocouple locations in the plan view of layers 4 & 5 are given in Appendix A5.2 and the positions inside the butter are given in the 3D drawing (Appendix A5.2). Six thermocouples were positioned on the six sides of the pallet to record the ambient temperatures on all sides. Five and six thermocouples were placed inside Blocks 31 & 38 respectively. Six sensors were positioned outside each of Blocks 31 & 38 for the local ambient temperatures on different sides of the blocks and the remaining six thermocouples were positioned in between the air channels as shown in Appendix A5.2.

The dimensions of the pallet were taken after each freezing and thawing trial to account for the bulging of the cartons and also the deformation of the pallet due to transportation from one storage room to another.

7.2.2 Half Pallet Trials

Trials 3, 4 and 5 used a half pallet experimental design that approximated the middle three layers (3, 4, and 5) of a seven high pallet. Medium density polystyrene sheets (50 mm thick) were placed above and below the top and bottom layers to insulate against heat transfer in the vertical direction. The carton configuration is shown in Figure 7.4. Thermocouples were located throughout the middle layer in the same way for all three trials as summarised in Figure 7.5. The main purpose of placing so many thermocouples was to quantify the temperature gradients along the air gaps and to collect information that indicated the presence and the direction of the air flows within the pallet. Figure 7.6 gives the positions of the thermocouples in Blocks 1 and 2. The same positions were used for Blocks 7 and 8. All thermocouples throughout in the layer were placed at the geometric centre of the half pallet which was at the vertical centre of the middle layer. The blocks were placed in a freezer at about -25°C for 10 weeks to freeze them completely and then the thermocouples were inserted by a drilling a 2 mm diameter hole and pushing the thermocouple into position. All the thermocouples had been previously calibrated in an water and ice slurry and were accurate within ±0.25°C.

The thermocouples were connected to a Campbell data logger (CR10X) to record the temperature profiles with a time interval of 15 minutes. Prior to starting the experiment, the pallet was held at a temperature of about 10°C to equilibrate for 2 weeks in a walk in chiller and then shifted to a –25°C walk-in freezer for the freezing trail. A single carton took about 120 hours at about -25°C to freeze all the water in the butter. It was expected that for the half pallet trials it could take 3-5 weeks for all the water to freeze depending on the extent of air penetration into the pallet.

After the completion of the freezing trial (when an equilibrium temperature of -25°C was achieved) the freezer was then turned off to start the thawing trail and a thermostat controlled heater was placed inside the freezer to control the temperature at about 20°C. The ambient temperature for the thawing trial was low for the first 22 hours of Trial PH -5 because of a lack of air circulation in the room. A pedestal fan was then placed in the room facing towards front wall to enhance the mixing of air in the room.

The directions of air flow in the freezer during freezing and thawing of the half pallet is given in Figure 7.7. During freezing trials the fan delivered air across the top of the pallet where it flowed down the back and recycled around the pallet at lower levels. This resulted in slightly cooler ambient temperatures at the top and rear of the pallet stack. During thawing the pedestal fan resulted in more circulation around the pallet with air traveling from the top of the pallet to the back and sides.

Trial 3 (PC – 3, PH – 3) was performed by stretch wrapping a half pallet which had under gone several freeze and thaw cycles creating bulginess and reducing the height of the pallet due to slumping. The approximate outer dimensions of the half pallet were (1182 × 820) × 738 mm. The bulging of the blocks partially filled the (30-40 mm) gaps that were initially between the adjacent cartons. This was to be expected considering the appreciable periods of time the butter was at 10°C or higher where the SFC of the milkfat is reduced to about 50-60% and the butter was softer.

The set up of Trial 4 (PC – 4, PH – 4) was the same as for Trial 3 but without any gaps between the blocks. By stacking the pallet with freshly manufactured butter and without stretch wrap it was expected that air gaps would be present through out the pallet and therefore faster heat transfer would result due to the potential for internal air flows. However in this trial the blocks were placed as tight as possible with hand stacking. The Trial 4 half pallet was set up on the top of the Trial 5 half pallet trial to save space and freezing and thawing resources. The thermocouples were placed in the same location as in Trial 3. The approximate outer dimensions of the half pallet without the polystyrene sheet were (1154mm × 840mm) × 810 mm. After freezing, the half pallet was kept at -21°C for 5 weeks prior to thawing to achieve uniform initial conditions.

Trial 5 was carried out to present the most extreme scenario likely to be experienced in industrial practice, with large potential for internal air flow through the pallet and subsequently faster heat transfer rates. For Trial 5 the cartons in all three layers were placed with gaps of 30-40 mm between

them to allow air flow between the cartons. The approximate outer dimensions of the cartons were (385 × 280) ×250 mm. The effective outer dimensions of the pallet were (1154 × 840) × 810 mm.

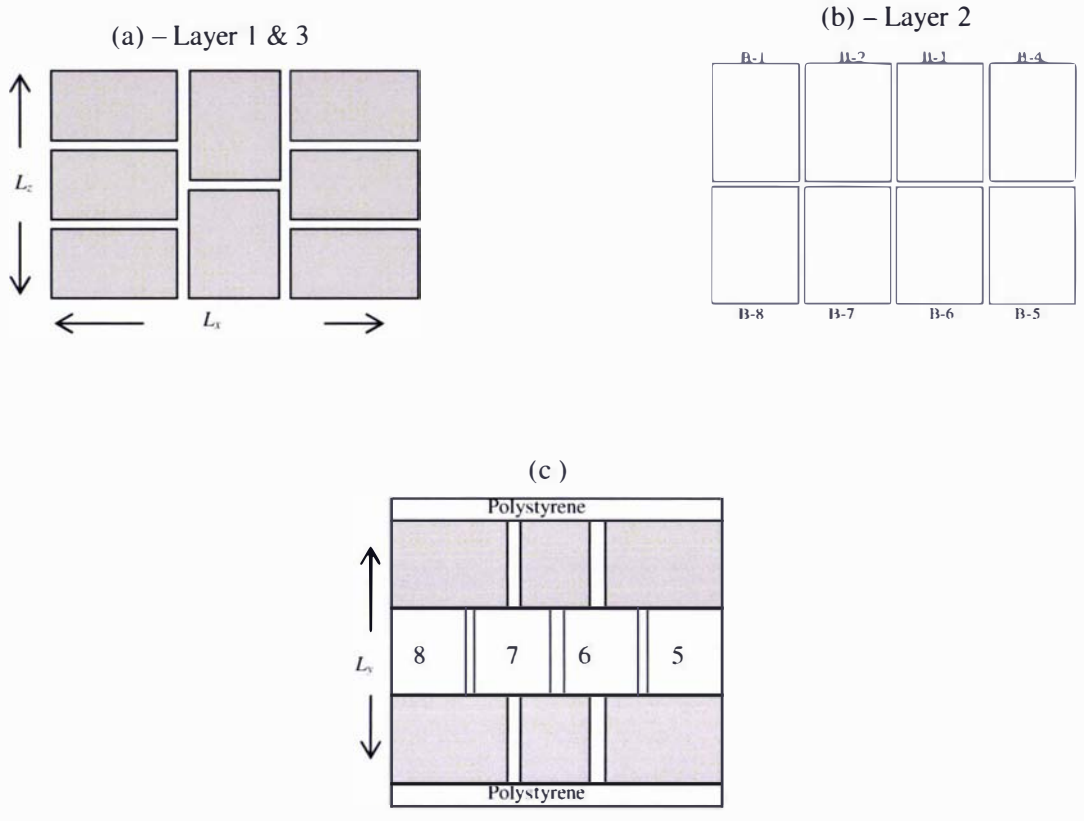

Figure 7.4: Plan views ((a) and (b)) and front elevation (c) of half pallet trails (Trials 3-5)

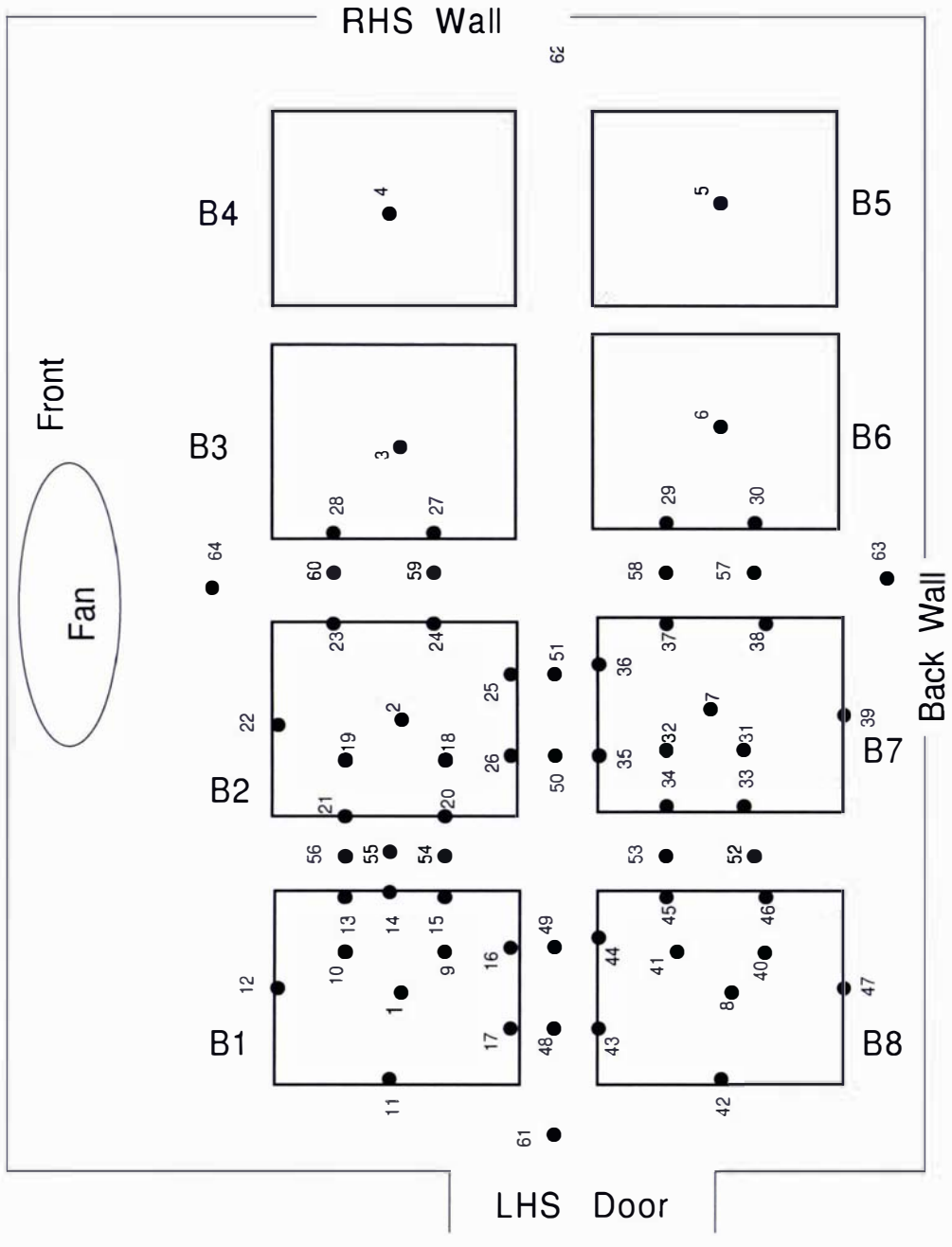

Figure 7.5: Position and code numbers of thermocouples in the middle layer of the three layered half pallet trials. (Note that diagram is not to real room scale)

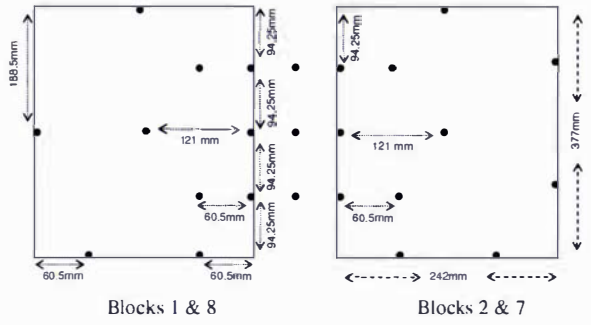

Figure 7.6: Position of the thermocouples in cartons 1, 2, 7 and 8 in half pallet Trials 3-5

(a)

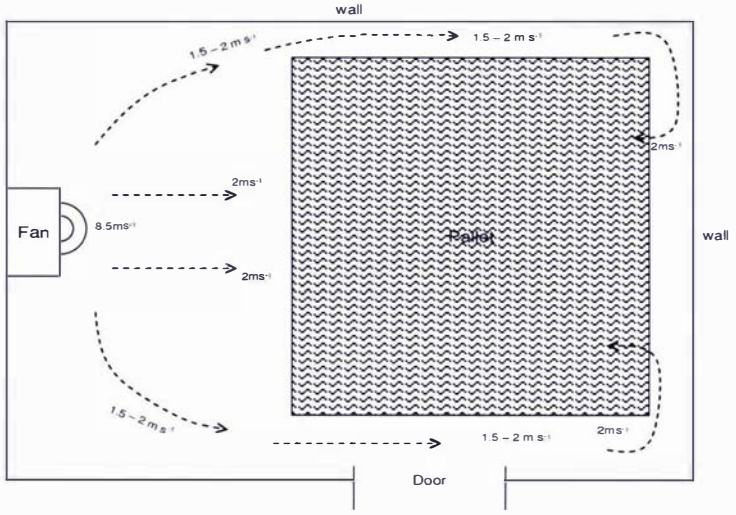

(b)

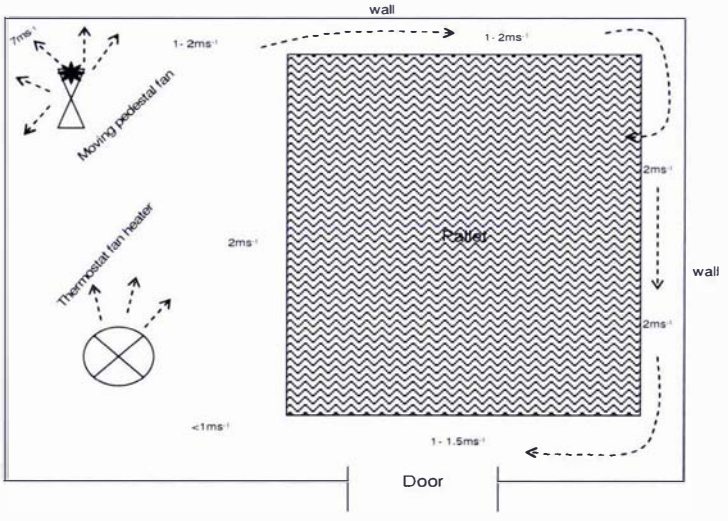

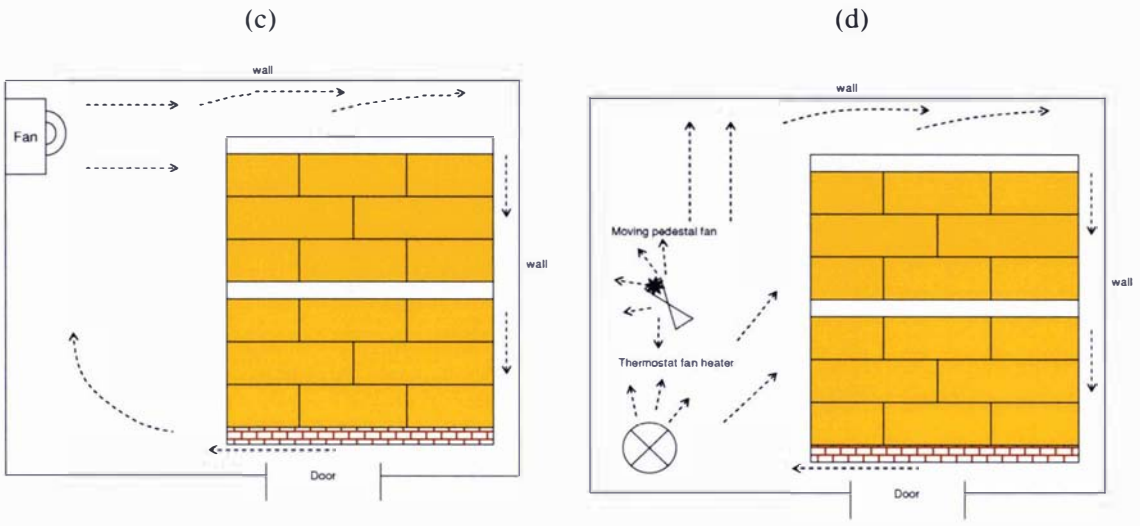

Figure 7.7: Direction of air flows in the experimental room (a): Plan view (freezing) (b): Plan view (thawing) (c): Elevation (freezing) (d): Elevation (thawing)

7.3 Experimental Results

This section summarises the experimental results for thawing and freezing of half and full pallets of butter. The detailed data for each thermocouple in the half and full pallets is given in the accompanying CD (Appendix A5.3).

7.3.1 Trial 1 – Wrapped Full Pallet

(a) Freezing (PC – 1)

Figure 7.8 shows the measured data for the freezing of the wrapped full pallet trial. Figure 7.8(a) gives the data for the six external faces of the pallet which were found to be quite uniform. The temperature of the bottom surface was a little higher due to slightly less air circulation through the base of the pallet. The temperature of the top surface was very slow to change compared to any other face due to the position of the data logger on the top of the pallet effectively insulating the pallet surface from the ambient conditions.

(a)

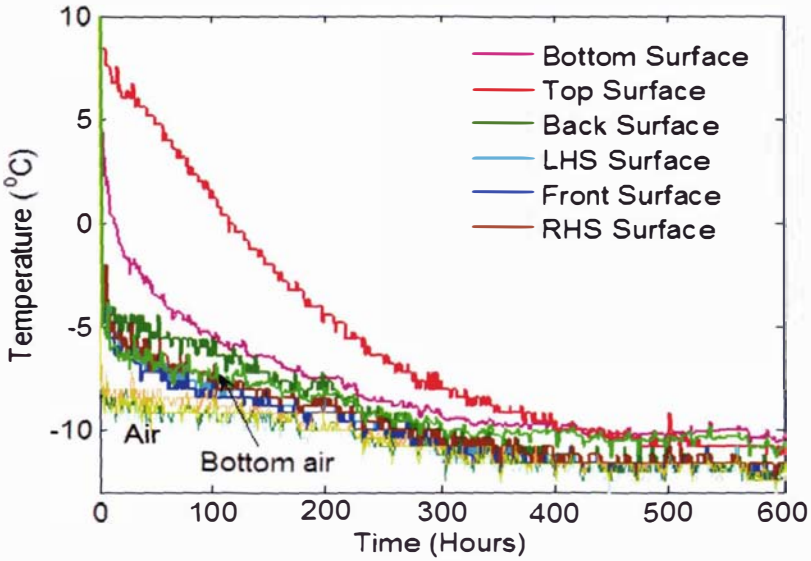
Temperature (°C)
Time (Hours)
Bottom Surface
Top Surface
Back Surface
LHS Surface
Front Surface
RHS Surface
Air
Bottom air

(b)

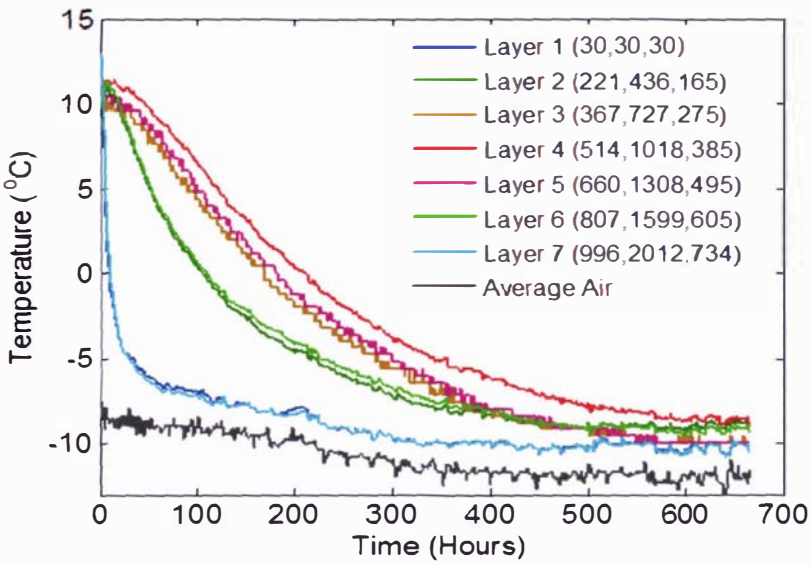
Temperature (°C)
Time (Hours)
Layer 1 (30,30,30)
Layer 2 (221,436,165)
Layer 3 (367,727,275)
Layer 4 (514,1018,385)
Layer 5 (660,1308,495)
Layer 6 (807,1599,605)
Layer 7 (996,2012,734)
Average Air

(c)

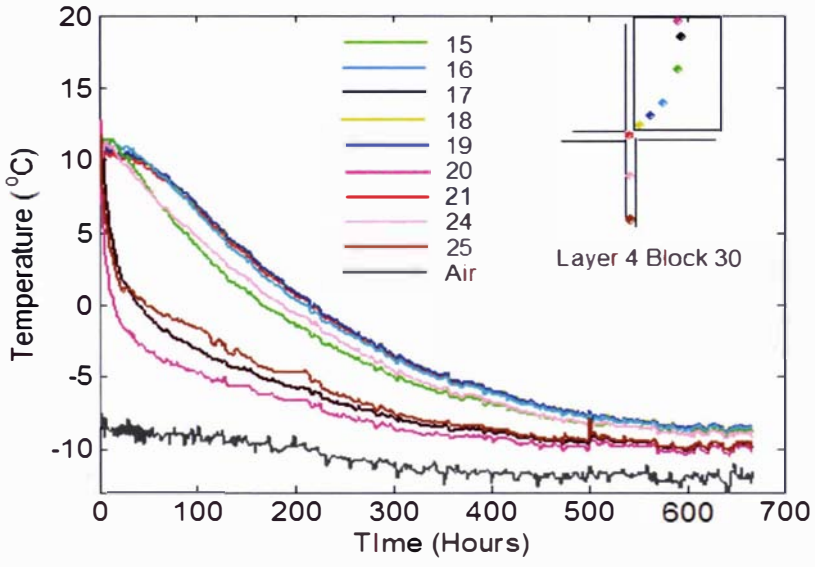

Figure 7.8: Experimental temperature profiles measured for trial PC – 1
(a) pallet faces (b) across the pallet diagonal from bottom LHS front corner to top RHS back corner - positions in mm indicated are relative to bottom LHS of pallet as in Figure 7.1
(c) across layer 4

Figure 7.8(b) gives the general trend of the heat transfer through the diagonal of the pallet. Heat transfer was quite symmetrical through the pallet. The measured positions in layers 1 & 7 had similar temperature profiles at the positions in layers 2 & 6 and in layers 3 & 5. The middle layer 4 had the slowest freezing position. The release of latent heat was either very slow or incomplete. Only the recorded positions on layers 2 & 6 showed evidence of release of latent heat after 600 hours and a slight raise in the temperature. The experiment was stopped after 675 hours due to the cost and time involved in conducting the trials.

Figure 7.8 (c) shows the temperature profiles throughout the middle layer (layer 4) of the pallet. Four positions (16, 18, 19, and 21) near the centre of the pallet had the similar temperature profiles. Thus the physical centre of the pallet was found to be the thermal centre of the pallet and the slow heat transfer from the top and bottom surfaces of the pallet did not significantly influence the pallet centre temperature.

From Figure7.8 (c) it is also clear that the heat transfer in the pallet is by conduction only. Positions 16 & 17 (inside the butter in block 30) were nearly at the same positions from the front and back

surfaces of the pallet as positions 24 & 25 but in the channel between the Blocks 26 & 27. There was little difference between the temperatures of each of the pairs indicating an absence of air circulation in these air gaps.

The top to bottom symmetry can also be observed from Figure 7.9, which gives the temperature profile of the centre of the butter blocks from top to bottom of the pallet. The temperature profile of the positions in the centres of the boxes in layer 3, 4, and 5 were exactly the same and were the slowest, showing there is negligible heat transfer from top to bottom in the pallet. The blocks at layers 2 & 6 cooled at the same rate at the beginning but then the block in layer 6 remained higher as did the block in layer 7. This was due to the slow rate of heat transfer from the top due to the data logger box.

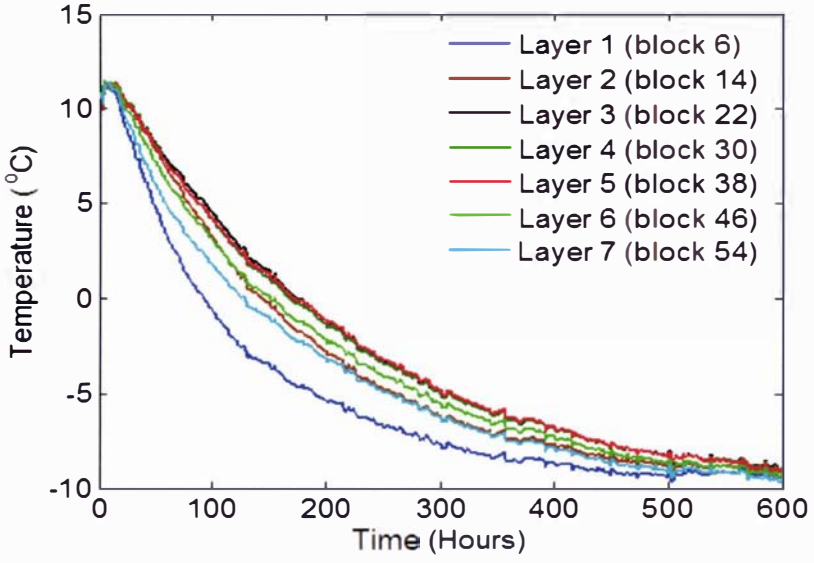

Figure 7.9: Experimental temperature profiles measured for trial PC – 1 at centre of the blocks (one on each layer) from top to bottom of the pallet

(b) Thawing (PH – 1)

Figure 7.10 shows the temperature profiles for the pallet undergoing heating. The surface temperatures of all four vertical sides were quite consistent whereas the heat transfer through the top and bottom was found to be slow as was observed in freezing trial. To try and prevent this data

logger box was placed on two wooden blocks to allow air flow over the top surface of the pallet, but in spite of this the air flows were lower compared to the sides of the pallet.

In Figure 7.10(b) for the temperature profiles of the positions on the diagonal down through the pallet, Layer 4 was again the slowest thawing position. The corners of layers 1 & 7 showed identical temperatures slightly higher than the ambient after about 400 hours indicating some variability in the air circulation around the pallet. The measured positions on layers 2 & 7 thawed quite consistently to about 4°C but then layer 7 thawed faster than layer 2. The same pattern was observed on layers 3 and 5.

A clear latent heat plateau can be seen in the thawing as the butter was kept in the freezer for long enough to freeze all the water in the butter before starting the experiment. The thawing of positions on layers 6 & 7 were faster than those on layers 2 & 3 showing that the heat transfer through the upper half and lower half of the pallet was not symmetrical. This was likely to be due to better air flow over the top of the pallet than at the ground level through the pallet base.

Figure 7.10 (c) shows the temperature profile measured through the middle layer of the pallet. Positions 18 & 19 on layer 4 were the slowest changing temperatures recorded in the pallet.

(a)

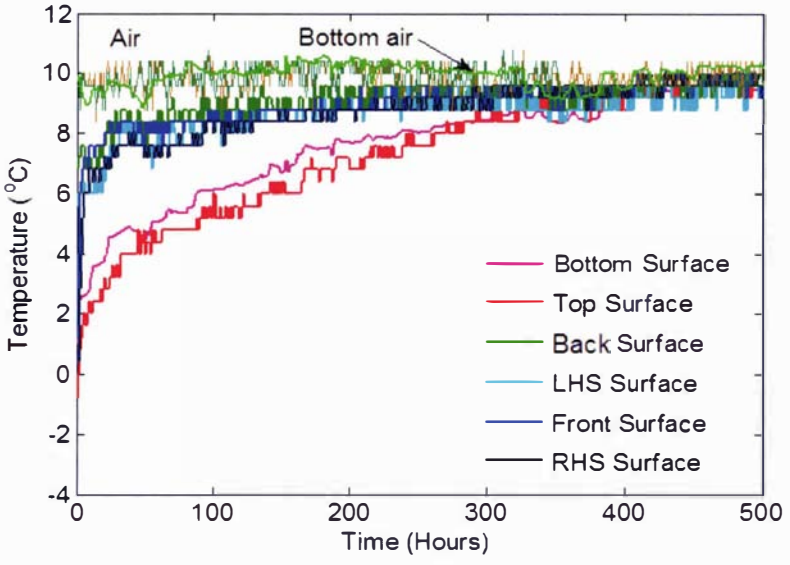

(b)

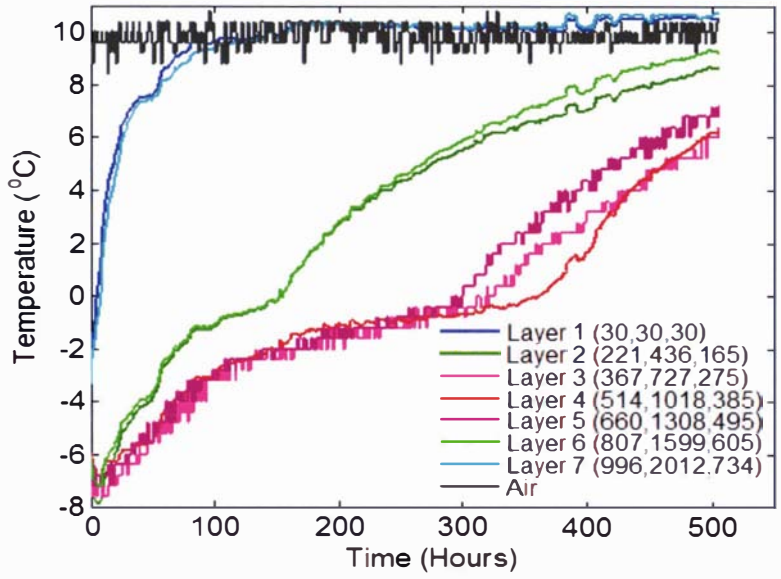

(c)

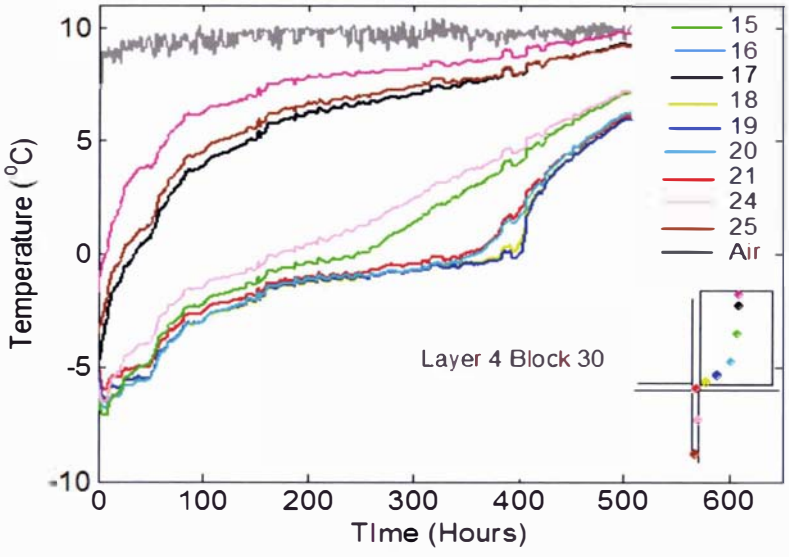

Figure 7.10: Experimental temperature profiles measured for trial PH – 1

(a). pallet faces (b). across the pallet diagonal from bottom LHS front corner to top RHS back corner - positions in mm indicated are relative to bottom LHS of pallet as in Figure 7.1

(c). across layer 4

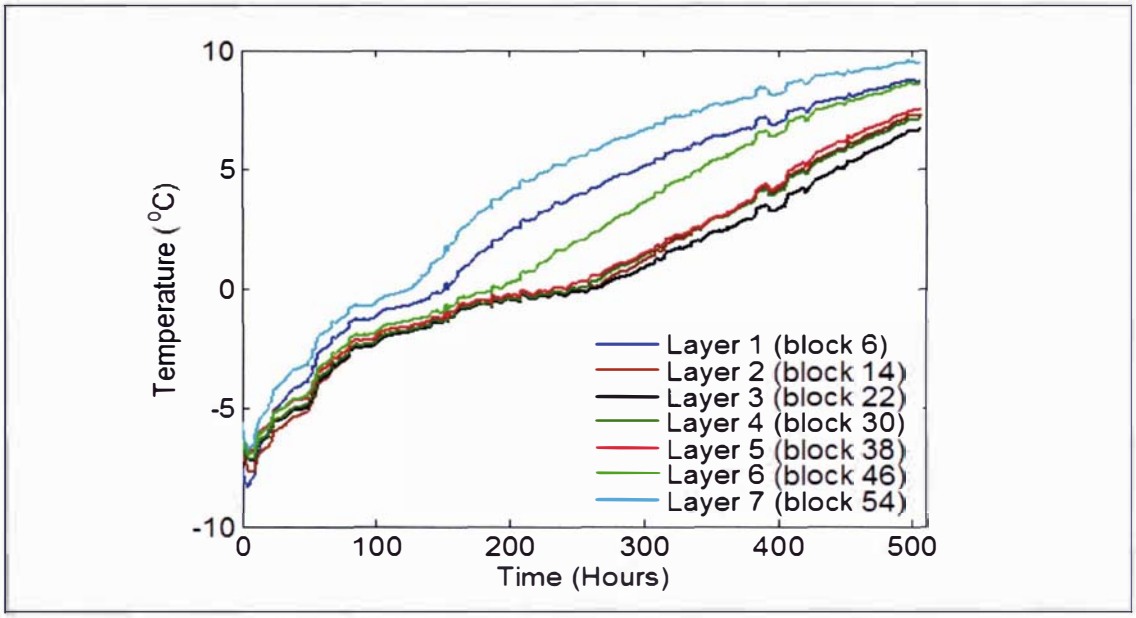

Figure 7.11: Experimental temperature profiles measured for trial PH – 1 at the centres of the blocks (one on each layer) from top to bottom of the pallet

Figure 7.11 shows the temperature profile of the centre of seven blocks (one in each layer) at the back of the pallet. The centre of the blocks on layer 2, 4 & 5 showed the same temperature profile and the centre of the Block 22 on layer 3 was found to be the slowest. This analysis confirmed that the upper half of the pallet heated slightly faster than the lower half.

As seen in Figure 7.2 the pallet base was also wrapped thereby preventing air flow through it. This would provide a good barrier to heat transfer as air cannot flow directly onto bottom face of the butter blocks on the bottom layer.

Overall the freezing and thawing of wrapped pallet shows that the heat transfer in pallet was conduction dominated. The geometric centre of the pallet was found to be the thermal centre of the pallet.

7.3.2 Trial 2 – Unwrapped Full Pallet

(a) Freezing – (PC – 2)

Figure 7.12 shows the recorded temperature profiles for cooling of the unwrapped full pallet. The ambient temperature on all sides of the pallet was very uniform except the bottom. Figure 7.12(a) shows that the temperature of the centre of the pallet faces followed the same trends as were observed in Trial 1 (PC – 1).

(a)

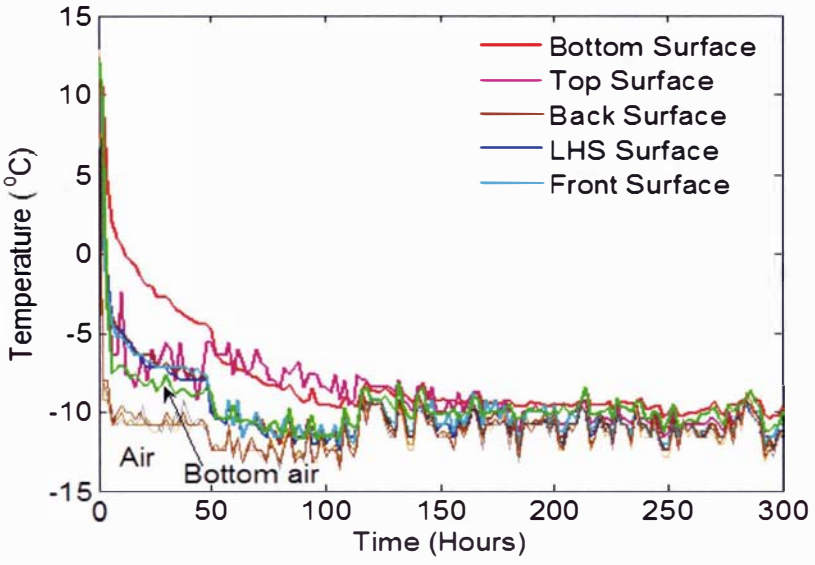
Bottom Surface
Top Surface
Back Surface
LHS Surface
Front Surface
Air
Bottom air
Temperature (°C)
Time (Hours)
15
10
5
0
-5
-10
-15
0
50
100
150
200
250
300

(b)

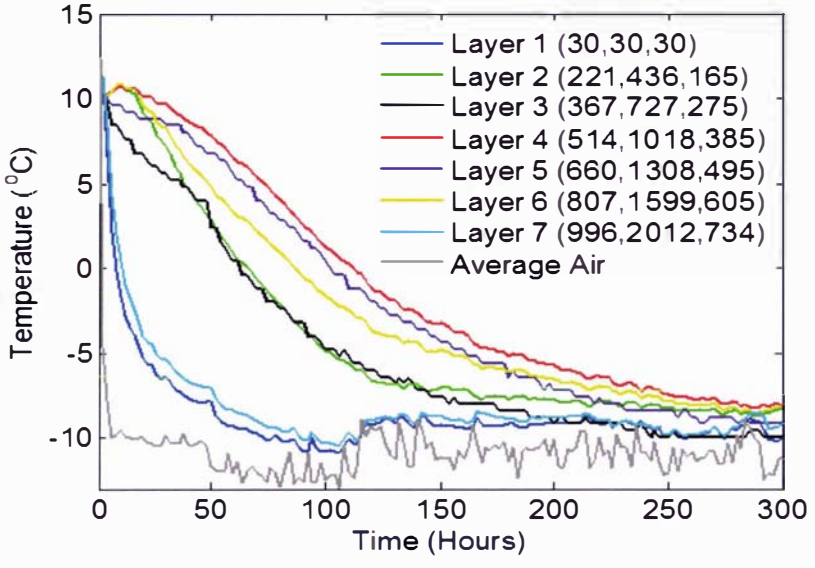
Layer 1 (30,30,30)
Layer 2 (221,436,165)
Layer 3 (367,727,275)
Layer 4 (514,1018,385)
Layer 5 (660,1308,495)
Layer 6 (807,1599,605)
Layer 7 (996,2012,734)
Average Air
Temperature (°C)
Time (Hours)
15
10
5
0
-5
-10
0
50
100
150
200
250
300

(c)

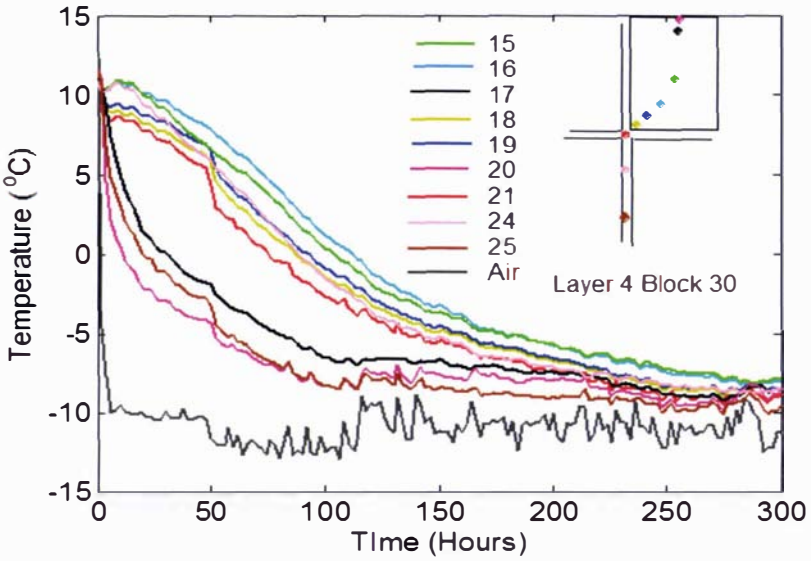

Figure 7.12: Experimental temperature profiles measured for trial PC – 2
(a). pallet faces (b). across the pallet diagonal from bottom LHS front corner to top RHS back corner - positions in mm indicated are relative to bottom LHS of pallet as in Figure 7.1
(c). across layer 4

Figure 7.12(b) shows the temperature profile on the diagonal of the pallet. Unlike the trends observed in Trial 1, the cooling profiles were not vertically symmetrical. Layers 3 & 5 were different, layers 2 & 6 were different, although layers 1 & 7 were found to be reasonably similar. Although the heat transfer throughout the pallet was not uniform, the slowest position was on the layer 4. The fact that similar rates of heat transfer over the top and bottom surfaces did not result in symmetry of heat transfer in the vertical direction suggests the possibility of irregular air flow internal to the pallet.

Figure 7.12(c) showed that the slowest freezing point was near position 16 (the diagonal position in layer 4). This shows that the most of the heat transfer was from the external face. The temperature profile at position 20 and the surface shows the heat transfer resistance due to the packaging. A similar but a smaller temperature difference can be seen between positions 18 & 21. All these factors showed that the heat transfer in the pallet was affected by the air flows in the gaps between adjacent blocks.

Figure 7.13 shows the temperature profile of the centre of all the blocks on the back side of the pallet. Block 6 on layer 1 was the fastest to cool due to heat conduction from two sides of the block being exposed to ambient. Although block 54 in layer 7 also had two faces exposed to ambient, it was found to change much slower than layer 1. This could be due to the data logger box which could have partially blocked the heat transfer from some part of the top face. The blocks on layers 4, 5, & 6 had very similar temperature profiles. The blocks in layers 2 & 3 were found to cool slightly faster than other three which could be due to different sized air gaps around these blocks.

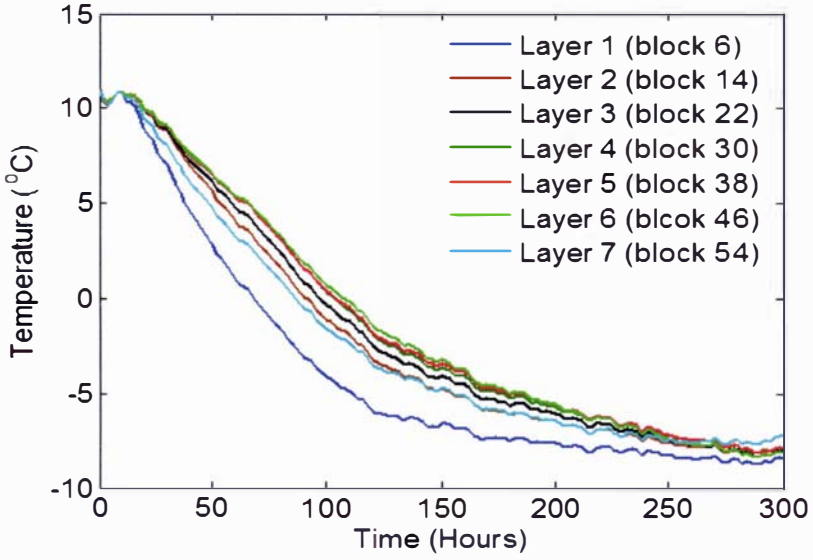

Figure 7.13: Experimental temperature profiles measured for trial PC – 2 at centers of the blocks (one on each layer) from top to bottom of the pallet

A comparison of slowest freezing position in the wrapped and unwrapped pallets is given in Figure 7.14 with the average ambient temperatures of both trials. By unwrapping the pallet, the freezing rates were accelerated as expected, although some of these differences were due to the differences in the ambient conditions. It took about 160 hours longer to reach to -5°C for the wrapped pallet even though the freezer conditions were within 2-3°C of those for the unwrapped trial.

The unwrapped trial was monitored for long enough to observe any slow release of latent heat and rebound in the temperature due to freezing. Even after 700 hours at about -10°C, the temperature of the slowest freezing position in the pallet remained higher than the ambient suggested that the latent was heat released very slowly over a long period of time and no significant rebound in temperature was observed.

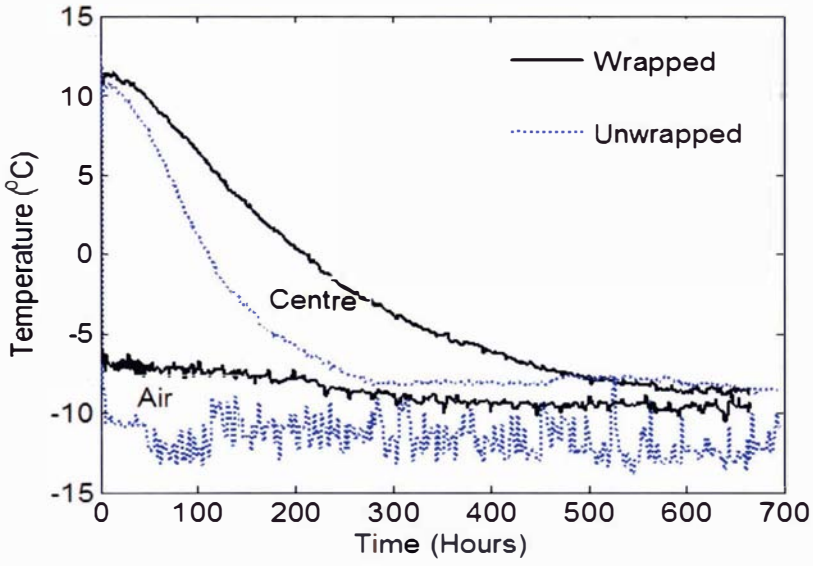

Figure 7.14: Comparison of the slowest cooling position (16) in the wrapped (PC – 1) and unwrapped (PC – 2) full pallet trials

Summarizing the freezing for the unwrapped full pallet trial it can be concluded that due to the shifting of the pallet with forklifts, the air gaps between the blocks were not consistent. The least air gaps were present in layer 4 where the whole layer was strapped with the plastic band to maintain the dimensions of the layer thus avoided any increase in the air gaps. Despite this the centre of the pallet was not the slowest cooling point, indicating that some air flow through the pallet did occur. The presence of these air gaps and subsequent internal air flow had a dramatic effect on the rate of heat transfer in the pallet.

(b) Thawing (PH – 2)

Figure 7.15 shows the measured temperature profile through the unwrapped full pallet during thawing. As in the previous experiments the ambient temperature on all sides of the butter pallet was found to be uniform except the bottom of the pallet which was found a little lower than the other faces. To compare the rate of heat transfer on different sides of the Block 31 all the positions on the faces of the block along with an average ambient temperature is given in Figure 7.15(a). Overall the two side faces had slower heat transfer than the inner and outer faces of Block 31. There was some heat transfer from Block 32 towards Block 30. There must have been significant airflow through the centre of the pallet for the inner face to heat more quickly than faces nearer the outside of the pallet.

These uneven rates of heat transfer affected the temperatures at the positions inside the Block 31 as shown in Figure 7.15(b). Position 15 (centre of the block) and position 11 (towards Block 30) were the slowest heating points, which shows that the block was heating from the side towards the Block 32 and there was negligible heat transfer from the side towards the block 30. The block also received some heating from the inner face towards its centre; most probably due to air flows occurring through the pallet.

(a)

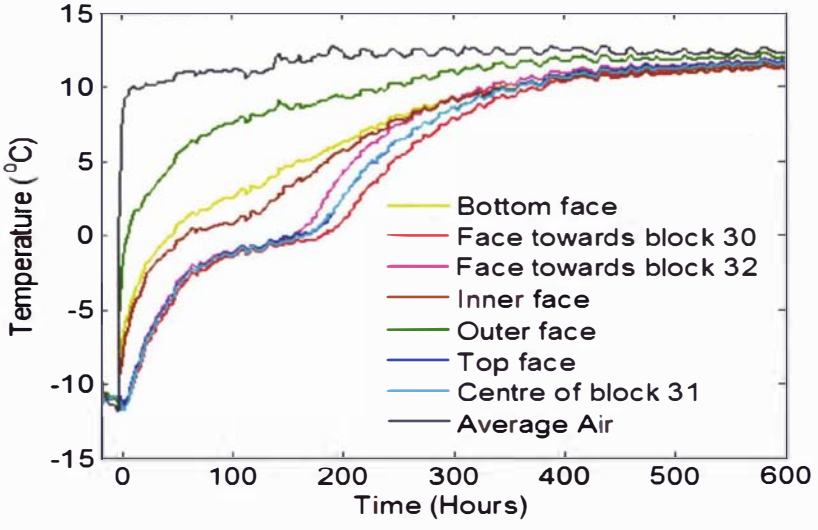

(b)

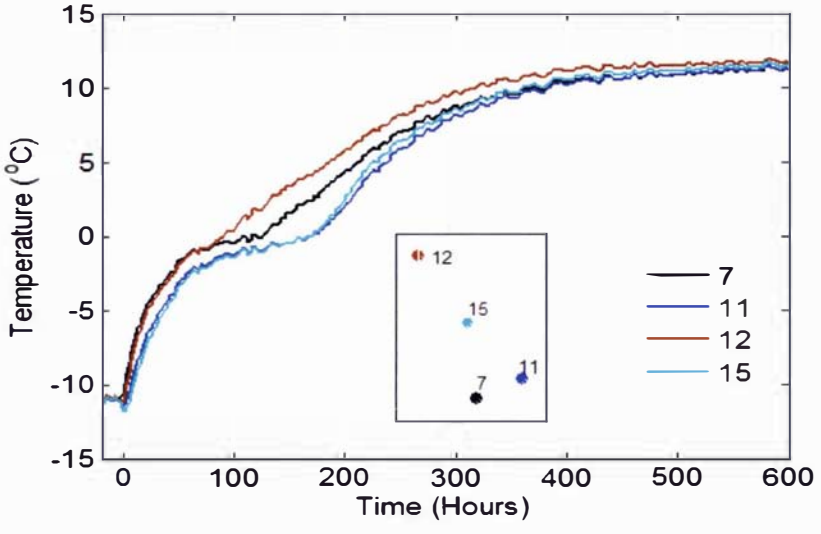

Figure 7.15: Experimental temperature profile measured for trial PC – 2
(a). centre of all the faces of the Block 31 (b): positions inside the Block 31

Figure 7.16 shows the temperature profiles of all the faces on Block 38. There is little evidence of air flow between Blocks 38 and 37. Some air flow is evident between Blocks 38 and 39 resulting in that face heating up faster. There was significant air flow occurring along the inner face. Although the blocks were tightly packed vertically, some heat transfer can be seen from the top and bottom faces. Overall the temperature profiles of the faces demonstrate uneven heat transfer rates which subsequently affected the rate of heating of the butter blocks.

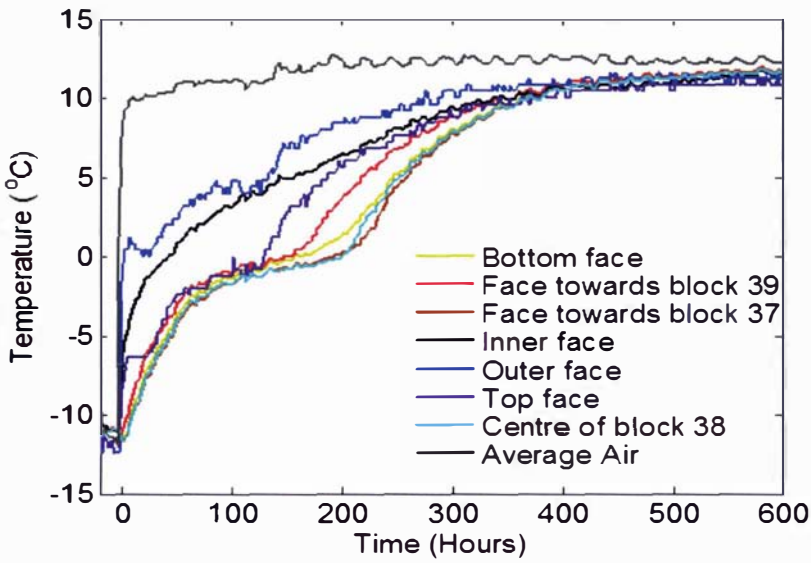

Figure 7.16: Experimental temperature profiles measured for trial PH – 2 at the centre of all the faces of the Block 38

Figure 7.17 shows the temperature profile of all the positions inside Block 38, which is placed between blocks 37 and 38. Most of the heat transfer was from the face exposed to ambient resulting in position 5 heating up most quickly. There was symmetry along the diagonal of the block where position 31 and 18 showed the same temperature except in the phase change region. Position 17 was at the same distance from the inner face as position 5 was from the internal face. The fact this was lower than the pallet centre shows that there was some heat transferring through the inner face as well. Position 19 which was 50 mm in from the top also heated up very slowly showing that there was much less heat transfer from top to bottom as was observed in Block 31.

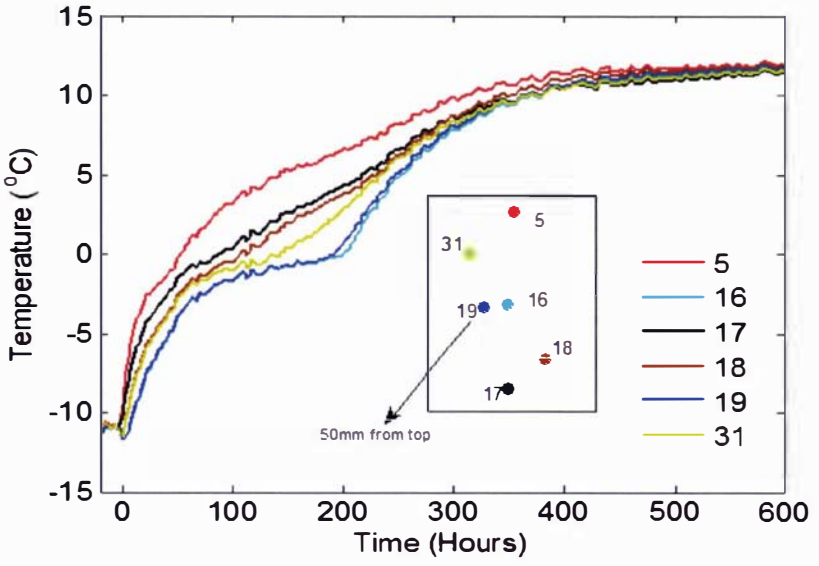

Figure 7.17: Experimental temperature profiles measured for trial PH – 2 at positions inside the Block 38

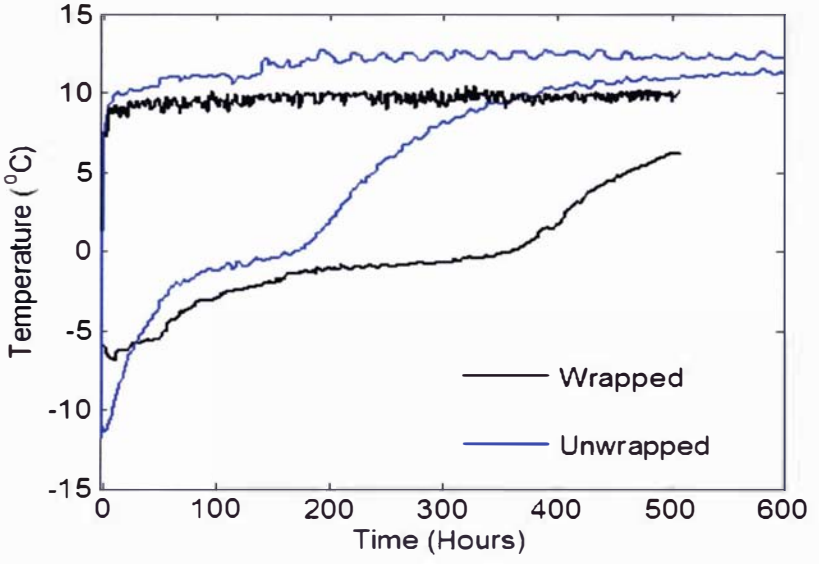

Figure 7.18: Comparison of thawing of wrapped (PH – 1) and unwrapped (PH – 2)in the full pallet trials

A comparison of the wrapped and unwrapped full pallet thawing is given in Figure 7.18. The measured slowest heating points in each configuration (position 16 in Block 30 for the wrapped trial and position 11 in Block 31 for the unwrapped trial) were compared. There were some differences

in the initial and ambient conditions, but as expected the wrapped trial took much longer to thaw as compared with the unwrapped trial, clearly demonstrating the impact of air flow through the pallet on the overall rates of heat transfer.

7.3.3 Trial 3 – Wrapped Loosely Stacked Half Pallet

(a) Freezing (PC – 3)

Figure 7.19 shows the temperature profiles for the external surfaces and at the centres of various blocks. Heat transfer rates through the surfaces were uneven. The Block 8 corner cooled faster compared to the Block 1 corner. From Figure 7.19(b) two clear groups of profiles are evident, consisting of outer and inner blocks showing that heat transfer occurred through the pallet by conduction. Blocks 3 and 4 were the slowest cooling blocks showing that the rate of heat transfer to this corner of the pallet was slowest. There was no difference in the rates of cooling for Blocks 6 & 7 and similarly the rate of cooling in Blocks 1 & 5 was found to be similar. The pallet's inner block temperatures (except Block 2) showed some temperature rebound due to the release of latent heat but the corner blocks showed no significant rebound.

(a)

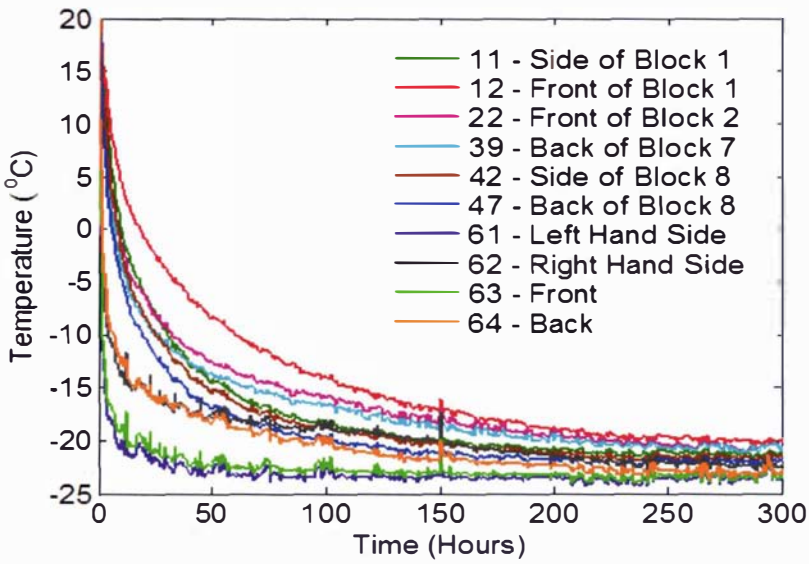

(b)

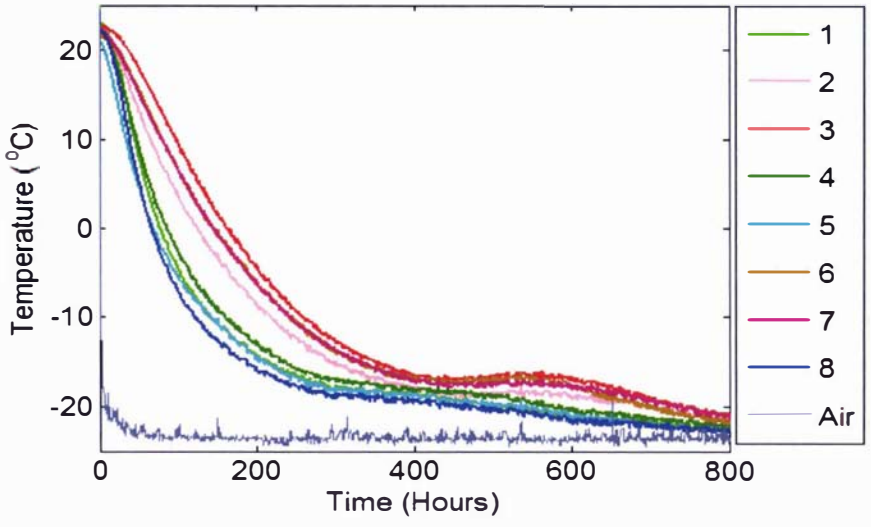

Figure 7.19: Experimental temperature profiles measured for trial PC – 3

(a). Temperature profile at the centre of the faces exposed to ambient

(b). Temperature profile at the centre of each block

Figure 7.20 shows a snapshot of the temperature in the middle layer of the pallet at the surfaces of the butter blocks and in the air channels between the adjacent blocks of butter. There was up to 5.3°C variations in the ambient temperature around the four sides of the pallet. At the front and the right hand side (towards the wall) of the pallet the temperature was higher than at the back and left hand side (towards the door). The difference was due to the direction of the air flowing in the freezer (Figure 7.7). If there was significant air flow between blocks then significant differences between temperatures in the air gaps and the adjacent block surfaces would be expected. Figure 7.20 clearly shows the consistent trend of increasing temperature towards the centre of the pallet and small differences between air gaps and adjacent butter surfaces temperatures. This behavior is consistent with heat transfer by conduction within the pallet, and there is no evidence of internal air circulation within the pallet.

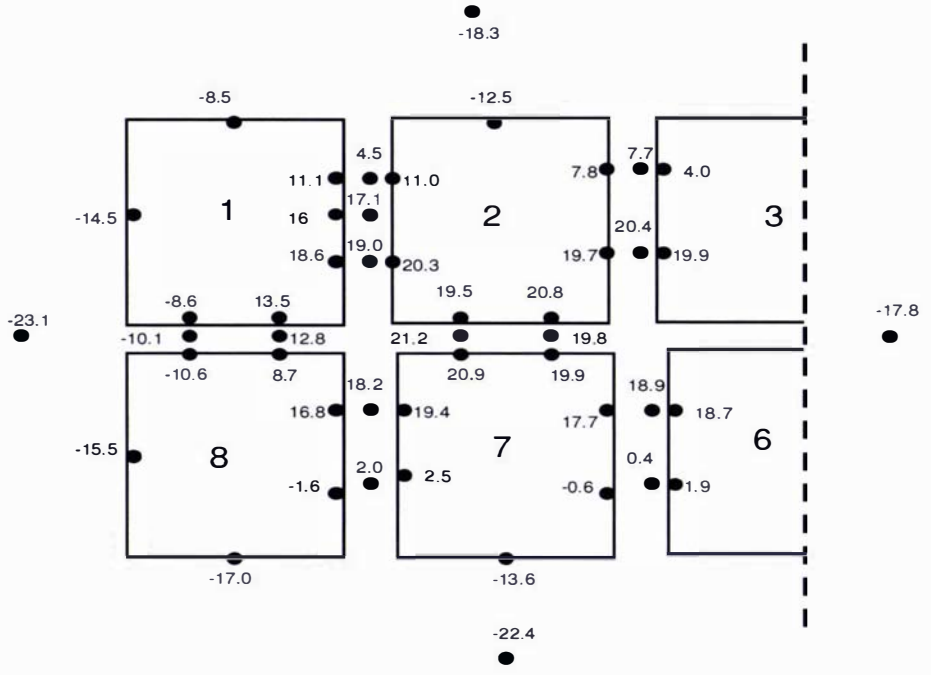

Figure 7.20: Temperature readings (between the blocks and corresponding butter surfaces) after 50 hours in Trial PC – 3

A further comparison of blocks 1and 8 and 2 and 7 was made to see if there was any symmetry through the pallet. Figure 7.21 shows the temperature profile at the internal positions of Blocks 1 and 8. Although the heat transfer through the faces of the pallet was not uniform, there was little temperature difference at positions 10 and 40 and between positions 9 and 41. Similarly Figure 7.21 (b) shows that there were not large differences in the temperature at the positions 18 and 32 but position 19 was found to cool slower than at position 31. Only at position 32 was some rebound in the temperature observed. All other position showed very little or no rebound in the temperature but did flatten out above the ambient temperature indicating slow freezing.

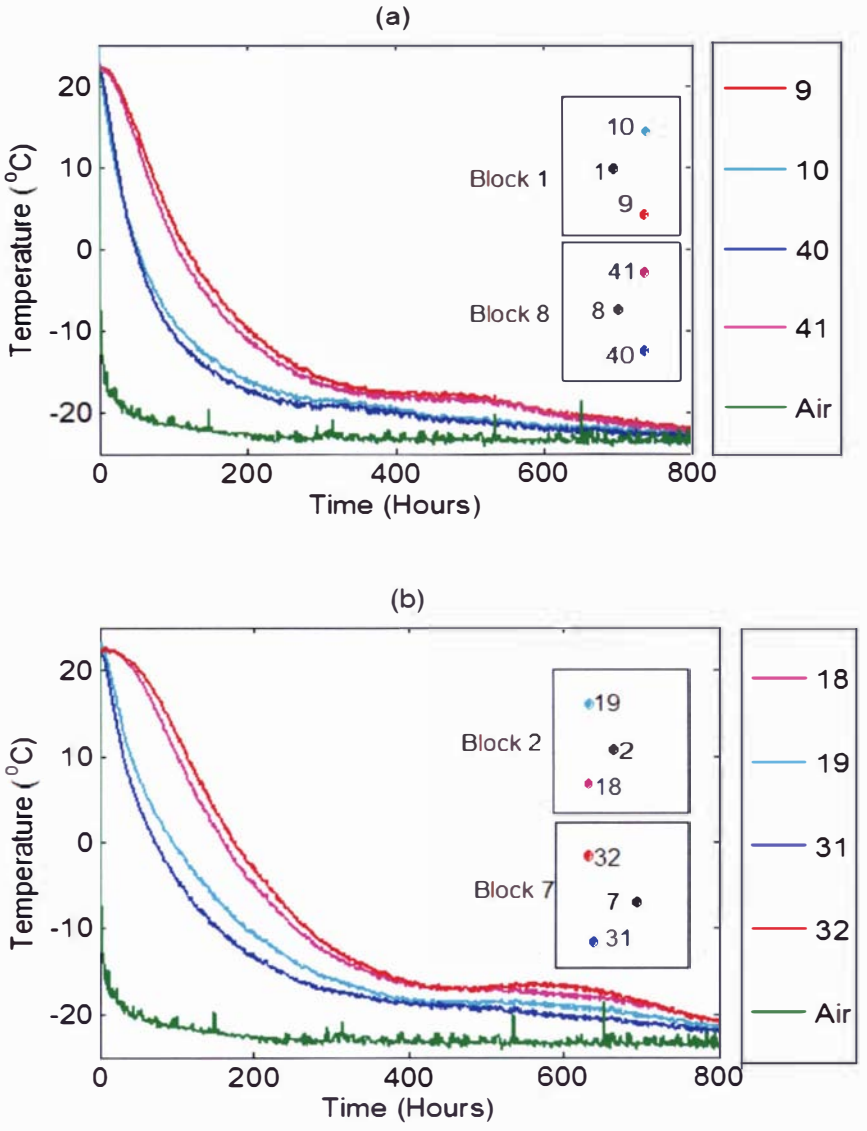

Figure 7.21: Experimental temperature profiles measured for the wrapped loosely stacked half pallet trial (PC – 3)

(a) Comparison of block 1 & 8 (b) Comparison of block 2 & 7

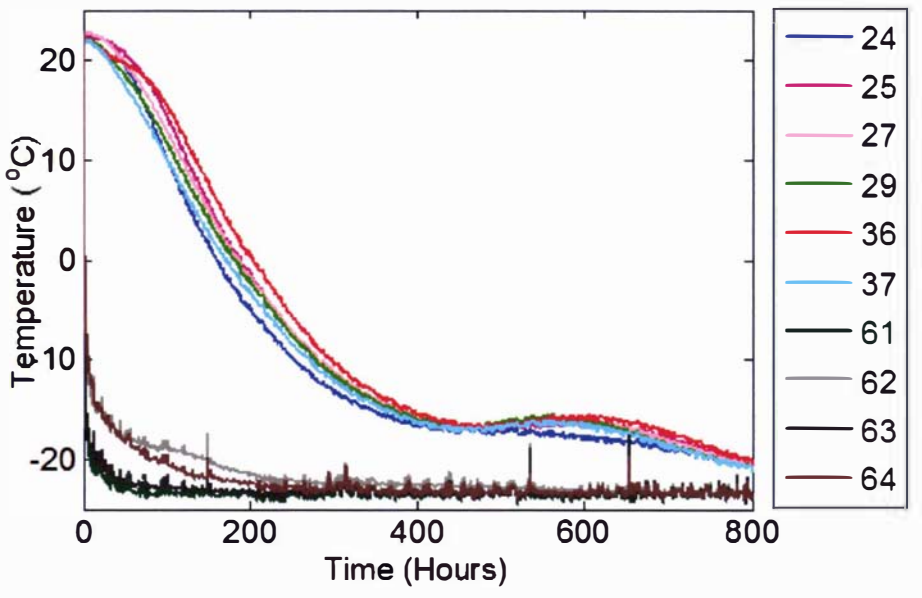

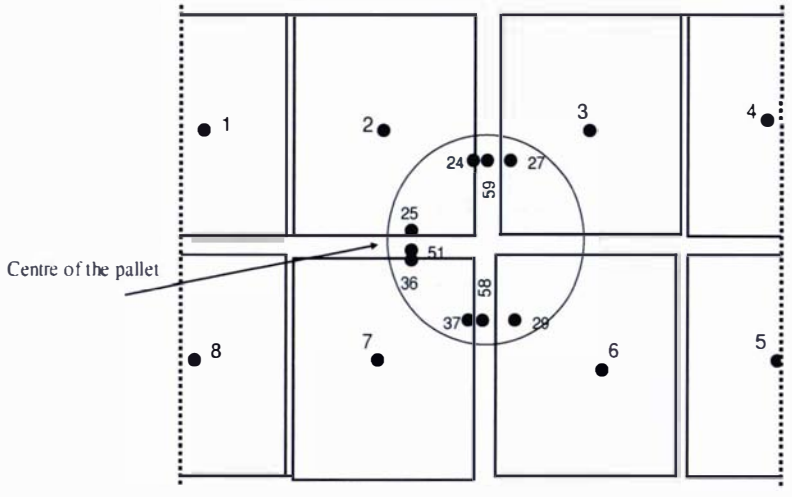

Figure 7.22

Figure 7.22: Experimental temperature profiles measured for the wrapped loosely stacked half pallet trial (PC – 3)

(a): Temperature profiles of the slowest freezing position along with the other positions around the centre of the half pallet.

(b): Schematic diagram of the centre of the pallet.

The slowest cooling point was near the geometric centre of the pallet as shown in Figure 7.22. Position 36 was found to cool the slowest but only slightly slower than the other central positions (27, 29 and 25).

(b) Thawing (PH – 3)

Figure 7-23(a) shows the temperature profiles at the centre of the external faces of Blocks 1, 2 7 and 8. The data is missing for about 41 hours due to a technical problem with the data logger but it is clear that the rate of heat transfer through all the faces was not same. Figure 23(b) gives the temperature profiles at the centres of each block and the ambient temperature around the four sides of the pallet. Blocks 1 and 8 had lower initial temperature than the other blocks. The centres of these blocks heated at different rates. Figure 7.24 shows the temperatures after 50 hours throughout the middle layer of the pallet. The front left hand side heated faster followed by the back of the pallet, then the right hand side. This was due to the placement of the fan heater in front of Blocks 1 and 2 and pedestal fan blowing air around the room. No significant temperature differences were found between air gaps and their adjacent butter surfaces except for between Blocks 1 and 2 where there were large differences near the external face. Overall the air flow within the pallet was insignificant and it appears that the heat transfer is by conduction only.

(a)

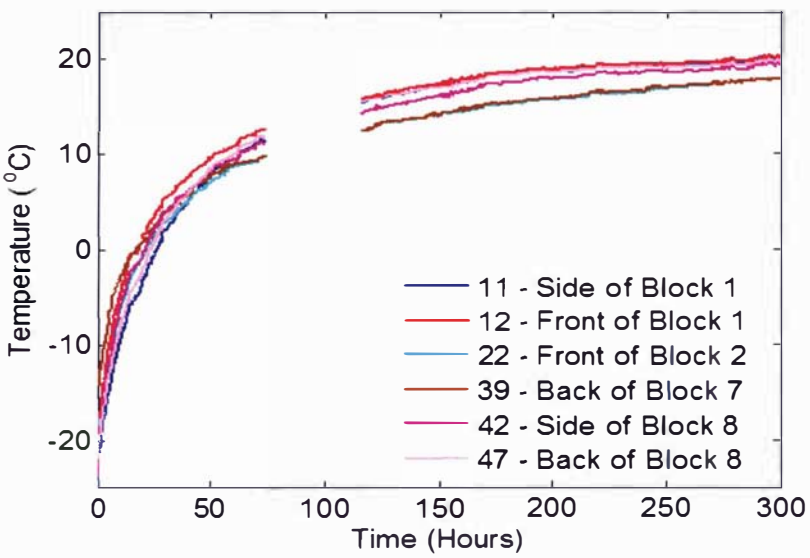

(b)

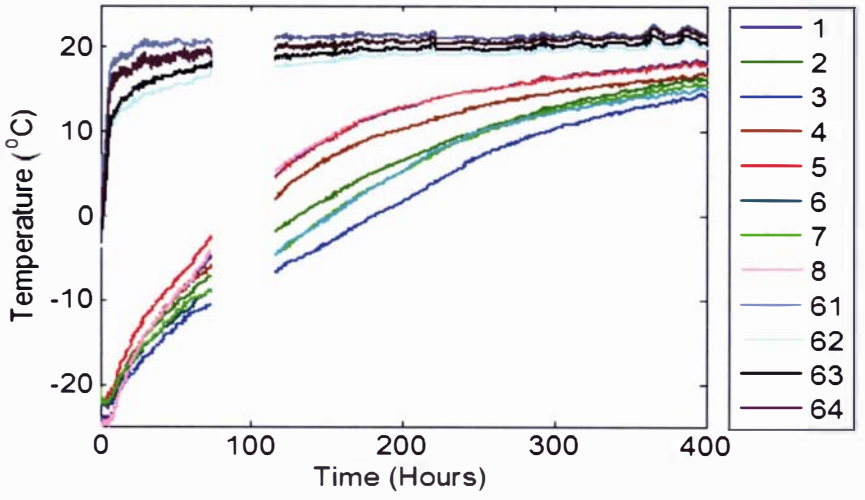

Figure 7.23 Experimental temperature profiles measured for trial PH – 3
(a). Temperature profile at the centre of the faces exposed to ambient
(b). Temperature profile at the centre of each block

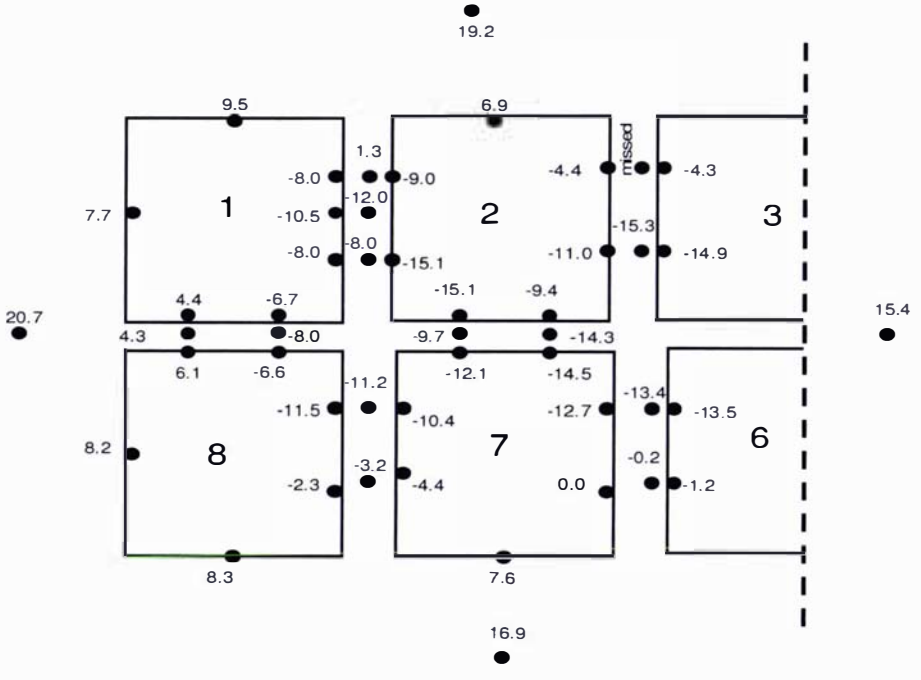

Figure 7.24: Temperature readings (between the blocks and corresponding butter surfaces) after 50 hours in Trial PH – 3

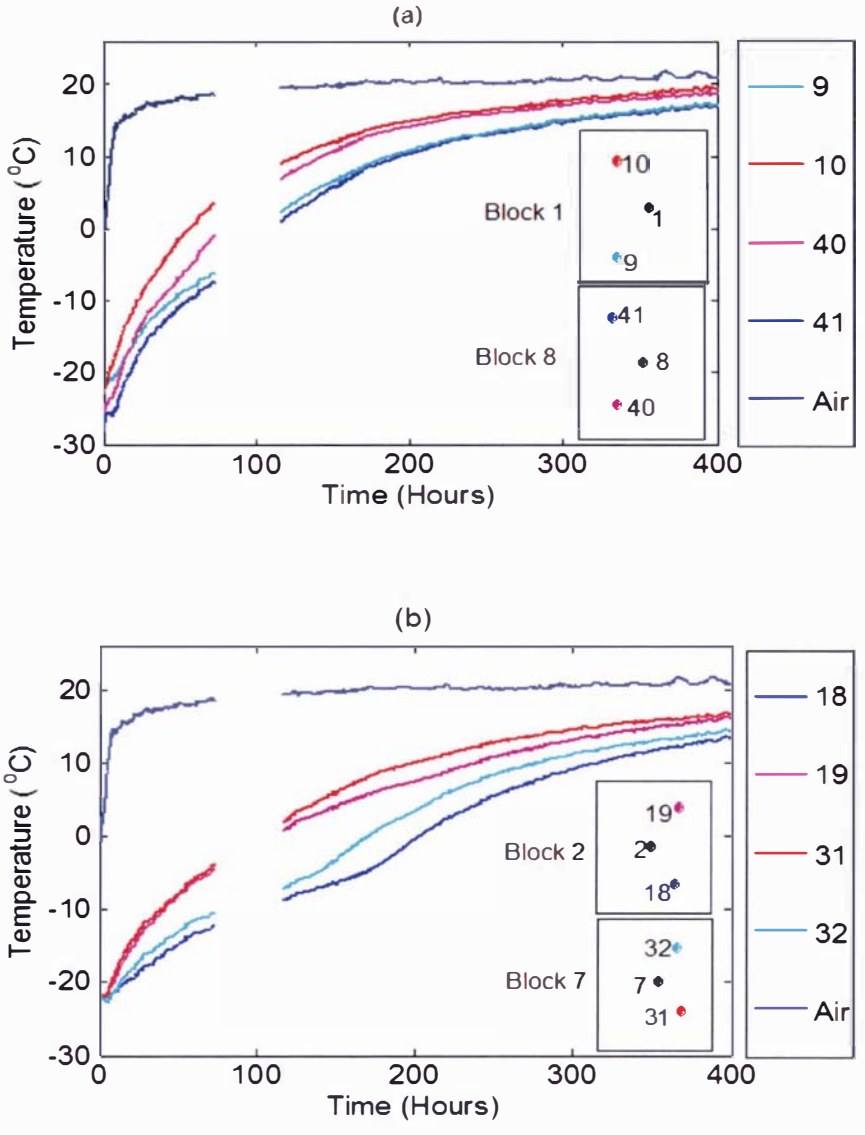

Figure 7.25: Experimental temperature profiles measured for the wrapped loosely stacked half pallet trial (PH – 3)

(a) Comparison of block 1 &8 (b) Comparison of block 2 & 7

A further comparison between Blocks 1 and 8 and between Blocks 2 and 7 is shown in Figure 7.25. These plots confirmed that there was inconsistency in the initial temperatures inside the blocks and therefore frozen water contents in the butter blocks may not be have been the same. Due to uneven heat transfer rates from the external faces, Block 1 heated up slighter quicker than Block 8 and Block 7 heated up quicker than Block 2. Despite these differences the physical centre of the pallets

(positions 36 and 27) was found to be the slowest thawing point in the wrapped loose stacked half pallet trial as shown in Figure 7.26.

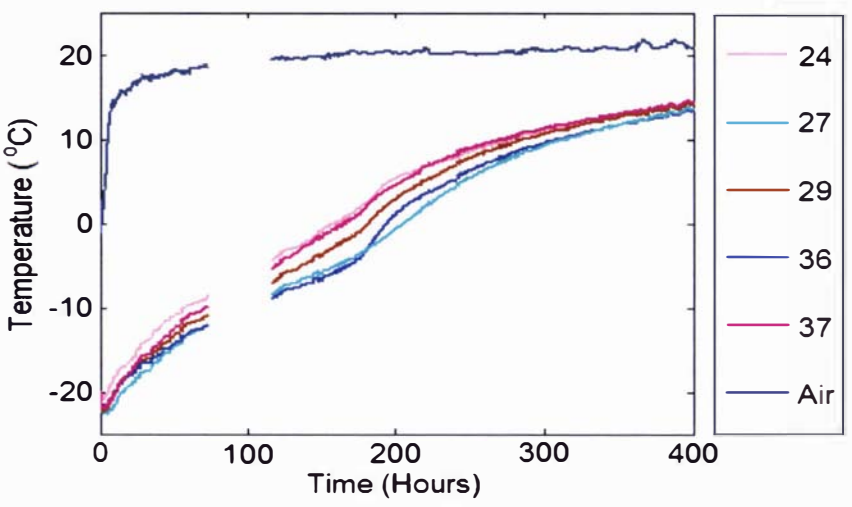

Figure 7.26: Experimental temperature profile measured for the slowest thawing position along with other positions around the centre of the half pallet (PH – 3)

7.3.4 Trial 4 – Unwrapped Tightly Stacked Half Pallet

(a) Freezing (PC – 4)

Figure 7.27(a) shows that the rate of heat transfer across the faces 11 and 42 and 12 and 22 was very uniform. There was also a temperature difference in the ambient conditions. The door side of the pallet and the surface temperatures on that side of Blocks 1 and 8 was found to be higher than the other surfaces showing a very little air flow on that side of the pallet.

Figure 7.27(b) shows the temperature profiles at the centre of each block. Two clear bands of temperatures can be seen. One band consists of the corner blocks 1, 4, 5 and 8 that cooled down quickly compared to the other band consisting of inner blocks 2, 3 and 7. All these positions showed a small rebound in the temperature due to the release of latent heat. The temperature profiles at positions 1 and 4, 2 and 3 and 5 and 8 were quite uniform indicating symmetry across the pallet.

(a)

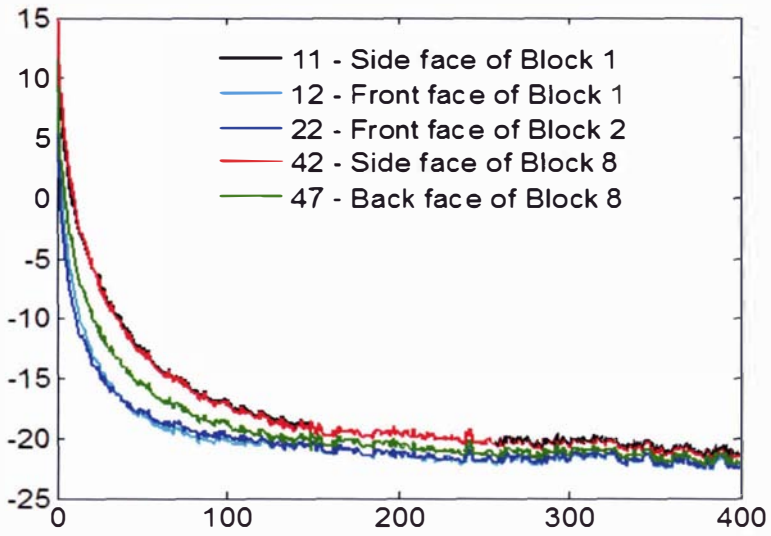

(b)

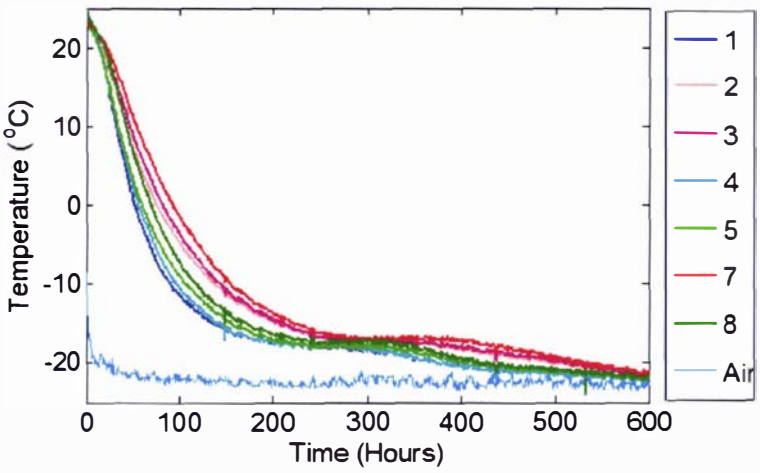

Figure 7.27: Experimental temperature profiles measured for Trial PC – 4

(a). Temperature profile at the centre of each block along with the average ambient temperature on four sides of the half pallet

(b). Temperature profile for the centres of all the blocks

Figure 7.28 shows the temperature at the surfaces and the air gaps between the blocks across the middle layer of the pallet, 50 hours after the start of the experiment. It was quite clear from the temperature readings that there were small temperature gradients between the air gaps and the

surfaces of the blocks near the external faces of the pallet. Since all the blocks were packed quite close so there was a possibility that the thermocouples positioned in between the individual blocks were touching the opposite blocks. The heat transfer through each block appeared to be predominated by conduction from all the faces exposed to ambient. Reasonably large air penetration appears to occur at the outward ends of the air gaps between the Blocks 1 and 2 and between Blocks 1 and 8. Smaller air penetration is evident at the outside ends of the air gaps between Blocks 2 and 3 and between Blocks 6 and 7. No air flow is evident further inside the pallet interior. The directions of the air circulation in between the individual blocks are shown in Figure 7.28. The thermal centre of the pallet seemed to be near the geometric centre of the pallet, indicating that heat transfer is pallet based, where heat transfer occurs primarily by conduction from the outside of the pallet inwards, but with some contribution by convection due to air flow penetration in the outer regions of the pallet only.

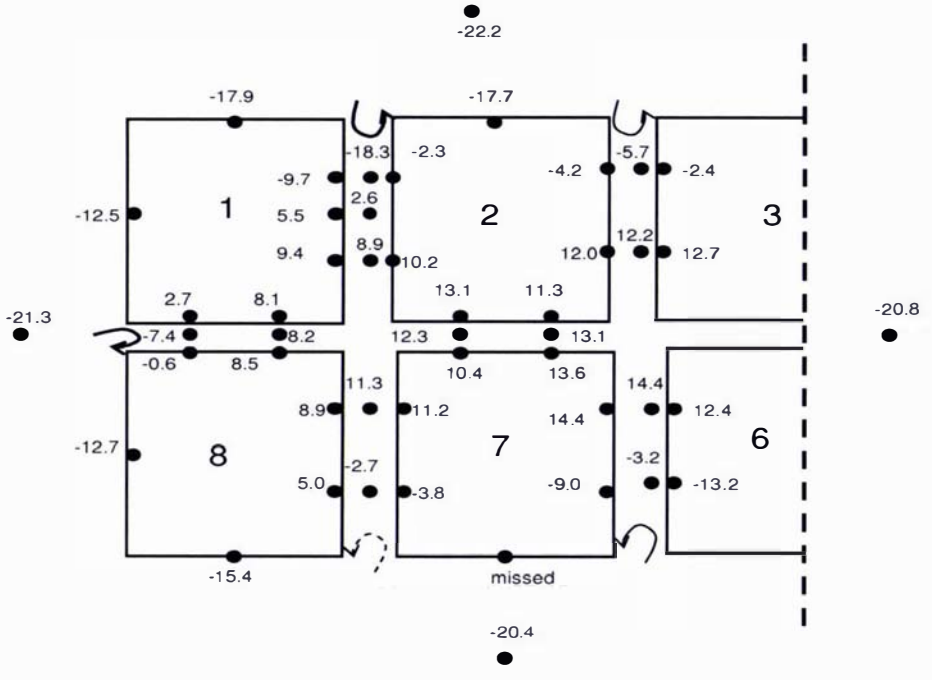

Figure 7.28: Temperature readings (between the blocks and corresponding butter surfaces) after 50 hours for Trial PC – 4

Figure 7.29 shows the comparison between blocks 1, 2, 7 and 8. Figure 7.29(a) shows that the temperature profiles at position 10 and 40 and 9 and 41 are quite different due to the effect of the different ambient temperatures on different sides of the pallet. In Blocks 2 and 7, the outer positions 19 and 31 were affected by the ambient conditions but there was little difference at positions more central to the pallet (18 and 32) as sown in Figure 7.29(b).

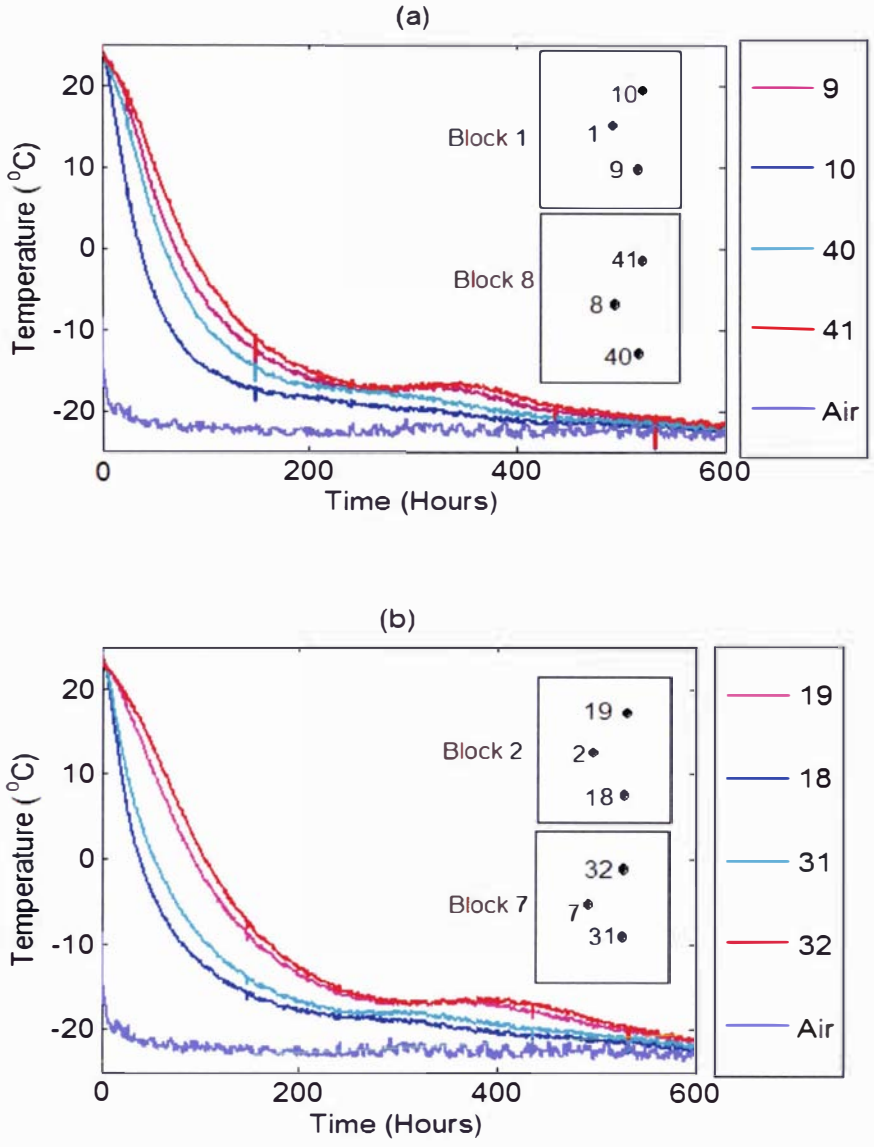

Figure 7.29: Experimental temperature profiles measured for the unwrapped half pallet trial (PC – 4)

(a) Comparison of block 1 and 8 (b) Comparison of block 2 and 7

At the centre of the pallet (Figure 7.30) the temperature at positions 24, 25, 27, 29, 36 and 37 are nearly identical and are the slowest freezing point of the pallet (thermal centre) of the pallet. Overall position 37 was the slowest moving position which also consistent with the rate of heat transfer through the front of the pallet (fan side) being slightly faster than from the back (wall side) of the pallet.

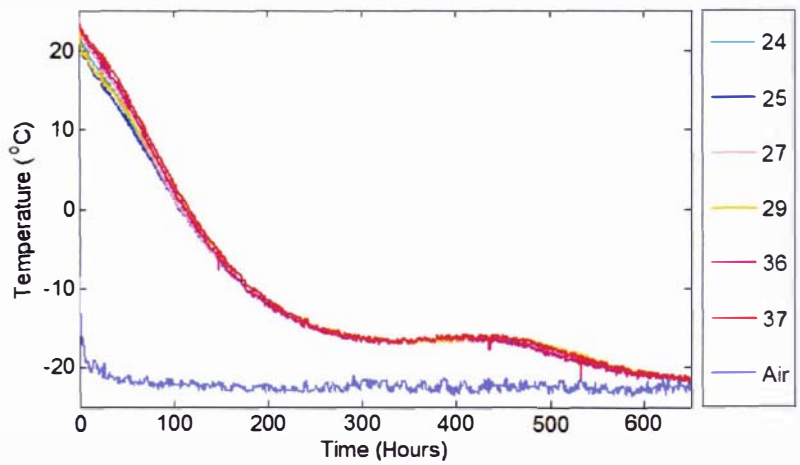

Figure 7.30: Experimental temperature profiles measured for the slowest freezing position along with other positions around the centre of the half pallet (PC – 4)

A comparison of the slowest freezing point between trials PC – 3 and PC – 4 under the same ambient and initial condition showed Trial PC – 3 took about 240 hours longer to reach -22°C. The difference in the temperature rebound due to ice crystallisation was about 190 hours although in both the freezing trials the maximum rebound in temperatures were found to be at about -16°C. It should be noted that the pallet dimensions in Trial PC – 3 were much larger than in Trial PC – 4. It appears that the additional air internal to the pallet acts as additional resistance to heat transfer thereby further slowing heat transfer rates whereas some convection in the air gaps towards the outside of the pallets accelerated the heat rate of heat transfer in Trial PC – 4. The net effect of the convection is a slightly faster overall heat transfer rate for the Trial 4 configuration.

(b) Thawing (PT – 4):

Figure 7.31(a) shows the surface temperatures of the blocks exposed to the ambient. Heat transfer from all the sides were not uniform as was observed in the previous half pallet experiments. Figure 7.31(b) shows the temperature profiles of the centre of all the butter blocks. Overall two clear groups can be seen as were observed in the freezing of this configuration. The temperature profiles

of positions 2 and 7, 4 and 5 and 3 and 6 were similar showing symmetry across the pallet. The pair of positions 2 and 7 heated up slightly faster than the other pair but overall there was little temperatures difference in the four positions. Position 1 heated up faster than position 8 but the difference was less than 5°C and probably due to the slightly lower ambient temperature on the two sides that Block 8 was exposed to.

(a)

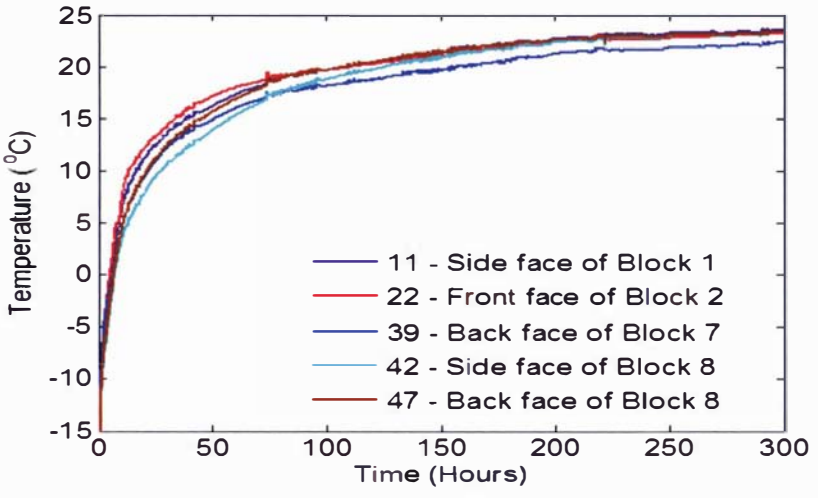

(b)

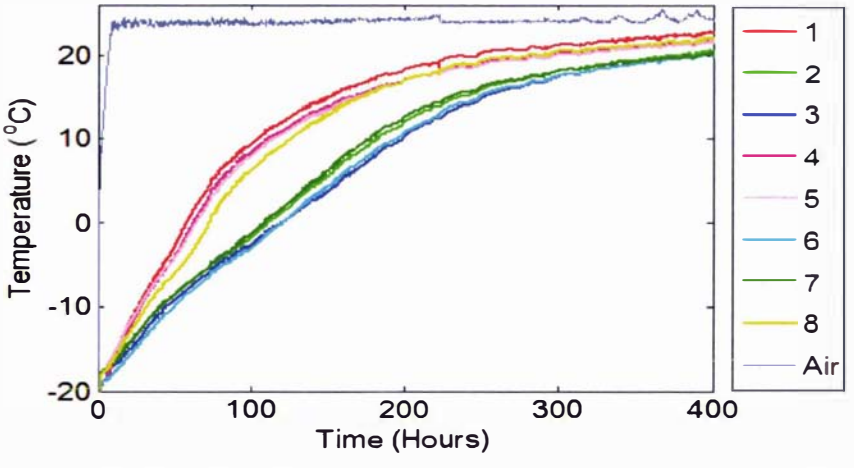

Figure 7.31:Experimental temperature profiles measured for Trial PH - 4

(a): Centre of all the faces exposed to ambient (the position 12 on block 1 is missing)

(b): Centres of all the blocks in the middle layer

Figure 7.32 shows the temperatures of the positions monitored at the surface and in the air channels between the adjacent blocks. The overall trend was nearly the same as was found in the freezing of this pallet.

The ambient temperature at the front and the right hand side (towards the door) of the pallet was higher than the other two sides. The geometric centre of the pallet was found to be the thermal centre of the pallet. Large temperature gradients were found along the channels between the adjacent blocks as for the freezing trial. The temperature at any point in between the carton gap and those of the butter surfaces adjacent to it were virtually the same, consistent with no significant air flow passing through the pallet except for gaps toward the outside of the pallet.

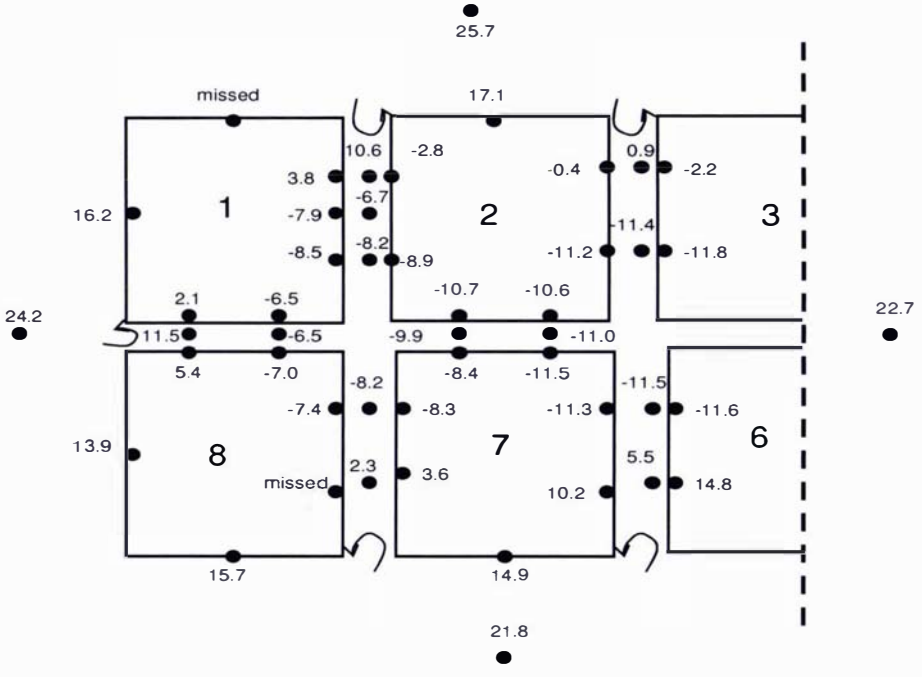

Figure 7.32: Temperature readings (between the blocks and corresponding butter surfaces) after 50 hours for Trial PH – 4

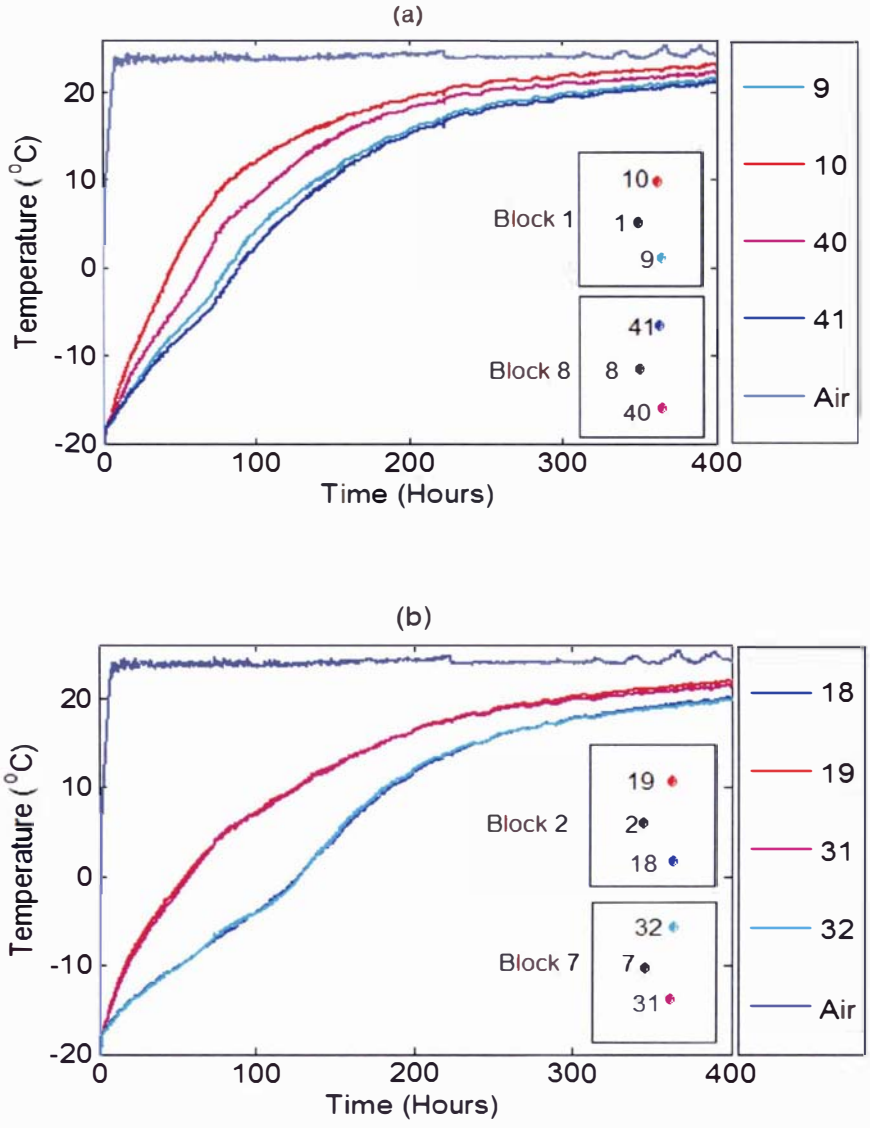

Figure 7.33: Experimental temperature profiles measured for Trial PH - 4
(a) Comparison of Blocks 1 & 8 (b) Comparison of Blocks 2 & 7

Figure 7.33 (a) & (b) compares the heating of Blocks 1 and 8 and Blocks 2 and 7 respectively. Since the heat transfer through around the pallet was not uniform, the rates of heating of Blocks 1 and 8 were different. Although the heat transfer to the faces exposed to ambient for Blocks 2 and 7 was found to be up to 1°C different this did not cause differences in the temperatures at positions the same distances from the surface in Blocks 2 and 7 as shown in Figure 7.33(b)

The slowest thawing points were found to be at position 27 and 36 which were around the centre of the half pallet as observed in the freezing experiment for of this trial (PC – 4).

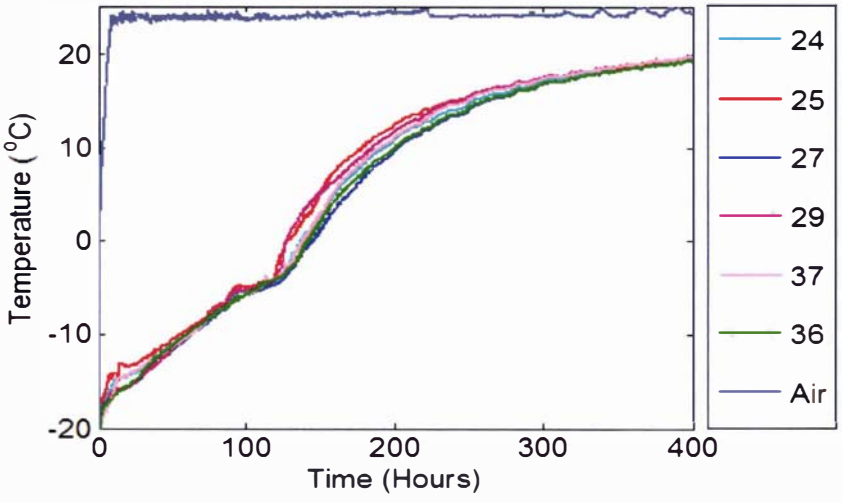

Figure 7.34: Experimental temperature profiles measured for the slowest thawing position along with the other position around the centre of the half pallet Trial PH – 4.

A comparison of trials PH – 3 and PH – 4 for the slowest thawing point showed that trial PH – 3 took more than 300 hours to reach 10°C from -20°C as compared to 180 hours taken by PH – 4 with less than 3°C difference in ambient temperatures.

Overall, in Trial 3 heat transfer was through conduction only whereas in Trial 4 it was dominated by conduction but some convection on the outer regions of the pallet was also evident.

7.3.5 Trial 5 - Unwrapped Loose Stacked Half Pallet

(a) Freezing (PC – 5a)

Figure 7.35 gives the temperature profiles for the centre of all the blocks during cooling of the pallet. The centre of Block 7, supercooled very quickly and the temperature stayed higher than the ambient for a long period of time suggesting slow freezing but no significant rebound in the temperature was observed. The centre of the blocks 3 and 4 cooled down together and were the slowest as anticipated by the directions of air flows around the pallet (Figure 7.7). The release of latent heat in block 3 was observed earlier than that observed in block 4. The central positions of

blocks 1, 2, 5, 6, and 8 cooled down almost together but the rebound in the temperature occurred at different times. The differences in crystallisation times (where rebound occurs) could be due to the stochastic nature of the crystallisation process as found in the individual block trials or due to different rates of heat transfer removing the latent heat within the blocks.

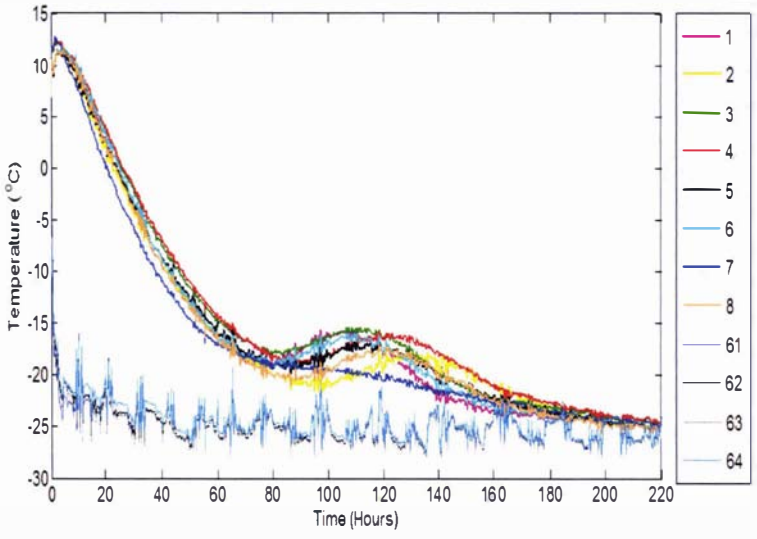

Figure 7.35: Experimental temperature profiles measured for the half pallet loosely stacked trial PC – 5 at the centre of all the blocks along with the ambient temperature on four sides of the half

Figure 7.36 shows the temperature profile for the all surfaces of blocks 1, 2, 7 and 8. The more internal surfaces cooled slower than the others. The heat transfer through the surfaces into blocks was quite uniform although there are a few points where regions are cooling very slowly (e.g. 21). This was probably due to two blocks bulging together and the thermocouple position not directly interacting with the air. Also there are points where heat transfer was found to be quite rapid (e.g. 17).

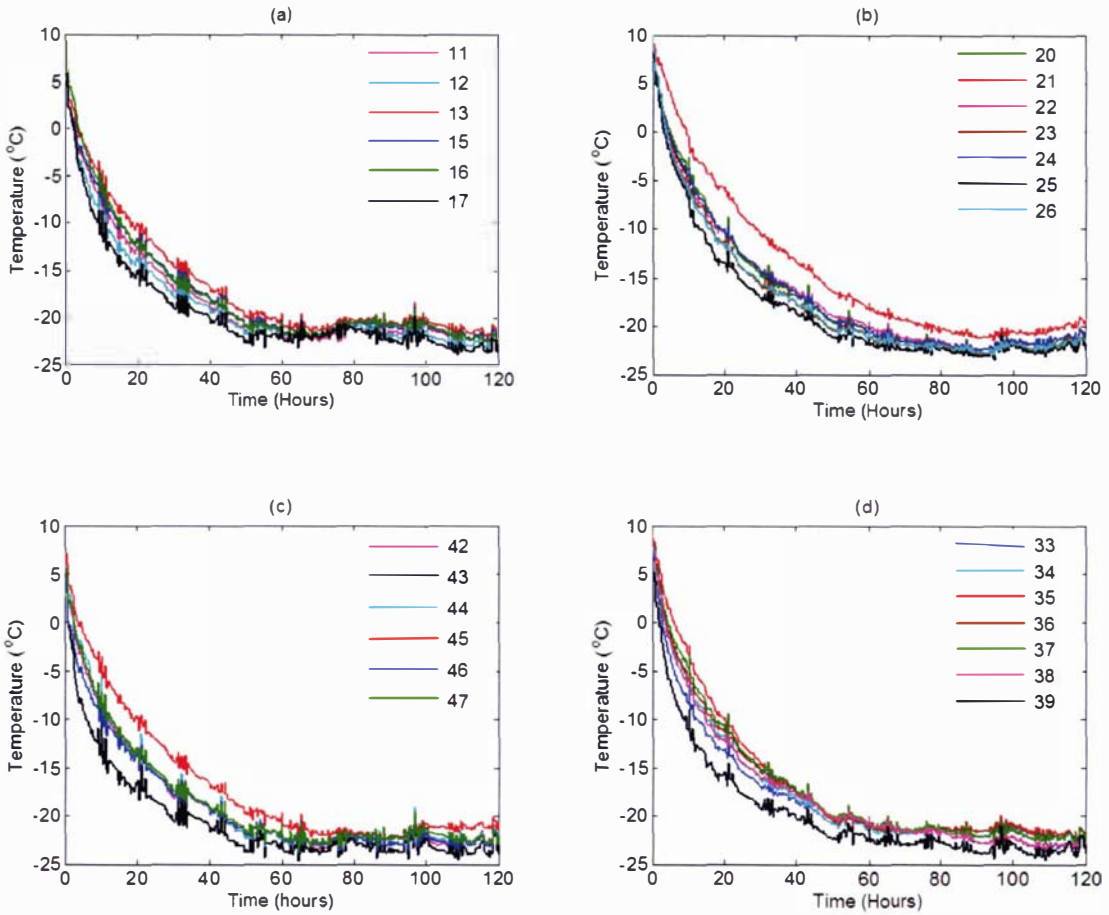

Figure 7.36: Experimental temperature profile measured for the positions at the surfaces of the blocks (PC – 5a)
(a) Block 1 (b) Block 2 (c) Block 8 (d) Block 7

Figure 7.37gives the temperature profiles for the middle layer of the trial, 50 hours after starting the experiment. All the recorded temperatures (position 60 was not recorded due to the thermocouple malfunction) in the air spaces between cartons were much lower than the adjacent carton surfaces, even in the centre of the pallet. This can only be due to significant air flow occurring through the pallet. By following the temperature changes with position through the flow channels it was possible to estimate the directions of air flow through the pallet. These are included in Figure 7.5 as arrows which trace the steady increase in air temperature as it flows through the pallet and is heated by the cartons. A simple heat balance (see Appendix A5.4) for the air flows in the channels between Blocks 1 and 2, Blocks 1 and 8 and Blocks 7 & 8 gave estimation of the velocities of air as 0.5 ms^{-1}, 0.18 ms^{-1} and 0.23 ms^{-1} respectively.

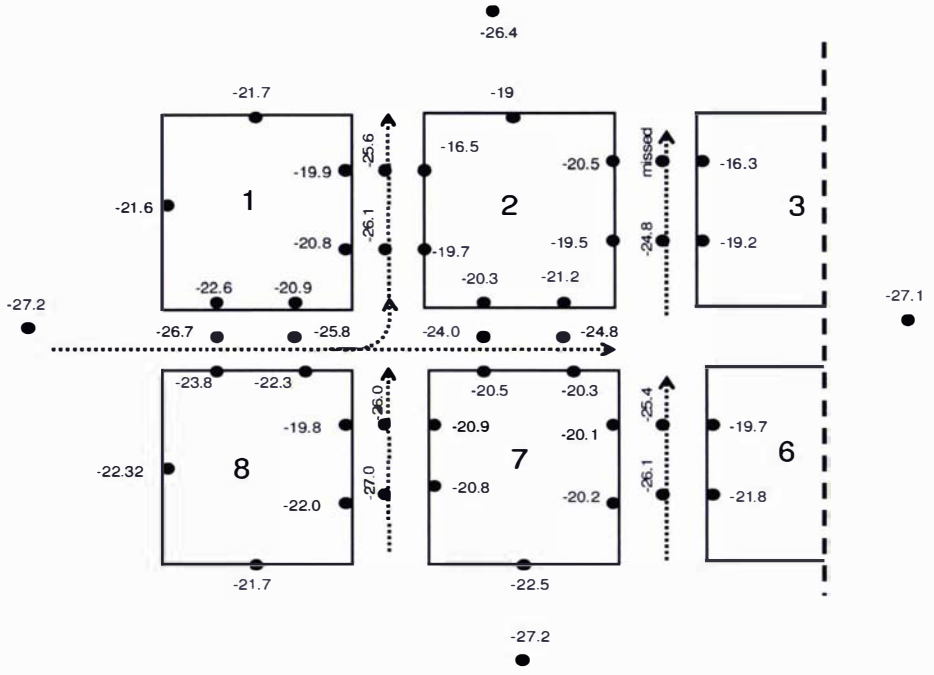

Figure 7.37: Temperature readings (between the blocks and corresponding butter surfaces) after50 hour for Trial PC – 5a

Figure 7.38 gives the temperature profile within blocks 1, 2, 7 and 8 along with the average ambient temperature. There is more conduction occurring from the sides of the blocks exposed to ambient. This resulted in position 10 and 40 cooling more quickly than positions 9 and 41 respectively.

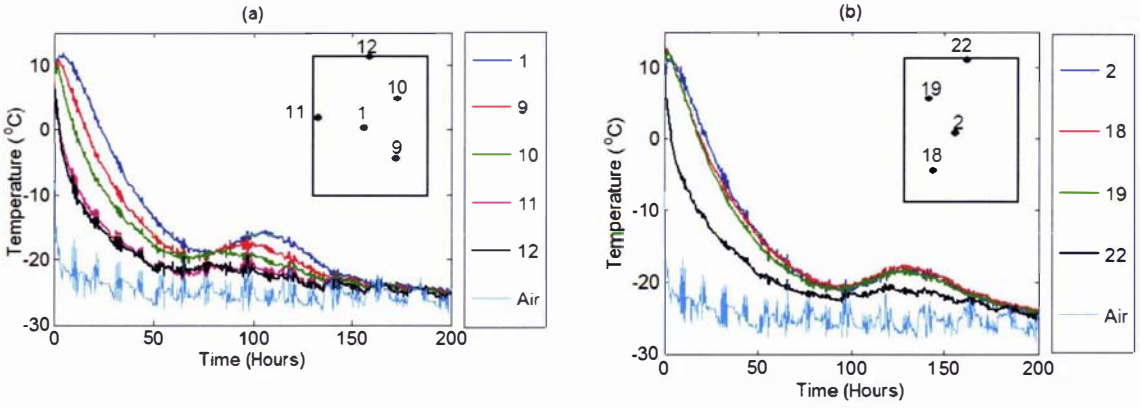

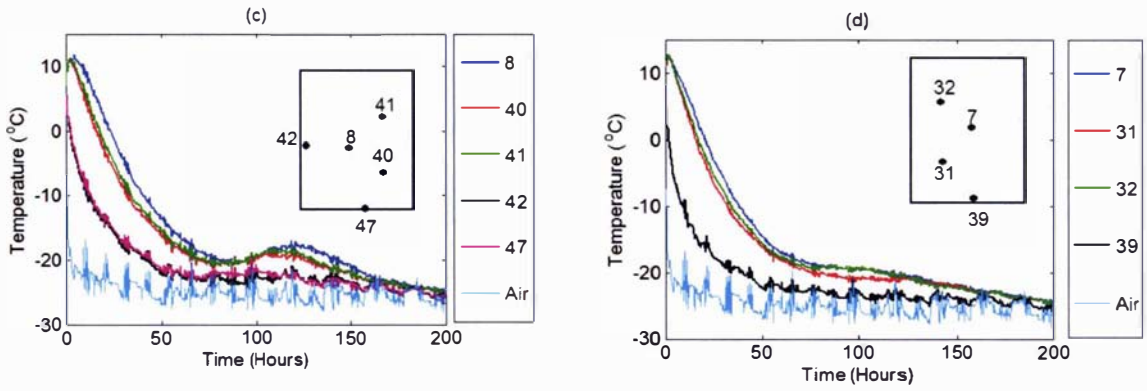

Figure 7.38: Experimental temperature profile measured for trial PC – 5a at the positions inside the blocks along with the average ambient temperature. (a) Block 1 (b) Block 2 (c) Block 8 (d) Block 7

The central temperatures of the corner blocks (1, 8 and 5) were almost the same until the nucleation event started. The centre of block 4 was cooled slightly slower than the others. Similarly there was little difference in the central temperatures of the four inner blocks before the start of the nucleation process. Moreover the maximum time difference in the rebound position for the centre of the blocks was smaller (about 10 hours) than that observed in the single block trials (UBC-1 and UBC-2 about 20 hours) in Chapter 4 performed under the uniform initial and ambient conditions.

Overall there were no real evidence to support the difference in rebound position and magnitude being a result of differences in heat transfer rates between the cartons. Therefore most likely the difference in rebound time was due to the stochastic nature of the crystallisation process.

Overall heat transfer into each carton was much more independent of other blocks, due to the different local air gap temperatures (due to the direction of the air flow through the pallet) around each block of butter. Because of the air flows through the pallet, the temperature distribution within block is not uniform and the centre is not necessarily the slowest cooling point.

(b) Thawing (PH – 5)

Figure 7.39 shows the temperature profile at the centres of all the butter cartons together with the ambient temperatures. As observed in the freezing trial (PC – 5) the blocks thawed in response to the air flow through the pallet rather than as a bulk mass of product. Block 3 was the slowest thawing block and block 5 was the fastest which was consistent with the overall airflow from the

back of the room and through the pallet. The temperatures at positions 1 and 8 and positions 2 and 4 were nearly identical showing symmetry across the pallet.

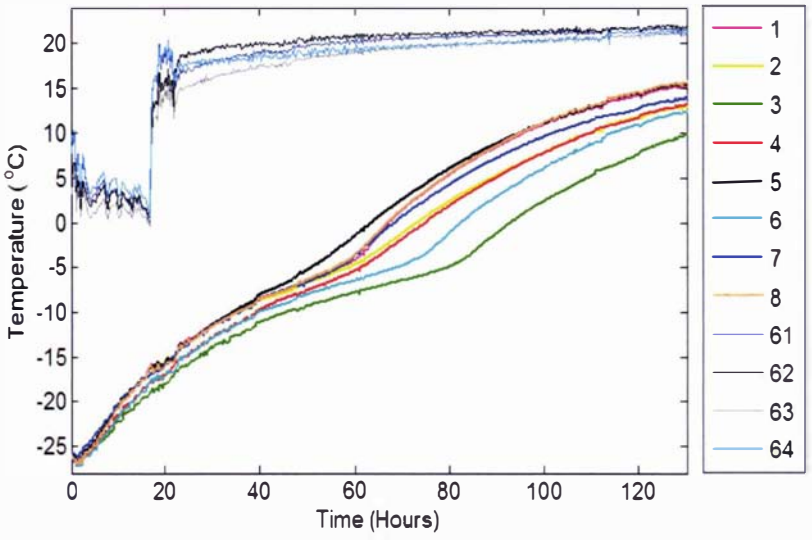

Figure 7.39: Experimental temperature profiles measured at the centre of each block along with the ambient temperature on four sides of the half pallet (PH – 5)

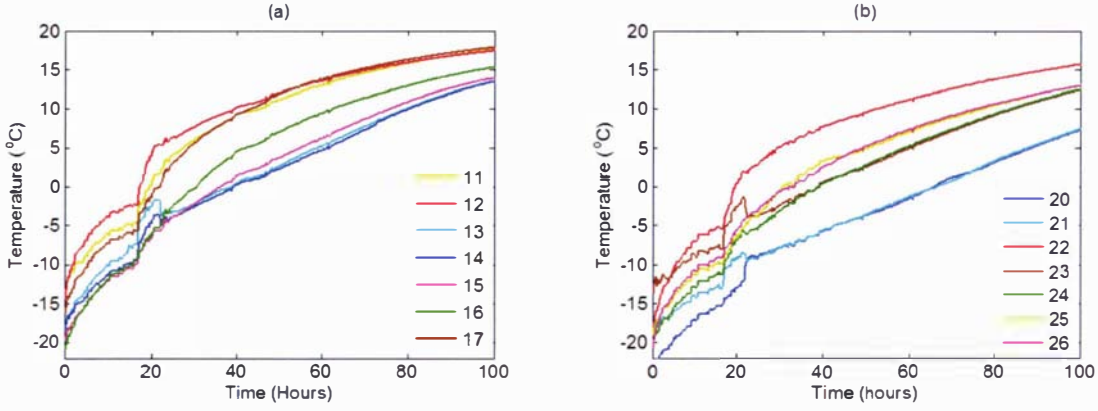

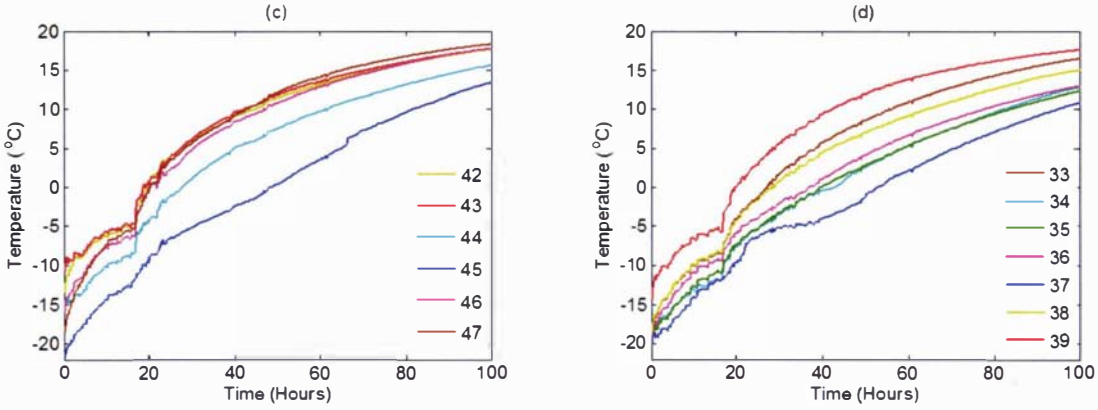

Figure 7.40: Experimental temperature profiles measured for trial PH – 5 at the surfaces of the blocks
(a) Block (b) Block 2 (c) Block 8 (d) Block 7

Figure 7.40 shows the temperature profile of all the surfaces temperatures in block 1, 2, 7, and 8. Large differences in the surface temperatures can be seen which confirm the uneven heating of the blocks. Surfaces more internal to the pallet heated the most slowly.

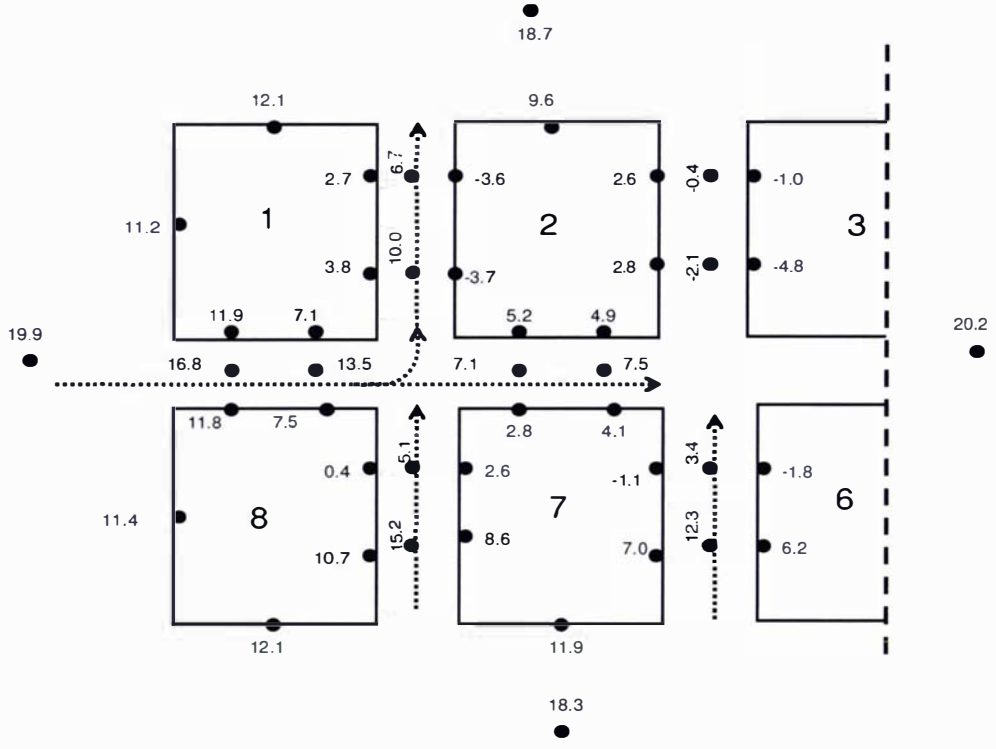

Figure 7.41: Temperature readings (between the blocks and corresponding butter surfaces) after 50 hours for Trial PH – 5

Figure 7.41 shows the temperatures throughout the middle layer of the pallet (PH – 5), 50 hours after the start of the experiment. As for freezing the air temperatures within the pallet were consistently higher than the temperature of the adjacent butter surfaces suggesting there was significant air flow in the gaps between cartons. The arrows show the direction of the air flowing through the pallet inferred from the direction of temperature decrease of the air as it travels through the pallet. Most of the air flowed through the gap between block 1 and 8. Some of the air flowed straight through the gap between cartons 2 and 7, and some flowed between cartons 1 and 2. A flow of air between cartons 7 and 8 and cartons 6 and 7 was also evident, although this was reduced because bulging of the cartons partially blocked the passage of air through this region of the pallet. There was no evidence of air flow through the gap between cartons 2 and 3 as the air temperature was intermediate between the temperatures of the butter surfaces on either side of the gap. The velocities between Blocks 1 and 2, Blocks 1 and 8 and Blocks 7 and 8 were found to be 0.058 ms^{-1}, 0.06 ms^{-1} and 0.016 ms^{-1} respectively using a simple energy balance of the air flowing in the gaps (see Appendix A5.4).

Figure 7.42 shows the temperature profile of cartons 1, 2, 7 and 8. The rate of heat transfer from external surfaces was faster than internal block surfaces due to the extra resistance related to air flow from the outside to the inside of the pallet.

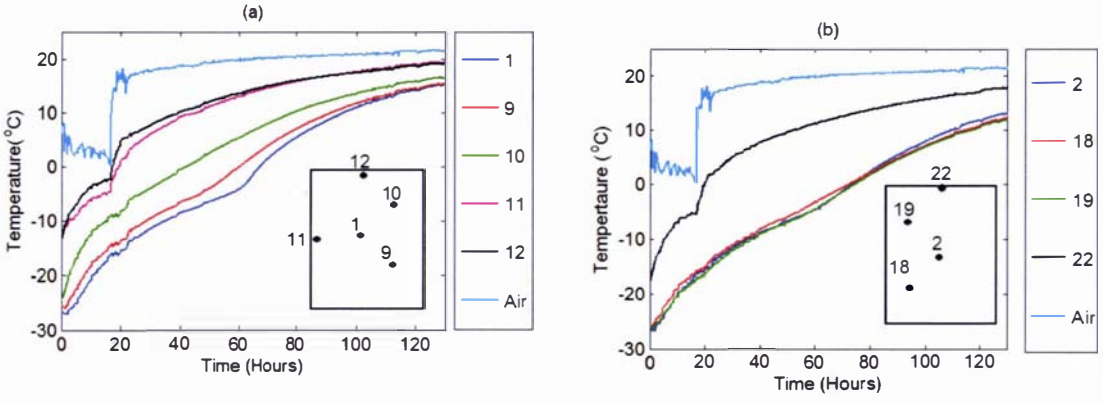

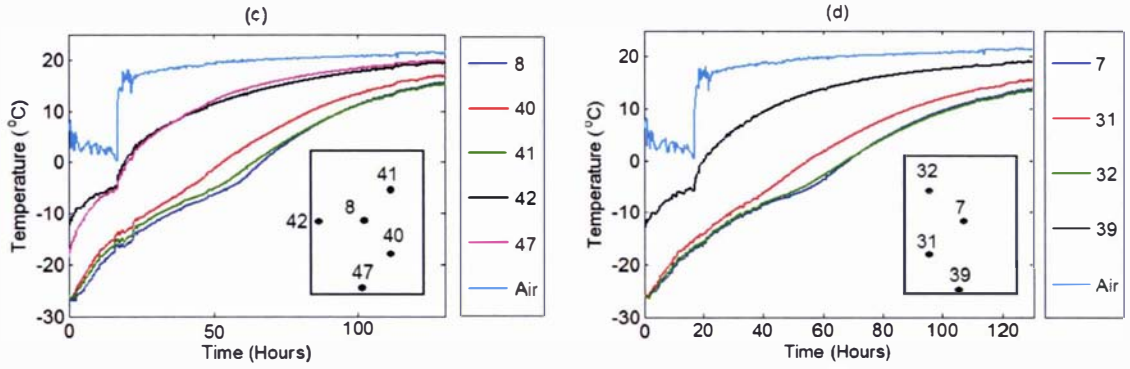

Figure 7.42: Experimental temperature profiles measured for trial PC – 5 inside the blocks along with the average ambient temperature.
(a) Block 1 (b) Block 2 (c) Block 8 (d) Block 7

It is clear from trials PC -5a and PH - 5 that airflow in unwrapped pallets can be very important to the overall heat transfer rates during freezing and thawing. Modelling the pallet thawing behaviour must consider this phenomenon where air flow results in more individual block heat transfer behaviour, but the rates of heat transfer over each surface depends on the position of the block within the pallet.

The freezing run was repeated after the end of the thawing run (PC – 5b). Although the gaps in between the blocks were partially filled due to the bulging of the blocks resulting from repeated heating and cooling of the pallet similar trends were observed as in the freezing of Trial 1 (PC – 5a). A comparison of the slowest freezing point (position 3) in both the runs is given in Figure 7.43. PC - 5a had a higher initial temperature and the freezing rebound occurred about 50 hours later than for PC – 5b.

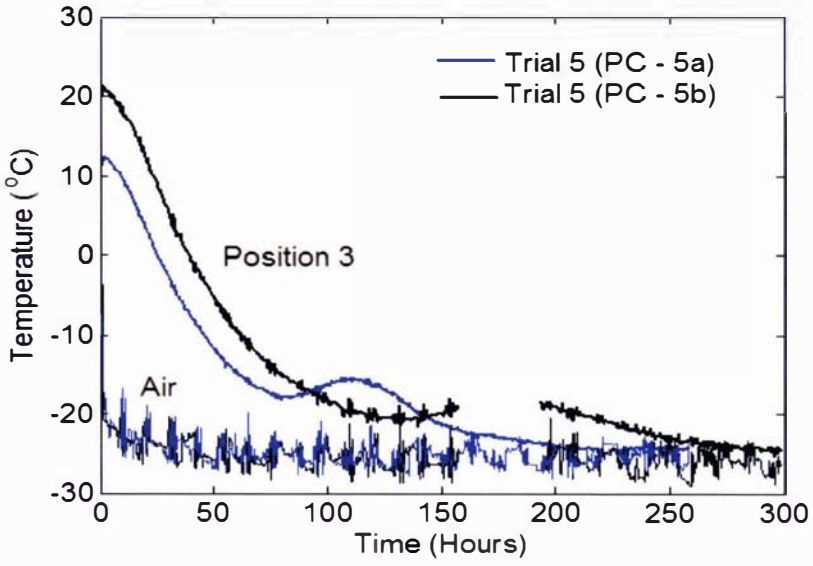

Figure 7.43: Comparison of the slowest freezing point for both the freezing runs of Trial 5 (PC – 5a and PC – 5b)

7.4 Conclusions

Figures 7.44(a) and (b) give a graphical summary of all the half pallet trials for freezing and thawing respectively. It can be seen that the unwrapped loosely stacked pallet (PC – 5, PH – 5) gave the fastest rate of freezing and thawing. The unwrapped tightly stacked half pallet (PC – 4, PH – 4) scenario was the second fastest and the wrapped loosely stacked half pallet trial (PC – 3, PH – 3) was the slowest. Similar observations were found on the full pallet scale pallet trials (Trials 1and 2) in industrial cool store facilities.

In unwrapped pallets, there is potential for significant air flow to occur through the pallet, thereby increasing heat transfer rates due to convective heat transfer by the air movement. This results in a more block based heating or cooling behaviour (thermal centre towards the centre of the block rather than the centre of the pallet). If the air gaps are reduced, this can effectively make air flows through the pallet insignificant thereby moving thawing /freezing behaviour back to a pallet based heat transfer behaviour where heat transfer is dominated by conduction and convective heat transfer due to air flow through the pallet is minor(centre of the pallet is the thermal centre). By wrapping the pallet, air flow can be effectively blocked but it was clear that amount of trapped air inside the pallet significant altered the heat transfer rate. In tightly packed unwrapped pallets an intermediate behavior can result where heat transfer in the inner regions of the pallet is by conduction only but

some air penetration can occur in the outer regions of the pallet. Prediction of heat transfer in a bulk pallet situation must consider all these factors.

(a)

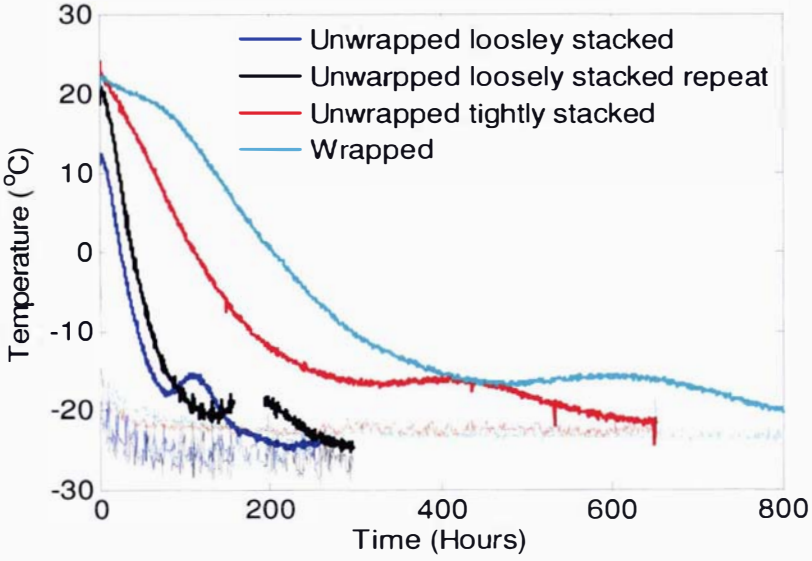

(b)

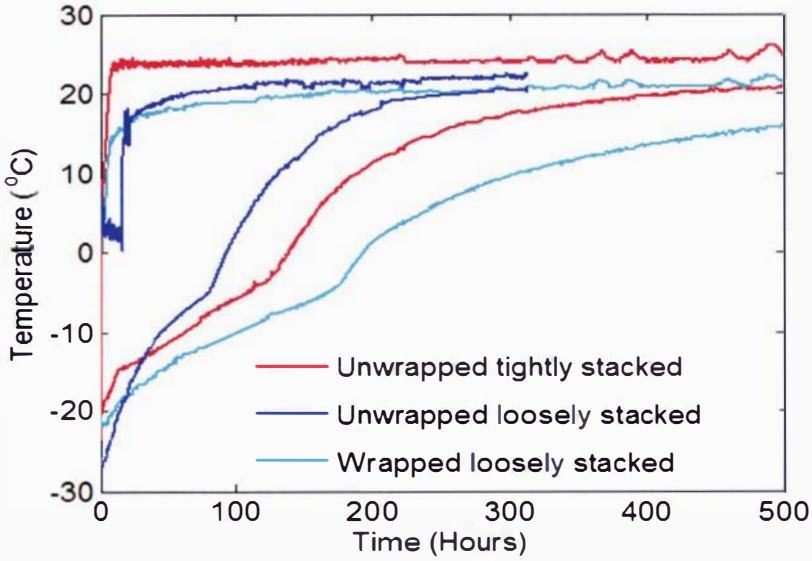

Figure 7.44: Comparison of slowest changing positions in the half pallet Trials 3-5 (a) Freezing (b) Thawing

CHAPTER 8

MODELING HEAT TRANSFER IN PALLETISED BUTTER

8.1 Introduction

This chapter evaluates simple approaches to adapt the thawing/freezing models for individual butter blocks developed in Chapters 5 & 6 to a stacked pallet scenario. A pallet of butter is a combination of butter, two types of packaging and air. There are many approaches to model freezing and thawing in such a system. Computational Fluid Dynamics (CFD) packages allow the actual convective and conductive heat transfer in the heterogeneous system to be approximated. However this kind of approach is not suitable for industrial use due to the requirement for a large amount of system input data and the need for expert personnel to operate the packages. Therefore, a simpler modeling approach is needed that can use system input data that is easily measurable in industrial situations e.g. pallet and carton dimensions, manufacturing details and ambient storage conditions etc.

Chapter 7 summarised the experimental data collected for the freezing and thawing of half and full pallets of butter. The heat transfer in a wrapped pallet behaved like a homogenous block of butter with the thermal centre being in the geometrical centre of the pallet and no convective heat flow within the pallet. This is because the plastic wrap around the pallet prevented air flow through the gaps between the butter blocks. In trials on an unwrapped, closely-stacked, pallet, the heat transfer rate was faster than would be expected from conduction only, despite there being no evidence of air flow through the pallet. In trials on an unwrapped loosely stacked pallet, the heat transfer rate was only slightly slower than for a single block of butter, due to a large amount of air flowing through the pallet between the blocks.

Analysis of the wrapped and unwrapped pallet trials showed that different modeling approaches were likely to be necessary to predict the thawing/freezing behaviour in the different scenarios depending on the amount of air flow within the pallet. At one extreme, with low internal air flows, the heat transfer within the pallet probably needed be modeled as conduction only within a

homogenous pallet-sized butter block with effective thermal properties set dependent on the amount of packaging and entrapped air. At other extreme, with high internal air flows, the pallet probably needed to be modeled as individual cartons with uneven heat transfer on each face, depending on the position in the pallet and the amount of air flow on each face.

In this chapter these different modeling approaches are assessed using the experimental data collected the Chapter 7.

8.2 Modeling Approaches

It is clear from the experimental data that two key factors influencing the palletized thawing/freezing behaviour are:

- The extent of air flow within the pallet.
- The amount of trapped air, and packaging within the bulk pallet.

Two broad approaches were used to model the heat transfer.

Changing from a fully wrapped pallet to one without wrapping which is loosely stacked gives internal airflow which shifts the heat transfer behaviour from one for which the thermal centre of the pallet is the geometric centre of the pallet to one for which the thermal centre is somewhere in the butter block that is slowest to change temperature. This suggests that the geometry to be modeled in this case should be an individual block with the rate of heat transfer on each face being different based on the extent of air flow through the different pathways in the pallet. This approach was applied for the following scenarios: the loosely stacked half pallet trials (PH – 5, PC – 5); and the unwrapped full pallet trials (PH – 2, PC – 2) as outlined in Chapter 7.

In the scenarios with trapped air/packaging within the pallet and little internal air flow,(conduction dominant) trapped air/packaging increases the dimensions of the pallet and also produces additional resistance to heat transfer within the pallet. The orientation of the air/packaging is either in parallel to or in series with the direction of the heat transfer depending on the location within the pallet. A simple approach is to model the whole pallet as one block with effective thermal properties dependent on the amount and distribution of air and packaging in the pallet. This approach is applicable to the wrapped full pallet trials (PH – 1, PC – 1), the wrapped loosely stacked half pallet trials (PH – 3, PC – 3) and the unwrapped tightly stacked half pallet trials (PH – 4, PC – 4) outlined in Chapter 7. In each case, the temperature predictions for either a corner block (1 or 8) and an

inner block (2 or 7) or the slowest heating/cooling position were compared with the experimental data.

8.2.1 Modeling Heat Transfer in Pallets With No Internal Airflow

The simplest approach to model heat transfer in pallets with no internal airflow is to assume it to be a homogenous block with effective thermal properties using the conduction-only model using equilibrium properties for predicting thawing (Equation 5-2 to 5-10) and the conduction-only model with the crystallization model for predicting freezing (Equation 6.1- 6.3), that were developed in Chapters 5 and 6 respectively. This modeling approach combines the heat transfer resistances of the air, two types of packaging (cardboard and plastic liner) and the butter based on their respective volume and mass fractions to provide effective thermal properties. The thermophysical properties of the butter, air and packaging components are summarized in Table 8.1.

Table 8.1: Pallet component thermal properties

Component	λ (WmK^{-1})	ρ ($kg\ m^{-3}$)	c ($kJ\ kg^{-1}\ K$)
Salted Butter	$\lambda_f = 0.28$	970	$c_f = 1.7$
	$\lambda_u = 0.20$		$c_u = 3.1$
Lactic Unsalted Butter	$\lambda_f = 0.29$	970	$c_f = 1.8$
	$\lambda_u = 0.22$		$c_u = 3.2$
Corrugated Carton[1]	0.061	200	1.340
Polyethylene Liner[1]	0.290	897	2.303
Air[2]	0.024	1.2	1.005

[1] ASHRAE , [2] Miles *et al.* (1993)

8.2.1.1 Calculation of the Volume of Air Gaps

The volume and masses of the whole pallet, the butter and the packaging were measured. The volume fraction of air was calculated from their difference between the values for the whole pallet and the sum of the values for the butter and packaging. The air in the outer layer of the packaging on all external faces was not included but instead included as a heat transfer resistance in the effective heat transfer coefficient. Table 8.2 gives the volume and mass fractions of all the components estimated in this way for the half and full butter pallet experiments. The volume fraction of air in the wrapped, closely stacked, full pallet was similar to that for the unwrapped closely stacked half pallet, as expected. The volume fraction of air in the wrapped loosely stacked

pallet was nearly double that of the tightly stacked pallets. . In the wrapped full pallet, the volume fraction of cardboard and plastic liner was slightly higher as compared with the two other configurations, due to some extra packaging between the pallet layers (in a seven pallet trial there is an average of 12/7=1.71 layers of top or bottom carton packaging per layer whereas there are 4/3=1.33 layers or top or bottom carton packaging per layer on a three layer half pallet).

8.2.1.2 Effective Thermal Conductivity Models

The effective thermal conductivity of a butter pallet depends on its configuration in terms of the location of the packaging and entrapped air, relative to the butter. In Chapter 3 details of commonly used theoretical models to calculate effective thermal conductivity and their application to calculate the thermal conductivity of butter were discussed. The Series and Parallel Models represent two effective conductivity extremes. The heterogeneous nature of the pallet includes two types of packaging, air and the bulk butter as its principle components. For the series model, the components are assumed to be thermally in series with respect to the direction of heat flow. In the parallel model, the components are considered as thermally in parallel with respect to the direction of heat flow. Obviously neither case is true for the pallet but the approximations may be sufficient for modeling purposes. In the middle layers of the pallet there is no significant heat transfer from the top to the bottom and the heat conduction occurs horizontally from the other four faces so the that air gaps and the packaging are predominantly in parallel to the heat transfer directions. Therefore, the Parallel Model appears to be the closest approximation to the pallet system. Another model that could be used is the Maxwell Eucken Model by considering butter as a continuous phase and the air and packaging as the dispersed phase. Equations (3-9), (3-10) and (3-12) give the Series, Parallel and the Maxwell Eucken Model respectively. Table 8.2 gives the thermal conductivity values for both the frozen (λ_f) and unfrozen (λ_u) temperature ranges using the three models for all the trials.

The estimated effective thermal conductivity values for both the half pallets show that, although the volume of air fraction doubles with loose stacking, the thermal conductivity values decreases only slightly. The effective thermal conductivity for the full wrapped pallet was higher than that for the unwrapped half pallet, despite the volume of air fraction being slightly higher. This is due to the higher butter thermal conductivity values used for the full pallet.

8.2.1.3 Effective Density

The effective density of the pallet was calculated using Equation (3-9) discussed in Chapter 3 using the mass fraction of air, butter and two types of packaging. Table 8.2 gives the values of effective density for all the pallet configurations.

8.2.1.4 Effective Specific Heat Capacity and Enthalpy

The effective specific heat and enthalpy of the pallet was calculated on a mass fraction basis with air, butter and packaging as the main components:

$$H_{eff} = \rho_b HV_b + c_a \rho_a V_a (T+40) + c_c \rho_c V_c (T+40) + c_s \rho_s V_s (T+40) \quad (8\text{-}1)$$

Where H_{eff} is the effective enthalpy of the pallet calculated on components basis, H is the measured enthalpy (Table 3.13) of butter (Note -40°C was used as a datum). It was assumed that the apparent specific heat capacity of butter changes in the frozen and unfrozen range but remains constant for the other components. The values used for the specific heat capacities of air (c_a), corrugated card board (c_c) and the plastic sheet (c_l) are given in Table 8.1

Table 8.1 also gives the effective values of specific heat capacity for the butter in frozen and unfrozen range for the freezing model. Figure 8.1 gives the difference between the enthalpy of butter and the effective enthalpy of the pallet of butter (B15). Figure 8.1 also shows the enthalpy estimated by correcting the enthalpy prorata to the change in effective density of the pallet ($H_{eff} = \rho_{cff} / \rho_b$). This approach ignores the thermal mass of the air and packaging components. There is little difference in the effective enthalpy from two approaches because the thermal mass of the non butter components is small. Therefore, for the sake of simplicity, the enthalpy was estimated from the effective density.

Table 8.2: Summary of the effective properties for butter half and full pallet used in model predictions

Configuration	Wrapped Full Pallet (PH – 1, PC – 1) (tightly packed)	Wrapped Half Pallet (PH – 3, PC – 3) (loose packed)	Unwrapped Half Pallet (PH – 4, PC – 4) (tightly packed)
Measured Length (L_x)	1.0380	1.1820	1.060
L_{xeff} (m) (inside)	1.0258	1.1695	1.0476
Measured Width (L_z)	0.7764	0.8200	0.7860
L_{zeff}(m) (inside)	0.7640	0.8075	0.7736
Measured height (Ly)	2.0430	0.7380	0.8450
L_{yeff}(m) (inside)	2.0252	0.7195	0.8262
ρ_{eff}	898	896	904
$\lambda_{u\,eff}$ (Parallel model) (WmK^{-1})	0.2055	0.1868	0.1885
$\lambda_{f\,eff}$(Parallel model) (WmK^{-1})	0.2692	0.2596	0.2620
$\lambda_{u\,eff}$ (Maxwell Eucken model) ($Wm^{-2}K^{-1}$)	0.2006	0.1822	0.1846
$\lambda_{f\,eff}$(Maxwell Eucken model) ($Wm^{-2}K^{-1}$)	0.2618	0.2521	0.2555
$\lambda_{u\,eff}$ (Series model) (WmK^{-1})	0.1675	0.1510	0.1597
$\lambda_{f\,eff}$(Series model) (WmK^{-1})	0.2012	0.1879	0.2020
C_{ueff} ($kJkg^{-1}$)	3.15	3.04	3.04
C_{feff}($kJkg^{-1}$)	1.79	1.68	1.68
Volume fraction of air V_a	0.015	0.024	0.0141
Volume fraction of butter V_b	0.9101	0.9094	0.9187
Volume fraction of cardboard V_c	0.0734	0.0652	0.0659
Volume fraction of liner V_l	0.0015	0.0014	0.0014
Mass fraction of air X_a	2.002×10^{-5}	3.219×10^{-3}	1.8634×10^{-3}
Mass fraction of butter X_b	0.9829	0.9847	0.9847
Mass fraction of cardboard X_c	0.0156	0.0139	0.0139
Mass fraction of liner X_l	0.0015	0.0014	0.0014

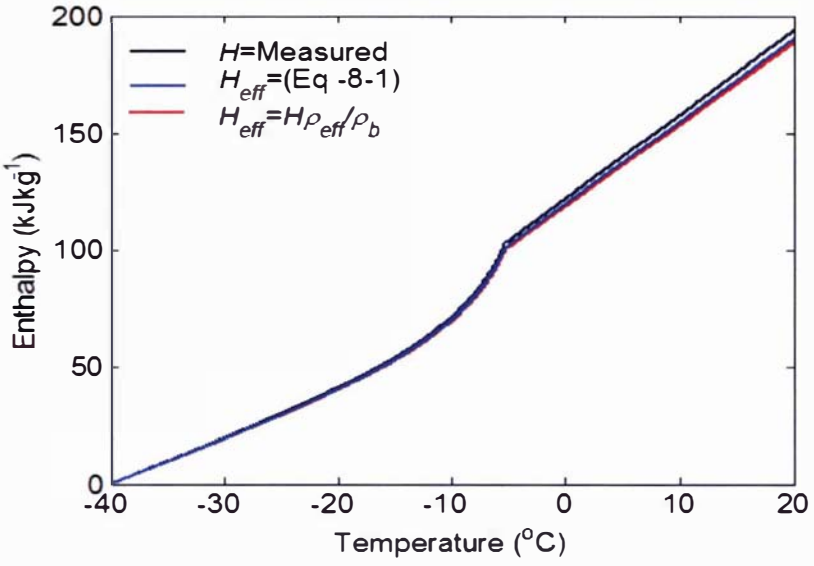

Figure 8.1: Comparison of measured enthalpy with the effective enthalpy for the unwrapped half pallet

8.2.1.5 Effective Heat Transfer Coefficients, Ambient and Initial Conditions:

The effective heat transfer coefficient for the faces of the cartons exposed to ambient air were estimated using Equation (5-1), assuming convection to the packaging surface, plus the additional resistance to heat transfer caused by the corrugated cardboard carton, the polyethylene liner and air gap in between the butter and the packaging. This was the same approach used for individual block butter trials outlined in Chapters 5 and 6. The convective heat transfer coefficients for the half pallet trials were estimated from the measured air velocities using Equation (5-9) for four sides of the pallet. For the top and the bottom of the pallet heat transfer coefficients were set to zero, due to negligible heat transfer in the vertical direction due to the presence of the polystyrene sheets on top and bottom. For the full pallet industrial trials, no data were available for the air velocities and, therefore, a typical value of 10 $Wm^{-2}K^{-1}$ was used for the convective heat transfer coefficient. Table 8.3 gives a summary of heat transfer coefficients, initial and ambient temperatures used in modeling for each trial.

Table 8.3: Input data for the full pallet and half pallet trials

Trial	Heat Transfer Coefficients, Ambient and Initial Temperature
PH - 1	$T_a(^\circ\mathrm{C}) = 10$ for all t $T_i(^\circ\mathrm{C}) = -6$ $h(\mathrm{Wm^{-2}K^{-1}}) = [4.8 \quad 4.8 \quad 3.5 \quad 3.5 \quad 4.8 \quad 4.8]^{\mathrm{I}}$
PC - 1	$T_a(^\circ\mathrm{C}) = 10^{-5}\left(t/3600\right)^2 - 0.013\left(t/3600\right) - 7.8455$ for all t $T_i(^\circ\mathrm{C}) = 10$ $h(\mathrm{Wm^{-2}K^{-1}}) = [5.3 \quad 5.3 \quad 0 \quad 0 \quad 5.3 \quad 5.3]$
PH- 3	$T_a(^\circ\mathrm{C}) = \begin{cases} 1.73\left(t/3600\right) + 3\times10^{-15} & 0 < t \le 30600 \\ 4\times10^{-4}\left(t/3600\right)^2 + 0.09t + 13.94 & 30600 < t \le 424800 \\ 5.0\times10^{-3}\left(t/3600\right) + 18.88 & t > 424800 \end{cases}$ $T_i(^\circ\mathrm{C}) = -22$ $h(\mathrm{Wm^{-2}K^{-1}}) = [5.3 \quad 5.3 \quad 0 \quad 0 \quad 5.3 \quad 5.3]$ (negligible heat transfer in vertical directions due to polystyrene sheets)
PC - 3	For front and left hand side of the pallet $T_a(^\circ\mathrm{C}) = \begin{cases} 2\times10^{-4}\left(t/3600\right)^2 - 0.095\left(t/3600\right) - 11.99 & t < 30600 \\ -17\times10^{-4}\left(t/3600\right) - 22.05 & t \ge 30600 \end{cases}$ $T_a(^\circ\mathrm{C}) = \begin{cases} 16\times10^{-4}\left(t/3600\right)^2 - 0.216\left(t/3600\right) - 16.10 & t < 288000 \\ -3\times10^{-4}\left(t/3600\right) - 23.22 & t \ge 288000 \end{cases}$ $T_i(^\circ\mathrm{C}) = 22$ $h(\mathrm{Wm^{-2}K^{-1}}) = [5.3 \quad 5.3 \quad 0 \quad 0 \quad 5.3 \quad 5.3]$
PH - 4	$T_a(^\circ\mathrm{C}) = \begin{cases} 2.17\left(t/3600\right) + 4\times10^{-15} & t < 39600 \\ 7\times10^{-6}\left(t/3600\right)^2 - 8\times10^{-4}\left(t/3600\right) + 23.8 & t \ge 39600 \end{cases}$ $T_i(^\circ\mathrm{C}) = -16$ $h(\mathrm{Wm^{-2}K^{-1}}) = [5.3 \quad 5.3 \quad 0 \quad 0 \quad 5.3 \quad 5.3]$

PC - 4

$$T_a\,(^{\circ}\mathrm{C}) = \begin{cases} -3.85\left(t/3600\right) - 4.61 & t < 10800 \\ 4\times10^{-3}\left(t/3600\right)^2 - 0.316\times10^{-4}\left(t/3600\right) - 15.25 & 10800 \le t < 167400 \\ 6\times10^{-6}\left(t/3600\right)^2 - 6.1\times10^{-3}\left(t/3600\right) - 21.086 & t \ge 167400 \end{cases}$$

$$T_i\,(^{\circ}\mathrm{C}) = 21.47$$

$$h\,(\mathrm{Wm^{-2}K^{-1}}) = [5.3 \quad 5.3 \quad 0 \quad 0 \quad 5.3 \quad 5.3]$$

[1] h = [front, back, left hand side, right hand side, top, bottom] faces

8.2.1.6 Results and Discussion

(a) Wrapped Full Pallet (Trial – 1)

Figure 8.2 gives the model predictions for the centre and surface temperatures during the full pallet thawing trial (PH-1) using the conduction only model with the Series, Parallel and Maxwell Eucken effective thermal conductivity models.

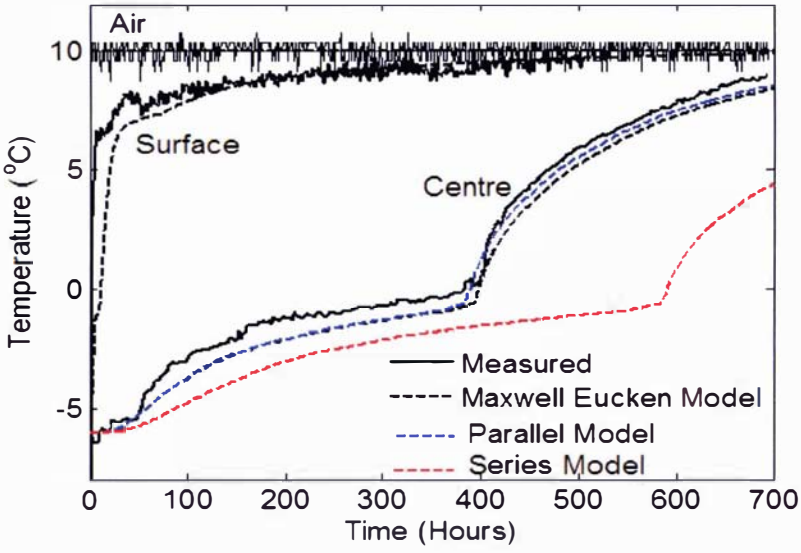

Figure 8.2: Measured thawing data for the centre of the wrapped full pallet trial (PH – 1) compared with model predictions using conduction only model with effective thermal properties calculated by Maxwell Eucken, Parallel and Series models

T_i=-6°C, T_a=10°C

R^2=0.9784 for centre using Maxwell Eucken Model

R^2=0.9848 for centre using parallel Model

R^2=0.12 for centre using series Model

Predictions using the Parallel and Maxwell Eucken models were closer to the measured data than the Series model which predicted the temperature to change far too slowly. The model predictions were a little lower than the actual data at temperatures below the initial freezing point, which could be due to the some uncertainty in the initial freezing point and, hence, enthalpy data. Above the initial freezing, the Parallel and Maxwell Eucken Models gave good agreement with the measured data.

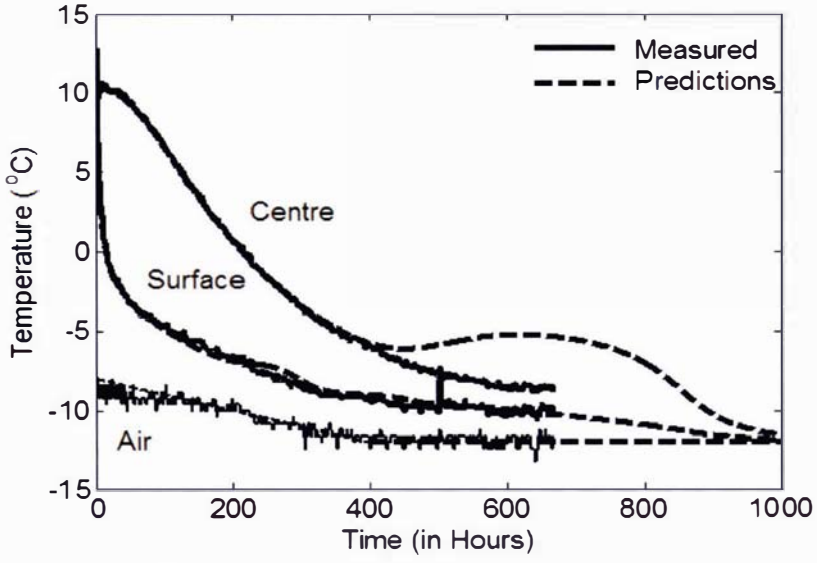

Figure 8.3: Measured freezing data for the centre of the wrapped full pallet trial (PC – 1) compared with model predictions using conduction only model with effective thermal properties calculated by the Parallel model. T_i =10°C, T_a=-11°C
R^2=0.9701 for centre using for first 400 hours
R^2=0.9301 for centre for 700 hours

Figure 8.3 gives the model predictions for the surface and pallet centre for the wrapped full pallet trial (PC – 1) for freezing. The effective thermal conductivity was calculated using the Parallel Model only. The model predicted the experimental data well up to 400 hours. The temperature rebound due to latent heat release on water crystallization was predicted to be earlier than measured. The rebound had just started when measurement were terminated after 600 hours due to the cost and time involved in carrying out the experiments. The butter used in this trial was lactic unsalted butter (B 19) which may have had different crystallisation kinetics than B19 (standard unsalted butter) for which the kinetics parameters were fitted (Chapter 6) which may explain the deviation in the predicted rebound from the actual rebound. A higher

value for the kinetic constant U would be expected to shift the rebound later in time. Overall, the freezing model shows similar behaviour for pallets as were observed for single blocks of butter (Chapter 6).

The effective property model performed very well for the wrapped whole pallet trials. These results indicate that the conduction only approach with effective properties given by the parallel thermal conductivity model is a reasonable basis to simulate heat transfer in butter where no internal air flow occurs. The modeling of unwrapped whole pallets is discussed in the section below.

(b) *Wrapped Half Pallet Trial (Trial – 3)*

The same modeling approach as above was taken for the wrapped half pallet trial where the loosely stacked layers of the pallet were wrapped with plastic film. As discussed in Chapter 7, the thawing of the three layered pallet was not uniform on all four sides. In addition, there was no heat transfer from top to bottom. Figure 8.4 gives the model predictions compared with the measured data for key positions in the pallet. Position 36 was the slowest heating position in the pallet. Position 3 was the centre of the Block 3. Positions 12, 22, 39 and 47 were the centres of the four faces exposed to the ambient for Blocks 1, 2 , 7 and 8 respectively (surface probes).

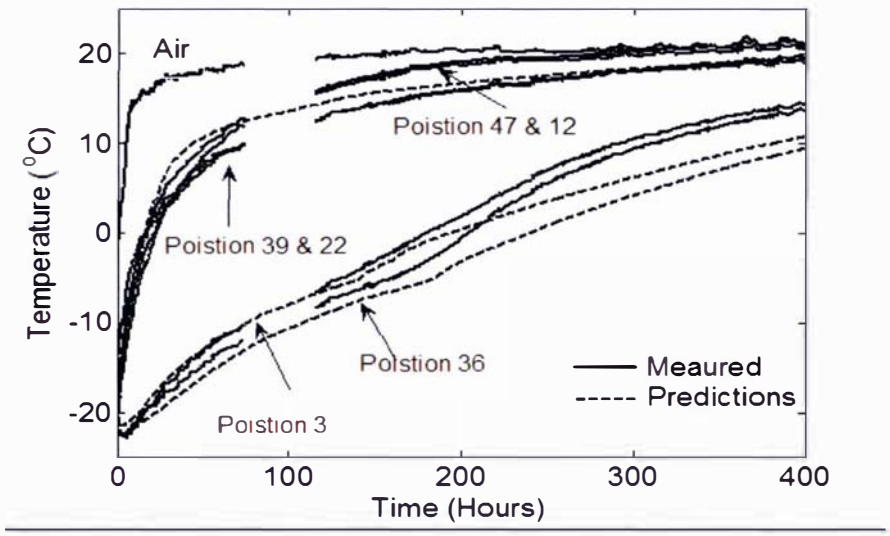

Figure 8.4: Measured data for the centre of the wrapped half pallet trial (PH – 3) during thawing compared with the conduction only model with effective thermal properties calculated by the Parallel model (Trial 3) with T_i=-23°C, T_a=20°C

The model predictions agreed reasonably well with the data below the initial freezing point of the butter. Above the initial freezing point, the predicted rate of temperature increase was very low (slower rate of heat transfer) compared with the measured data. These differences could be due to uncertainty in the input data. The source of uncertainty could be due to the specific heat capacity of butter which varies significantly between 0°C and 20°C. Salted butter has a peak at 10°C (Figure 3.18). In this range the specific heat capacity varies from about 3 $kJkg^{-1}{}^{o}C^{-1}$ to about 4 $kJg^{-1}{}^{o}C^{-1}$ with an average of 3.69 $kJkg^{-1}{}^{o}C^{-1}$ (the value used in the model). The difference could also have been due (at least in part) to the butter not being fully frozen at the start of the experiment in which case the total enthalpy change was over estimated. Another simulation was made using the enthalpy data collected for unfrozen salted butter (Figure 3.18(b)). Figure 8.5 shows the comparison of the measured data for Position 36 of the pallet with the models predictions using enthalpy data for completely frozen and unfrozen butter. The measured data lies between these predictions suggesting that incomplete freezing of the butter is a possible explanation for some of the differences between measured and predicted temperatures. This suggests that the butter pallet layers needed to be placed in the freezer for longer period of time before thawing.

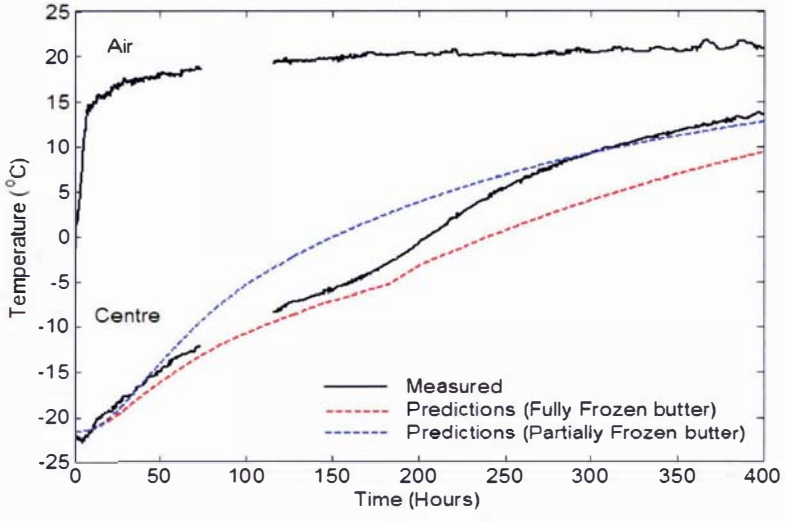

Figure 8.5: Predictions for the wrapped half pallet trial (PH – 3) using enthalpy for the fully and partially frozen butter compared with the measured data

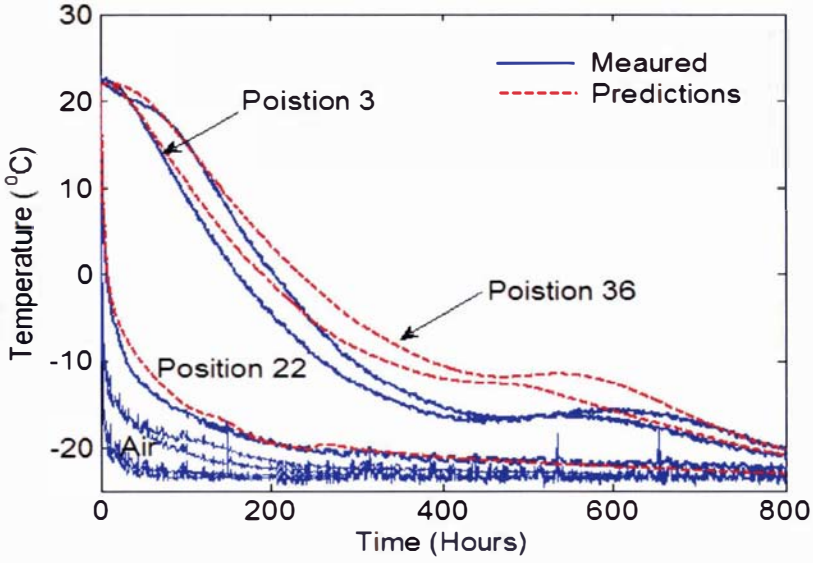

Figure 8.6: Comparison of measured data for the freezing of wrapped loosely stacked half pallet trial (PC - 3) considering heat transfer as conduction only with effective thermal properties based on the parallel model. T_i=22°C, T_a=-23°C

Figure 8.6 shows the measured and predicted temperature profile for different positions in the wrapped half pallet trial (PC-3) during freezing. The model showed good agreement with the measured data for Position 22 on the surface of the pallet. As for the thawing, the predicted temperature changed slower than the measured temperature profile for both Positions 3 and 36. The rebound was also predicted to occur earlier as compared with the measured data. However, the time to reach about -20°C was predicted to be the same for both the positions. The reason for the model giving slower changes in temperature than the measured data can not be explained as by the reasons suggested for the differences found for the thawing trial. Some of the inaccuracy of prediction can probably be explained by uncertainty in the estimation of thermal properties in general and the crystallisation kinetics parameters. However, the conduction model with parallel estimation of effective thermal conductivity approach seems only to work when the volume fraction of air in the pallet is not too large. The results suggest that, as the volume fraction of air increases and the potential for internal convection of air or natural radiation heat transfer increases the modeling approach starts to fall down.

(c) Unwrapped Tightly Packed Half Pallet Trial (Trial – 4)

(a)

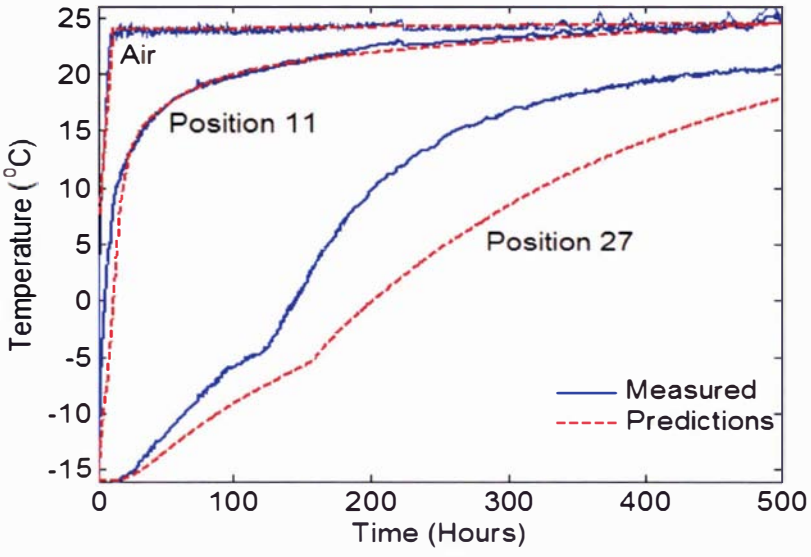

(b)

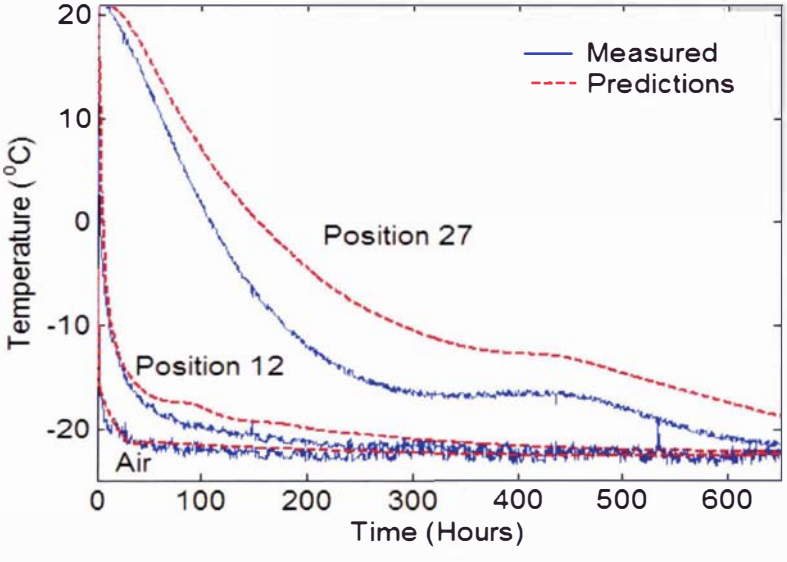

Figure 8.7: Comparison of model predictions with the measured data for the unwrapped half pallet trial (PH – 4) considering heat transfer as conduction only with effective thermal properties based on the parallel model.

(a)Thawing with T_i =-16°C, T_a=23°C (b) Freezing with T_i =21°C, T_a=-22°C

Figure 8.7 gives the model predictions for the unwrapped half pallet trials (PC–4) and (PH–4) using the same approach as above. As observed for the wrapped half pallet trial, temperatures predicted by the model within the butter blocks were lower than the measured data for both thawing and freezing, but there was a different reason. Due to the half pallet being unwrapped, there was some air movement into the outer regions of the pallet that accelerated the thawing and freezing, whereas the model assumed conduction only with effective thermal properties. There was evidence of convection in the outer sides of the pallet that speeded up the freezing and thawing mechanism (Chapter 7).

8.2.2 Modeling Heat Transfer in Pallets with Internal Airflow

The experimental results summarized in Chapter 7 for trials on unwrapped, loosely stacked, half pallets show that significant air flows can occur within the pallet, suggesting that modeling heat transfer in the pallet as only conduction is less appropriate. An alternative approach is to model each block in the pallet individually (as in Chapter 5 & 6) using different heat transfer rates on each face depending on the position in the pallet to account for heat transfer caused by internal air flow.

A simple approach is to treat the air channels within the pallet as additional resistance to heat transfer that increase as the path length from the pallet surface increase and decrease as the air velocity through the channel increases. Taking this approximation, a methodology to calculate the effective heat transfer coefficients on each surface from the experimental temperature differences between the surfaces and the air gaps was developed.

The effective surface heat transfer coefficients for the faces of cartons exposed to ambient air were estimated as previously by considering convection and radiation to the external surface of the pallet plus the additional resistance to heat transfer contributed by the corrugated cardboard carton, the polyethylene liner and the air in between the butter and the packaging:

$$\frac{1}{h} = \frac{1}{h_a} + \frac{d_c}{\lambda_c} + \frac{d_l}{\lambda_l} + \frac{d_a}{\lambda_a} \qquad (8\text{-}2)$$

In the experimental trials, the temperatures of the butter surface and the air gap immediately next to it were measured for a number of internal air channels. Assuming that the heat transfer coefficient

from the air in the gap to the butter surface adjacent to the gap is h, then these data can be used to estimate the heat flux at a particular point on the face using:

$$q = h(T_f - T_s) \tag{8-3}$$

where T_f is the temperature of the air flowing in the gap between the cartons and T_s is the temperature at the surface of the butter. The average heat flux for an internal face was then expressed in terms of the difference between the air temperature outside the pallet (T_a) and the temperature of the carton surface (T_s) as:

$$q = h_{eff}(T_a - T_s) \tag{8-4}$$

In this way, the effective heat transfer coefficient (h_{eff}) accounts for the resistance to heat transfer due to limited air flow through the pallet interior as well as the local resistance calculated in equation (8-2). Although this approximation gives correct average heat flows across the face, heat flows are overestimated near the centre of the pallet (as the temperature difference is large) and are underestimated near the outside of the pallet (as the temperature difference is small).
By simple rearrangement of Equations (8-3) and (8-4), an expression to estimate the effective heat transfer coefficients for internal was derived:

$$h_{eff} = h\frac{(T_f - T_s)}{(T_a - T_s)} \tag{8-5}$$

The way h_{eff} is calculated it is possible to have negative values for h_{eff} so for the sake of completion if the calculated value of h_{eff} is negative it will be considered 0 giving no heat conduction through that side of the block.

For the unwrapped, loosely stacked, half pallet trial (PC-5, PH-5), effective heat transfer coefficients were directly estimated from the measured temperature profile using Equation (8-5). For the unwrapped full pallet trial (PC-2, PH-2), no similar internal temperature measurements were made and, therefore, an estimation of the heat transfer coefficients were determined from fitted surface measured temperatures to predict the rates heat transfer.

The conductive heat transfer model developed in Chapter 5 (Equations (5-2) to (5-10)) was used to predict thawing in each block of butter in the pallet by replacing h by h_{eff}. Similarly the conduction only model for freezing individual blocks developed in Chapter 6 (Equations (6-1) to (6-3)) was used to predict cooling in blocks of butter in the pallet was used by replacing h by h_{eff}.

(a) Unwrapped Loose Stacked Half Pallet (Trial – 5)

The heat transfer coefficients on the inner faces of Blocks 2 & 7 for first 60 hours of freezing are given in Figure 8.8 (b). The estimates of the heat transfer coefficients were very consistent throughout the 60 hours (note that the regular discontinuities occurring every 8 hours were due to freezer room defrost and can be ignored). An average value for each position on each face were estimated and used for model inputs. Figure 8.8(b) shows the positions on surface of the blocks where the temperature was measured and the value of the heat transfer coefficient used for that position. The heat transfer coefficients on the top and bottom of each carton were set to zero as negligible thermal gradients were observed in the vertical direction in the half pallet. The heat transfer coefficients for the faces exposed to ambient were estimated using Equation (8-2). The effective heat transfer coefficient decreased as the length of the air flow path increased. The effective heat transfer coefficients at the same positions on opposite sides of the pallet (e.g. Positions 15 & 20 and 13 & 21) had very similar values. The average heat transfer coefficients used in the model are given in Table 8.4

(a)

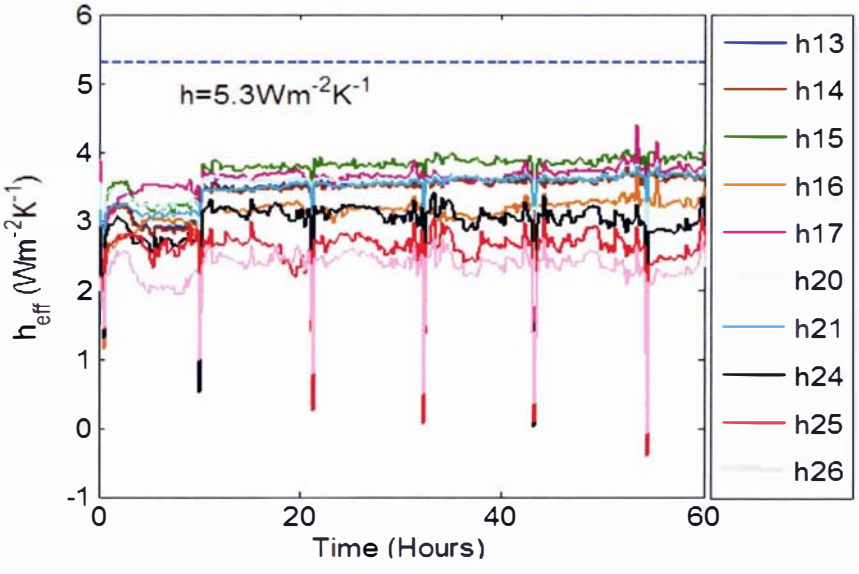

(b)

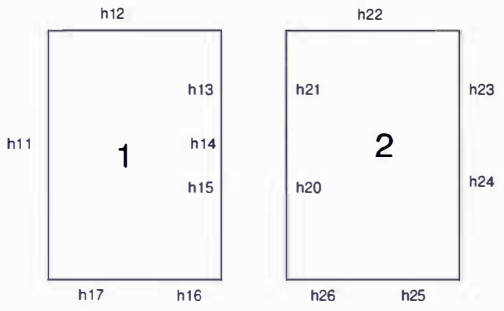

Figure 8.8: Effective heat transfer coefficient for freezing of Block 2 and 7 in unwrapped half pallet trial (PC – 5)

(Positions corresponding to those given in the plan view of the blocks in Figure 8.8(b)

Table 8.4: Effective heat transfer coefficients **(W m^{-2} K^{-1})** ***used in the model to predict freezing in trial PC – 5***

h13	h14	h15	h16	h17	h20	h21	h23	h24	h25	h26
3.5	3.4	3.7	3.1	3.6	3.5	3.5	missed	3.0	2.6	2.3

The heat transfer coefficients for the inner faces were also predicted for Blocks 7 & 8 during thawing (Figure 8.9).The greater variation in the effective heat transfer coefficients with time was due to poorer control of the air circulation in the room for this trial. At approximately 17 hours, a pedestal fan was placed into the room to improve the air flow generally resulting in less variable calculated heat transfer coefficients thereafter. The air velocities in the thawing trial were lower than those in the freezing trial for the same pallet resulting in lower effective heat transfer coefficients values. The effective heat transfer coefficients were averaged for times below 17 hours and above 22hours and used in the model. The heat transfer coefficients used in the model are given in Table 8.5

(a)

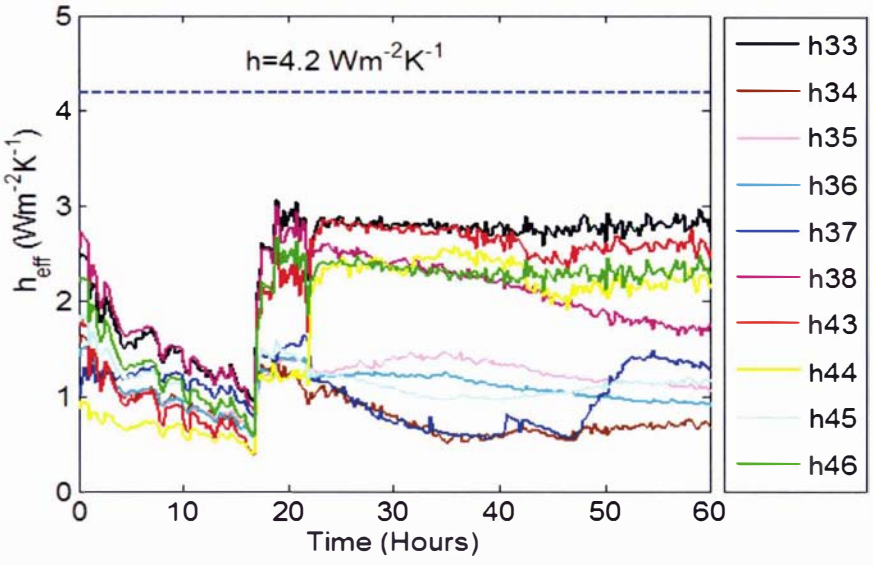

(b)

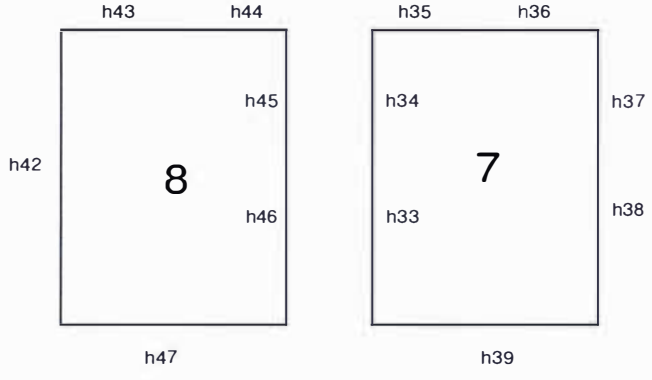

Figure 8.9: (a) Effective heat transfer coefficient for freezing of Block 7 and 8 in unwrapped half pallet trial (PH – 5)

(Positions corresponding to those given in the plan view of the blocks in Figure 8.9(b)

Table 8.5: Effective heat transfer coefficients ($W\ m^{-2}K^{-1}$) *used in the model to predict thawing in trial PH – 5*

Time (hours)	h33	h34	h35	h36	h37	h38	h43	h44	h45	h46
t < 17	1.5	1.0	1.0	1.0	1.1	1.6	0.9	0.7	1.2	1.2
t ≥ 17	2.8	0.8	1.3	1.1	1.0	2.2	2.6	2.2	1.1	2.3

All the other input data for predicting freezing in Blocks 1 and 2 and thawing in Blocks 7 and 8 is given in Table 8.6.

Table 8.6: Input data for unwrapped loosely stacked trial

Trial	Ambient and Initial Temperature
PC - 5	$T_a(^oC) = \begin{cases} -0.224\left(t/3600\right) - 18.5 & t < 104400 \\ -25 & t \geq 104400 \end{cases}$ $T_i\left(^oC\right) = 10,\ 12.14$
PH - 5	$T_a(^oC) = \begin{cases} 3.5 & 0 < t \leq 68400 \\ -2.5\times10^{-3}\left(t/3600\right)^2 + 0.29\left(t/3600\right) + 11.23 & 68400 < t \leq 212400 \\ -8\times10^{-5}\left(t/3600\right)^2 + 0.03\left(t/3600\right) + 18.18 & t > 212400 \end{cases}$ $T_i(^oC) = -21.5$

Figure 8.10 shows the measured data compared with the model predictions using the block by block effective heat transfer coefficient model for freezing Blocks 1 & 2. The exterior surface predictions agreed well with the measured temperatures (Block 1). The model shows good agreement with the measured data for all other positions in the blocks with the exception of the magnitude of the temperature rebound for the centre of the butter in Block 1 and the timing of the rebound in Block2. Due to the stochastic nature of the crystallization process the rebounds in all blocks occurred at different times.

(a)

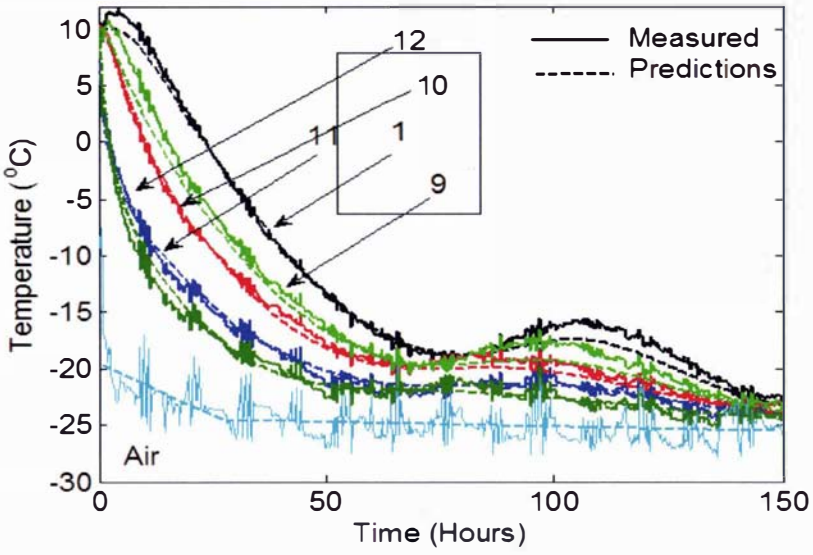

(b)

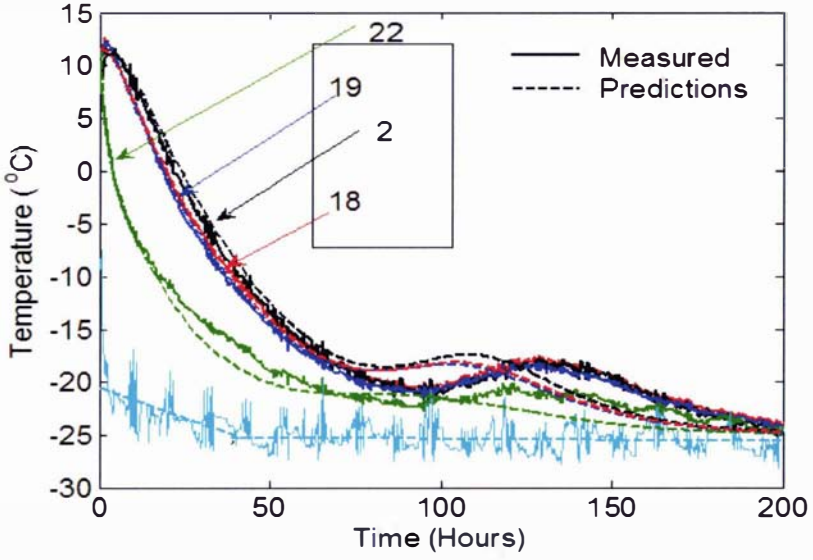

Figure 8.10: Measured data compared with the model prediction for freezing of unwrapped loosely stacked half trial with gaps (PF – 3) with T_i= 11°C, T_a=-25°C

(a) Block1 (R^2=0.9936 for centre)

(b) Block 2 (R^2=0.9654 for centre)

(a)

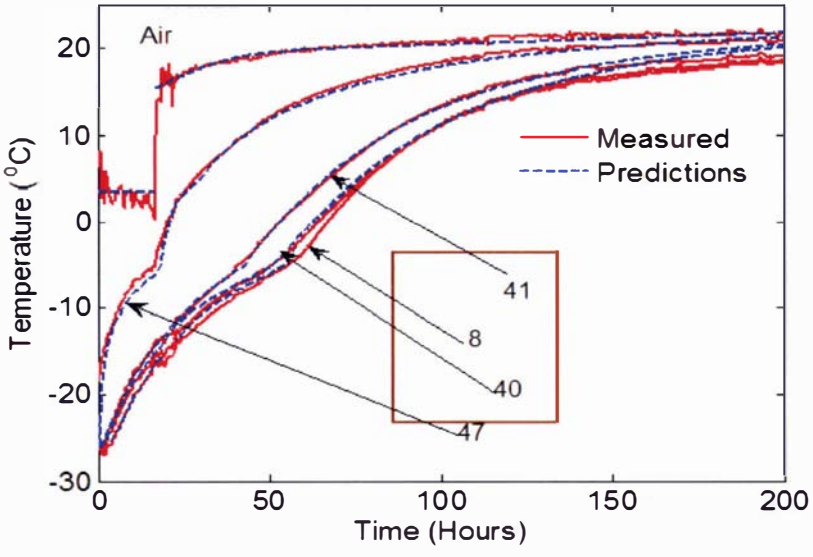

(b)

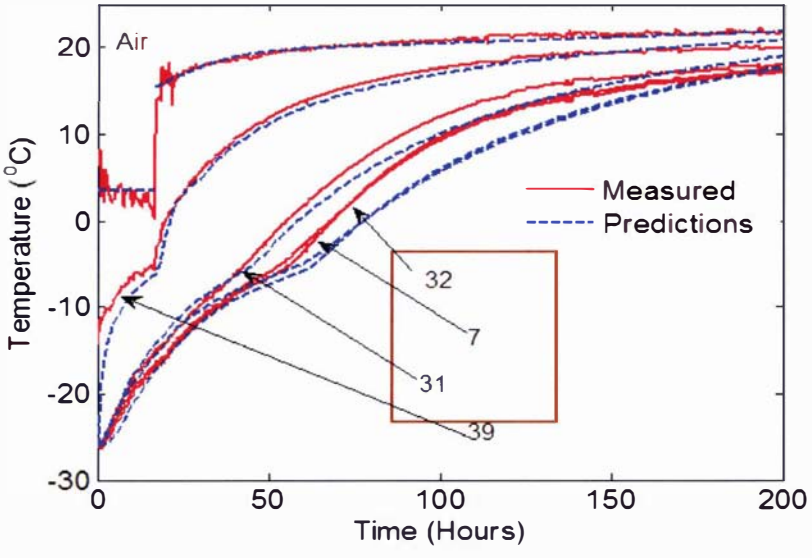

Figure 8.11: Measured data compared with the model prediction for thawing of unwrapped loosely stacked half pallet trial with gaps (PH - 5) with T_i= -25°C, T_a=20°C

(a) Block8 (R^2=0.9962 for centre)

(b) Block 7 (R^2=0.9751 for centre)

Figure 8.11 shows the model predictions for thawing compared with the experimental data for Blocks 7 and 8. In general the model gave good agreement with the measured temperature data for thawing.

The way in which the effective heat transfer coefficients were calculated gave average values across each face to which the heat transfer model was applied. This resulted in under-prediction of surface heat fluxes for the points of the interior faces near the outside of the pallet and over-prediction of heat fluxes further into the pallet. This trend is evident in Figure 8.11(b), where rates of heat transfer at interior positions in block 7 were predicted to be slightly slower than experimentally measured.

Overall, this modeling approach gave reasonable predictions for the pallet layer containing gaps between the blocks. The model validation demonstrates that useful predictions for the thawing of bulk butter can be obtained with a relatively simple heat transfer model. In practical use of the model, the temperature profiles throughout a pallet would not be known and, therefore, the effective heat transfer coefficients could not be easily estimated. It would be expected that they would be strong functions of the magnitude of the air flow through different regions of the pallet. This would in turn be dependent on the directions and velocities of the air flowing on to the pallet exterior and the looseness of the pallet stacking (i.e. the width of the air gaps between adjacent cartons). If the pallet was stacked very tightly, the amount of air flowing within the pallet would be very low and, therefore, a different set of heat transfer coefficients (presumably lower) would be needed for those scenarios.

Further testing of the approach requires repeated experimental trials in which more defined and constant air flow patterns through the pallet are achieved for both thawing and freezing scenarios so that a systematic method to predict h_{eff} values can be developed.

(b) Model Predictions for the Unwrapped Full Pallet Trial:

The unwrapped full pallet trial was an industrial trial with some air gaps between blocks due to repeated movement of the pallet by forklift. The air gaps in between the cartons were not as open as in trial PC–5. To predict freezing and thawing in the unwrapped full pallet trial, Block 30 was chosen as a representative inner block in the central layer of the pallet. The effective heat transfer coefficients were manually estimated from observations of the relative rates of heating around the block. Table 8.7 gives the input data used.

Table 8.7: Input data for unwrapped tight packed full pallet trial

Trial	Ambient and Initial Temperature
PH - 2	$T_a(^oC) = \begin{cases} -2\times10^{-3}\left(t/3600\right)^2 + 0.0453\left(t/3600\right) + 8.6676 & t < 180000 \\ -6\times10^{-6}\left(t/3600\right)^2 + 0.0072\left(t/3600\right) + 10.266 & t \geq 180000 \end{cases}$ $T_i\left(^oC\right) = -11$ $h\left(Wm^{-2}K^{-1}\right) = [5.3 \quad 1 \quad 0 \quad 0 \quad 0.5 \quad 0.5]$
PC - 2	$T_a(^oC) = \begin{cases} 2.12\left(t/3600\right) + 5.3 & t < 31320 \\ 1.5\times10^{-3}\left(t/3600\right) + 23.76 & t > 212400 \end{cases}$ $T_i(^oC) = -17.5$ $h\left(Wm^{-2}K^{-1}\right) = [3.7 \quad 0.3 \quad 0 \quad 0 \quad 0.3 \quad 0.3]$

Figure 8.12(a) gives the model predictions for the freezing of the unwrapped full pallet trial for Block 30. The model predicted the measured data well for Block 30 at the surface and at position 17, showing that the air side heat transfer coefficient was accurately fitted for the industrial setting. For Positions 15 and 16, the predicted cooling rates were slightly faster than observed experimentally. For position 19, the model predicted slower heat transfer rates than the measured data. The predicted temperature rebound due to the ice formation was after about 250 hours for Block 31. Although no rebound was observed in the experimental data as shown in Figure 8.13(b), the measured temperature stayed above the ambient for a very long period of time consistent with the slow release of the latent heat of water. The difference in the rebound could be explained by uncertainty in the crystallisation kinetics.

(a) - Block 30

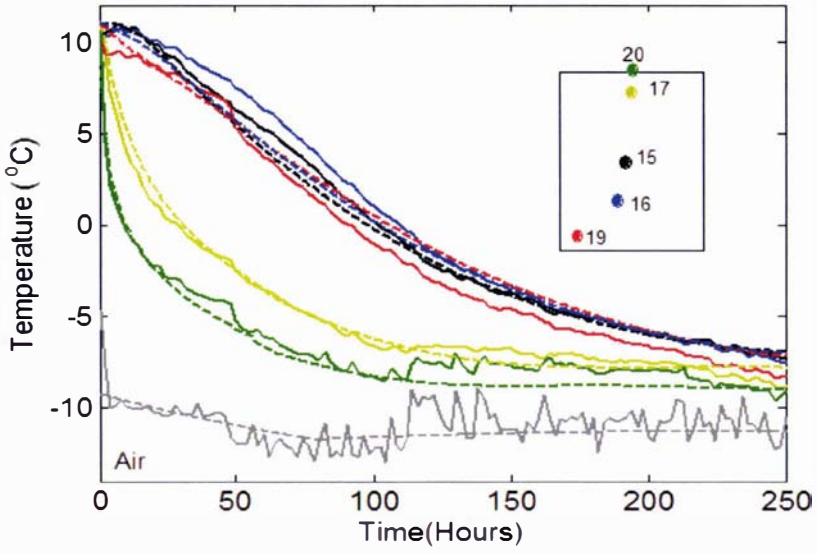

(b) - Block 30

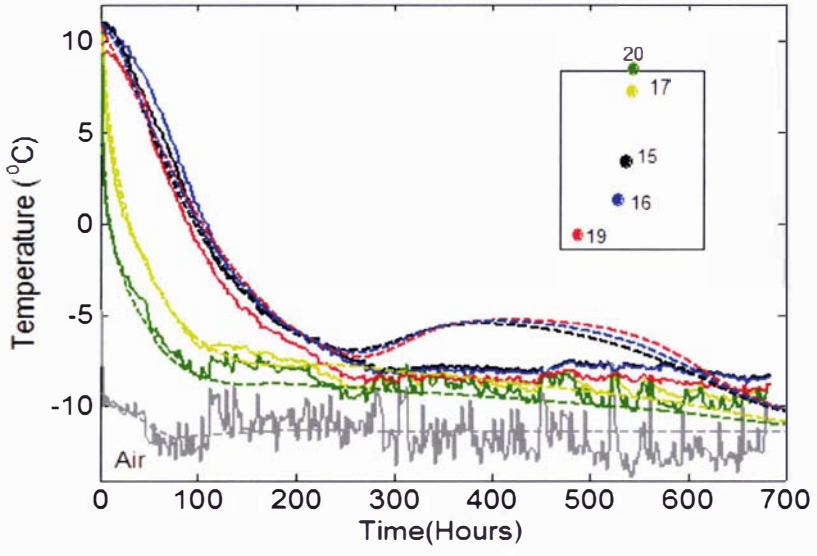

(c) – Block 31

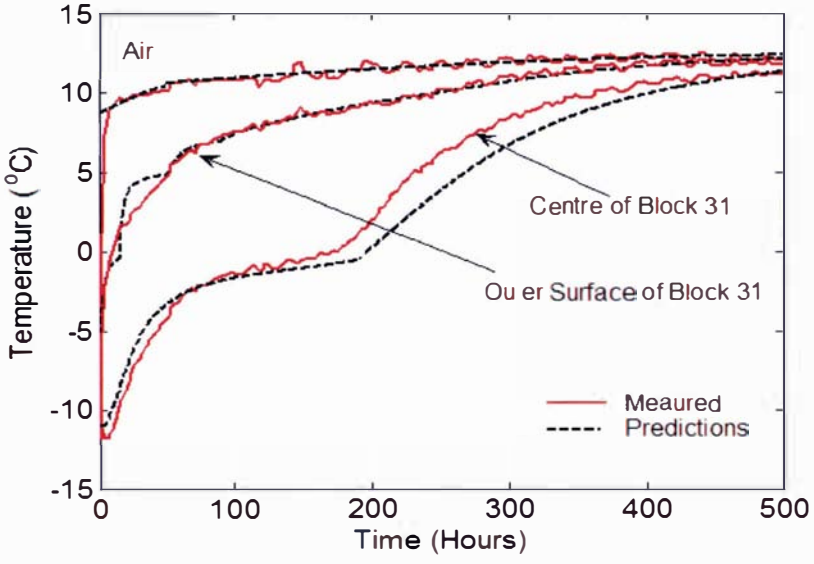

Figure 8.12: Comparison of the model predictions with measured data for the unwrapped full pallet trial ((PH – 2) & (PC – 2))

(a) and (b): Freezing in Block 30 with T_i= 10°C, T_a=-11°C

(c): Thawing in Block 31 with T_i= -11°C, T_a=11°C

Figure 8.12(c) gives the model prediction for the surface and the centre for the thawing of Block 31 in the pallet. The heat transfer coefficients used in the model predictions are given in Table 8.5. The model agreed well with the measured data for both positions.

Overall the model using the fitted heat transfer coefficients for single blocks gave good predictions for both the Trials PH – 2 and PC – 2 for both thawing and freezing. However further work is needed to develop methods to estimate the internal heat transfer coefficients for different scenarios likely to occur in the dairy industry.

(b) Model Predictions for Trial 4:

Trial 4 (unwrapped closely stacked half pallet) was set up by packing the blocks manually together as much as possible. This trial represented the best-case scenario in an industrial situation where the pallet is not moved from one place to another causing air gaps between the cartons. For predicting heat transfer in Trial 4, the heat transfer coefficients on the internal faces of all the blocks were calculated using Equation (8-5). It was found that the heat transfer coefficients were below zero for

most of the positions. For the positions 13, 21, 23, 28, 38, 30, 33, 46, and 48 the heat transfer was not negative due to some air movement at those places as being exposed to ambient. An average value of effective heat transfer coefficients on each face was used for modeling the freezing of Block 7. Figure 8.13 gives the effective heat transfer coefficients used for modeling freezing and thawing of Block 7. All other input data used for modeling are shown in Table (8.1).

(a)

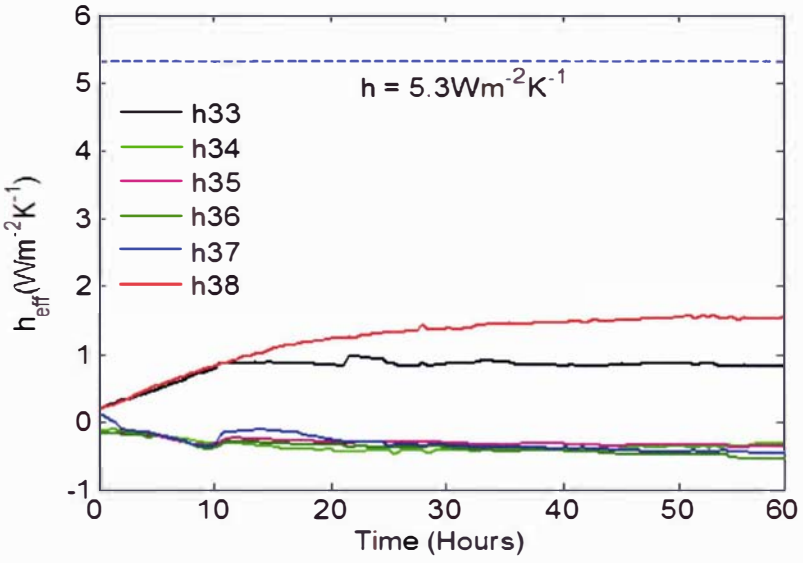

(b)

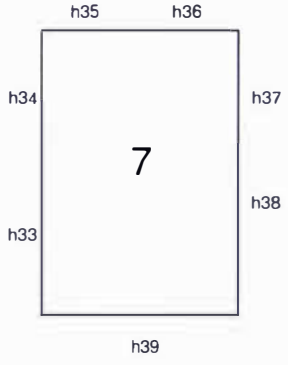

Figure 8.13: (a) Effective heat transfer coefficient for freezing of Block 7 in unwrapped closely stacked half pallet trial (PC – 4) for Block 7

(Positions corresponding to those given in the plan view of the blocks in Figure 8.13(b)

Block 7

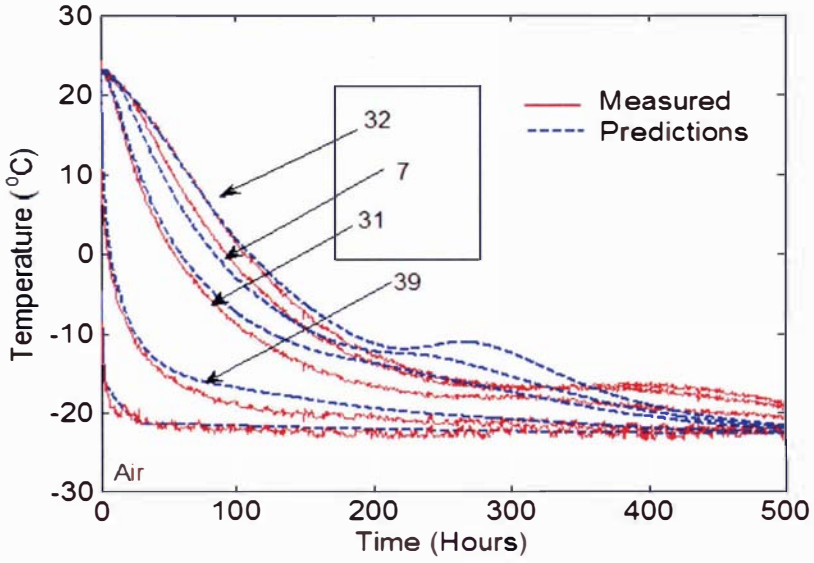

Figure 8.14: Measured freezing data compared with the model prediction for unwrapped closely stacked half pallet trial (PC – 4) with T_i = 21°C, T_a= -21°C

Figure 8.14 gives the model predictions for Block 7 with only one surface exposed to ambient. The model predicted a slower drop in temperature for Position 31 in the beginning, due to a slightly lower heat transfer coefficient. For all other positions, the model agreed well with the experimental data.

For thawing of Trial 4 (PH-4), Block 7 was chosen for the model prediction. There was no heat transfer from the smaller inner (end) face and so the heat transfer coefficient was set to zero for that face as for the top and the bottom of the block. An average heat transfer coefficient of 0.3W m^{-2} K^{-1} and 1 W m^{-2} K^{-1} was used on the two other inner (side) faces (Figure 8.13 (a)) and a heat transfer coefficient of 5.3 $Wm^{-2}K^{-1}$ was used for the face exposed to the ambient. Figure 8.15 gives the model predictions for the thawing of Block 7 in Trial PH-4. The model gave good agreement for the surface and all other positions in the block.

Overall, for Trial 4 the approach of predicting freezing and thawing in unwrapped half pallet trial on a block by block basis worked successfully.

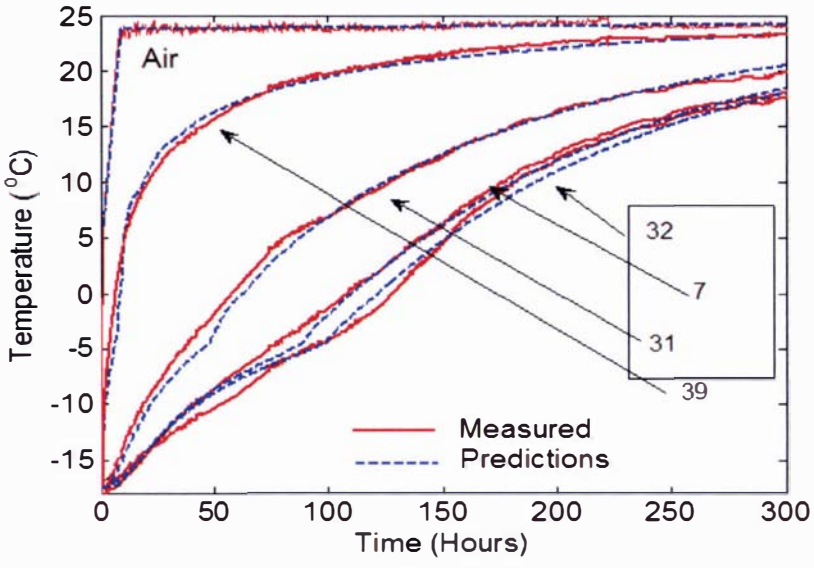

Figure 8.15: Measured data for thawing of Block 7 in thawing of unwrapped half pallet trial with no gaps (Trial PH-4) with T_i= -18°C, T_a=22°C

8.3 Conclusions

From the models developed and applied on different industrial scenarios for freezing and thawing of palletized butter, the following conclusion can be drawn from an industrial point of view:

- For wrapped palletised butter where there is no internal air flow, a model considering the heat transfer within the pallet by conduction only with effective thermal properties estimated from the parallel model gave good predictions.
- The same approach starts to fall down as the amount of air in the wrapped pallet increases.
- For unwrapped palletized butter where significant airflows exists within the pallet, the approach of predicting heat transfer on block by block basis using effective heat transfer coefficients gave good predictions.
- For unwrapped tightly packed butter pallets the individual block effective heat transfer coefficient model can give reasonable predictions if the rate of heat transfer over the inner face of the carton is set to zero and the effective heat transfer coefficients on the inner sides of the block are set to reflect the extent of air penetration into the outer regions of the pallet.
- Further experimental and/or modeling work is required in order to develop guidelines for estimating effective heat transfer coefficient values for internal block face for industrial scenarios.

CHAPTER 9

CONCLUSIONS AND RECOMMENDATIONS

9.1 Conclusions

- The specific heat capacity of butter differs for cooling and heating operations due to significant supercooling and delayed crystallization of the fat fraction of butter at temperatures well below the equilibrium phase change temperature during cooling. This reduces the heat capacity for cooling relative to that for heating.

- A conduction-only model using the equilibrium thermal properties can be used to adequately predict the thawing of butter blocks when the water in the butter is completely frozen before thawing. Measured temperature-dependent specific heat capacity data for butter for which the water phase was not frozen, gave accurate predictions for the conduction-only model. These values included data for melting of some of the fat fraction.

- To predict the freezing behavior of butter blocks, which included the freezing of the water phase, a differential form of the Avrami equation (which models the kinetics of crystallization) was combined with a standard three dimensional heat conduction model. This model gave good predictions of the measured data for the freezing of a butter block when fitted kinetic parameters were used.

- Freezing and thawing models developed for the individual blocks were extended to predict heat transfer in palletized butter in different industrial scenarios. For wrapped palletised butter (for which no internal air flows occur), a conduction-only model gave accurate predictions when effective thermal properties predicted by the parallel model were used.

- For an unwrapped palletized butter, (for which there is significant airflow occurs through the pallet) the approach of predicting heat transfer on a block-by-block basis using effective convective heat transfer coefficients on a surface-by-surface basis looks promising but

methods to predict the heat transfer coefficient of internal air flow and pallet geometry were not adequate and require further development.

- Some industrial pallet configurations behave in an intermediate fashion. Internal air flow is at such a level that a conduction-only model is not appropriate, but the air flow is not high enough that a block-by-block modeling approach can be expected to be accurate. A model that combines a conduction-only model with an effective convective heat transfer coefficients on the surfaces exposed to air flows gives good predictions using block by block basis approach in such a case.

9.2 Recommendations

- It is recommended that the nucleation and growth kinetics constants for the Avrami equation are independently defined by means of isothermal experiments, or equivalent to improve the model predictions under all cooling conditions.

- A population balance modelling approach for the freezing process may allow prediction of the fluctuation in the position of the temperature rebound observed in nearly identical experimental trials.

- Further experimental and/or modelling work is required in order to develop guidelines to estimate the effective heat transfer coefficient values as a function of air flow conditions and pallet configuration for more accurate predictions of heat transfer in unwrapped palletised butter in industrially relevant scenarios.

REFERENCES

Abraham, F. (1974). Homogenous Nucleation Theory. New York, Academic Press.

AlfaLaval (1980). Dairy Handbook Sweden, Alfa - Laval AB.

Angell, C. A. (1982). Supercooled Water in Water - a Comprehensive Treatise. F. Franks. New York, Plenum Press. **7:** 1-82.

ASHARE (1989). Ashrae Handbook - Fundamentals American Society of Heating, Refrigeration and Air Conditioning Engineers Atlanta, Tullie Circle.

ASTM (2005). Standard Test Method for Determining Specific Heat Capacity by Differential Scanning Calorimetry, E1269.

Auldist, M. J.,S. Coats,G. L. Rogers and G. H. McDowell (1995). "Changes in the Composition of Milk from the Healthy and Mastitic Dairy Cows During the Lactation Cycle." Australian Journal of experimental agriculture **35**: 427-436.

Avrami, M. (1939). "Kinetics of Phase Change 1." Journal of Chemical Physics **7**: 1103 - 1112.

Avrami, M. (1940). "Kinetics of Phase Change Ii." Journal of Chemical Physics **8**: 212-224.

Avrami, M. (1941). "Kinetics of Phase Change Iii." Journal of Chemical Physics **9**: 177-184.

Ballentynes, C. (2001). Personal Communication. Palmerston North, Fonterra Co-Operative Group Ltd.

Becker, B. R. and B. A. Fricke (1999). "Freezing Times of Regularly Shaped Food Items." Int. Comm. Heat Mass Transfer **26**(5): 617-626.

Boston, G.,K. Palfreyman,D. Illingworth,E. Cant and R. Keen (2001). Milkfat Product a Digtp Manual - Version 2001. New Zealand Dairy Research Institute, Cheese & Milkfat Technology New Zealand Dairy Research Institute**:** 1-44.

Bronshteyn, V. L. and P. L. Steponkus (1995). "Nucleation and Growth of Ice Crystals in Concentrated Solutions of Ethylene." Cryobiology **32**(1-22).

Broto, F. and D. Clausse (1976). "A Study of the Freezing of Supercooled Water Dispersed within Emulsions by Differential Scanning Calorimetry." Journal of Phys C: Solid State Phys **9**: 4251-4257.

Butler, M. (2001). "Instability Formulation and Directional Dendritic Growth of Ice Studied by Optical Interfermetry." Crystal growth and Design **1**: 1-11.

Cant, P. A. E.,K. R. Palfreyman,G. D. Boston and A. K. h. MacGibbon (1997). Milkfat Products, NZDRI.

Carslaw, H. S. and J. C. Jaeger (1959). Conduction of Heat in Solids Oxford, Claredon Press.

Chang, H. D. and L. C. Tao (1981). "Correlation of Enthalpies of Food Systems." Journal of Food Science **46**: 1493.

Chen, A. C. and S. Nagy (1987). "Prediction and Correlation of Freezing Point Depression of Aqueous Solutions " Transaction of the ASAE **30**(4): 1176.

Chen, C. S. (1986). "Effective Molecular Weight of Aqueous Solutions and Liquid Foods Calculated from the Freezing Point Depression." Journal of Food Science **51**(6): 1537.

Chen, C. S. (1987a). "Sorption Isotherm and Freezing Point Depression Equations of Glycerol Solutions." Transaction of the ASAE **30**(1): 279.

Chen, C. S. and S. Nagy (1987). "Prediction and Correlation of Freezing Point Depression of Aqueous Solution." Transaction of the ASAE **30**(4): 1176-1180.

Choi, Y. and M. R. Okas (1986). Transport Phenomena. Effects of Temperature and Composition on the Thermal Properties of Foods in Food Engineering and Process Application, Vol 1. M. Maguer and P. Jelen. London, Applied Science. **1**.

Christian, J. W. (1965). The Theory of Transformation in Metals and Alloys. Physical Metallurgy. R. W. Cahn. Amsterdam, North Holland**:** 443-539.

Chubik, Y. A. and A. I. Maslov (1965). Handbook of Thermophysical Constants of Food Products and Semi-Products (in Russian). Moscow.

Clark, P. E.,C. R. Waldenland and R. P. Cross (1946). "Specific Heat of Vegetable Oils from 0 to 250°c." Ind. Eng. Chem. **38**(3): 350.

Clarkson, C. E. and T. Malkin (1934). "Journal of Chemical Society." **666**.

Cleland, A. C. (1990). Food Refrigeration Process Analysis, Design and Simulatio. New York, Elsevier Applied Science.

Cleland, A. C.,D. J. Cleland and R. L. Earle (1982). "The Effect of Freezing Rate on the Accuracy of Numerical Freezing Calculations." International Journal of

Refrigeration **5**: 294-301.

Cleland, A. C.,D. J. Cleland and S. D. White (2005). Cost -Effective Refrigeration. Palmerston North, New Zealand, Massey University.

Cleland, D. J. (1985). Prediction of Freezing and Thawing Times for Foods. Palmerston North, Massey University. **PhD**.

Cleland, D. J. and A. C. Cleland (1991). Rads. Release 3.1. Palmerston North, Massey University.

Cleland, D. J., A. C. Cleland, R. L. Earle and S. J. Byrne (1987c). "Prediction of Freezing and Thawing Times for Multi-Dimensional Shapes by Numerical Methods." International Journal of Refrigeration **10**: 32-39.

Conochie, J. (1964). "The Thermal Conductivity of Butter and Cheese." Australian Journal of Dairy Technology **19**: p90.

Crank, J. and P. Nicholson (1947). "A Practical Method for Numerical Integration of Solutions of Partial Differential Equations of Heat Conduction Type." Proc. Cam. Phil. Soc **43**: 50.

Delgado, A. E. and D. W. Sun (2001). "Heat and Mass Transfer Modles for Predicting Freezing Processes - a Review." Journal of Food Engineering **47**: 157-174.

Dickerson, R. W. (1968). Thermal Properties of Food. The Freezing Preservation of Food. D. K. Tressler, W. B. van Arsdel and M. R. Copley. Westport, CT, AVI Publishing Co.

Dufour, L. and R. Defay (1963). Thermodynamics of Clouds. New York, Academic Press.

Dumas, J. P.,M. Krichi,M. Strub and Y. Zeraouli (1994). "Models for the Heat Transfers During the Transformations inside an Emulsion - 1. Crystallisation of The Undercooled Droplets." Journal of Heat and Mass Transfer **37**(5): 737-746.

Early, R. (1992). The Technology of Dairy Products. New York, Balckie & Sons Ltd.

Erickson, M. and Y. Hung, Eds. (1997). Quality in Frozen Food. New York, USA, Chapman & Hall.

Eyres, N. R.,D. R. Hartree,J. Ingham,R. Jackson,R. J. Sarjant and J. B. Wagstaff (1946). "The Calculation of Variable Heat Flow in Solids." Transaction of the Royal Society London **A240**: 1.

Fennema, O. R.,W. D. Powrie and E. H. Marth (1973). Low Temperatures Preservation of

Foods and Living Matters. New York, Marchel Dekker, Inc.

Franks, F. (1985). Biophysics and Biochemistry at Low Temperatures. London, Cambridge University Press.

Franks, F.,S. F. Mathias,P. Galfre,S. D. Webster and D. Brown (1983). "Ice Nuclation and Freezing in Undercooled Cells." Cryobiology **20**: 298-309.

Franks, F.,S. F. Mathias and K. Trafford (1984). "The Nucleation of Ice in Undercooled Water and Aqueous Polymer Solutions " Colloids Surfaces **11**: 275-309.

Frede, E. (2002). Butter/ Properties and Analysis. Kiel, Germany Elsevier Science Ltd 220 - 236.

Frede, E.,D.Precht and K. H. Peters (1978). Milchwirtsch **29**: 1684.

Ginzburg, A. S.,M. A. Gromov and G. I. Krasovskaya (1975). Thermal Properties of Food Products and Materials (in Russian). Moscow.

Ginzburg, A. S.,G. I. Krasovskaya and M. A. Gromov (1985). Thermal Properties of Food Products (Czech Translation). Prague.

Griffen, V. J. and P. G. Laye (1992). Differential Thermal Analysis and Differential Scanning Calorimetry. Thermal Analysis: Techniques and Application. E. L. Charsley and S. B. Warrington. Cambridge, Royal society of chemsitry.

Hagemann, J. W. (1988). Thermal Behavior and Polymorphism of Acylglycerides. Crystallization and Polymorphism of Fats and Fatty Acids. N. Garti and K. Sato. New York, Marcel Dekker, Inc.

Harper, J. W. and C. W. Hall (1981). Dairy Technology and Engineering. Wetport, Conn. USA, AVI Publishing Company Inc.

Heldmen, D. R. (1974). "Predicting the Relationship between the Unfrozen Water Fraction and Temperature During Food Freezing Using Freezing Point Depression." Transaction of the ASAE **17**: 63-66.

Hobbs, P. V. (1974). Ice Physics. London, Oxford University Press.

Houska, M. (1994). Milk, Milk Products and Semi products. Prague, Institute of Agriculture and Food Information.

Jamieson, D. J. and D. J. Cleland (1993). Modelling of Bulk Stacked Cheese Cooling in Coolstore. I.I.F. - I.I.R. - Commissions B1. B2, D1, D2/3. Palmerston North.

Johnson, W. A. and R. Mehl (1939). Transaction of the AIME **185**: 416.

Katz, J. L. and F. Spaepen (1978). "A Kinetic Approach to Nuclation in Condensed Systems." Phil. Mag., **B37**: 137-148.

Kefford, B.,M. P. Christian,B. J. Sutherland,J. J. Mayes and C. Grainger (1995). "Seasonal Influence on Cheddar Cheese Manufacture of Diet Quality and Stage Lactation" Journal of dairy research **62**: 529-537.

Kenneth, A. J. (2004). Kinetics Processes. Weinheim, Wiley-Vch Berlag GmbH & Co. KGa A.

Knoop, E. and A. Wortmann (1962). 16th International Dairy Congress, Copenhagen, 16th International Dairy Congress.

Kolmogorov, A. N. (1937). "Izv. Akad. Nauk Ussr, Ser. Mat." **3**: 355.

Lees, M. (1966). "A Linear Three Level Difference Scheme for Quasilinear Parabolic Equations." Mathematics of Computation **20**: 516-522.

Levy, F. L. (1981). "A Modified Maxwell-Eucken Equation for Claculating the Thermal Conductivity of Two Component Solutions or Mixtures." International Journal of Refrigeration **4**(4): 223-225.

Lindsay, D. T. and S. J. Lovatt (1994). "Further Enthalpy Values of Foods Measured by an Adiabatic Calorimeter." Journal of Food Engineering **23**(4): 609-620.

L. Riedel, Kältetechnik, 8, 374 (1956).

L. Riedel, Kältetechnik, 9, 38 (1957).

Lu, M. (1999). Determination of the Distribution of Water Droplet Size in Butter and Margarine Using Pulsed Field Gradient-Nmr and Confocal Scanning Laser Microscopy Chemistry. Palmerston North, Massey University. **Master of Science**

Lucey, J. A. and P. F. Fox (1992). "Rennet Coagulation Properties of Late-Lactation Milk. Effect of Ph Adjustment by Addition of Ca Cl_2, Variation in Rennet Level and Blending with Mid-Lactation Milk." Irish journal of Agriculture and Food Research **31**: 172-184.

MacGibbon, A. K. H. (1993). Milkfat and Butter: Seasonal Changes in Composition and Properties Palmerston North, NZDRI.

MacGibbon, A. K. H. and W. D. McLennan (1987). "Hardness of New Zealand Patted Butter: Seasonal and Regional Variations." New Zealand Journal of Dairy Science and Technology **22**: 143-156.

Macklin, W. and B. Ryan (1968). Growth Velocities of Ice in Supercooled Water and Aqueous Sucrose Solutions The Philosophical Magazine. **17:** 83-87.

Mannapperuma, J. D. and R. P. Singh (1988). "Prediction of Freezing and Thawing Times of Foods Using a Numerical Method Based on Enthalpy Formulation." Journal of Food Science **53**(2): 626-630.

McDowell, F. H. (1953). The Buttermakers Manual, New Zealand University Press.

McPherson, A. V. and B. J. Kitchen (1981). Australian Journal of Dairy Technology **36**(1): 7-10.

Mercer, W. B. (1988). Fritz and Ammix Buttermaking Process, NZDRI.

Michelmore, R. W. and F. Franks (1982). "Nucleation Rate of Ice in Undercooled Water and Aqueous Solutions of Polyethylene Glycol." Cryobiology **19**: 163-171.

Middleton, J. (1996). Physical Properties of Dairy Products New Zealand, MAF Quality Management Ministry of Agriculture

Miles, C. A.,v.-B. G and V. C. H (1983). Calculation of Thermal Properties of Food. Physical Properties of Food. R. Jowitt, Applied science publishers**:** 269-313.

Miles, C. A.,Z. Mayer,J. M. Michael and M. Houska (1997). "Estimation of Initial Freezing Point of Foods from Composition Data." International Journal of Food Science and Technology **32**: 389-400.

Miyawaki, O.,T. Abe and T. Yano (1989). "A Numerical Method to Describe Freezing of Foods When Supercooling Occurs." Journal of Food Engineering **9**: 143-151.

Mohsenin, N. N. (1980). Thermal Properties of Foods and Agricultural Materials. London, Gordon and Breach Science Publisher.

Moline, S. W.,J. A. Sawdye,A. J. Short and A. P. Rinfret (1961). "Thermal Properties of Foods at Low Temperatures I." Food Technology **14**(5): 228.

Muhr, A. and J. Blanshard (1986). "Effect of Polysaccharide Stabilizers on the Rate of Growth of Ice." Journal of Food Technology **21**: 683-710.

Mulder, H. (1947). Zuivelonderzock. The Hague, Algemeene Nederlandsche Zuivelbond.

Mulder, H. (1953). Netherland Milk Dairy Journal **7**(199): 149.

Mulder, H.,F. C. A. D. Braver and T. G. Welle (1956). Netherlands Milk Dairy Journal **10**(199): 206, 214, 230.

Mulder, H. and P.Walstra. (1974). The Milkfat Globule. Slough , UK, Commonwealth

Precht, D. (1980). Fetta Seifen Anstrichm **82**: 142.

Precht, D. (1988). Fat Crystal Structure in Cream and Butter. Crystallization and Polymorphism of Fats and Fatty Acids. N. Garti and K. Sato. New York Marchel Dekker. **31:** 305-355.

Precht, D. and W. Buchheim (1980). Milchwissenschaft **35**: 684.

Pruppacher, H. R. and J. D. Klett (1997). Microphysics of Clouds and Precipitation. D. Reidal. Holland, Dordrecht.

Rahman, S. (1995). Food Properties Handbook. New York, CRC Press.

Ramussen, D. H. (1982). "Energetic of Homogenous Nucleation, Approach to a Physical Spinodal." Journal of Crystal growth **56**: 45-55.

Rasmussen, D. H. and C. R. Loper (1976). "A Rapid Method for Isothermal Nucleation Rate Measurement." Acta Metallurg **24**(117-123).

Rasmussen, H.,M. R. Applebly,G. L. Leedom,S.V.Babu and R. J. Naumann (1983). "Homogenous Nucleation Kinetics." Journal of Crystal growth **64**: 229-238.

Rémy, J. (1987). "Modern Freezing Facilities." International Journal of Refrigeration **10**: 165-174.

Riedel, L. (1951). "The Refrigeration Required to Freeze Fruits and Vegetables." Refrigeration Engineering **59**: 670.

Robertson, T. R.,F. B. Thompson and A. C. Cleland (1998). "Measuring Thermal Conductivity Thermal Resistance of Corrugated Made Simple." Packag. Technol. Eng **7**(8): 48-50.

Rogowski, R. Z. (2005). "The Kinetics of Nucleation in in Homogenous Media Based on Classical Avrami Model." Material Science Poland **23**(4): 961-.

Sarge, S. M.,E. Gmelin,W. H. Hohne,H. K. Cammenga,W. Hemminger and W. Eysel (1994). "The Caloric Calibration of Scanning Calorimeters." Thermochimica Acta **247**: 129-168.

Scwartzberg, H. G. (1976). "Effective Heat Capacities for the Freezing and Thawing of Foods." Journal of Food Sciene **41**: 152-156.

Skripov, v. P. (1974). Metastable Liquids. New York, Wiley.

Staph., H. E. (1949). "Specific Heat of Foodstuffs." Refrigerating Engineering **57**(8): 767.

Succar, J. and K. Hayakawa (1990). "A Method to Determine the Initial Freezing Point of

Foods." Journal of Food Science **55**(6): 1171.

Tang, J.,S. Sokhansanj,S. Yannacopoulos and S. O. Kasap (1991). "Specific Heat of Lentil Seeds by Differential Scanning Calorimetry." Transaction of the ASAE **34**: 517-522.

Turnbull, D. (1956). Phase Changes, Solid State Physics. New York, Acad Press Inc.

Turnbull, D. and J. C. Fisher (1949). "Rate of Nucleation in Condensed System." Journal of Chemical Physics **17**: 71-73.

Tverdokhleb, G. V. (1957). "L. L. A. Raksti 6: 485 " Cited in Dairy Science Abstract **22**(31): (1960).

van-Bersesteyn, E. C. H. and P. Walstra (1972). "Off. Org. K. Ned. Zuivelbond " **63**: 1112.

van-Krevelen, D. W. (1990). Properties of Polymers. Amsterdam, Elsevier Applied Science.

Walstra, P. (1974). Netherland Milk Dairy Journal **28**(3).

Walstra, P. (2003). Physical Chemistry of Foods. New York, Marchel Dekker Inc.

Wang, J.,J. K. Carson,M. F. North and D. J. Cleland (2006). "A New Approach to Modelling the Effective Thermal Conductivity of Heterogeneous Materials " Journal of Heat and Mass Transfer **49**(17-18): 3075-3083.

Wendlandt, W. W. (1986). Thermal Analysis. New York, Wiley.

Widmann, G. and R. Riesen (1987). Thermal Analysis: Terms , Methods and Application. D. A. Huthig. Heidelberg, Germany, Verlag GmbH.

Willix, J.,S. J. Lovatt and N. D. Amos (1998). "Additional Thermal Conductivity Values of Food Measured by Guarded Hot Plate." Journal of Food Engineering **37**(2): 159-174.

Winton, A. L. and K. B. Winton (1945). The Analysis of Foods. New York.

WolfschoonPombo, A. F. (1991). "A Simple Cryoscopic Method for the Prediction of Water Activity in Butter." Milchwissenschaft **46**(2): 3498-1000.

WolfschoonPombo, A. F. and A. D. Lima (1983). "A Cryoscopic Method for Salt (Nacl) Conent Detrmination in Butter." Milchwissenschaft **38**(6): 349-351.

Wood, G. R. and A. G. Walton (1970). "Homogenous Nuclation of Ice from Water." Journal of Applied Physics **41**: 3027-3036.

Wortmann, A. (1965). Fette Seifen Anstrichem **67**: 279.

Wright, M. E. and J. G. Porterfield (1970). "Specific Heat of Spanish Peanuts." Transaction of the ASAE **13**(4): 508-510.

Yamada, M.,M. Tago,S. Fukusako and A. Horibe (1993). "A Melting Point and Supercooling Characteristics of Molten Salt." Thermochim Acta **218**: 401-411.

Yang, W.,S. Sokhansanj and L. Tabil (1997). "Measurement of Heat Capacity for Borage Seeds by Differential Scanning Calorimetry." Journal of Food Processing and Preservation **21**: 395-407.

Yinnon, H. and D. R. Uhlmann (1983). "Application of the Thermo Analytical Techniques to the Study of Crystallisation Kinetics in Glass Forming Liquids. Part 1: Theory." Journal of Non-Crystal Solids **54**: 253-275.

Appendix -A1: NOMENCLATURE

a	Nucleation rate constant	$s^{-1}m^{-3}$
A	Constant	$kJkg^{-1}$
A'	Constant	$kJkg^{-1}$
B	Constant	$(kJ\ K\ kg^{-1})$
B'	Constant	$(kJ\ K\ kg^{-1})$
B''	Bounded water	
$\underline{b}$	Constant	$Wm^{-1}K^{-2}$
C	Volumetric specific heat capacity	$Jm^{-3}K^{-1}$
$\underline{c}$	Constant	Wm^{-1}
c	Constant	$(kJ\ kg^{-1}K^{-1})$
c'	Constant	$(kJ\ kg^{-1}K^{-1})$
c''	Constant	
c_f	Specific heat capacity below initial freezing point	$Jkg^{-1}K^{-1}$
c_p	Specific heat capacity at T	$Jkg^{-1}K^{-1}$
c_u	Specific heat capacity above initial freezing point	$Jkg^{-1}K^{-1}$
$\underline{d}$	Constant	$Wm^{-1}K^{-2}$
d	distance	m
d_a	Thickness of air gap	m
d_p	Thickness of packaging	m
dH_{if}	Latent heat of freezing at T_{if}	Jkg^{-1}
E	Molecular weight ratio	
f	Constant	
F	Fraction frozen	
G	Linear growth rate	ms^{-1}
ΔG^*	Critical value of free energy change	
ΔG_*^*	Free energy of activation of self diffusion	
ΔG_c	Free energy change.	
g	Growth constant	$ms^{-1}K^{-1}$
H	Enthalpy	$kJkg^{-1}$
H_{eff}	Effective enthalpy	$kJkg^{-1}$
H_{if}	Enthalpy at initial freezing point	$kJkg^{-1}$
H_o	Enthalpy at temperature equals to zero	$kJkg^{-1}$

ΔH	Molar enthalpy of fusion of ice	Jkg^{-1}
ΔH_f	Molar latent heat of crystallization	$kJkg^{-1}$
h	Heat transfer coefficient	$Wm^{-2}K^{-1}$
h_a	Air side heat transfer coefficient	$Wm^{-2}K^{-1}$
h_{eff}	Effective heat transfer coefficient	$Wm^{-2}K^{-1}$
J	Nucleation rate	$s^{-1}m^{-3}$
K	Avrami Constant	
LF	Latent heat of freezing at T	Jm^{-3}
Lx	Length	m
Ly	Height	m
L_z	Width	m
M_w	Molecular weight of water	
n	Avrami index	
n_1	Number of molecules	
$n_o(r^*)$	Number of critical cluster	
p_{ice}	Vapor pressure of ice	
p_{liquid}	Vapor pressure of supercooled liquid	
Q	Internal heat generation	Wm^{-3}
q	Heat flow rate	Wm^{-3}
r	radius	m
r^*	Critical radius	m
S	Salt fraction	
s	surface	
T	Temperature	
T_a	Ambient Temperature	
T_i	Initial temperature	
T_{if}	Initial freezing point	
T_m	Equilibrium freezing temperature	
T_{ref}	Reference temperature	°C
t	time	second
t_p	Preconditioning time	
U	Crystallization constant	$ms^{-1}K^{-1}$
v_a	Velocity of air	ms^{-1}
V	Volume of droplet	m^3

V_a	Volume fraction of air	
V_b	Volume fraction of butter	
V_c	Volume fraction of cardboard	
V_l	Volume fraction of liner	
X	Mass fraction of a component	
X_a	Mass fraction of air	
X_b	Mass fraction of butter	
X_c	Mass fraction of cardboard	
X_i	Mass fraction of i^{th} term	
X_l	Mass fraction of liner	
X_p	Mass fraction of protein	
X_s	Mass fraction of salt	
X_{si}	Mass fraction of solute before freezing	
X_{bw}	Mass fraction of bounded water	
X_w	Mass fraction of water	
x	Distance in direction of length	m
y	Distance in direction of height	m
z	Distance in direction of width	m
Φ	Reduced temperature (supercooling)	
ρ	Density	kgm^{-3}
ρ_{ice}	Density of ice	kgm^{-3}
ρ_*	Relative density	
θ	$273.15+T$	K^{-1}
$\Delta\theta$		
β	Molar freezing point constant of water	$kgK\ kg^{-1}mole$
λ	Thermal conductivity	$Wm^{-1}K^{-1}$
λ_f	Thermal conductivity below initial freezing point	$Wm^{-1}K^{-1}$
λ_u	Thermal conductivity above initial freezing point	$Wm^{-1}K^{-1}$
τ	$(\theta^3(1-\theta)^2)^{-1}$	
τ_ϕ	$(\Phi^3(1-\Phi)^2)^{-1}$	

Appendix-A2: Standard Methods Used to Measure the Composition of Butter

Lactose – Auto analyzer

Hoffman W S (1937), J. Biol.Chem., 120, 51-55
NZTM3: 6.3

Fat by Roese Gottlieb

IDF Provisional Standard 16C: 1987 Cream. Determination of fat content (Roese Gottlieb Reference Method). International Dairy Federation, Brussels.

Lactate- Enzymatic

Boehringer Mannheim (1995). Methods of Enzymatic Bioanalysis and Food Analysis Using Test-Combinations. Lactic acid test kit catalogue number 1 112 821. Boehringer Mannheim Biochemica GmbH Mannheim Germany.

Butter Moisture

IDF Provisional Standard 137: 1986 Butter. Determination of water content (Routine Method). International Dairy Federation, Brussels.
NZTM3: 12.4

Non Protein Nitrogen

IDF Provisional Standard 20B: 1993 *Milk*. Determination of Nitrogen Content. Part 4: Determination of non-protein nitrogen content. International Dairy Federation, Brussels.
NZTM3:15.3

Salt using Autotitrator

International standard ISO 15648: 2004, IDF 179: 2004
Butter – determination of salt content. Potentiometric Method.
NZTM3: 9.20

Solids-Not-Fat (SNF)

Wilster, G.H. Testing Dairy Products and dairy plant sanitation. Second Edition. Testing butter for composition. pp 31-32. OSC Cooperative Association, Oregon 1948.
NZTM3:12.1

Nitrogen on Liquid using Kjeltec

IDF Provisional Standard 20B: 1993 *Milk*. Determination of Nitrogen Content. Part 1: Kjldahl Method. International Dairy Federation, Brussels.
NZTM3: 15.4

Solid Fat Content

The fat was extracted from the butter by melting, centrifuging and filtering it. The sample was crystallised using a standard temperature/time regime. The solid fat content was determined using low resolution pulsed NMR. This method calculates the percentage solid fat content from the solid and liquid signals generated from the relaxation of the nuclei in the sample after a magnetic pulse is applied at 90° to the magnetic field in which the sample was placed.

MacGibbon AKH and McLennan WD (1987)
Hardness survey of New Zealand patted butter: seasonal and regional variations. New Zealand Journal of Dairy Science and Technology, 22, 143-156.

Triglycerides by HPLC

Fat samples were analyzed by a reversed-phase high-performance liquid chromatography (HPLC) method with an evaporative light scattering detector (ELSD). Using a binary solvent system the method separates the triglycerides into distinct peaks, on the basis of chain length and number of double bonds.All solvents were HPLC grade (BDH, Poole, UK) and nitrogen and helium (oxygen-free grade) supplied by BOC Gases (Palmerston North, NZ). The fat samples were dissolved in 1,2-Dichloroethane to 10 mg/mL solution. The injection volume was 10 µL.Reversed-phase chromatography was performed on a Waters™ LC Module I Plus (Waters Associates, Milford, MA) that incorporated a quaternary pumping system, carousel autosampler and helium sparging unit. The chromatography column was a Waters Nova-Pak™ C18, 4 µm, 3.9 × 150 mm (Part No. WAT086344, Lot No. W02481) with a precolumn module that contained inserts of the same solid phase. The chromatography column was jacketed and maintained at 20°C, by water circulated from a bath (LKB Bromma 2219 Multitemp II, Thermostatic Circulator). Triglycerides were detected with a Varex MKIII ELSD, (Alltech Associates Inc., Deerfield, Illinois, USA). Nitrogen gas was directed to the ELSD at a pressure of 80 psi with the flow at the nebulizer kept at 2.00 standard L/min (SLPM). The ELSD drift tube temperature was set at 70°C.The peak data sampling rate was 2 points/s acquired through a BUS/LACE interface with Waters Millennium 2010 Software System (Version 2.15, Waters Associates, Milford, MA).

The mobile phase gradient program is shown in Table 1. The mobile phase composition changed linearly between each step.

Table 1. Mobile phase gradient program used for triglyceride separation at 1 mL/min flow rate (A = acetonitrile, B = dichloromethane).

TIME (Min)	% of each solvent	
	A	B
	90	10
20	90	10
100	65	35
110	50	50
115	50	50
115.1	90	10
125	90	10

Reference

The Composition of New Zealand Milk Fat Triacylglycerols by Reversed-Phase High-Performance Liquid Chromatography by N.P. Robinson and A.K.H. MacGibbon published in JAOCS, Vol. 75, no. 8 (1998)

Appendix - A3: Numerical Formulation of Model

A 3.1: Finite Difference Method (Explicit Method)

Finite difference explicit scheme was used for the numerical solution of the heat transfer equation.

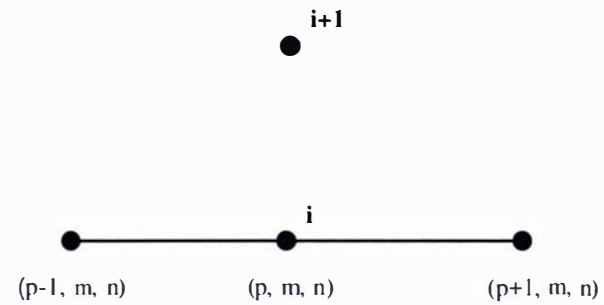

Figure: definition of a node with i as time level

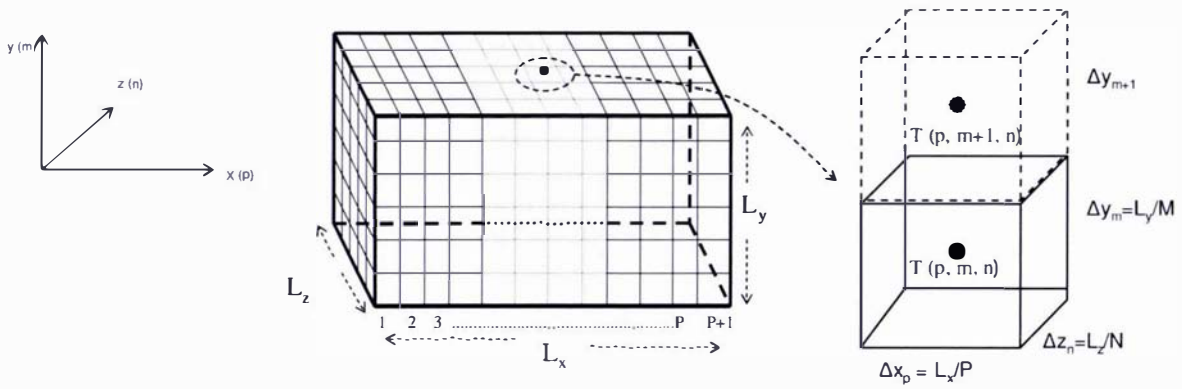

Figure: Division of block into P+1, M+1, N+1 nodes
(a) Axis direction (b) Three dimensional grid for a solid block (c) Two adjoining nodes

A3.2: Thermal conductivity

$\lambda^{i}_{(p+1/2,\,m,\,n)}$ was evaluated at $\frac{1}{2}(T^{i}_{(p+1,\,m,\,n)} + T^{i}_{(p,\,m,\,n)})$ and
$\lambda^{i}_{(p-1/2,\,m,\,n)}$ was evaluated at $\frac{1}{2}(T^{i}_{(p-1,\,m,\,n)} + T^{i}_{(p,\,m,\,n)})$

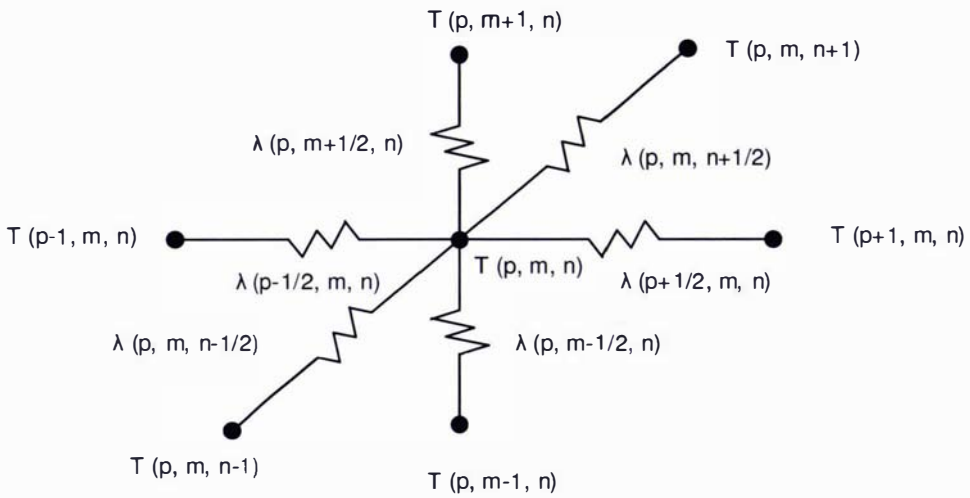

Figure Calculation of thermal conductivity for finite difference method

A3.3: Heat transfer coefficient (h) and ambient temperature (T_a)

$h = [h(1) \quad h(2) \quad h(3) \quad h(4) \quad h(5) \quad h(6)]$

similarly

$T_a = [T_a(1) \quad T_a(2) \quad T_a(3) \quad T_a(4) \quad T_a(5) \quad T_a(6)]$

where 1, 2, 3, 4, 5 and 6 correspond to the faces

$x = 0$, $x = L_x$, $y = 0$, $y = L_y$, $z = 0$, and $z = L_z$ respectively

A3.4: MATLAB code for the numerical solution for thawing of butter blocks

Please see attached CD

Block.m (Script File)

roh.m (Density)

K.m (Thermal Conductivity)

TtoH.m(Initial enthalpy from temperature input)

htooT(h).m(Calculation of Temperature at the end of each time step from enthalpy)

Appendix -A4: MATLAB code for the numerical solution for freezing of butter blocks

Please see attached CD

BlockF.m (Script File)

La.m (latent Heat Calculation)

J.m (Calculation of *J* function)

K.m (Thermal Conductivity)

Appendix - A5: Plans of Thermocouples Positions and Data for Pallet Trials

A5.1: Plan of Thermocouples in the Full Pallet Trials 1 & 2

There were 46 thermocouples all together.

LAYER 1 (bottom):
No of thermocouples used in this layer = 5

No	Position of the thermocouple
1	Box 1 at (30,30,30)mm for diagonal
2	Bottom Box 3 (surface)
3	Between slots (ambient)
4	Box 6 (at the centre of the box 6)
5	Box 6 (between box and butter) in corner towards centre of layer

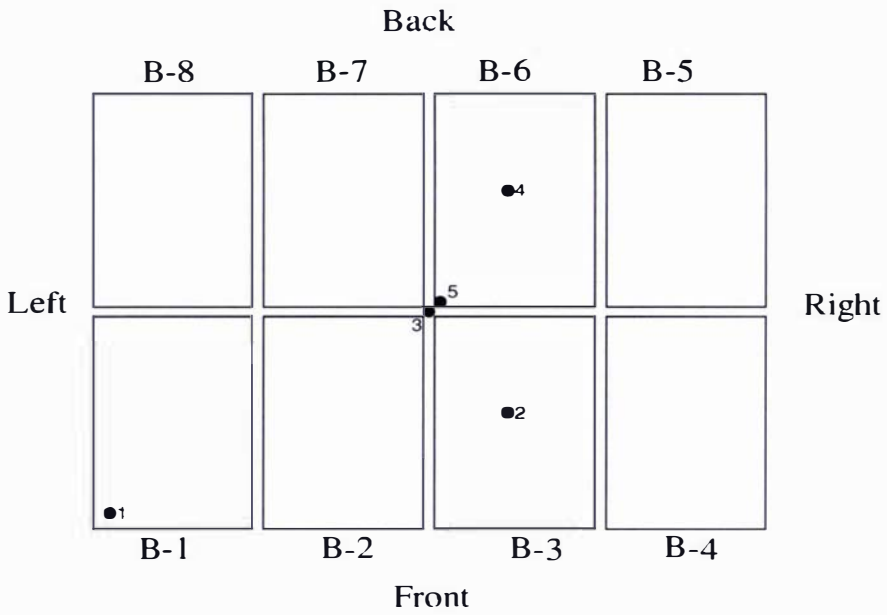

LAYER 2
No of TC used = 4

No.	Position of the thermocouple
6	Box 9 for diagonal at(221,436,165)mm
7	Box 14 for centre
8	Centre of pallet on top of layer 2
9	Indirect path between box 16 and 9 on top of L2 180mm in (x direction)

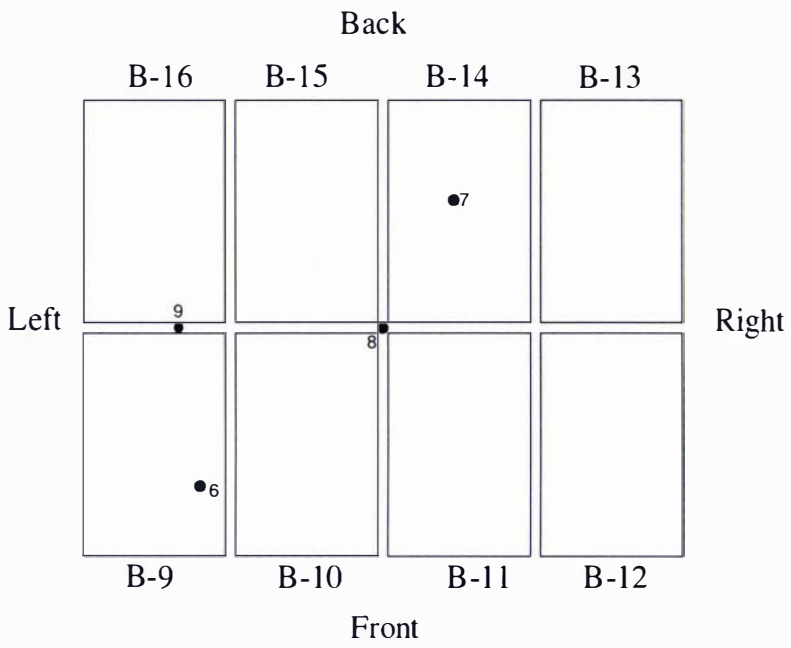

LAYER 3
No of thermocouples used = 5

No.	Position of the thermocouple
10	Centre of box 23
11	Centre of box 24
12	Centre of box 22
13	In box 24 diagonal at (367,727,275)mm
14	In air between box 22 and 18

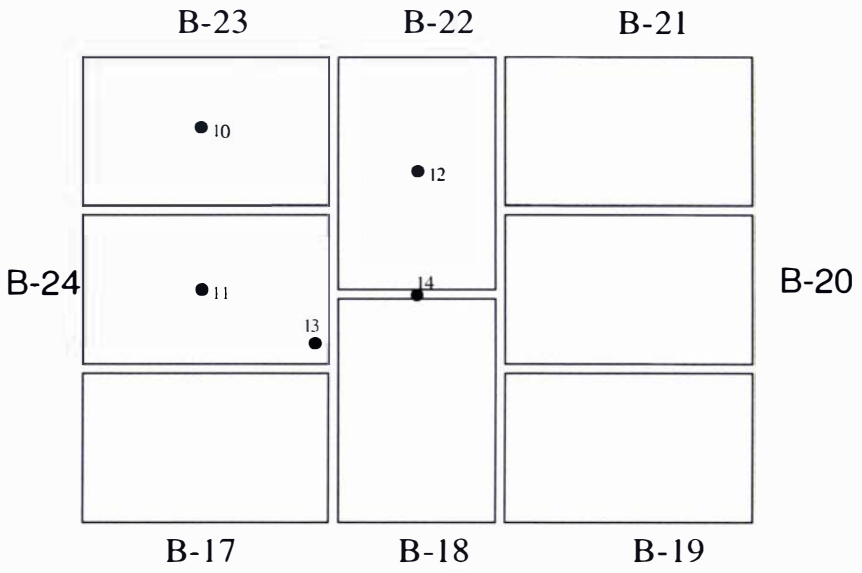

LAYER 4
No of thermocouples used = 11

No.	Position of the thermocouple
15	Box 30 centre
16	Box 30 on diagonal at (513.5,1017.5, 385)mm
17	Box 30 3cm in from the face in the centre of the box
18	Corner towards centre in box 30 between box and butter
19	Near corner in butter (1.5,Centre of box 30,1.5)
20	Between butter and box same point as OO(in Y and X direction)
21	Centre of pallet
22	Indirect path between 32 and 25 (120,870+195,Centre)
23	Indirect path between 31 and 26 (385,870+188,C)
24	Indirect path between 27 and 26(Centre,185+870,200)
25	Indirect path between 27 and 26(centre,175+870,50)

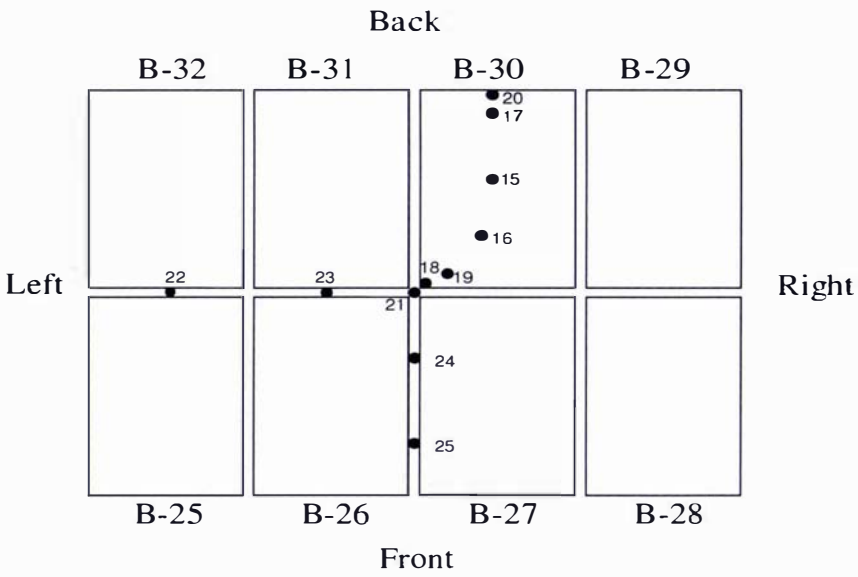

LAYER 5

No of thermocouples used = 3

No.	Position of the thermocouple
26	Centre box 38
27	Diagonal (660,1308,495)
28	Centre in air between the box 38 and 34

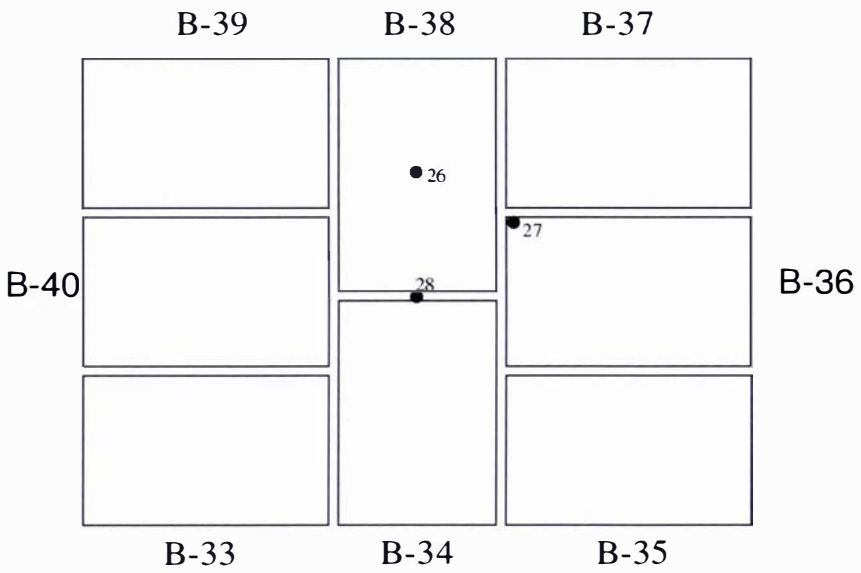

LAYER 6
No of thermocouples used = 6

No.	Position of the thermocouple
29	Centre of box 46
30	For diagonal in box 45 at (807,1599,605)
31	Centre of box 42
32	Centre of box 41
33	In the indirect path between 48 and 41
34	In the centre in air

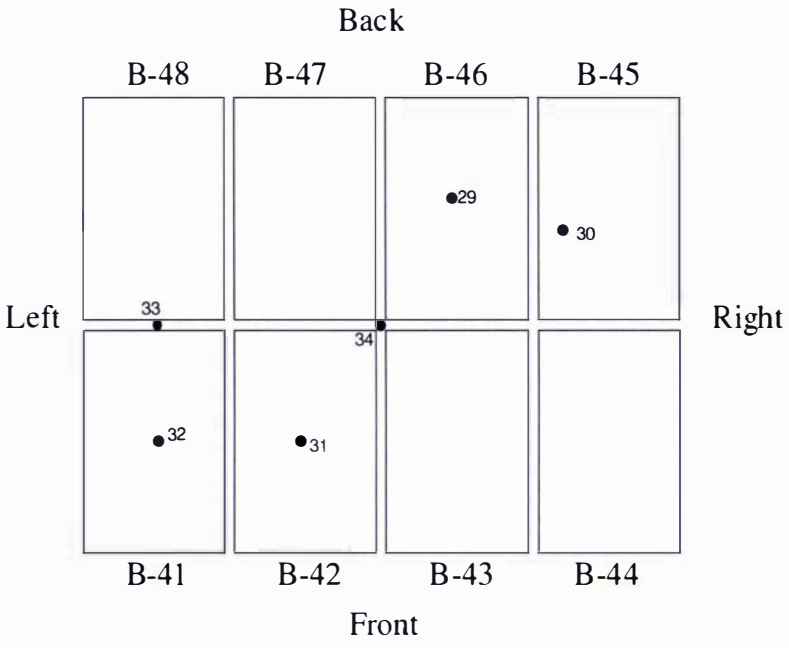

LAYER 7 (Top layer)
No of TC used = 3

No.	Position of the thermocouple
35	Between liner and box (under two layers)
36	Centre of 54
37	Corner of box 53 for diagonal at (996,2012,734)

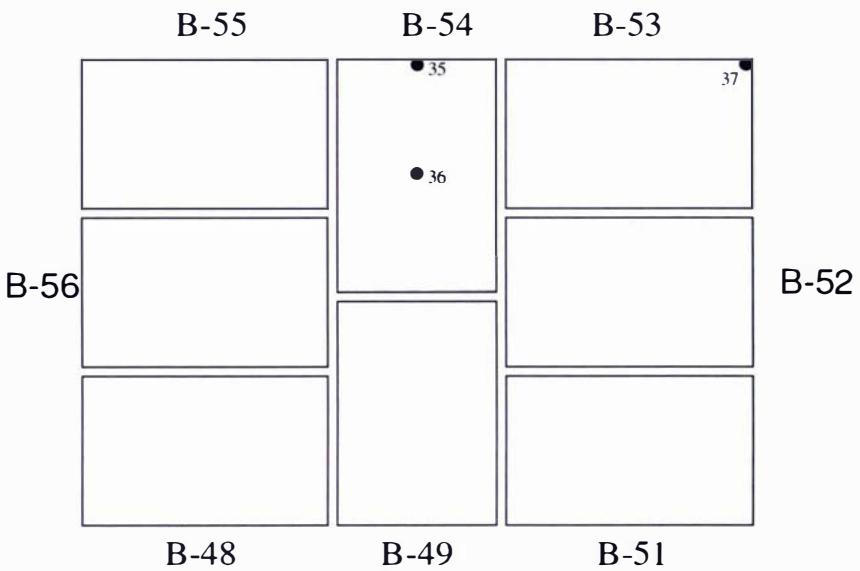

Ambient and Surface:

No	Position
38	Top of pallet under data logger
39	Back face (in the middle)
40	LHS face (in the middle)
41	Back ambient
42	Top ambient
43	Front face(in the middle)
44	RHS ambient
45	Front ambient
46	RHS on face(in the middle)

A5.2: Plan of Thermocouples in the Thawing of unwrapped Full Pallet Trial (PH-2)

Ambient Positions on six faces of Pallet	
26	LHS
27	RHS
28	Back
29	Bottom
30	Front
39	Top

Centre of each layer in air	
37	Centre of layer 6
21	Centre of layer 5
33	Centre of layer 4
4	Centre of layer 3

others	
2	on layer 5 between block 38, 39
34	on layer 4 between block 31,32,25,26
36	On layer 4 between block 28,29
20	on layer 3 between block 22, 23
38	on layer 3 top of block 22,23,24

(a)

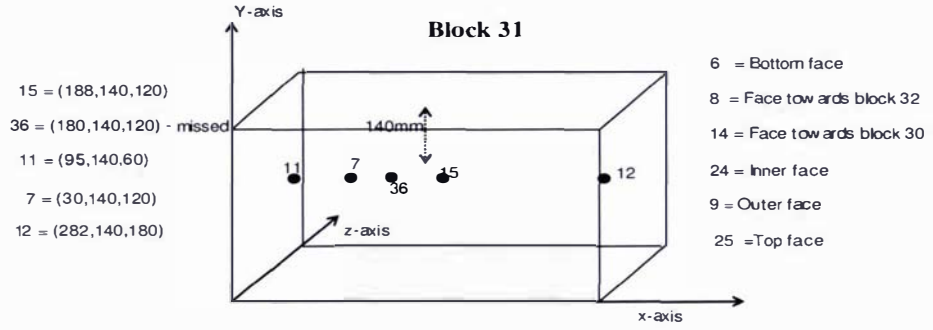

(b)

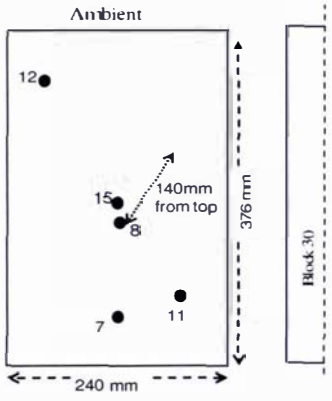

(a)

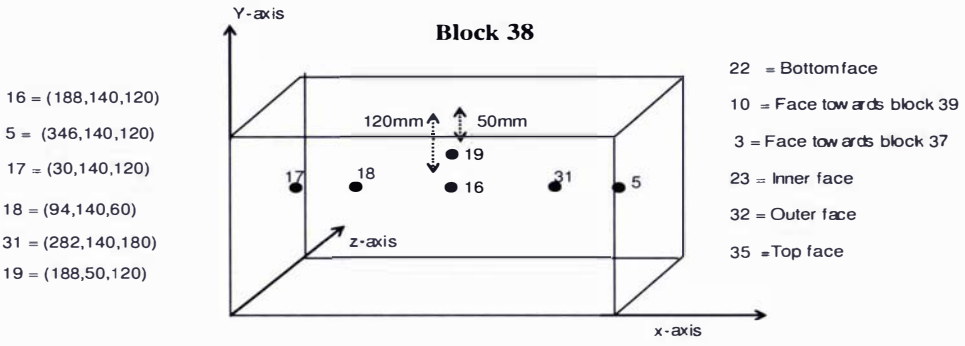

(b)

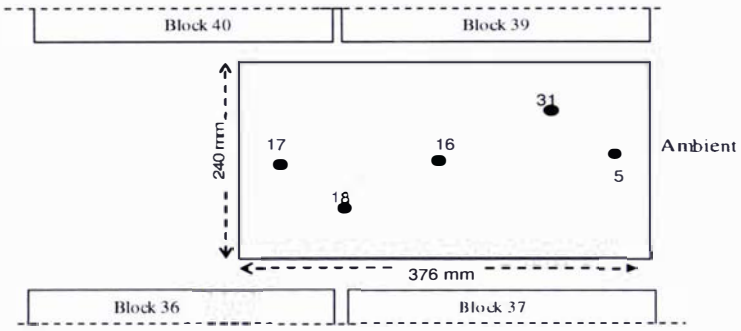

A5.3: Data for Full and Half Pallet Trials:

The data for all the trials is given in accompanying CD. The name of the text file corresponds to the trial number. Number of columns shows the number of position. Last two columns give the average ambient temperatures and time.

A5.4: Heat Balance:

$$q\rho C_{pa}(\Delta\theta_{air}) = 2\int hH(\theta_a - \theta_s)dx$$

$$q = \frac{2hHA\Delta\theta_{a\to s}}{\rho C_{pa}(\Delta\theta_{air})}$$

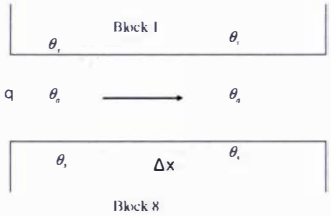

where
h = effective heat transfer coefficient ($Wm^{-2}K^{-1}$)
H = Block height (m)
q = Air flow rate (m^3s^{-1})

C_{pa}= specific heat capacity if air
2 comes from the fact that there are two faces exposed to the air

Thawing Trial:

$\theta_a - \theta_s = 16.8 - 11.9 = 4.9^{\circ}C$

$\theta_a - \theta_s = 13.5 - 7.1 = 6.4^{\circ}C$

on average = $5.65^{\circ}C$

$\Delta\theta_{air} = 16.8 - 13.5 = 3.3^{\circ}C$

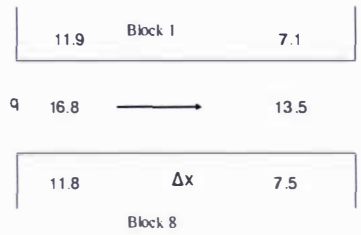

e.g: Between Blocks 1 & 8

$$q = \frac{(2)(3)(0.25)(0.28)(5.65)}{(1000)(1.2)(3.3)} = 6\times10^{-4} m^3 s^{-1}$$

area of the gap = (0.04)(0.25)=0.01m^2
Thus

$v = 0.06 ms^{-1}$

Similarly

Between Blocks 1 & 2

q = 0.7 x 10^{-3}

v = 0.05ms^{-1}

Between Blocks 7 & 8

q = 0.21 x 10^{-3}

v = 0.02ms^{-1}

Freezing Trial

Using the same approach the air velocities were calculated for freezing trial:

Between Blocks 1 & 8

q = 1.8 x 10^{-3}

v = 0.18ms^{-1}

Between Blocks 1 & 2

q = 1.64 x 10^{-3}

v = 0.46ms^{-1}

Between Blocks 7 & 8

q = 3.27 x 10^{-3}

v = 0.23ms^{-1}